



# Combined Actions

Investigation on Widened Deck KW03.01

by

**Xu Yan**

Graduation thesis to fulfill the requirement of  
Master of Science in  
Structural Engineering (Structural Mechanics) in  
Faculty of Civil Engineering and Geosciences at  
Delft University of Technology

**Author: Xu Yan**

**Student Number: 4735307**

**Project Duration: 15<sup>th</sup> March 2020 – 31<sup>st</sup> March 2020**

**Thesis Committee:**

Dr. ir. drs. C.R. Braam (Chariman)	Delft University of Technology
Dr.ir. P.C.J. (Pierre) Hoogenboom	Delft University of Technology
Ir. J.M. (Lambert) Houben	Delft University of Technology
Ing. Eelco de Winter	Royal HaskoningDHV
Ing. Rob Soetekouw	Royal HaskoningDHV

## Acknowledgement

I am very much grateful to my daily supervisor Eelco de Winter and Rob Soetekouw in Royal HaskoningDHV, who kindly provided me with help for all the data files required during the graduation project. They also patiently helped me on improving my thesis writing, making my paper much easier to be read. When working with them, their professionalism moved me. It is my honor to work with people who are skillful and experienced like them.

I would also like to thank my professor René Braam, the chairman of my committee. The knowledge I required when solving problem about cracking and prestressing is mainly learnt from his lessons, Concrete Structure. In addition, when I was confused by expressions from book and even Eurocode, Mr. Braam can always provide me a clear and thorough explanation. I would like to thank my another professor Pierre Hoogenboom. His taught me the knowledge about plate structure. The theory of discrete element model used in my thesis is learnt from his lessons, Plate and Slabs.

The last but not the least, I want to thank Lambert Houben. Mr. Houben helped me to fill register tables before the beginning of my thesis and introduced Mr. Hoogenboom to me so that I can have a complete thesis committee. Without his help, I cannot get start on my thesis.

It is my pleasure to have an opportunity to work at Royal HaskoningDHV, which kindly provides the laptop and the access to powerful softwares. People here are all friendly and helpful. I would like to address special thanks to Tim Pouwels and Shuhong Tan. Mr. Pouwels helped me to search data from the files which have hundreds pages. And the calculation carried by SCIA, which I referred to in my thesis, is the work done by Mr. Pouwels in the past. Mrs. Tan, my fellow nation, helped me a lot on overcoming language and culture barriers. Working with her really relieved my homesick. The conversations with her are really helpful and appreciated.

Many thanks to my friends with whom I enjoyed the two-and-half years in Netherlands. Every moment spent with them is a great memory and appreciated.

In the end, I would like to express the greatest thanks to my family, who brought me up and supports my study at TU Delft financially and mentally. Their love is a priceless fortune for me which encourages me being brave to overcome every trouble I come across!

## Table of Contents

<b>1</b>	<b>Abstract</b>	<b>1</b>
<b>2</b>	<b>Glossary</b>	<b>2</b>
<b>3</b>	<b>List of Acronyms and Abbreviations</b>	<b>4</b>
<b>4</b>	<b>Introduction</b>	<b>5</b>
4.1	Background Information	5
4.2	Motivation and Problem Statement	6
4.3	Research Questions	8
4.4	Scope and Limitation	9
<b>5</b>	<b>Reading Guide</b>	<b>10</b>
<b>6</b>	<b>Input Data</b>	<b>11</b>
6.1	Time History of Construction	11
6.2	Material Properties and Environmental Conditions	12
6.3	Prestressing Tendons	13
<b>7</b>	<b>Models</b>	<b>15</b>
7.1	General	15
7.2	Reason of Using Three-layer Models	15
7.3	Mean Thickness	16
7.3.1	Sketch of Models	16
7.3.2	Imposed Deformation Calculated by Realistic Model 1 and Simplified Model 1	17
7.3.2.1	In-plane Imposed Deformation in Old Deck	17
7.3.2.2	In-plane Imposed Deformation in Connection	20
7.3.2.3	In-plane Imposed Deformation in New Deck	23
7.3.3	Data of Mean Imposed Deformation	26
7.4	Mean Width	26
7.4.1	Sketch of Models	26
7.4.2	Imposed Deformation Calculated by Realistic Model 2 and Simplified Model 2	27
7.4.2.1	In-plane Imposed Deformation in Old Deck	28
7.4.2.2	In-plane Imposed Deformation in Connection	28
7.4.2.3	In-plane Imposed Deformation in New Deck	29
7.4.3	Data of Mean Imposed Deformation	29
7.5	Conclusion	30

<b>8</b>	<b>Mechanics for Structural Analysis</b>	<b>31</b>
8.1	General	31
8.2	Disadvantage of Mechanics 1	31
8.3	Advantage of Mechanics 2	32
8.4	Conclusion	33
<b>9</b>	<b>Calculation</b>	<b>34</b>
9.1	General	34
9.2	Results of SCIA and the Simple Approach	34
9.3	Sources of Different Stress Resulting from Imposed Deformation and Prestress Consumption in Proportion	36
9.3.1	Models and Mechanics	36
9.3.2	Elastic Modulus	36
9.3.3	Imposed Deformation	37
9.3.4	Contribution of Each Source	38
9.4	Discussion	40
9.4.1	General	40
9.4.2	Improving the Calculation Carried out by SCIA	40
9.4.3	Reducing Prestress Consumption	41
<b>10</b>	<b>Conclusions</b>	<b>43</b>
<b>11</b>	<b>Recommendations</b>	<b>44</b>
11.1	General	44
11.2	About Models	44
11.3	About Factor $t_0$ and Creep Factor $\phi t, t_0$ to Evaluate Elastic Modulus of Concrete and Imposed Deformation	44
11.4	About Expressions to Evaluate Elastic Modulus of Cracked Concrete	44
11.5	About Mechanics Used during Calculation	44
11.6	About Reducing Prestress Consumption	44
<b>12</b>	<b>References</b>	<b>45</b>
<b>A1</b>	<b>Examples of Imposed Deformation Resulting in Tensile Stress</b>	<b>46</b>
<b>A2</b>	<b>Data of Calculation Carried out by SCIA</b>	<b>48</b>
A2.1	General	48
A2.2	Stress Resulting from Imposed Deformation at Time $t = 40515$ days	48
A2.3	Stress Resulting from Prestressing at Time $t = 40515$ days	49
A2.4	Prestress Consumption in Proportion	50
A2.5	Out-of-plane Moment	50
A2.6	Input Data	51

A2.6.1	Material Properties	51
A2.6.2	Imposed Deformation	52
<b>A3</b>	<b>Calculation of Thermal Deformation</b>	<b>53</b>
<b>A4</b>	<b>Expressions to Evaluate the Material Properties of Concrete at Time <math>t</math> days</b>	<b>56</b>
<b>A5</b>	<b>Expressions to Calculate Cross-sectional Calculation at Time <math>t</math> days</b>	<b>58</b>
A5.1	General	58
A5.2	Cross-sectional Properties of Concrete Deck	58
A5.3	Cross-sectional Properties of Prestressing Cables	58
A5.4	Stress Resulting from Loads	59
<b>A6</b>	<b>Expressions to Calculate the Remaining Prestressing Force in Model with Uniform Cross-section Mean Dimensions at Time <math>t</math> days</b>	<b>60</b>
<b>A7</b>	<b>The Impact of Prestressing Steps</b>	<b>63</b>
A7.1	General	63
A7.2	Results	63
A7.3	Discussion	65
A7.3.1	Imposed Deformation	65
A7.3.2	Remaining Prestressing Force	65
A7.4	Conclusion	66
<b>A8</b>	<b>Dimensions and Material Properties of Models Required to Calculate Prestress Loss</b>	<b>67</b>
A8.1	Simplified Model 1	67
A8.2	Realistic Model 1	69
A8.3	Simplified Model 2	71
A8.4	Realistic Model 2	73
<b>A9</b>	<b>Calculation of Prestress Loss (Old Deck)</b>	<b>76</b>
A9.1	General	76
A9.2	All in One Step (Old Deck)	76
A9.2.1	Calculation Related to $P1, 7 - t^\infty$ ( $t^\infty = 11 \text{ years} + 29 \text{ days}$ )	77
A9.2.2	Calculation Related to $P1, 7 - t^\infty$ ( $t^\infty = 111 \text{ years}$ )	79
A9.3	Three Steps (Old Deck)	81
A9.3.1	Calculation Related to $P1, 3 - t^\infty$ ( $t^\infty = 11 \text{ years} + 29 \text{ days}$ )	82
A9.3.2	Calculation Related to $P2, 7 - t^\infty$ ( $t^\infty = 11 \text{ years} + 29 \text{ days}$ )	84
A9.3.3	Calculation Related to $P3, 28 - t^\infty$ ( $t^\infty = 11 \text{ years} + 29 \text{ days}$ )	86
A9.3.4	Calculation Related to $P1, 3 - t^\infty$ ( $t^\infty = 111 \text{ years}$ )	88
A9.3.5	Calculation Related to $P2, 7 - t^\infty$ ( $t^\infty = 111 \text{ years}$ )	90

A9.3.6	Calculation Related to $P3, 28 - t^\infty$ ( $t^\infty = 111$ years)	92
<b>A10</b>	<b>Calculation of Increment of Prestressing Force Applied in Each Step (Old Deck)</b>	<b>94</b>
A10.1	Calculation of $\Delta P1, 3 - 7$ (Old Deck)	94
A10.2	Calculation of $\Delta P1, 3 - 28$ (Old Deck)	96
A10.3	Calculation of $\Delta P2, 7 - 28$ (Old Deck)	98
A10.4	Increment of Prestressing Force Applied in Each Step	100
<b>A11</b>	<b>Calculation of Prestress Loss (New Deck)</b>	<b>101</b>
A11.1	General	101
A11.2	All in One Step (New Deck - South)	101
A11.2.1	Calculation Related to $P1, 7 - t^\infty$ ( $t^\infty = 11$ years + 29 days)	102
A11.2.2	Calculation Related to $P1, 7 - t^\infty$ ( $t^\infty = 111$ years)	104
A11.3	All in One Step (New Deck - North)	106
A11.3.1	Calculation Related to $P1, 7 - t^\infty$ ( $t^\infty = 11$ years + 29 days)	107
A11.3.2	Calculation Related to $P1, 7 - t^\infty$ ( $t^\infty = 111$ years)	109
<b>A12</b>	<b>Mechanics 1</b>	<b>111</b>
A12.1	General	111
A12.2	Properties of Cross-section	111
A12.3	Response under 'Imposed Deformation'	112
A12.4	Response under 'Mechanical Load'	113
<b>A13</b>	<b>Mechanics 2</b>	<b>114</b>
A13.1	General	114
A13.2	Split Layers and Deformation Compatibility	114
A13.3	General Elasticity Matrices	115
A13.4	Specific Elasticity Matrix	116
A13.5	Restore Compatibility	118
A13.6	In-plane Strain and Stress Resulting from Imposed Deformation	118
<b>A14</b>	<b>Comparison of Mechanics 1 and Mechanics 2</b>	<b>120</b>
A14.1	General	120
A14.2	Conditions 1	121
A14.2.1	Aim and Expectation	121
A14.2.2	Input Data	121
A14.2.3	Results	121
A14.2.4	Conclusion	122
A14.3	Conditions 2	123
A14.3.1	Aim and Expectation	123
A14.3.2	Input Data	123

12.1.1	Results	123
A14.3.3	Conclusion	124
A14.4	Conditions 3	125
A14.4.1	Aim and Expectation	125
12.1.2	Input Data	125
12.1.3	Results	125
A14.4.2	Conclusion	126
A14.5	Conditions 4	127
A14.5.1	Aim and Expectation	127
A14.5.2	Input Data	127
A14.5.3	Results	127
A14.5.4	Conclusion	129
A14.6	Conclusion	129
<b>A15</b>	<b>Impact of Timing to Make Connection on the Resulting Stress</b>	<b>130</b>
A15.1	General	130
A15.2	Time History of Construction	130
A15.3	Results (Making Connection at Time $\Delta t_{II} - III = 7 \sim 18250$ days)	131
A15.4	Results (Making Connection at Time $t = 7 \sim 90$ days)	133
A15.5	Prestress Consumption without Cracking	134
A15.6	Examples	136
A15.7	Discussion	139
A15.8	Conclusion	139
<b>A16</b>	<b>Relation between Mean Normal Stiffness and Imposed deformation in a Tensile Member</b>	<b>140</b>
A16.1	Bond Stress – Slip Relationship	140
A16.2	Primary Cracks Only	140
A16.2.1	Stress Distribution	140
A16.2.2	Shape Factors for Primary Cracks	142
A16.2.3	Slip at Crack and Transition Length	142
A16.2.4	Mean Normal Stiffness inside Transition Zone	143
A16.2.5	Mean Normal Stiffness of Cracked Tensile Member (Primary Cracks Only)	144
A16.3	Primary and Secondary Cracks	145
A16.3.1	Stress Distribution	145
A16.3.2	Shape Factors for Primary and Secondary Cracks	146
A16.3.3	Idealized Crack Pattern	147
A16.3.4	Mean Normal Stiffness of Idealized Crack Pattern	148
A16.3.5	Mean Normal Stiffness of Cracked Tensile Member	149
A16.4	Crack Pattern	149
A16.4.1	Formation Process of Crack Pattern	149
A16.4.2	Crack Pattern when $\Delta \epsilon_{II} < \Delta \epsilon \leq \Delta \epsilon_{III}$ (Stage 2)	150
A16.4.3	Crack Pattern when $\Delta \epsilon_{III} < \Delta \epsilon \leq \Delta \epsilon_{IV}$ (Stage 3)	151

A16.5	Mean Normal Stiffness of Cracked Tensile Member (Primary and Secondary Cracks)	152
A16.6	Conclusion	153
<b>A17</b>	<b>Calculation of Mean Normal Stiffness</b>	<b>154</b>
A17.1	General	154
A17.2	Input Data	154
A17.2.1	Dimensions	154
A17.2.2	Material Properties and Imposed Deformation	154
A17.3	Expressions of Equivalent Normal Force	155
A17.4	Results	156
A17.5	Conclusion	159
<b>A18</b>	<b>Expressions to Evaluate the Effective Area of Rebar</b>	<b>160</b>
<b>A19</b>	<b>Impact of Cracking on Prestress Consumption in Proportion</b>	<b>162</b>
A19.1	General	162
A19.2	Re-calculated Examples	162
A19.3	Additional Calculation	164
A19.4	Conclusion	168
<b>A20</b>	<b>Impact of Reduced Prestressing Force on Prestress Consumption</b>	<b>169</b>
A20.1	General	169
A20.2	Results	169
A20.3	Conclusion	171
<b>A21</b>	<b>Expressions for Elastic Modulus of Concrete</b>	<b>172</b>
A21.1	General	172
A21.2	Discussion	172
A21.3	Conclusion	173

## Table of Tables

Table 1: Basic Data of Time History of Construction.	11
Table 2: Other Data of Time History of Construction.	11
Table 3: Basic Data of Material Properties and Environmental Conditions of Old Decks.	12
Table 4: Basic Data of Material Properties and Environmental Conditions of Connections.	12
Table 5: Basic Data of Material Properties and Environmental Conditions of New Decks.	13
Table 6: Coordinates of Tendons in Old Decks.	13

Table 7:Coordinates of Tendons in New Decks.	13
Table 8:Data of Tendons in Old Decks.	14
Table 9:Data of Tendons in New Decks.	14
Table 10:Summary of Mean Imposed Deformation Calculated in Section 7.3.	26
Table 11:Summary of Mean Imposed Deformation Calculated in Section 7.4.	29
Table 12:Elastic Modulus of Concrete in South.	36
Table 13:Imposed Deformation in South.	37
Table 14:Imposed Deformation in South (SCIA).	37
Table 15:Imposed Deformation in South (Simple Approach).	38
Table 16:Models, Mechanics, Elastic Modulus of Concrete and Imposed Deformation Used in Each Step.	38
Table 17:Stress Resulting from Imposed Deformation from Step 0 to Step 3 in South and Contribution to Difference in Each Step.	39
Table 18:Stress Resulting from Imposed Deformation from Step 0 to Step 3 in North and Contribution to Difference in Each Step (Axis 1-2).	40
Table 19:Stress Resulting from Imposed Deformation from Step 0 to Step 3 in North and Contribution to Difference in Each Step (Axis 2-3).	40
Table 20:Stress Resulting from Imposed Deformation Calculated by SCIA.	49
Table 21:Stress Resulting from Prestressing in Old Decks.	49
Table 22:Stress Resulting from Prestressing in South New Deck.	49
Table 23:Stress Resulting from Prestressing in North New Deck.	49
Table 24:Prestress Consumption Calculated basing on the Results from SCIA.	50
Table 25:Out-of-plane Moment and Normal Stress in New Decks.	51
Table 26:Strength and Deformation Characteristics for Concrete.	56
Table 27:Values of $kh$ .	61
Table 28:Dimensions of Old Deck in Simplified Model 1.	67
Table 29:Dimensions of New Deck in Simplified Model 1.	67
Table 30:Dimensions of Connection in Simplified Model 1.	67
Table 31:Material Properties of Prestressing Cables in Old Deck.	67
Table 32:Material Properties of Prestressing Cables in New Deck.	67
Table 33:Material Properties of Concrete in Old Deck at Time $t = 3 \text{ days}$ .	68
Table 34:Material Properties of Concrete in Old Deck at Time $t = 7 \text{ days}$ .	68
Table 35:Material Properties of Concrete in Old Deck at Time $t = 28 \text{ days}$ .	68
Table 36:Material Properties of Concrete in New Deck at Time $t = 7 \text{ days}$ .	68
Table 37:Dimensions of Old Deck in Realistic Model 1.	69
Table 38:Dimensions of New Deck in Realistic Model 1.	69
Table 39:Dimensions of Connection in Realistic Model 1.	69

Table 40:Material Properties of Prestressing Cables in Old Deck.	69
Table 41:Material Properties of Prestressing Cables in New Deck.	69
Table 42:Material Properties of Concrete in Old Deck at Time $t = 3$ days.	70
Table 43:Material Properties of Concrete in Old Deck at Time $t = 7$ days.	70
Table 44:Material Properties of Concrete in Old Deck at Time $t = 28$ days.	70
Table 45:Material Properties of Concrete in New Deck at Time $t = 7$ days.	70
Table 46:Dimensions of Old Deck in Simplified Model 2.	71
Table 47:Dimensions of New Deck in Simplified Model 2.	71
Table 48:Dimensions of Connection in Simplified Model 2.	71
Table 49:Material Properties of Prestressing Cables in Old Deck.	71
Table 50:Material Properties of Prestressing Cables in New Deck.	71
Table 51:Material Properties of Concrete in Old Deck at Time $t = 3$ days.	72
Table 52:Material Properties of Concrete in Old Deck at Time $t = 7$ days.	72
Table 53:Material Properties of Concrete in Old Deck at Time $t = 28$ days.	72
Table 54:Material Properties of Concrete in New Deck at Time $t = 7$ days.	72
Table 55:Dimensions of Old Deck in Simplified Model 2.	73
Table 56:Dimensions of New Deck in Simplified Model 2.	73
Table 57:Dimensions of Connection in Simplified Model 2.	73
Table 58:Material Properties of Prestressing Cables in Old Deck.	73
Table 59:Material Properties of Prestressing Cables in New Deck.	74
Table 60:Material Properties of Concrete in Old Deck at Time $t = 3$ days.	74
Table 61:Material Properties of Concrete in Old Deck at Time $t = 7$ days.	74
Table 62:Material Properties of Concrete in Old Deck at Time $t = 28$ days.	74
Table 63:Material Properties of Concrete in New Deck at Time $t = 7$ days.	75
Table 64:Prestress Loss and Remaining Prestressing Force Calculated by All in One Step at time $t = 11$ years.	76
Table 65:Prestress Loss and Remaining Prestressing Force Calculated by All in One Step at time $t = 111$ years.	76
Table 66:Immediate Loss of Step 1 from Time $t = 7$ days to Time $t = 11$ years + 29 days.	77
Table 67:Elastic Loss of Step 1 from Time $t = 7$ days to Time $t = 11$ years + 29 days.	77
Table 68:Friction Loss of Step 1 from Time $t = 7$ days to Time $t = 11$ years + 29 days.	77
Table 69:Shrinkage Loss of Step 1 from Time $t = 3$ days to Time $t = 11$ years + 29 days.	78
Table 70:Creep Loss of Step 1 from Time $t = 7$ days to Time $t = 11$ years + 29 days.	78
Table 71:Relaxation Loss of Step 1 from Time $t = 7$ days to Time $t = 11$ years + 29 days.	78
Table 72:Immediate Loss of Step 1 from Time $t = 7$ days to Time $t = 111$ years.	79
Table 73:Elastic Loss of Step 1 from Time $t = 7$ days to Time $t = 111$ years.	79
Table 74:Friction Loss of Step 1 from Time $t = 7$ days to Time $t = 111$ years.	79

Table 75: Shrinkage Loss of Step 1 from Time $t = 3$ days to Time $t = 111$ years.	80
Table 76: Creep Loss of Step 1 from Time $t = 7$ days to Time $t = 111$ years.	80
Table 77: Relaxation Loss of Step 1 from Time $t = 7$ days to Time $t = 111$ years.	80
Table 78: Prestress Loss and Remaining Prestressing Force Calculated by Three Steps at time $t = 11$ years.	81
Table 79: Prestress Loss and Remaining Prestressing Force Calculated by Three Steps at time $t = 111$ years.	81
Table 80: Immediate Loss of Step 1 from Time $t = 3$ days to Time $t = 11$ years + 29 days.	82
Table 81: Elastic Loss of Step 1 from Time $t = 3$ days to Time $t = 11$ years + 29 days.	82
Table 82: Friction Loss of Step 1 from Time $t = 3$ days to Time $t = 11$ years + 29 days.	82
Table 83: Shrinkage Loss of Step 1 from Time $t = 3$ days to Time $t = 11$ years + 29 days.	83
Table 84: Creep Loss of Step 1 from Time $t = 3$ days to Time $t = 11$ years + 29 days.	83
Table 85: Relaxation Loss of Step 1 from Time $t = 3$ days to Time $t = 11$ years + 29 days.	83
Table 86: Immediate Loss of Step 2 from Time $t = 7$ days to Time $t = 11$ years + 29 days.	84
Table 87: Elastic Loss of Step 2 from Time $t = 7$ days to Time $t = 11$ years + 29 days.	84
Table 88: Friction Loss of Step 2 from Time $t = 7$ days to Time $t = 11$ years + 29 days.	84
Table 89: Shrinkage Loss of Step 2 from Time $t = 7$ days to Time $t = 11$ years + 29 days.	85
Table 90: Creep Loss of Step 2 from Time $t = 7$ days to Time $t = 11$ years + 29 days.	85
Table 91: Relaxation Loss of Step 2 from Time $t = 7$ days to Time $t = 11$ years + 29 days.	85
Table 92: Immediate Loss of Step 3 from Time $t = 28$ days to Time $t = 11$ years + 29 days.	86
Table 93: Elastic Loss of Step 3 from Time $t = 28$ days to Time $t = 11$ years + 29 days.	86
Table 94: Friction Loss of Step 3 from Time $t = 28$ days to Time $t = 11$ years + 29 days.	86
Table 95: Shrinkage Loss of Step 3 from Time $t = 28$ days to Time $t = 11$ years + 29 days.	87
Table 96: Creep Loss of Step 3 from Time $t = 28$ days to Time $t = 11$ years + 29 days.	87
Table 97: Relaxation Loss of Step 3 from Time $t = 28$ days to Time $t = 11$ years + 29 days.	87
Table 98: Immediate Loss of Step 1 from Time $t = 3$ days to Time $t = t^\infty$ days.	88
Table 99: Elastic Loss of Step 1 from Time $t = 3$ days to Time $t = t^\infty$ days.	88
Table 100: Friction Loss of Step 1 from Time $t = 3$ days to Time $t = t^\infty$ days.	88
Table 101: Shrinkage Loss of Step 1 from Time $t = 3$ days to Time $t = t^\infty$ days.	89
Table 102: Creep Loss of Step 1 from Time $t = 3$ days to Time $t = t^\infty$ days.	89
Table 103: Relaxation Loss of Step 1 from Time $t = 3$ days to Time $t = t^\infty$ days.	89
Table 104: Immediate Loss of Step 2 from Time $t = 7$ days to Time $t = t^\infty$ days.	90
Table 105: Elastic Loss of Step 2 from Time $t = 7$ days to Time $t = t^\infty$ days.	90
Table 106: Friction Loss of Step 2 from Time $t = 7$ days to Time $t = t^\infty$ days.	90
Table 107: Shrinkage Loss of Step 2 from Time $t = 7$ days to Time $t = t^\infty$ days.	91
Table 108: Creep Loss of Step 2 from Time $t = 7$ days to Time $t = t^\infty$ days.	91

Table 109:Relaxation Loss of Step 2 from Time $t = 7$ days to Time $t = t^\infty$ days.	91
Table 110: Immediate Loss of Step 3 from Time $t = 28$ days to Time $t = t^\infty$ days.	92
Table 111:Elastic Loss of Step 3 from Time $t = 28$ days to Time $t = t^\infty$ days.	92
Table 112:Friction Loss of Step 3 from Time $t = 28$ days to Time $t = t^\infty$ days.	92
Table 113:Shrinkage Loss of Step 3 from Time $t = 28$ days to Time $t = t^\infty$ days.	93
Table 114:Creep Loss of Step 3 from Time $t = 28$ days to Time $t = t^\infty$ days.	93
Table 115:Relaxation Loss of Step 3 from Time $t = 28$ days to Time $t = t^\infty$ days.	93
Table 116:Immediate Loss of Step 1 from Time $t = 3$ days to Time $t = 7$ days.	94
Table 117:Elastic Loss of Step 1 from Time $t = 3$ days to Time $t = 7$ days.	94
Table 118:Friction Loss of Step 1 from Time $t = 3$ days to Time $t = 7$ days.	94
Table 119:Shrinkage Loss of Step 1 from Time $t = 3$ days to Time $t = 7$ days.	95
Table 120:Creep Loss of Step 1 from Time $t = 3$ days to Time $t = 7$ days.	95
Table 121:Relaxation Loss of Step 1 from Time $t = 3$ days to Time $t = 7$ days.	95
Table 122:Immediate Loss of Step 1 from Time $t = 3$ days to Time $t = 28$ days.	96
Table 123:Elastic Loss of Step 1 from Time $t = 3$ days to Time $t = 28$ days.	96
Table 124:Friction Loss of Step 1 from Time $t = 3$ days to Time $t = 28$ days.	96
Table 125:Shrinkage Loss of Step 1 from Time $t = 3$ days to Time $t = 28$ days.	97
Table 126:Creep Loss of Step 1 from Time $t = 3$ days to Time $t = 7$ days.	97
Table 127:Relaxation Loss of Step 1 from Time $t = 3$ days to Time $t = 7$ days.	97
Table 128:Immediate Loss of Step 2 from Time $t = 7$ days to Time $t = 28$ days.	98
Table 129:Elastic Loss of Step 2 from Time $t = 7$ days to Time $t = 28$ days.	98
Table 130:Friction Loss of Step 2 from Time $t = 7$ days to Time $t = 28$ days.	98
Table 131:Shrinkage Loss of Step 2 from Time $t = 7$ days to Time $t = 28$ days.	99
Table 132:Creep Loss of Step 2 from Time $t = 7$ days to Time $t = 28$ days.	99
Table 133:Relaxation Loss of Step 2 from Time $t = 7$ days to Time $t = 28$ days.	99
Table 134:Prestress Loss and Remaining Prestressing Force Calculated by All in One Step at time $t = 11$ years + 29 days.	101
Table 135:Prestress Loss and Remaining Prestressing Force Calculated by All in One Step at time $t = 111$ years.	101
Table 136:Immediate Loss from Time $t = 7$ days to Time $t = t^\infty$ days.	102
Table 137:Elastic Loss from Time $t = 7$ days to Time $t = t^\infty$ days.	102
Table 138:Friction Loss from Time $t = 7$ days to Time $t = t^\infty$ days.	102
Table 139:Shrinkage Loss from Time $t = 7$ days to Time $t = t^\infty$ days.	103
Table 140:Creep Loss from Time $t = 7$ days to Time $t = t^\infty$ days.	103
Table 141:Relaxation Loss from Time $t = 7$ days to Time $t = t^\infty$ days.	103
Table 142:Immediate Loss from Time $t = 7$ days to Time $t = t^\infty$ days.	104

Table 143:Elastic Loss from Time $t = 7$ days to Time $t = t^\infty$ days.	104
Table 144:Friction Loss from Time $t = 7$ days to Time $t = t^\infty$ days.	104
Table 145:Shrinkage Loss from Time $t = 7$ days to Time $t = t^\infty$ days.	105
Table 146:Creep Loss from Time $t = 7$ days to Time $t = t^\infty$ days.	105
Table 147:Relaxation Loss from Time $t = 7$ days to Time $t = t^\infty$ days.	105
Table 148:Prestress Loss and Remaining Prestressing Force Calculated by All in One Step at time $t = 11$ years + 29 days.	106
Table 149:Prestress Loss and Remaining Prestressing Force Calculated by All in One Step at time $t = 111$ years.	106
Table 150:Immediate Loss from Time $t = 7$ days to Time $t = t^\infty$ days.	107
Table 151:Elastic Loss from Time $t = 7$ days to Time $t = t^\infty$ days.	107
Table 152:Friction Loss from Time $t = 7$ days to Time $t = t^\infty$ days.	107
Table 153:Shrinkage Loss from Time $t = 7$ days to Time $t = t^\infty$ days.	108
Table 154:Creep Loss from Time $t = 7$ days to Time $t = t^\infty$ days.	108
Table 155:Relaxation Loss from Time $t = 7$ days to Time $t = t^\infty$ days.	108
Table 156:Immediate Loss from Time $t = 7$ days to Time $t = t^\infty$ days.	109
Table 157:Elastic Loss from Time $t = 7$ days to Time $t = t^\infty$ days.	109
Table 158:Friction Loss from Time $t = 7$ days to Time $t = t^\infty$ days.	109
Table 159:Shrinkage Loss from Time $t = 7$ days to Time $t = t^\infty$ days.	110
Table 160:Creep Loss from Time $t = 7$ days to Time $t = t^\infty$ days.	110
Table 161:Relaxation Loss from Time $t = 7$ days to Time $t = t^\infty$ days.	110
Table 162:Material Properties Applied under Conditions 1.	121
Table 163:Imposed Deformation Applied under Conditions 1.	121
Table 164:Material Properties Applied in Conditions 2.	123
Table 165:Imposed Deformation Applied in Conditions 2.	123
Table 166:Material Properties Applied in Conditions 3.	125
Table 167:Imposed Deformation Applied in Conditions 3.	125
Table 168:Material Properties Applied in Conditions 4.	127
Table 169:Imposed Deformation Applied in Conditions 4.	127
Table 170:Basic Data of Time History of Construction.	130
Table 171:Other Data of Time History of Construction.	131
Table 172:Compressive Stress Resulting from Prestressing at time $t = t^\infty$ $t^\infty = 111$ years.	131
Table 173:Ratio between Maximum Tensile Stress and Prestress.	134
Table 174:Dimensions of the Connection.	154
Table 175:Basic Dimensions of Reinforcement.	154
Table 176:Dimensions of Effective Area.	154
Table 177:Basic Data of Material Properties and Environmental Conditions.	155

Table 178:Material Properties of Concrete at Time $t = 36500$ days.	155
Table 179:Fictitious Elastic Modulus $E_f$	172

## Table of Figures

Figure 1:Comparison between Free and Restrained Deformation.	5
Figure 2:Schematised $N - \varepsilon$ Diagram of Reinforced Concrete Tensile Member.	6
Figure 3:On-site Picture, Satellite Image and Effect Picture of Deck KW03.01.	7
Figure 4:Sketch of Widened Deck KW03.01.	7
Figure 5:Distribution of Tendons in the North New Deck.	8
Figure 6:Time History of Construction.	11
Figure 7:Sketch of Tendons.	13
Figure 8:Sketch of Realistic Model 1 (Decks in South).	16
Figure 9:Sketch of Simplified Model 1 (Decks in South).	16
Figure 10:In-plane Imposed Deformation in Realistic Model 1 and Simplified Model 1 (Old Deck).	17
Figure 11:Coefficient $\beta_H$ in Old and New Deck.	18
Figure 12:Coefficient $\varphi_0$ in Old Deck.	19
Figure 13:Coefficient $\varphi_0$ in New Deck.	19
Figure 14:Coefficient $\beta_{ct}, t_0$ in Old Deck.	19
Figure 15:Difference of Coefficient $\beta_{ct}, t_0$ in Old Deck from Time $t = t_{IV}$ to Time $t = t_V$ .	19
Figure 16:Coefficient $\beta_{ct}, t_0$ in New Deck.	19
Figure 17:Difference of Coefficient $\beta_{ct}, t_0$ in New Deck from Time $t = t_{IV}$ to Time $t = t_V$ .	19
Figure 18:In-plane Imposed Deformation in Realistic Model 1 and Simplified Model 1 (Connection).	20
Figure 19:Drying Shrinkage and Autogenous Shrinkage in Connection at Time $t = t_{IV}$ and Time $t = t_V$ .	21
Figure 20:Coefficient $\beta_{dst}, t_s$ in Connection at Time $t = t_{IV}$ and Time $t = t_V$ .	21
Figure 21:Coefficient $kh$ in Connection.	21
Figure 22:Relation between Coefficient $kh$ and Notional Size $h_0$ .	22
Figure 23:Notional Size $h_0$ in Connection.	22
Figure 24:In-plane Imposed Deformation in Realistic Model 1 and Simplified Model 1 (New Deck).	23
Figure 25:Drying Shrinkage and Autogenous Shrinkage in Old and New Deck at Time $t = t_{IV}$ and Time $t = t_V$ .	24
Figure 26:Relation between Coefficient $kh$ and Notional Size $h_0$ .	24
Figure 27:Notional Size $h_0$ .	24

Figure 28:Coefficient $\beta ds$ in Old Deck.	25
Figure 29:Coefficient $\beta ds$ in Connection and New Deck.	25
Figure 30:Sketch of Realistic Model 2 (Decks in North).	27
Figure 31:Sketch of Simplified Model 2 (Decks in North).	27
Figure 32:In-plane Imposed Deformation in Realistic Model 2 (Old Deck).	28
Figure 33:In-plane Imposed Deformation in Realistic Model 2 (Connection).	28
Figure 34:In-plane Imposed Deformation in Realistic Model 2 (New Deck).	29
Figure 35:Sketch of Simplified Model 1 (Decks in South).	30
Figure 36:Sketch of Simplified Model 2 (Decks in North).	30
Figure 37:Strain Distribution Calculated by Mechanics 1 (M1).	32
Figure 38:Stress Distribution Calculated by Mechanics 1 (M1).	32
Figure 39:Strain Distribution Calculated by Mechanics 2 (M2).	33
Figure 40:Stress Distribution Calculated by Mechanics 2 (M2).	33
Figure 41:Stress Calculated by SCIA in South.	35
Figure 42:Stress Calculated by Mechanics 2 (M2) with and without Cracking in South.	35
Figure 43:Stress Calculated by SCIA in North at Axis 1-2.	35
Figure 44:Stress Calculated by SCIA in North at Axis 2-3.	35
Figure 45:Stress Calculated by Mechanics 2 (M2) with and without Cracking in North.	35
Figure 46:Stress Resulting from Imposed Deformation from Step 0 to Step 3 in South.	39
Figure 47:Stress Resulting from Imposed Deformation from Step 0 to Step 3 in North.	39
Figure 48:Stress Resulting from Imposed Deformation in South with Different Timing to Make Connection.	42
Figure 49:Stress Resulting from Imposed Deformation in North with Different Timing to Make Connection.	42
Figure 50:Rectangular Reservoir Containing a Cooled Liquid.	46
Figure 51:Cylindrical Reservoir Containing a Heated Liquid.	46
Figure 52:Beam Subjected to Distributed Load and Cooling.	47
<i>Figure 53:Stress Resulting from Imposed Deformation Calculated by SCIA.</i>	48
Figure 54:Overview of Cross-sections in New Decks.	50
Figure 55:Development of Elastic Modulus of Concrete C35.	53
Figure 56:Development of Elastic Modulus of Concrete C45.	53
Figure 57:Development of Elastic Modulus of Concrete C35 in Proportion.	54
Figure 58:Development of Elastic Modulus of Concrete C45 in Proportion.	54
Figure 59:Temperature Development versus Time.	54
Figure 60:Temperature Development versus Height.	54
Figure 61:Relaxation Factor in Hardening Concrete.	55
Figure 62:Cross-section.	58

Figure 63:Distribution of Elastic Deformation.	62
Figure 64:Prestressing Steps of Old Decks.	63
Figure 65:Prestressing Steps of New Decks.	63
Figure 66:Prestress Loss Calculated by Three Steps at Time $t = 4015 \text{ days}$ (11 years).	64
Figure 67:Prestress Loss Calculated by Time $t = 40515 \text{ days}$ 111 years.	64
Figure 68:Prestress Loss Calculated by All in One Step at Time $t = 4015 \text{ days}$ (11 years).	64
Figure 69:Prestress Loss Calculated by All in One Step at Time $t = 40515 \text{ days}$ (111 years).	64
Figure 70:Side View of Half Realistic Model 1.	69
Figure 71:Sketch of Top View of Half Deck 1.	73
Figure 72:Sketch of Top View of Half Deck 2.	73
Figure 73:Composited Cross-section.	111
Figure 74:External Normal Force $N_i^*$ , External Normal Force $N^{**}$ and Compensating Moment $M^{**}$ .	112
Figure 75:Superposition.	112
Figure 76:Sketch of Strain and Stress.	113
Figure 77:Top and Side View of Composited Deck.	114
Figure 78:'Gaps' due to Free Deformation.	115
Figure 79:'Restored Compatibility'.	115
Figure 80:Sketch of Split Deck.	117
Figure 81:Material Properties, Imposed Deformation and the Sketch of Expectation (Strain) under Conditions 1.	122
Figure 82:Strain Distribution Calculated by Mechanics 1 (M1) under Conditions 1.	122
Figure 83:Strain Distribution Calculated by Mechanics 1 (M1) and Mechanics 2 (M2) under Conditions 1.	122
Figure 84:Material Properties, Imposed Deformation and the Sketch of Expectation (Stress) under Conditions 1.	122
Figure 85:Stress Distribution Calculated by Mechanics 1 (M1) under Conditions 1.	122
Figure 86:Stress Distribution Calculated by Mechanics 1 (M1) and Mechanics 2 (M2) under Conditions 1.	122
Figure 87:Material Properties, Imposed Deformation and the Sketch of Expectation (Strain) under Conditions 2.	124
Figure 88:Strain Distribution Calculated by Mechanics 1 (M1) under Conditions 2.	124
Figure 89:Strain Distribution Calculated by Mechanics 1 (M1) and Mechanics 2 (M2) under Conditions 2.	124
Figure 90:Material Properties, Imposed Deformation and the Sketch of Expectation (Stress) under Conditions 2.	124
Figure 91:Stress Distribution Calculated by Mechanics 1 (M1) under Conditions 2.	124

Figure 92:Stress Distribution Calculated by Mechanics 1 (M1) and Mechanics 2 (M2) under Conditions 2.	124
Figure 93:Material Properties, Imposed Deformation and the Sketch of Expectation (Strain) under Conditions 3.	126
Figure 94:Strain Distribution Calculated by Mechanics 1 (M1) under Conditions 3.	126
Figure 95:Strain Distribution Calculated by Mechanics 1 (M1) and Mechanics 2 (M2) under Conditions 3.	126
Figure 96:Material Properties, Imposed Deformation and the Sketch of Expectation (Stress) under Conditions 3.	126
Figure 97:Stress Distribution Calculated by Mechanics 1 (M1) under Conditions 3.	126
Figure 98:Stress Distribution Calculated by Mechanics 1 (M1) and Mechanics 2 (M2) under Conditions 3.	126
Figure 99:Material Properties and Imposed Deformation in the South Part ( $\Delta t_{II} - III = 28 \text{ days}$ ).	128
Figure 100:Three-Dimensional Image of Strain Resulting from All Imposed Deformation in Conditions 4.	128
Figure 101:Material Properties and Imposed Deformation in the South Part ( $\Delta t_{II} - III = 28 \text{ days}$ ).	128
Figure 102:Three-Dimensional Image of Strain Resulting from All Imposed Deformation in Conditions 4.	128
Figure 103:Y-View of Figure 100.	129
Figure 104:Y-View of Figure 102.	129
Figure 105:Sketch of Edges in the South Part.	132
Figure 106:Final Resulting Stress in the South Part without Cracking.	132
Figure 107:Sketch of Edges in the North Part.	132
Figure 108:Final Resulting Stress in the North Part without Cracking.	132
Figure 109:Sketch of Edges in the South Part.	133
Figure 110:Final resulting Stress in the South Part without Cracking (7~90 days).	133
Figure 111:Sketch of Edges in the North Part.	133
Figure 112:Final resulting Stress in the North Part without Cracking (7~90 days).	133
Figure 113:Sketch of Edges in the South Part.	134
Figure 114:Consumption of Prestress in the South Part without Cracking (7~90 days).	134
Figure 115:Sketch of Edges in the North Part.	135
Figure 116:Consumption of Prestress in the North Part without Cracking (7~90 days).	135
Figure 117:Material Properties and Imposed Deformation in South ( $\Delta t_{II} - III = 7 \text{ days}$ ).	136
Figure 118:Stress Calculated by Mechanics 1 (M1) in South ( $\Delta t_{II} - III = 7 \text{ days}$ ).	136
Figure 119:Stress Calculated by Mechanics 1 (M1) and Mechanics 2 (M2) in South ( $\Delta t_{II} - III = 7 \text{ days}$ ).	136

Figure 120:Material Properties and Imposed Deformation in South ( $\Delta t_{II} - III = 14 \text{ days}$ ).	136
Figure 121:Stress Calculated by Mechanics 1 (M1) in South ( $\Delta t_{II} - III = 14 \text{ days}$ ).	136
Figure 122:Stress Calculated by Mechanics 1 (M1) and Mechanics 2 (M2) in South ( $\Delta t_{II} - III = 14 \text{ days}$ ).	136
Figure 123:Material Properties and Imposed Deformation in South ( $\Delta t_{II} - III = 28 \text{ days}$ ).	137
Figure 124:Stress Calculated by Mechanics 1 (M1) in South ( $\Delta t_{II} - III = 28 \text{ days}$ ).	137
Figure 125:Stress Calculated by Mechanics 1 (M1) and Mechanics 2 (M2) in South ( $\Delta t_{II} - III = 28 \text{ days}$ ).	137
Figure 126:Material Properties and Imposed Deformation in North ( $\Delta t_{II} - III = 7 \text{ days}$ ).	137
Figure 127:Stress Calculated by Mechanics 1 (M1) in North ( $\Delta t_{II} - III = 7 \text{ days}$ ).	137
Figure 128:Stress Calculated by Mechanics 1 (M1) and Mechanics 2 (M2) in North ( $\Delta t_{II} - III = 7 \text{ days}$ ).	137
Figure 129:Material Properties and Imposed Deformation in North ( $\Delta t_{II} - III = 14 \text{ days}$ ).	138
Figure 130:Stress Calculated by Mechanics 1 (M1) in North ( $\Delta t_{II} - III = 14 \text{ days}$ ).	138
Figure 131:Stress Calculated by Mechanics 1 (M1) and Mechanics 2 (M2) in North ( $\Delta t_{II} - III = 14 \text{ days}$ ).	138
Figure 132:Material Properties and Imposed Deformation in North ( $\Delta t_{II} - III = 28 \text{ days}$ ).	138
Figure 133:Stress Calculated by Mechanics 1 (M1) in North ( $\Delta t_{II} - III = 28 \text{ days}$ ).	138
Figure 134:Stress Calculated by Mechanics 1 (M1) and Mechanics 2 (M2) in North ( $\Delta t_{II} - III = 28 \text{ days}$ ).	138
Figure 135:Bond Stress - Slip Curve Obtained by a Pull-out Test.	140
Figure 136:Force Balance in Half Transition Zone.	141
Figure 137:Sketch of Stress Distribution in Transition Zone (Primary Cracks Only).	142
Figure 138:Force Balance in Rebar within Half Transition Zone.	143
Figure 139:Force Balance in Cracked Tensile Member when a New Crack is about to Occur (Primary Cracks Only).	144
Figure 140:Spring Form of Tensile Member (Primary Cracks Only).	145
Figure 141:Sketch of Shape Factor in Transition Zone when $b = 0$ (Secondary and Primary Cracks).	146
Figure 142:Sketch of Shape Factor in Transition Zone when $b = 1$ (Secondary and Primary Cracks).	146
Figure 143:Sketch of Stress Distribution in Transition Zone (Idealize Crack Pattern).	148
Figure 144:Force Balance in Cracked Tensile Member when a New Crack is about to Occur (Primary and Secondary Cracks).	149
Figure 145:Formation process of Crack Pattern.	149
Figure 146:Crack Pattern when Primary Cracks are not at Their Maximum.	150
Figure 147:Crack Pattern when Primary Cracks are at Their Maximum.	151
Figure 148:Crack Pattern when Secondary Cracks are not at Their Maximum.	152

Figure 149:Crack Pattern when Secondary Cracks are at Their Maximum.	152
Figure 150:Spring Form of Tensile Member (Primary and Secondary Cracks).	153
Figure 151: $N - \delta$ Diagram of Connection in the South Part of Widened Deck KW03.01.	157
Figure 152:Details A.	158
Figure 153:Details B.	158
Figure 154:Details C.	159
Figure 155:Sketch of $N - \delta$ Diagram in 'Pink Book'.	159
Figure 156:Effective Area in Tensile Member.	160
Figure 157:Sketch of Effective Area.	161
Figure 158:Material Properties and Imposed Deformation in South ( $\Delta t_{II} - III = 28 \text{ days}$ ).	163
Figure 159:Stress Calculated by Mechanics 1 (M1) and Mechanics 2 (M2) in South ( $\Delta t_{II} - III = 28 \text{ days}$ ).	163
Figure 160:Stress Calculated by Mechanics 2 (M2) with and without Cracking in South ( $\Delta t_{II} - III = 28 \text{ days}$ ).	163
Figure 161:Prestress Consumption Calculated by Mechanics 2 (M2) with and without Cracking in South ( $\Delta t_{II} - III = 28 \text{ days}$ ).	163
Figure 162:Material Properties and Imposed Deformation in North ( $\Delta t_{II} - III = 28 \text{ days}$ ).	164
Figure 163:Stress Calculated by Mechanics 1 (M1) and Mechanics 2 (M2) in North ( $\Delta t_{II} - III = 28 \text{ days}$ ).	164
Figure 164:Stress Calculated by Mechanics 2 (M2) with and without Cracking in North ( $\Delta t_{II} - III = 28 \text{ days}$ ).	164
Figure 165:Prestress Consumption Calculated by Mechanics 2 (M2) with and without Cracking in North ( $\Delta t_{II} - III = 28 \text{ days}$ ).	164
Figure 166:Material Properties and Imposed Deformation in the South Part ( $\Delta t_{II} - III = 28 \text{ days}$ ).	165
Figure 167:Stress Distribution in Example 3 Calculated by Mechanics 1 (M1) Corresponding to a Series of Elastic Modulus Applied to Connection.	165
Figure 168:Material Properties and Imposed Deformation in the South Part ( $\Delta t_{II} - III = 28 \text{ days}$ ).	165
Figure 169:Stress Distribution in Example 3 Calculated by Mechanics 2 (M2) Corresponding to a Series of Elastic Modulus Applied to Connection.	165
Figure 170:Front-view of Figure 167.	166
Figure 171:Front-View of Figure 169.	166
Figure 172:Material Properties and Imposed Deformation in the South Part ( $\Delta t_{II} - III = 28 \text{ days}$ ).	167
Figure 173:Stress Distribution in Example 3 Calculated by Mechanics 2 (M2) Corresponding to a Series of Elastic Modulus Applied to New Decks.	167
Figure 174:Front-view of Figure 173.	167
Figure 175:Mean Elastic Modulus of Concrete under Out-of-plane Loads.	168

Figure 176:Final Resulting Stress in South Corresponding to Different Prestressing Forces per Cable.	169
Figure 177:Prestress Consumption in South Corresponding to Different Prestressing Forces per Cable.	169
Figure 178:Final Resulting Stress in North Corresponding to Different Prestressing Forces per Cable.	170
Figure 179:Prestress Consumption in North Corresponding to Different Prestressing Forces per Cable.	170
Figure 180:Determine of Bending Stiffness from $M - \kappa$ Diagram	173

## Appendices

A1	Examples of Imposed Deformation Resulting in Tensile Stress
A2	Data of Calculation Carried out by SCIA
A2.1	General
A2.2	Stress Resulting from Imposed Deformation at Time $t = 40515$ days
A2.3	Stress Resulting from Prestressing at Time $t = 40515$ days
A2.4	Prestress Consumption in Proportion
A2.5	Out-of-plane Moment
A2.6	Input Data
A2.6.1	Material Properties
A2.6.2	Imposed Deformation
A3	Calculation of Thermal Deformation
A4	Expressions to Evaluate the Material Properties of Concrete at Time $t$ days
A5	Expressions to Calculate Cross-sectional Calculation at Time $t$ days
A5.1	General
A5.2	Cross-sectional Properties of Concrete Deck
A5.3	Cross-sectional Properties of Prestressing Cables
A5.4	Stress Resulting from Loads
A6	Expressions to Calculate the Remaining Prestressing Force in Model with Uniform Cross-section Mean Dimensions at Time $t$ days
A7	The Impact of Prestressing Steps
A7.1	General
A7.2	Results
A7.3	Discussion
A7.3.1	Imposed Deformation
A7.3.2	Remaining Prestressing Force
A7.4	Conclusion

- A8 Dimensions and Material Properties of Models Required to Calculate Prestress Loss
  - A8.1 Simplified Model 1
  - A8.2 Realistic Model 1
  - A8.3 Simplified Model 2
  - A8.4 Realistic Model 2
- A9 Calculation of Prestress Loss (Old Deck)
  - A9.1 General
  - A9.2 All in One Step (Old Deck)
    - A9.2.1 Calculation Related to  $P1, 7 - t^\infty$  ( $t^\infty = 11 \text{ years} + 29 \text{ days}$ )
    - A9.2.2 Calculation Related to  $P1, 7 - t^\infty$  ( $t^\infty = 111 \text{ years}$ )
  - A9.3 Three Steps (Old Deck)
    - A9.3.1 Calculation Related to  $P1, 3 - t^\infty$  ( $t^\infty = 11 \text{ years} + 29 \text{ days}$ )
    - A9.3.2 Calculation Related to  $P2, 7 - t^\infty$  ( $t^\infty = 11 \text{ years} + 29 \text{ days}$ )
    - A9.3.3 Calculation Related to  $P3, 28 - t^\infty$  ( $t^\infty = 11 \text{ years} + 29 \text{ days}$ )
    - A9.3.4 Calculation Related to  $P1, 3 - t^\infty$  ( $t^\infty = 111 \text{ years}$ )
    - A9.3.5 Calculation Related to  $P2, 7 - t^\infty$  ( $t^\infty = 111 \text{ years}$ )
    - A9.3.6 Calculation Related to  $P3, 28 - t^\infty$  ( $t^\infty = 111 \text{ years}$ )
- A10 Calculation of Increment of Prestressing Force Applied in Each Step (Old Deck)
  - A10.1 Calculation of  $\Delta P1, 3 - 7$  (Old Deck)
  - A10.2 Calculation of  $\Delta P1, 3 - 28$  (Old Deck)
  - A10.3 Calculation of  $\Delta P2, 7 - 28$  (Old Deck)
  - A10.4 Increment of Prestressing Force Applied in Each Step
- A11 Calculation of Prestress Loss (New Deck)
  - A11.1 General
  - A11.2 All in One Step (New Deck - South)
    - A11.2.1 Calculation Related to  $P1, 7 - t^\infty$  ( $t^\infty = 11 \text{ years} + 29 \text{ days}$ )
    - A11.2.2 Calculation Related to  $P1, 7 - t^\infty$  ( $t^\infty = 111 \text{ years}$ )
  - A11.3 All in One Step (New Deck - North)
    - A11.3.1 Calculation Related to  $P1, 7 - t^\infty$  ( $t^\infty = 11 \text{ years} + 29 \text{ days}$ )
    - A11.3.2 Calculation Related to  $P1, 7 - t^\infty$  ( $t^\infty = 111 \text{ years}$ )
- A12 Mechanics 1
  - A12.1 General
  - A12.2 Properties of Cross-section
  - A12.3 Response under 'Imposed Deformation'
  - A12.4 Response under 'Mechanical Load'
- A13 Mechanics 2

- A13.1 General
- A13.2 Split Layers and Deformation Compatibility
- A13.3 General Elasticity Matrices
- A13.4 Specific Elasticity Matrix
- A13.5 Restore Compatibility
- A13.6 In-plane Strain and Stress Resulting from Imposed Deformation
- A14 Comparison of Mechanics 1 and Mechanics 2
  - A14.1 General
  - A14.2 Conditions 1
    - A14.2.1 Aim and Expectation
    - A14.2.2 Input Data
    - A14.2.3 Results
    - A14.2.4 Conclusion
  - A14.3 Conditions 2
    - A14.3.1 Aim and Expectation
    - A14.3.2 Input Data
    - A14.3.3 Conclusion
  - A14.4 Conditions 3
    - A14.4.1 Aim and Expectation
    - A14.4.2 Conclusion
  - A14.5 Conditions 4
    - A14.5.1 Aim and Expectation
    - A14.5.2 Input Data
    - A14.5.3 Results
    - A14.5.4 Conclusion
  - A14.6 Conclusion
- A15 Impact of Timing to Make Connection on the Resulting Stress
  - A15.1 General
  - A15.2 Time History of Construction
  - A15.3 Results (Making Connection at Time  $\Delta t_{II - III} = 7 \sim 18250$  days)
  - A15.4 Results (Making Connection at Time  $t = 7 \sim 90$  days)
  - A15.5 Prestress Consumption without Cracking
  - A15.6 Examples
  - A15.7 Discussion
  - A15.8 Conclusion
- A16 Relation between Mean Normal Stiffness and Imposed deformation in a Tensile Member

- A16.1 Bond Stress – Slip Relationship
- A16.2 Primary Cracks Only
  - A16.2.1 Stress Distribution
  - A16.2.2 Shape Factors for Primary Cracks
  - A16.2.3 Slip at Crack and Transition Length
  - A16.2.4 Mean Normal Stiffness inside Transition Zone
  - A16.2.5 Mean Normal Stiffness of Cracked Tensile Member (Primary Cracks Only)
- A16.3 Primary and Secondary Cracks
  - A16.3.1 Stress Distribution
  - A16.3.2 Shape Factors for Primary and Secondary Cracks
  - A16.3.3 Idealized Crack Pattern
  - A16.3.4 Mean Normal Stiffness of Idealized Crack Pattern
  - A16.3.5 Mean Normal Stiffness of Cracked Tensile Member
- A16.4 Crack Pattern
  - A16.4.1 Formation Process of Crack Pattern
  - A16.4.2 Crack Pattern when  $\Delta\varepsilon_{II} < \Delta\varepsilon \leq \Delta\varepsilon_{III}$  (Stage 2)
  - A16.4.3 Crack Pattern when  $\Delta\varepsilon_{III} < \Delta\varepsilon \leq \Delta\varepsilon_{IV}$  (Stage 3)
- A16.5 Mean Normal Stiffness of Cracked Tensile Member (Primary and Secondary Cracks)
- A16.6 Conclusion
- A17 Calculation of Mean Normal Stiffness
  - A17.1 General
  - A17.2 Input Data
    - A17.2.1 Dimensions
    - A17.2.2 Material Properties and Imposed Deformation
  - A17.3 Expressions of Equivalent Normal Force
  - A17.4 Results
  - A17.5 Conclusion
- A18 Expressions to Evaluate the Effective Area of Rebar
- A19 Impact of Cracking on Prestress Consumption in Proportion
  - A19.1 General
  - A19.2 Re-calculated Examples
  - A19.3 Additional Calculation
  - A19.4 Conclusion
- A20 Impact of Reduced Prestressing Force on Prestress Consumption
  - A20.1 General
  - A20.2 Results

- A20.3 Conclusion
- A21 Expressions for Elastic Modulus of Concrete
  - A21.1 General
  - A21.2 Discussion
  - A21.3 Conclusion

## 1 Abstract

Structures may be subjected to both mechanical loads and imposed deformation. On one hand, the mechanical loads include, for example, the self-weight of the construction work (CEN, 2001), the action from normal use by person, furniture and movable objects, vehicles (CEN, 2001), snow (CEN, 2003), wind (CEN, 2005), execution (CEN, 2005), etc. On the other hand, when the deformation of a structure is restrained, imposed deformation occurs (Breugel, 2013, p. 1). The sources of deformation can be various, not only environmental conditions, such as temperature and humidity changes, but also chemical or physical actions, such as sulphate ingress or creep (H.W.Reinhardt, 2014, p. 454).

If the shortening of a structure is restrained, the structure will be subjected to imposed deformation which results in tensile stress. Since the tensile strength of concrete is relatively low, concrete structures, such as tunnels, bridges and pavement roads, always suffer a high risk of cracking (S.Y.Gu, 2008, p. 1). Even if the concrete structure is prestressed, the tensile stress resulting from imposed deformation would consume the compressive stress in concrete and raise the risk of cracking. If the crack width exceeds the limit, leakage, corrosion and even structural failure may happen.

According to the schematised  $N - \varepsilon$  diagram of reinforced concrete (Breugel, 2013, p. 9), the development of cracking caused by imposed deformation and mechanical load are different. Suppose the cracking is caused by imposed deformation, there is a developing stage for cracking. It means the cracks caused by imposed deformation could be either fully or not fully developed. However, suppose the cracking is caused by mechanical loads, the cracks could only be fully developed.

The stiffness of fully or not fully cracked members are different. The stress resulting from imposed deformation in a structure is related to the stiffness of the structure. Therefore, cracking has significant impact on the magnitude of stress resulting from imposed deformation. Therefore, when a structure is subjected to imposed deformation and mechanical load together, it is necessary to take the impact of cracking into account during structure design.

The combination of imposed deformation and mechanic loads is referred to as combined actions. It is common to use FEM software to analyse the stress resulting from the combined actions during structure design when cracking has to be taken into account. However, FEM analysis only is not enough. It is also necessary to check the results calculated by FEM software to avoid mistakes, for example a wrong input.

There is a project called 'Approach Ring South, Groningen' (Herepoort, 2019). In the project, widened deck KW03.01 is subjected to a combination of imposed deformation and prestressing force. FEM software called SCIA is used to calculate the prestress consumption in the widened deck KW03.01. According to the data file of the project, 41% in maximum of the compressive stress resulting from prestressing is consumed when the structure is subjected to combined actions, which is much more than the engineering experience. As a result, a simple approach is required to check whether the prestress consumption in widened deck KW03.01 suits the expectation or not, where the prestress consumption is calculated by FEM software.

## 2 Glossary

To avoid misunderstanding, hereby provides definition of some keywords which are mentioned in this paper.

**The Simple Approach:** A method carried out to check whether the prestress consumption in widened deck KW03.01 suits the expectation or not, where the prestress consumption is calculated by FEM software.

**Prestress Consumption:** Compressive stress in concrete which is consumed by the tensile stress resulting from imposed deformation. Different from prestress loss in prestressing cables.

**Prestress Consumption in Proportion:** Ratio of stress resulting from imposed deformation and compressive stress resulting from prestressing.

**Mechanic Load:** The self-weight of the construction work (CEN, 2001), the actions from normal use by person, furniture and movable objects, vehicles (CEN, 2001), snow (CEN, 2003), wind (CEN, 2005), execution (CEN, 2005), etc.

**Imposed Deformation:** Restrained deformation. In this paper, if not emphasised, the imposed deformation is in-plane only.

**Restrained Deformation:** The deformation of a member or structure which is prevented by the supports or boundary conditions. The deformation may be caused by environmental change and/or chemical and physical reactions (H.W.Reinhardt, 2014).

**Environmental Change:** Temperature and humidity changes, etc.

**Chemical and Physical Reactions:** Sulphate ingress and abrasion, etc.

**Combined Actions:** Combination of imposed deformation and/or mechanical loads.

**Tensile Member:** Reinforced concrete member which is subjected to axial normal force and imposed deformation.

**Cracking Force:** Normal force applied to a reinforced concrete tensile member when the first crack appears.

**Cracking Strain:** Strain in a reinforced concrete tensile member when the first crack appears.

**Cracking Strength:** Stress in a concrete tensile member when the first crack appears in the tensile member.

**Hydration:** Procedure of a series of chemical reactions during which, In the presence of water, the silicates and aluminates of cement form products which is firm and hard mass (A.M. Neville, J.J. brooks, 2010, p. 12). Hydration of concrete causes autogenous shrinkage in concrete.

**Heat of Hydration:** The quantity of heat (in joules) per gram of unhydrated cement, evolved upon complete hydration at a given temperature (A.M. Neville, J.J. brooks, 2010, p. 13).

**Cooling:** The loss of heat of hydration because the temperature of concrete is higher than the environment it exposed to. Cooling of concrete causes thermal contraction in concrete.

**Thermal Contraction:** Shrinking of concrete as it is cooling down.

**Drying Shrinkage:** Shrinkage of concrete caused by withdraw of water from hardened concrete exposed to unsaturated environment (A.M. Neville, J.J. brooks, 2010, p. 235).

**Autogenous Shrinkage:** Shrinkage of concrete caused by loss of water used up in hydration and except in massive concrete structures (A.M. Neville, J.J. brooks, 2010, p. 234).

**Creep:** Additional deformation to the elastic deformation in concrete when it is subjected to sustained constant stress (A.M. Neville, J.J. brooks, 2010, p. 212).

**Impact of Connection:** The strain and stress in widened deck KW03.01 resulting from the imposed deformation which is caused by the appearance of connection. The connections are built between old decks and new decks.

**Impact of Cracking:** Cracking decreases the stiffness of concrete member and the stiffness of concrete member is related to the magnitude of stress resulting from imposed deformation. As a result, the strain and stress calculated with and without cracking in widened deck KW03.01 are different. The difference is called the impact of cracking.

**Input Data:** Date of time history, material properties and combined actions to be used in the simple approach.

**Time History of Construction:** Data of important timing when the old decks, new decks and connections of widened deck KW03.01 are constructed.

### 3 List of Acronyms and Abbreviations

To avoid misunderstanding, hereby provides definition of all acronyms and abbreviations which are mentioned in this paper.

**FEM:** Finite element model.

## 4 Introduction

### 4.1 Background Information

When the deformation of structure caused by environmental change and/or chemical and physical reactions is restrained, imposed deformation is produced (Breugel, 2013). An example of imposed deformation is shown in Figure 1. The temperature drop  $\Delta T$  is expected to cause a shortening of the bar in Figure 1. In Figure 1(a), the bar is shortened freely because the right-hand end of the bar is free. However, in Figure 1(b), the bar is fixed on both ends. So, the shortening of the bar Figure 1(b) is not free but restrained by the supports at the ends of the bar. Such a restrained deformation is referred to as imposed deformation.

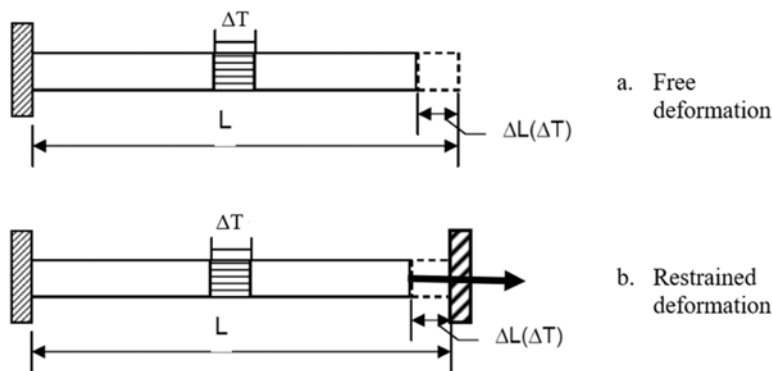


Figure 1: Comparison between Free and Restrained Deformation.

Suppose the deformation prevented by the supports or boundaries is strain, the imposed deformation is referred to as imposed strain  $\Delta\epsilon$ . Similarly, suppose the deformation prevented by the supports or boundaries is curvature, the imposed deformation is referred to as restrained curvature  $\Delta\kappa$ . Examples of structures subjected to imposed deformation are shown in Appendix A1.

As shown in Appendix A1, a structure may be subjected to both imposed deformation and mechanical loads at same time. The combination of imposed deformation and mechanical loads is referred to as combined actions.

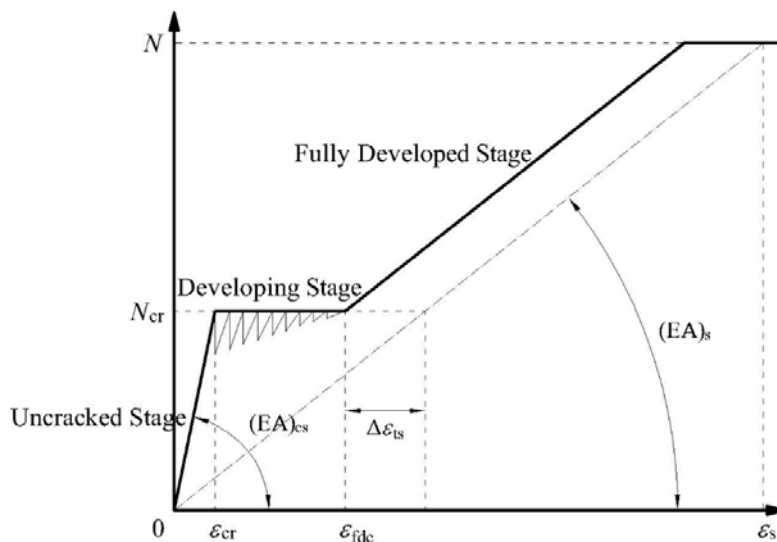
Suppose the shortening of a structure is restrained, tensile stress would appear. Since the tensile strength of concrete is relatively low, concrete structures, such as tunnels, bridges and pavement roads, always suffer a high risk of cracking (S.Y.Gu, 2008, p. 1). If the concrete structure is prestressed, the tensile stress resulting from imposed deformation will consume the prestress which also raises the risk of cracking. If the crack width exceeds the limit, leakage, corrosion and even structural failure will happen.

Cracking may happen when a reinforced concrete tensile member, or in short tensile member, is subjected to normal force  $N$  and/or impose deformation  $\Delta\epsilon$ . As shown in Figure 2, cracking of a tensile member consists of three stages (Breugel, 2013, p. 9). The first stage is uncracked stage, starting from point  $(0,0)$  to point  $(\epsilon_{cr}, N_{cr})$  where  $N_{cr}$  and  $\epsilon_{cr}$  represent the cracking force and cracking strain. In first stage,  $N < N_{cr}$  and  $\Delta\epsilon < \epsilon_{cr}$ , the tensile member is uncracked and linear elastic. When  $N = N_{cr}$  or  $\Delta\epsilon = \epsilon_{cr}$ , the first crack appears and cracking comes to the second stage. Suppose the cracking is caused by mechanical loads, the normal force  $N$  applied to the tensile member would be constant. In this case, all possible cracks would appear together at same time. However, suppose the cracking is caused by imposed deformation, instead of mechanic loads, the imposed strain  $\Delta\epsilon$  applied to the tensile member would be constant. When first crack appears, the normal stiffness of tensile member decreases. As a result, with a constant imposed deformation, the normal force in tensile member drops below the cracking force  $N_{cr}$ . Further cracks will not appear unless the imposed strain keeps increasing, making the normal force in the tensile member exceeds the cracking force  $N_{cr}$  again. For simplicity, when cracking is in second stage, it is assumed that the normal force in tensile member is constant and equals to the cracking force  $N_{cr}$ . When the maximum cracks appear, cracking

comes to the third stage. The mean strain of cracked tensile member at this moment is denoted as  $\varepsilon_{fdc}$ . In this stage, the crack pattern is taken fully developed. So, the third stage is referred to as fully developed stage, while the second stage, where the crack pattern is not fully developed, is referred to as developing stage.

As mentioned above, cracking caused by imposed deformation and mechanical loads are different. Those caused by imposed deformation consists of three stages, while those caused by mechanical loads consists of only the first stage and the third stage. As a result, when a tensile member is subjected to both imposed deformation and mechanical loads, the crack pattern can be either fully or not fully developed.

The mean stiffness of not fully cracked tensile member is larger than that of fully cracked one, which is expected to result in different magnitudes of stress in concrete when further imposed deformation is applied. Therefore, when a combination of imposed deformation and mechanical loads is applied, the structure should be designed with the combination instead of equivalving imposed deformation into mechanical loads, so that it is enabled to take not fully cracked pattern into account.



*\*It is assumed that the rebar will not be broken due to cracking. In this case, the mean strain of the tensile member is equal to the mean strain of rebar  $\varepsilon_s$ . Therefore, the mean strain of tensile member is referred to as the mean strain of rebar  $\varepsilon_s$  in this diagram.*

Figure 2: Schematised  $N - \varepsilon$  Diagram of Reinforced Concrete Tensile Member.

## 4.2 Motivation and Problem Statement

The combination of imposed deformation and mechanic loads is referred to as combined actions. It is common to use FEM software to analyse the stress resulting from the combined actions during structure design when cracking is taken into account. However, FEM analysis only is not enough. It is also important to check the results from FEM software to make sure that the results are reliable.

There is a project called 'Approach Ring South, Groningen', where the viaduct of main roadway N7 over the Laan Corpus den Hoorn in Groningen was widened (Herepoort, 2019). The viaduct deck is called KW03.01. Figure 3 shows the on-site picture, the satellite image of deck KW03.01 before being widened and the effect picture after being widened. The aim of the project is to improve traffic flow, accessibility, safety and quality of life. Extra lanes, new connections and level crossings will make the twelve-kilometre ring road safer and make city and region more accessible.



Figure 3: On-site Picture, Satellite Image and Effect Picture of Deck KW03.01.

The existing decks were built in 2009, which consists of two parts with same dimensions (Herepoort, 2007, p. 5). For simplicity, the existing decks of KW03.01 being widened are referred to as old decks, while the newly casted decks to widened existing decks are referred to as new decks.

After being prestressed, new decks were connected to old decks by connections (Herepoort, 2019). So, the widened deck KW03.01 consists of three parts: the old decks built in 2009, the new decks built in 2019 and the connections. The sketch of the widened deck KW03.01 is shown in Figure 4. The thickness of the decks varies from  $h = 550$  mm at the ends to  $h = 850$  mm at mid-support, where the mean thickness is  $h = 700$  mm.

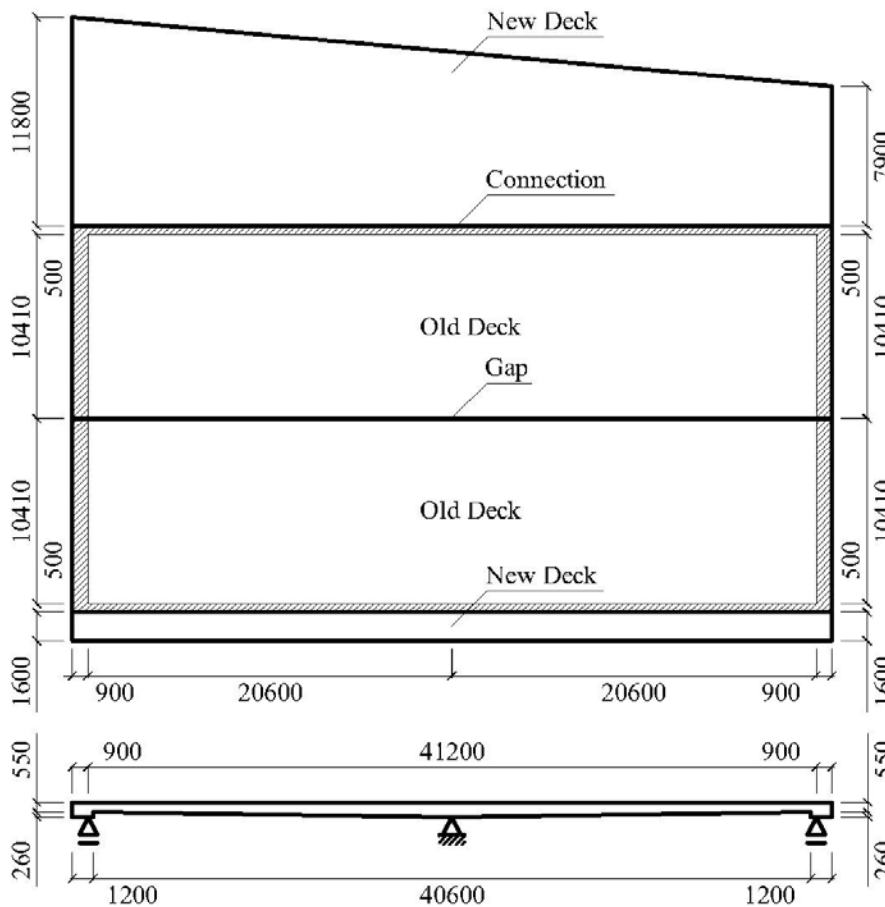


Figure 4: Sketch of Widened Deck KW03.01.

Old decks and new decks are prestressed while the connections are not. Since connections are made after old decks and new decks being prestressed, the thermal deformation of old decks and new decks is assumed to be free. As results, old decks and new decks only suffer the shortening due to drying, hydration and creep, while connections suffer the thermal deformation and the shortening due to cooling, drying and hydration. As shown in Figure 4, the width of new deck in north is variable. However, the distribution of prestressing tendons inside the deck, see Figure 5, enables it to deform without any bending (Herepoort, 2019).

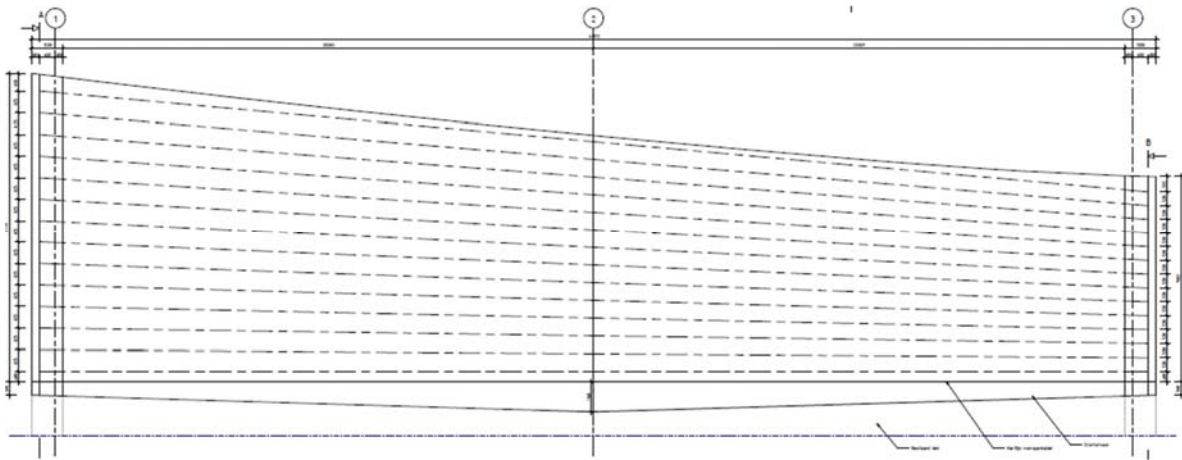


Figure 5: Distribution of Tendons in the North New Deck.

The thermal deformation and the shortening due to drying, hydration and creep are time-dependent, which grow faster in the early age and get slow gradually as the time goes. New decks were built at a time  $\Delta t = 11$  years after old decks being built. After new decks being built, new decks are expected to deform faster than old decks. Therefore, after being connected, the old decks are expected to prevent the deformation of new decks, resulting in in-plane imposed deformation. Similar to shortening of new decks, the shortening of connections also results in in-plane imposed deformation. In addition to the imposed deformation, the prestressing force applied to old decks and new decks is acting in-plane as well. So the widened deck KW03.01 is subjected to combined actions in-plane.

During the structure design of widened deck KW03.01, FEM software called SCIA is used to calculate the stress resulting from imposed deformation, or in short resulting stress. The results of SCIA is shown in Appendix A2. As shown in Appendix A2.4, the resulting stress consumes 41% in maximum of the compressive stress resulting from prestressing, which is much more than engineering experience. So, a simple approach is required to check whether the prestress consumption calculated by SCIA is reliable or not.

As shown in Section 4.1, the mean stiffness of not fully cracked tensile member is larger than that of fully cracked one, which is expected to result in different magnitudes of stress in concrete when further imposed deformation is applied. Therefore, to obtain a reasonable prestress consumption by the simple approach, the impact of cracking has to be taken into account.

### 4.3 Research Questions

To carry out the simple approach mentioned in Section 4.2, four research questions have to be answered. Hereby summarized the research questions.

1. What are the models to be used during the simple approach?

To answer this question, dimensions of the model has to be determined.

2. What is the mechanics to be used to calculate the impact of connection?

In addition to the models to be used during the simple approach, the mechanics for structural analysis is important as well. Without the mechanics for structural analysis, the stress resulting from the combined actions,

especially the imposed deformation, cannot be calculated. To get reliable prestress consumption at the end of the simple approach, a reliable mechanics for structural analysis is necessary.

3. How much is the prestress consumption calculated by the simple approach?

To answer this question, the answer to the first two research questions are required. Otherwise, the calculation of prestress consumption cannot be carried out. The prestress consumption calculated by the simple approach will be compared with that calculated by FEM software to answer the final research question.

4. Whether the prestress consumption calculated by FEM software is reliable?

This is the final research question of this thesis. To answer this question, the answer to the third research questions is required.

#### 4.4 Scope and Limitation

The simple approach is to check the mean prestress consumption which is calculated basing on the mean imposed deformation and the mean dimensions. For simplicity, it is assumed that the stress distribution resulting from combined actions is linear. However, the stress distribution resulting from combined actions is non-linear.

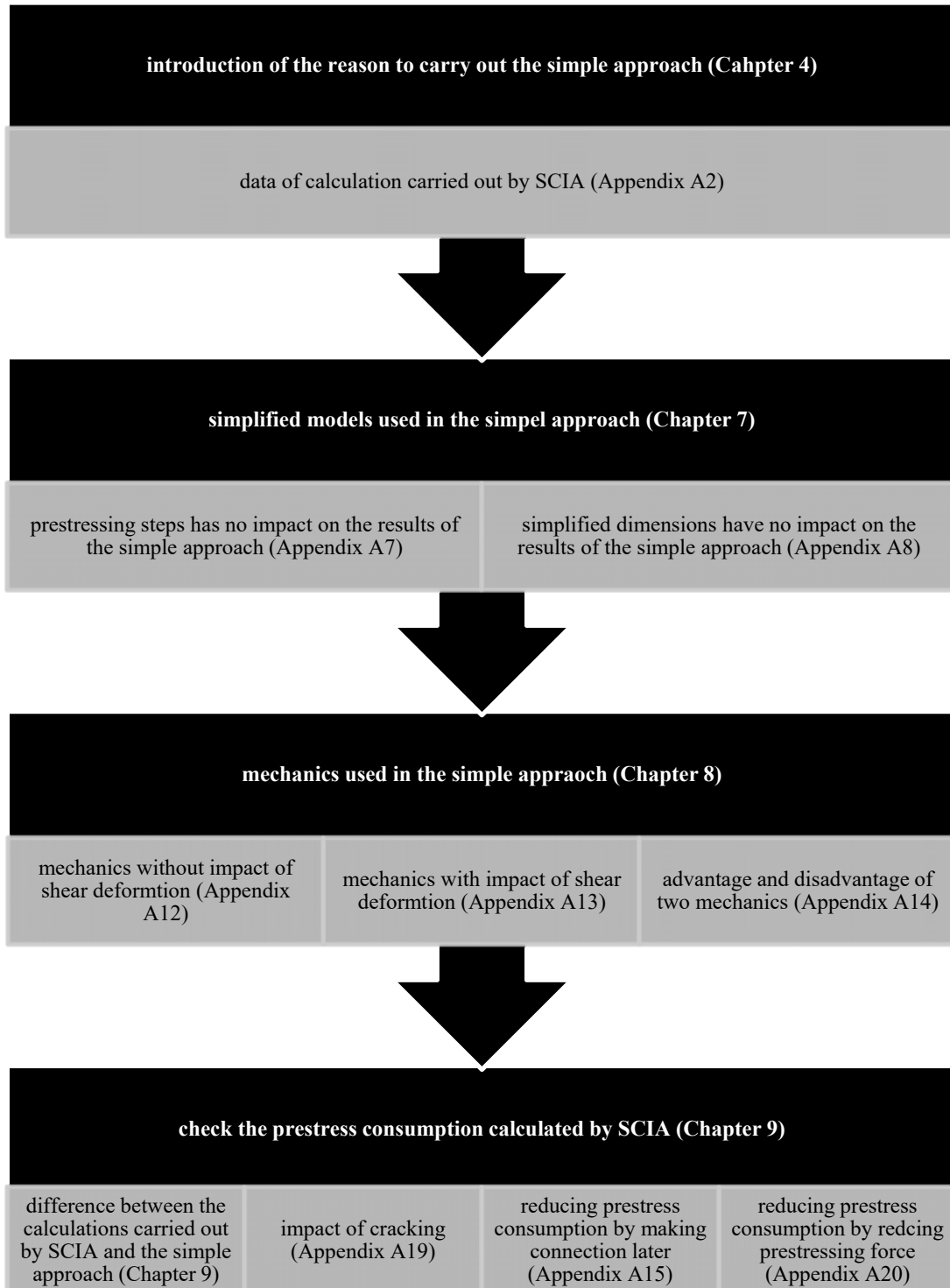
In the simple approach, prestress is taken constant and uniformly distributed in old decks and new decks. The prestress loss consists of the losses due to elastic deformation, friction, shrinkage, creep and relaxation. For simplicity, prestress loss is calculated without the impact of imposed deformation, see Appendix A15.1. However, in reality, tensile stress resulting from imposed deformation decreases the shortening of the decks and, therefore, decreases the prestress loss. Similarly, compressive stress resulting from imposed deformation increases the shortening of the decks and, therefore, increases the prestress loss. For simplicity, the impact of imposed deformation on the prestress loss mentioned above is neglected. So the prestress consumption calculated by the simple approach is conservative in the tensed area but not in the compressed area.

In the simple approach, cracking is taken into account. The cracked area is taken as the parts of widened deck KW03.01 where tensile stress resulting from combined actions exceeds the cracking strength of concrete, and the tensile stress resulting from combined actions is calculated without the impact of cracking. However, in real case, cracking decreases the stiffness of the decks and, therefore, decreases the tensile stress resulting from combined actions. Since it is not effective to estimate the crack pattern step by step, the cracked area of the decks are estimated without the impact of cracking. It is expected that the cracked area estimated in the simple approach is larger than that in reality.

As a result, the simple approach can give a general prestress consumption which **can** be used to check the reliability of the results calculated by FEM software. But the prestress consumption **cannot** be used directly to the structural design, for example to determine the exact stress at specific position in the widened deck KW03.01 or to determine the amount of reinforcement required.

## 5 Reading Guide

There are eleven chapters and twenty appendix in this paper. To avoid readers getting lost when reading this paper, a flow chart is provided below as a brief reading guide to show the relation between chapters and appendix.



## 6 Input Data

### 6.1 Time History of Construction

Both the material properties of concrete and the in-plane imposed deformation are related to the age of concrete. To inform the age of concrete in the old decks, new decks and connections, time history of construction (Herepoort, 2019) is summarized. As shown in Figure 6, there are five important timing during the construction of widened deck KW03.01.

- $t_I$  the timing when the construction of old decks was finished
- $t_{II}$  the timing when the construction of new decks was finished
- $t_{III}$  the timing when the construction of connections was finished, also referred to as the timing to make connection
- $t_{IV}$  the timing when the connections were stiff enough to restrain the deformation of free shrinkage/creep, or in short to produce imposed deformation
- $t_V$  the target timing to calculate the remaining prestress force, the imposed deformation and the resulting strain and stress, also referred to as  $t_{\infty}$

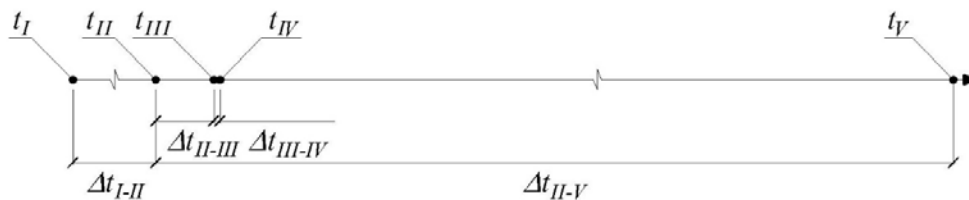


Figure 6: Time History of Construction.

The data of time history of construction is shown in Table 1 and Table 2.

timing of <b>old deck</b> being built	$t_I$	0 years
timing of <b>new deck</b> being built	$t_{II}$	11 years
timing of <b>connection</b> being built	$\Delta t_{II-III}$	28 days
connected age of <b>connection</b>	$\Delta t_{III-IV}$	1 days
target time after <b>new deck</b> being built	$\Delta t_{II-V}$	36500 days

\* $\Delta t_{III-V} = 1$  days which means it takes one day for the concrete in connections to get stiff enough to produce imposed deformation, see Appendix A3.

Table 1: Basic Data of Time History of Construction.

timing of connection being stiff	$\Delta t_{II-IV}$	29 days
connected age of <b>old deck</b>	$\Delta t_{I-IV}$	4044 days
connected age of <b>new deck</b>	$\Delta t_{II-IV}$	29 days
target age of <b>old deck</b>	$\Delta t_{I-V}$	40515 days
target age of <b>connection</b>	$\Delta t_{III-V}$	36472 days
target age of <b>new deck</b>	$\Delta t_{II-V}$	36500 days

\*The data in Table 2 is evaluated basing on the data in Table 1.

Table 2: Other Data of Time History of Construction.

## 6.2 Material Properties and Environmental Conditions

As shown in Section 6.1, the material properties of concrete are related to the age of concrete, while the age of concrete in old decks, new decks and connections are not same. For simplicity, here only summarized the material properties of concrete at time  $t = 28$  days. In addition, the material properties of prestressing cables and the environmental conditions of the widened deck KW03.01 are also summarized, see Table 3, Table 4 and Table 5.

The material properties of concrete at other time in addition to  $t = 28$  days are also used in this case study. The expressions used to evaluate these data are shown in Appendix A3. For the convenience of reading, the data is not summarized here.

Environment	relative humidity	RH	75 %
Cement (CEM III/B)	coefficient related to cement	$s$	0.25
Concrete (C35/45)	characteristic strength	$f_{ck}$	35 MPa
	gravity	$\gamma_c$	25 kN/m <sup>3</sup>
	compressive strength	$f_{cm}$	43 MPa
	tensile strength	$f_{ctm}$	3.2 MPa
	elastic modulus	$E_{cm}$	34 GPa
	poisson's ratio	$\nu$	0.2
	coefficient of thermal expansion	$\alpha_c$	0.00001 /°C
Prestressing Cable (Y1860)	area of cross-section per cable	$\bar{A}_p$	1800 mm <sup>2</sup>
	number of cables in the north one	$n$	25
	number of cables in the south one	$n$	25
	elastic modulus	$E_p$	195 GPa

Table 3: Basic Data of Material Properties and Environmental Conditions of Old Decks.

Environment	relative humidity	RH	75 %
Cement (CEM III/B)	coefficient related to cement	$s$	0.25
Concrete (C35/45)	characteristic strength	$f_{ck}$	35 MPa
	gravity	$\gamma_c$	25 kN/m <sup>3</sup>
	compression strength	$f_{cm}$	43 MPa
	elastic modulus	$E_{cm}$	34 GPa
	poisson's ratio	$\nu$	0.2
	coefficient of thermal expansion	$\alpha_c$	0.00001 /°C

Table 4: Basic Data of Material Properties and Environmental Conditions of Connections.

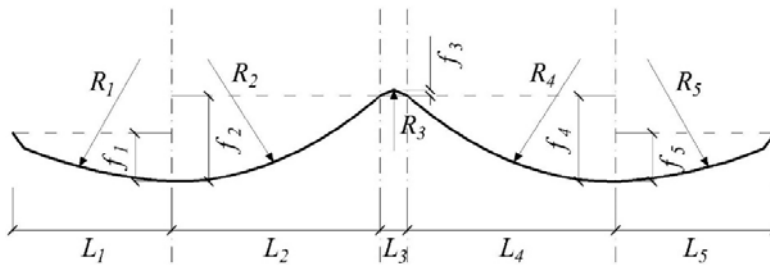
Environment	relative humidity	RH	75 %
Cement (CEM III/B)	coefficient related to cement	$s$	0.25
Concrete (C45/55)	characteristic strength	$f_{ck}$	45 MPa
	gravity	$\gamma_c$	25 kN/m <sup>3</sup>
	compression strength	$f_{cm}$	53 MPa
	elastic modulus	$E_{cm}$	36 GPa
	poisson's ratio	$\nu$	0.2
	coefficient of thermal expansion	$\alpha_c$	0.00001 /°C

Prestressing Cable (Y1860)	area of cross-section per cable	$\bar{A}_p$	2850 mm <sup>2</sup>
	number of cables in the north one	$n$	14
	number of cables in the south one	$n$	3
	elastic modulus	$E_p$	195 GPa

Table 5: Basic Data of Material Properties and Environmental Conditions of New Decks.

### 6.3 Prestressing Tendons

The shape of prestressing tendons in the old and the new decks are similar (Herepoort, 2007) (Herepoort, 2019). The sketch of prestressing tendons in both old deck and new deck is shown in Figure 7. The coordinates of points on the prestressing tendons in old decks and new decks are summarized in Table 6 and Table 7.



\*The linear part of tendons in new decks are not shown in Figure 7.

\*\* $L_i$ , the horizontal length of tendon curve  $i$

\*\*\* $R_i$ , is the radius of tendon curve  $i$

\*\*\*\* $f_i$ , is the vertical height of tendon curve  $i$

Figure 7: Sketch of Tendons.

-600,275	600,366	1600,413	2600,453	3600,488	4600,520	5600,546
6600,569	7600,588	8000,594	8600,602	9600,608	10600,606	11600,596
12600,578	13600,553	14600,520	15600,480	16600,431	17600,375	18600,310
19600,238	19861,218	20600,190	21339,218	21600,238	22600,310	23600,375
24600,431	25600,480	26600,521	27600,554	28600,579	29600,596	30600,607
31600,608	32600,603	33200,596	33600,590	34600,571	35600,549	36600,523
37600,491	38600,456	39600,415	40600,369	41800,275		

\*The data in Table 6 is form of  $(x, z)$ .

\*\*  $x$ , the horizontal position of certain point in longitudinal direction

\*\*\* $z$ , the vertical distance from certain point to the top-surface of deck

Table 6: Coordinates of Tendons in Old Decks.

<b>0,275</b>	<b>250,286</b>	<b>750,308</b>	<b>1000,320</b>	2630,385	4270,437	5900,475
7540,499	9170,510	10810,506	12440,488	14070,457	15710,411	17340,352
18980,279	20610,192	20670,188	20730,185	20780,183	20840,181	20900,179
20960,178	21070,176	21190,175	21310,176	21420,178	21480,179	21540,181
21600,183	21650,185	21710,188	21770,192	23400,279	25040,352	26670,411
28310,457	29940,488	31570,506	33210,510	34840,499	36480,475	38110,437
39750,385	<b>41380,320</b>	<b>41630,308</b>	<b>42130,286</b>	<b>42380,275</b>		

\*The data in Table 7 is form of  $(x, z)$ .

\*\*  $x$ , the horizontal position of certain point in longitudinal direction

\*\*\* $z$ , the vertical distance from certain point to the top-surface of deck

\*\*\*\*The tendons of which the coordinates in bold is not shown in Figure 7.

Table 7: Coordinates of Tendons in New Decks.

According to Table 6, Table 7 and Figure 7, the horizontal length  $L_i$  and the vertical height  $f_i$  of tendon curve  $i$  can be determined. Substitute the horizontal length  $L_i$  and the vertical height  $f_i$  into Expression 1 to evaluate the radius  $R_i$  of tendon curve  $i$ . Then, substitute the horizontal length  $L_i$  and the radius  $R_i$  into Expression 2 to evaluate the total angular rotation of tendon. The results are summarized in .

$$R_i = \frac{L_i^2}{8 \cdot f_i} \quad (1)$$

\*For Tendon Curve 3,  $L_i$  in Expression 1 has to be replaced by  $L_i/2$ .

$$\theta = \sum \frac{L_i}{R_i} \quad (2)$$

\*Since the prestressing is applied from two sides of tendon, to evaluate the angular rotation for prestress loss, Expression 2 has to be replaced by  $\theta = \frac{1}{2} \sum L_i/R_i$

tendon length	$L_1$	9.2	m
	$L_2$	11.3	m
	$L_3$	1.5	m
	$L_4$	11.3	m
	$L_5$	9.2	m
total length	$L$	42.4	m
deflection	$f_1$	0.3	m
	$f_2$	0.4	m
	$f_3$	0.0	m
	$f_4$	0.4	m
	$f_5$	0.3	m
radius	$R_1$	132.4	m
	$R_2$	168.6	m
	$R_3$	9.6	m
	$R_4$	167.7	m
	$R_5$	131.6	m
angular rotation	$\theta$	0.4	

Table 8: Data of Tendons in Old Decks.

tendon length	$L_1$	8.17	m
	$L_2$	11.44	m
	$L_3$	1.16	m
	$L_4$	11.44	m
	$L_5$	8.17	m
total length	$L$	42.38	m
deflection	$f_1$	0.13	m
	$f_2$	0.40	m
	$f_3$	0.02	m
	$f_4$	0.40	m
	$f_5$	0.13	m
radius	$R_1$	192.00	m
	$R_2$	192.00	m
	$R_3$	10.00	m
	$R_4$	192.00	m
	$R_5$	192.00	m
angular rotation	$\theta$	0.32	

Table 9: Data of Tendons in New Decks.

## 7 Models

### 7.1 General

As shown in Section 4.2, realistic dimensions of the widened deck KW03.01 is variable. For simplicity, the model with realistic dimensions is referred to as realistic model. It is expected that, suppose simplified models with mean thickness and width are used, the calculations carried out with simplified models would be much easier than those carried out with realistic models.

As shown in Chapter 1, the aim of this thesis is to provide a simple approach to check the prestress consumption calculated during the structure design of widened deck KW03.01. As shown in Section 4.4, the simple approach is to check the mean prestress consumption which is calculated basing on the mean imposed deformation and the mean dimensions. However, according to the expressions in Appendix A6, the magnitude of imposed deformation is related to the dimensions of models. Therefore, before simplified models being used, it has to be proved that using simplified models has no impact on the magnitude of mean imposed deformation. Otherwise, simplified models are not usable. As a result, investigation is carried out to check whether it is possible or not to use simplified models.

During the investigation, calculations with mean thickness and mean width are carried out respectively to prove that the mean thickness and the mean width can be applied. Suppose the mean imposed deformation calculated by mean thickness and mean width is close to that calculated by realistic dimensions, simplified models would be used instead of realistic models for the convenience of calculation.

According to Section 6.1, imposed deformation is produced when connections get stiff enough. As a result, according to Table 1 and Table 2, the magnitude of imposed deformation in widened deck KW03.01 is the increment of free deformation from time  $t = 11$  years + 29 days to time  $t = 111$  years. As shown in Section 4.2, old decks and new decks only suffer the shortening due to drying, hydration and creep, while connections suffer the shortening due to cooling, drying and hydration. Therefore, the source of imposed deformation in old decks and new deck are shrinkage and creep, while those in connections are shrinkage and thermal deformation.

### 7.2 Reason of Using Three-layer Models

As shown in Section 4.2, impact of cracking has to be taken into account during the simple approach. According to engineering experience and the results calculated by SCIA, see Appendix A2, connections between old decks and new decks are expected to be in tension. Since the tensile strength of concrete is relatively small, connections would be cracked due to tension.

As shown in Appendix A16, cracking decreases the stiffness of connection. As shown in Appendix A19, when the stiffness of connection decreases to 40% or less, there would be a large impact on the stress resulting from imposed deformation. As a result, to take the impact of cracking into account, models with three layers are used, where the layers represent old decks, connection and new decks respectively.

### 7.3 Mean Thickness

#### 7.3.1 Sketch of Models

In terms of mean thickness, the models of the south part of the widened deck KW03.01 are used. One is Realistic Model 1. In Realistic Model 1, the cushion at the ends of the deck is neglected. As a result, the thickness of the deck  $h$  in realistic model varies from 550 mm at the ends to 850 mm at the mid-support. The sketch of Realistic Model 1 is shown in Figure 8. The other is Simplified Model 1. In Simplified Model 1, instead of using variable thickness, a mean thickness of the deck  $h = 700$  mm is applied. The sketch of Simplified Model 1 is shown in Figure 9.

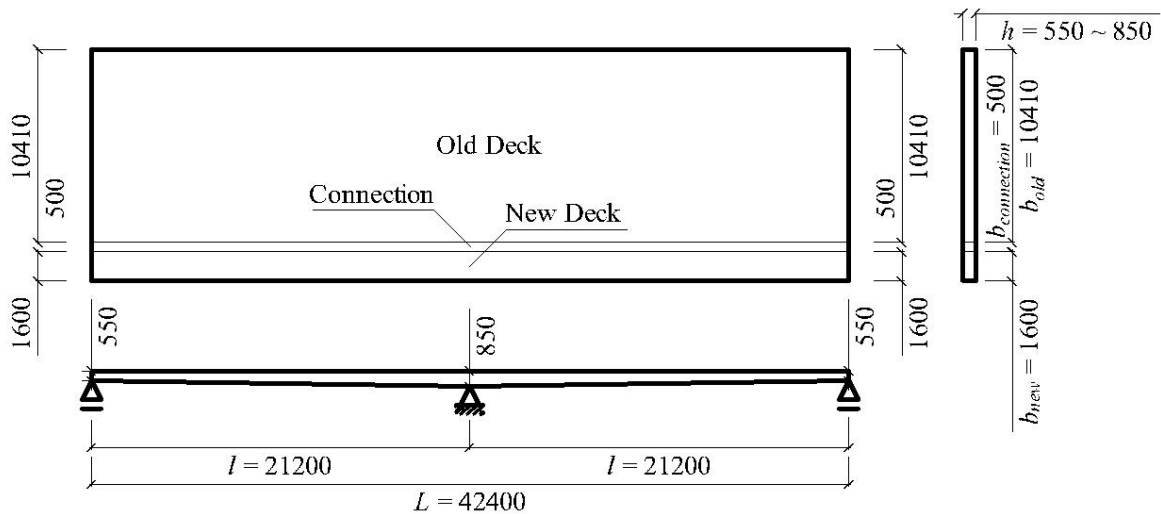


Figure 8: Sketch of Realistic Model 1 (Decks in South).

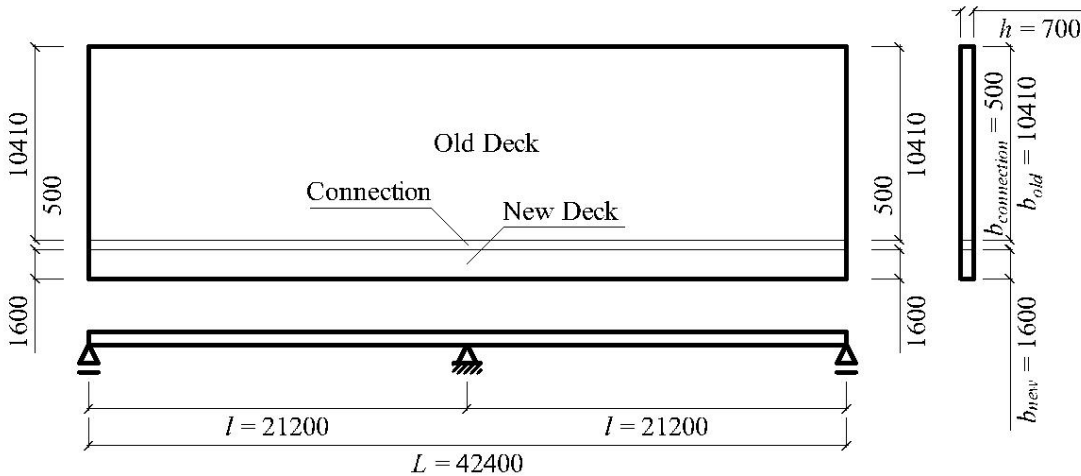


Figure 9: Sketch of Simplified Model 1 (Decks in South).

### 7.3.2 Imposed Deformation Calculated by Realistic Model 1 and Simplified Model 1

The distributions of imposed deformation along the deck are calculated by both Realistic Model 1 and Simplified Model 1. The imposed deformation of Simplified Model 1 is calculated basing on the data shown in Appendix A9.3.3, Appendix A9.3.6 and Appendix A11.2. The imposed deformation of Realistic Model 1 is calculated in a similar way as that of Simplified Model 1, where the difference is that the dimensions of Realistic Model 1 are not constant but expressed into a function of  $x$ , see Appendix A8.

As a result, the imposed deformation in Realistic Model 1 is a function of  $x$  as well. For simplicity, here only summarized the results of the calculation.

#### 7.3.2.1 In-plane Imposed Deformation in Old Deck

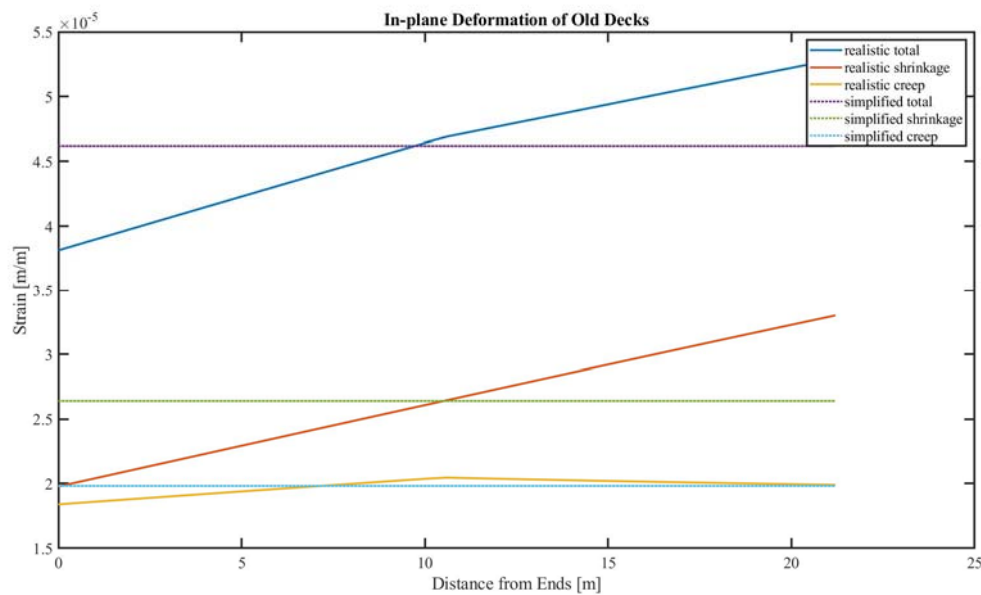


Figure 10: In-plane Imposed Deformation in Realistic Model 1 and Simplified Model 1 (Old Deck).

In Figure 10, the bold lines represent the distribution of imposed deformation Realistic Model 1 while the dashed lines represent the distribution of imposed deformation Simplified Model 1. The shrinkage shown in Figure 10 is the summation of drying shrinkage and autogenous shrinkage.

As shown in Figure 10, in terms of the creep in realistic model, point  $x = 10.6$  m is the turning point of the diagram of creep. This is caused by the coefficient  $\beta_H$ . According to Expression 37, the relation between creep and the coefficient  $\beta_H$  is as follow:

$$\varphi(t, t_0) = \varphi_0 \cdot \beta_c(t, t_0) \quad (3)$$

where:

$\varphi_0$  is the notional creep coefficient

$$= \varphi_{RH} \cdot \beta(f_{cm}) \cdot \beta(t_0)$$

$\varphi_{RH}$  is the coefficient related to the effect of relative humidity on the notional creep coefficient

$$= 1 + \frac{1-RH/100}{0.1 \cdot \sqrt[3]{h_0}} \quad (f_{cm} \leq 35 \text{ Mpa})$$

$$= \left[ 1 + \frac{1-RH/100}{0.1 \cdot \sqrt[3]{h_0}} \cdot \alpha_1 \right] \cdot \alpha_2 \quad (f_{cm} > 35 \text{ Mpa})$$

$h_0$  is the notional size

$$= 2A_c(x)/u(x)$$

$\beta_c(t, t_0)$  is the coefficient related to the development of creep after loading

$$\beta_H = [(t - t_0) / (\beta_H + t - t_0)]^{0.3}$$

$\beta_H$  is the coefficient related to relative humidity and notional size

$$= 1.5[1 + (0.012RH)^{18}]h_0 + 250 \cdot \alpha_3 \leq 1500 \cdot \alpha_3 \quad (f_{cm} > 35 \text{ Mpa})$$

As shown in Figure 11, in the old deck, the value of coefficient  $\beta_H$  reaches the upper limit  $1500 \cdot \alpha_3$  at point  $x = 10.6$  m. The value of coefficient  $\beta_H$  is variable for points  $x < 10.6$  m, while it is a constant for points  $x \geq 10.6$  m. So, in the old deck, the slope of the diagram of creep changes significantly at point  $x = 10.6$  m. However, in the new deck, the values of coefficient  $\beta_H$  are always smaller than upper limit  $1500 \cdot \alpha_3$ . As a result, in the new deck, there is no turning point in the diagram of creep, see Figure 24.

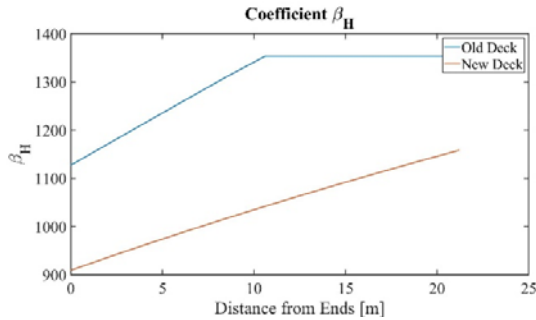


Figure 11: Coefficient  $\beta_H$  in Old and New Deck.

In addition to the turning point, from point  $x = 0$  m to point  $x = 21.2$  m, the creep in old deck increases when  $x < 10.6$  m while decreases when  $x \geq 10.6$  m. This is caused by the coefficient  $\varphi_0$  and coefficient  $\beta_c(t, t_0)$ . The relation between creep and the coefficients is shown in Expression 3.

The in-plane imposed deformation  $\Delta\varepsilon_{cc}$  from creep is the increment of free creep from time  $t = t_{IV}$  to time  $t = t_V$ .

$$\Delta\varepsilon_{cc} = \varepsilon_{cc}(t_V) - \varepsilon_{cc}(t_{IV}) = \varphi_0 \cdot [\beta_c(t_V, t_0) - \beta_c(t_{IV}, t_0)] \cdot \varepsilon_{el}$$

On one hand, coefficient  $\varphi_0$  is calculated by on  $\varphi_{RH}$  which is a function of notional size  $h_0$ . Since the notional size  $h_0$  is a function of  $x$ , the coefficient  $\varphi_0$  is not a constant but decreases from point  $x = 0$  m to point  $x = 21.2$  m, see Figure 12. On the other hand, coefficient  $\beta_c(t, t_0)$  is calculated by duration  $t - t_0$  and coefficient  $\beta_H$ . Due to the impact of both duration  $t - t_0$  and coefficient  $\beta_H$ , the value of  $\beta_c(t_V, t_0) - \beta_c(t_{IV}, t_0)$  is variable from point  $x = 0$  m to point  $x = 21.2$  m, which increases when  $x < 10.6$  m while is constant when  $x \geq 10.6$  m, see Figure 14 and Figure 15.

So, when  $x < 10.6$  m, the speed of the increment of  $\beta_c(t_V, t_0) - \beta_c(t_{IV}, t_0)$  is faster than that of the decrement of coefficient  $\varphi_0$ , resulting a rising of  $\Delta\varepsilon_{cc}$ . However, when  $x \geq 10.6$  m,  $\beta_c(t_V, t_0) - \beta_c(t_{IV}, t_0)$  becomes a constant, resulting a drop of  $\Delta\varepsilon_{cc}$ .

In the new deck, from point  $x = 0$  m to point  $x = 21.2$  m, coefficient  $\varphi_0$  keeps dropping while  $\beta_c(t_V, t_0) - \beta_c(t_{IV}, t_0)$  keeps rising, see Figure 13 and Figure 17. The speed of the increment of  $\beta_c(t_V, t_0) - \beta_c(t_{IV}, t_0)$  is slower than that of the decrement of coefficient  $\varphi_0$ . As a result, in the new deck,  $\Delta\varepsilon_{cc}$  keeps dropping from point  $x = 0$  m to point  $x = 21.2$  m, see Figure 24.

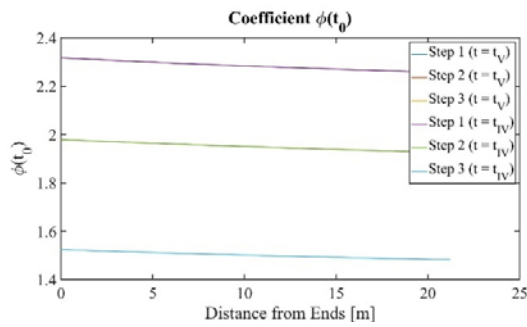


Figure 12: Coefficient  $\phi_0$  in Old Deck.

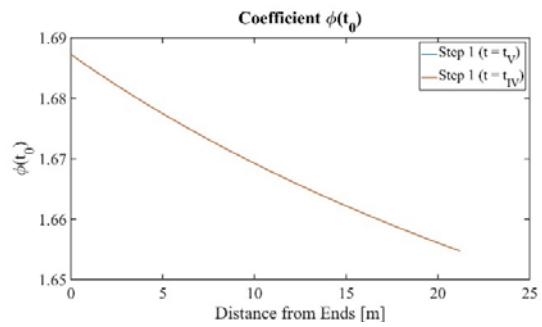


Figure 13: Coefficient  $\phi_0$  in New Deck.

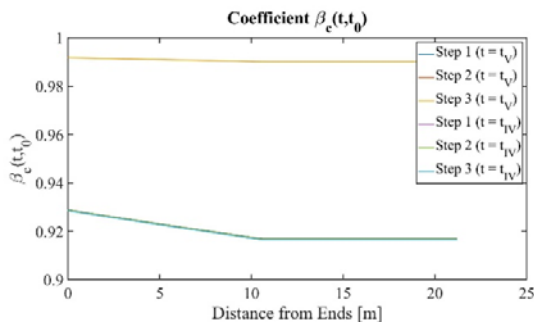


Figure 14: Coefficient  $\beta_c(t, t_0)$  in Old Deck.

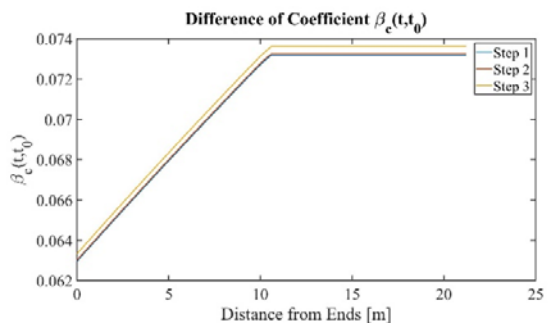


Figure 15: Difference of Coefficient  $\beta_c(t, t_0)$  in Old Deck from Time  $t = t_{IV}$  to Time  $t = t_V$ .

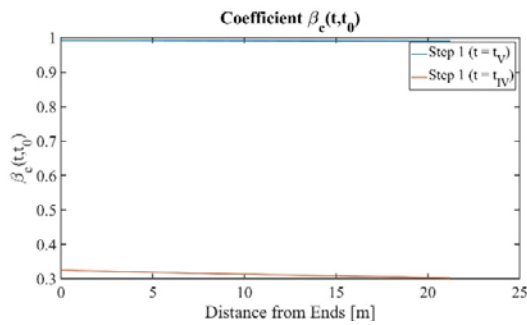


Figure 16: Coefficient  $\beta_c(t, t_0)$  in New Deck.

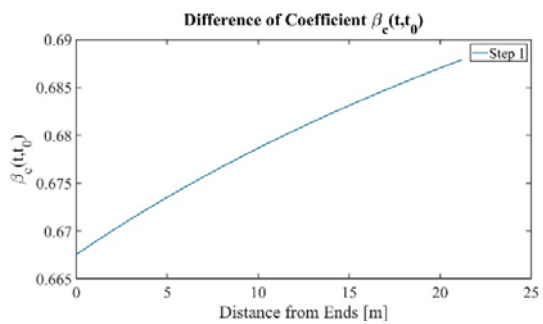


Figure 17: Difference of Coefficient  $\beta_c(t, t_0)$  in New Deck from Time  $t = t_{IV}$  to Time  $t = t_V$ .

### 7.3.2.2 In-plane Imposed Deformation in Connection

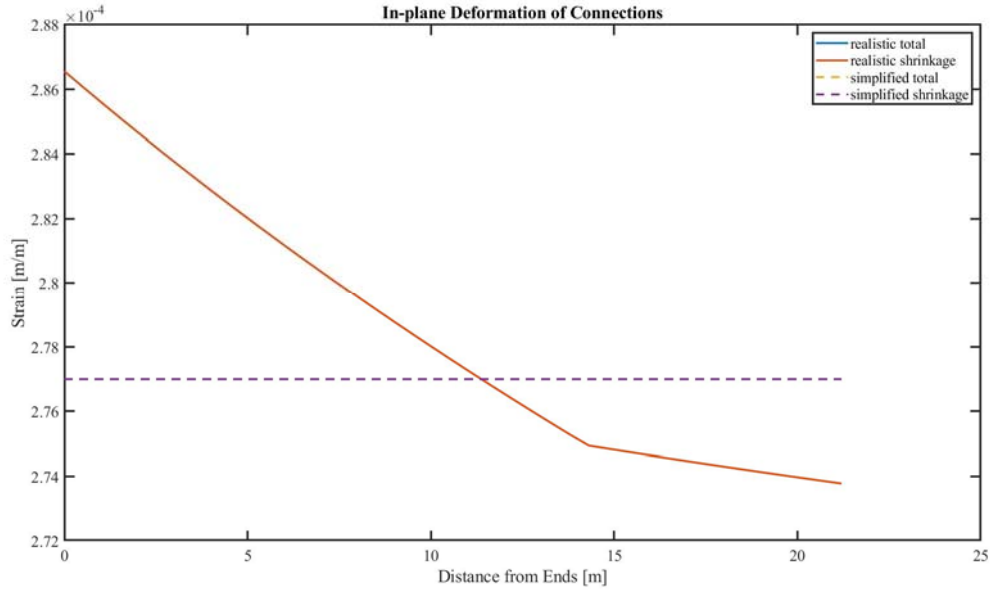


Figure 18: In-plane Imposed Deformation in Realistic Model 1 and Simplified Model 1 (Connection).

In Figure 18, the bold lines represent the distribution of imposed deformation Realistic Model 1 while the dashed lines represent the distribution of imposed deformation Simplified Model 1. The shrinkage shown in Figure 18 is the summation of drying shrinkage and autogenous shrinkage. Since the imposed deformation due to thermal contraction is constant, see Appendix A3, it has no impact on proving the usability of simplified models and, therefore, is not taken into account in Figure 18.

As shown in Figure 18, in terms of the shrinkage in realistic model, point  $x = 14.3$  m is the turning point of the diagram of total shrinkage. This is caused by the coefficient  $k_h$ . According to Expression 36, considering that there is not prestressing in connection, the relationship between total shrinkage at time  $t$  and the coefficient  $k_h$  is as follow:

$$\varepsilon_{cs} = \varepsilon_{cd}(t) + \varepsilon_{ca}(t) \quad (4)$$

where:

- $\varepsilon_{cd}(t)$  is the drying shrinkage  
 $= \beta_{ds}(t, t_s) \cdot k_h \cdot \varepsilon_{cd,0}$
- $k_h$  is the coefficient depending on the notional size  $h_0$ , see Figure 26
- $\beta_{ds}(t, t_s)$  is the coefficient related to drying shrinkage  
 $= (t - t_s) / (t - t_s + 0.04 \sqrt{h_0^3})$
- $\varepsilon_{cd,0}$  is the basic drying shrinkage

The in-plane imposed deformation  $\Delta\varepsilon_{cs}$  from shrinkage is the increment of free shrinkage from time  $t = t_{IV}$  to time  $t = t_V$ . As shown in Figure 19, at time  $t = t_{IV}$  and time  $t = t_V$ , the drying shrinkage is variable in the longitudinal direction of the half deck while the autogenous one is constant. As a result, the variance of in-plane deformation  $\Delta\varepsilon_{cs}$  from shrinkage in the longitudinal direction of the half deck is only from the drying shrinkage  $\Delta\varepsilon_{cd}$ .

$$\Delta\varepsilon_{cd} = \varepsilon_{cd}(t_V) - \varepsilon_{cd}(t_{IV}) = [\beta_{ds}(t_V, t_s) - \beta_{ds}(t_{IV}, t_s)] \cdot k_h \cdot \varepsilon_{cd,0}$$

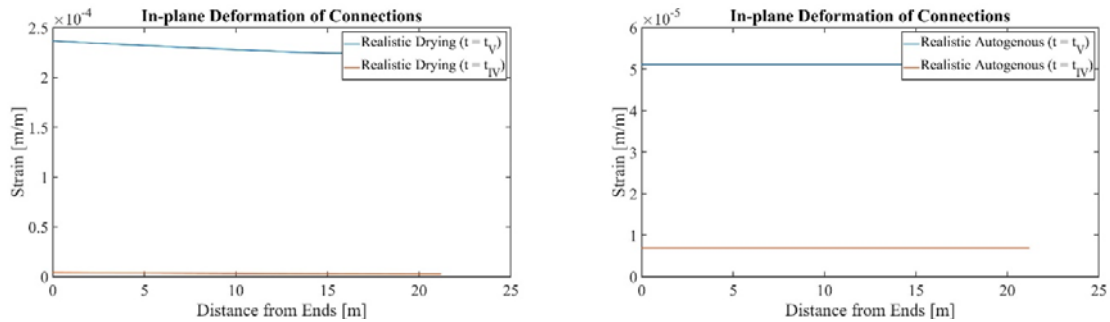


Figure 19: Drying Shrinkage and Autogenous Shrinkage in Connection at Time  $t = t_{IV}$  and Time  $t = t_V$ .

It is shown in Figure 20 that there is no turning point in the diagram of coefficient  $\beta_{ds}(t, t_s)$  at time  $t = t_{IV}$  and time  $t = t_V$ . However, as shown in Figure 21, turning point occurs at point  $x = 14.3$  m in the diagram of coefficient  $k_h$ . As shown in Figure 23, the notional size  $h_0$  in connection varies from 262 mm to 314 mm. Substitute the notional size  $h_0$  into Figure 22, turning point appears when  $h_0 = 300$  mm. Substitute  $h_0 = 300$  mm into Figure 23, it is corresponding to point  $x = 14.3$  m. So, a turning point appears in the diagram of coefficient  $k_h$  and, therefore, appears in the diagram of total shrinkage.

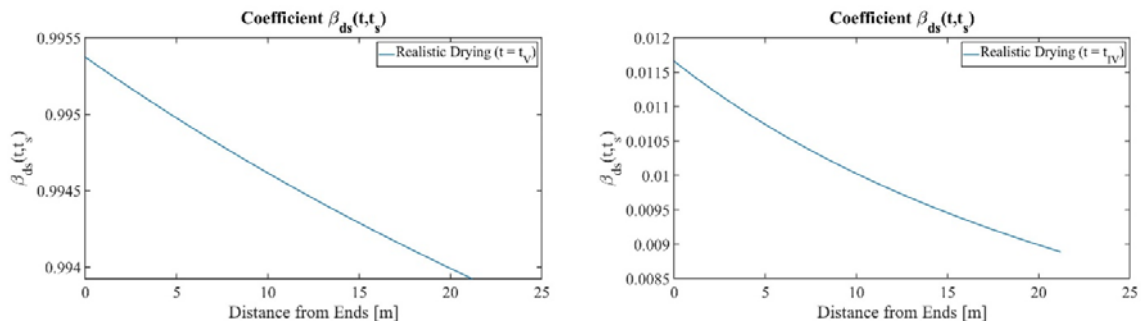


Figure 20: Coefficient  $\beta_{ds}(t, t_s)$  in Connection at Time  $t = t_{IV}$  and Time  $t = t_V$ .

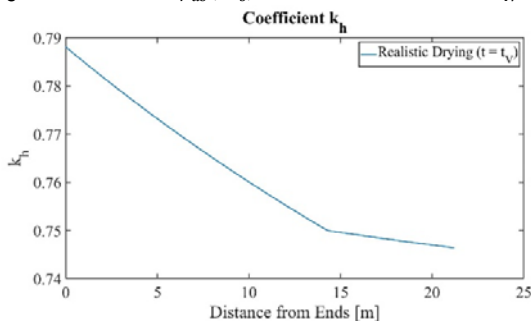


Figure 21: Coefficient  $k_h$  in Connection.

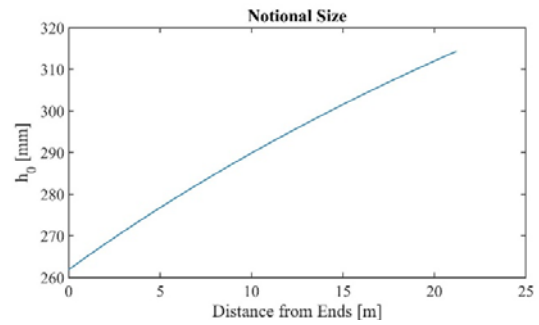
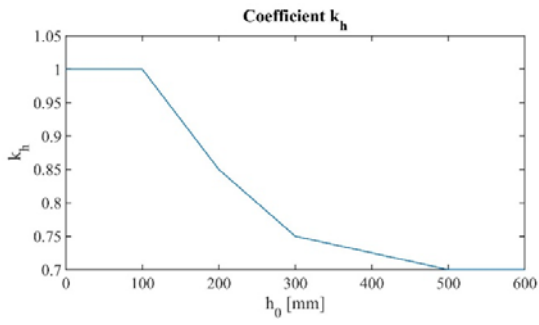


Figure 22: Relation between Coefficient  $k_h$  and Notional Size  $h_0$ . Figure 23: Notional Size  $h_0$  in Connection.

### 7.3.2.3 In-plane Imposed Deformation in New Deck

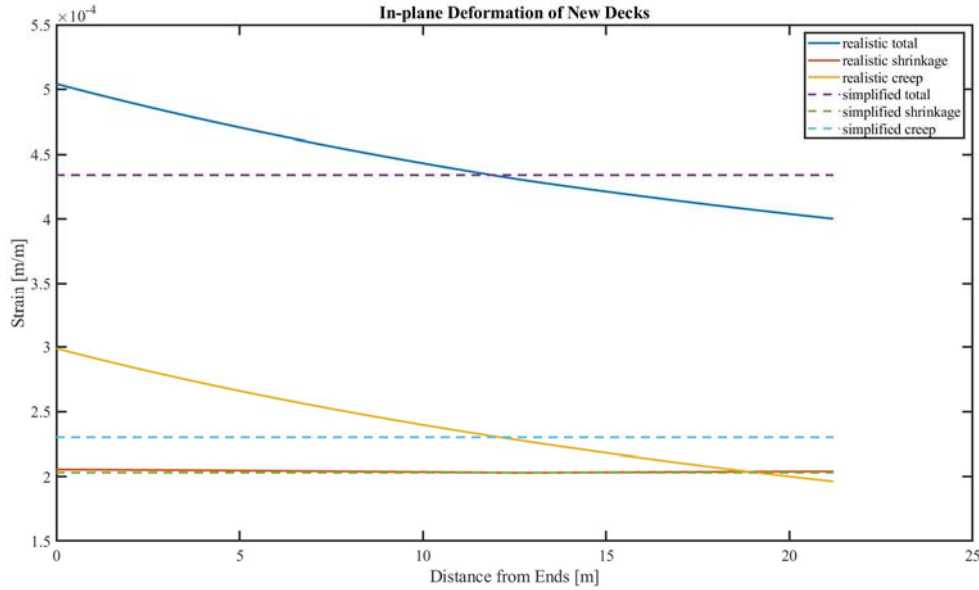


Figure 24: In-plane Imposed Deformation in Realistic Model 1 and Simplified Model 1 (New Deck).

As shown in Figure 10, Figure 18 and Figure 24, a larger height of cross-section results in a larger in-plane imposed deformation from shrinkage in old deck, which is opposite to the situations in connection and old deck. This is caused by the coefficient  $k_h$ . According to Expression 36, the relationship between drying shrinkage and the coefficient  $k_h$  is as follow:

$$\varepsilon_{cs} = \varepsilon_{cd}(t) + \varepsilon_{ca}(t) \quad (5)$$

where:

- $\varepsilon_{cd}(t)$  is the drying shrinkage  
 $= [\beta_{ds}(t, t_s) - \beta_{ds}(t_p, t_s)] \cdot k_h \cdot \varepsilon_{cd,0}$
- $k_h$  is the coefficient depending on the notional size  $h_0$ , see Figure 26
- $\beta_{ds}(t, t_s)$  is the coefficient related to drying shrinkage  
 $= (t - t_s) / (t - t_s + 0.04 \sqrt{h_0^3})$
- $\beta_{ds}(t_p, t_s)$  is the coefficient related to drying shrinkage  
 $= (t_p - t_s) / (t_p - t_s + 0.04 \sqrt{h_0^3})$
- $\varepsilon_{cd,0}$  is the basic drying shrinkage

The in-plane imposed deformation  $\Delta\varepsilon_s$  from shrinkage is the increment of free shrinkage from time  $t = t_{IV}$  to time  $t = t_V$ . As shown in Figure 19, at time  $t = t_{IV}$  and time  $t = t_V$ , the drying shrinkage is variable in the longitudinal direction of the half deck while the autogenous one is constant. As a result, the variance of in-plane deformation  $\Delta\varepsilon_{cs}$  in the longitudinal direction of the half deck is only from the drying shrinkage  $\Delta\varepsilon_{cd}$ .

$$\Delta\varepsilon_{cd} = \varepsilon_{cd}(t_V) - \varepsilon_{cd}(t_{IV}) = [\beta_{ds}(t_V, t_s) - \beta_{ds}(t_{IV}, t_s)] \cdot k_h \cdot \varepsilon_{cd,0}$$

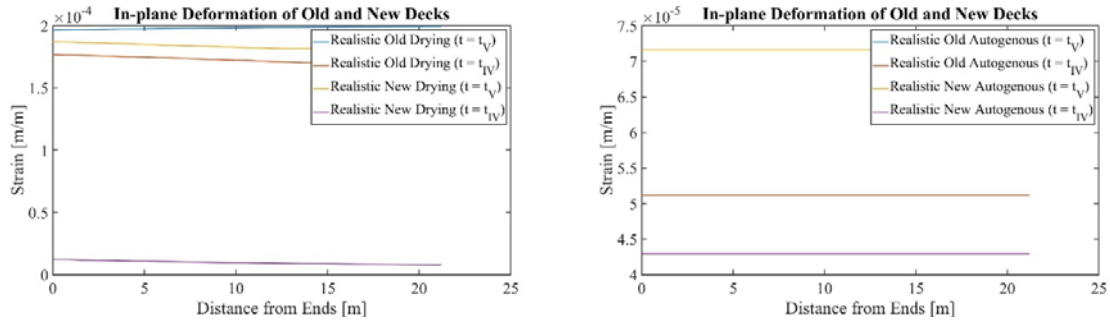


Figure 25: Drying Shrinkage and Autogenous Shrinkage in Old and New Deck at Time  $t = t_{IV}$  and Time  $t = t_V$ .

The coefficient  $\beta_{ds}(t_V, t_s)$  and  $\beta_{ds}(t_{IV}, t_s)$  in old deck are shown in Figure 28, while those in connection and new deck are shown in Figure 29. In these figures, a larger height of cross-section results in a larger the difference between coefficient  $\beta_{ds}(t_V, t_s)$  and  $\beta_{ds}(t_{IV}, t_s)$ .

As shown in Figure 27, the notional size  $h_0$  of the old deck is always larger than 500 mm. Substitute the notional size  $h_0$  into Figure 26, the coefficient  $k_h$  in old deck is a constant. So, the magnitude of the in-plane imposed deformation  $\Delta\epsilon_s$  from shrinkage is dominated by the difference between coefficient  $\beta_{ds}(t_V, t_s)$  and  $\beta_{ds}(t_{IV}, t_s)$ , and, therefore, a larger height of cross-section results in a larger in-plane imposed deformation from shrinkage in old deck.

However, when it comes to the connection and new deck, the notional size  $h_0$  is between 100 mm and 500 mm. Substitute the notional size  $h_0$  into Figure 26, a larger  $h_0$  results in a smaller coefficient  $k_h$  in connection and new deck which dominates the magnitude of the in-plane imposed deformation  $\Delta\epsilon_s$  from shrinkage, and, therefore, a larger height of cross-section results in a smaller in-plane imposed deformation from shrinkage in old deck.

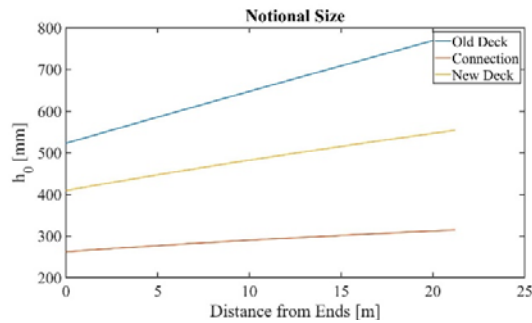
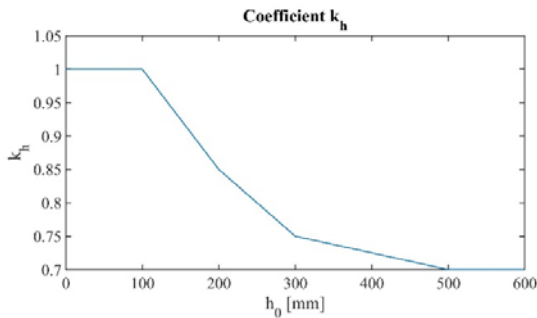


Figure 26: Relation between Coefficient  $k_h$  and Notional Size  $h_0$ . Figure 27: Notional Size  $h_0$ .

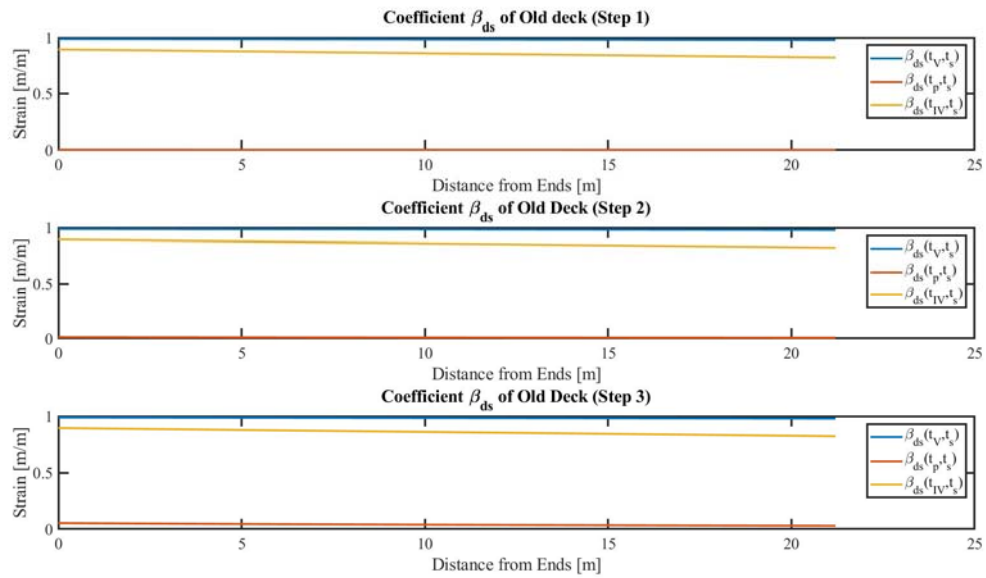


Figure 28: Coefficient  $\beta_{ds}$  in Old Deck.

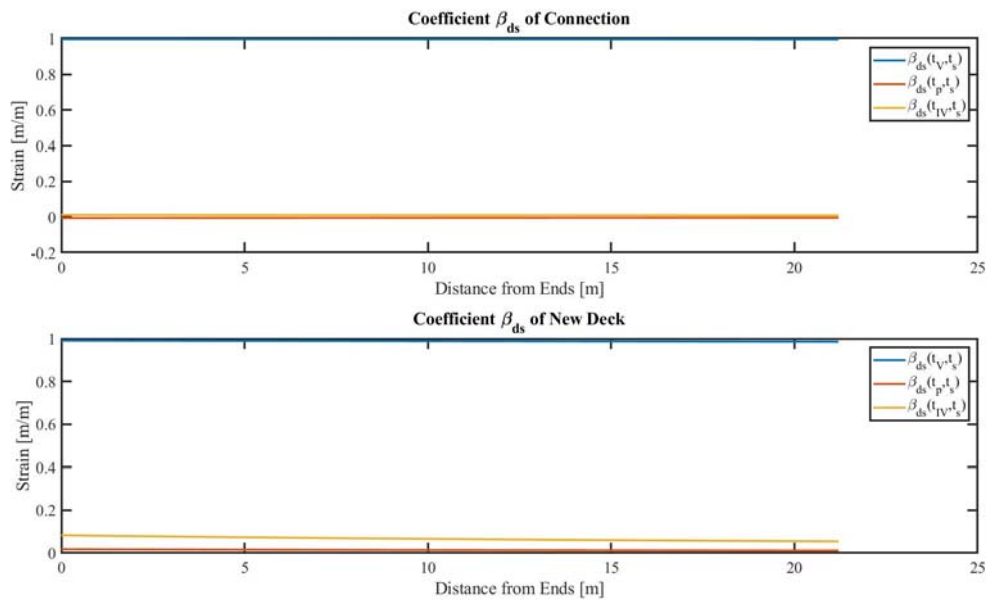


Figure 29: Coefficient  $\beta_{ds}$  in Connection and New Deck.

### 7.3.3 Data of Mean Imposed Deformation

The mean imposed deformation calculated by both Realistic Model 1 and Simplified Model 1 are shown in Table 10. According to Table 10, the mean imposed deformation of Realistic Model 1 is close to those of Simplified Model 1. As a result, simplified models with mean thickness can be used in the following calculation.

Name of Data		Simplified Model		Realistic Model	
Old Decks					
imposed deformation	$\Delta\varepsilon$	4.64E-05	m/m	4.62E-05	m/m
shrinkage strain	$\Delta\varepsilon_{cs}(t)$	2.65E-05	m/m	2.64E-05	m/m
creep strain	$\Delta\varepsilon_{cc}(t)$	1.99E-05	m/m	1.98E-05	m/m
Connection					
imposed deformation	$\Delta\varepsilon$	3.89E-04	m/m	3.91E-04	m/m
shrinkage strain	$\Delta\varepsilon_{cs}(t)$	2.77E-04	m/m	2.79E-04	m/m
thermal strain	$\Delta\varepsilon_{thermal}$	1.12E-04	m/m	1.12E-04	m/m
New Decks					
imposed deformation	$\Delta\varepsilon$	4.37E-04	m/m	4.39E-04	m/m
shrinkage strain	$\Delta\varepsilon_{cs}(t)$	2.03E-04	m/m	2.04E-04	m/m
creep strain	$\Delta\varepsilon_{cc}(t)$	2.34E-04	m/m	2.35E-04	m/m

Table 10: Summary of Mean Imposed Deformation Calculated in Section 7.3.

## 7.4 Mean Width

### 7.4.1 Sketch of Models

In terms of mean width, the models of the north part of the widened deck KW03.01 are used. One is Realistic Model 2. In Realistic Model 2, the width of the deck  $b$  in realistic model varies from 7900 mm at one end to 11800 mm at the other end. The sketch of Realistic Model 2 is shown in Figure 30. The other is Simplified Model 2. In Simplified Model 2, instead of using variable thickness, a mean width of the deck  $b = 9850$  mm is applied. The sketch of Simplified Model 2 is shown in Figure 31. It is proved in Section 7.3 that the mean thickness can be applied. So, in Realistic Model 2 and Simplified Model 2, the mean thickness is applied.

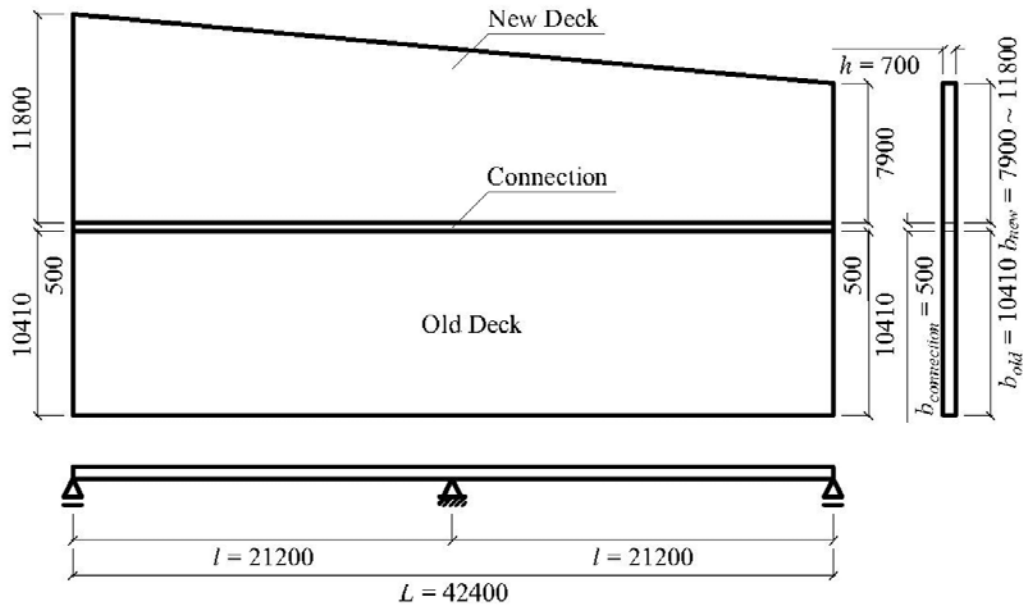


Figure 30: Sketch of Realistic Model 2 (Decks in North).

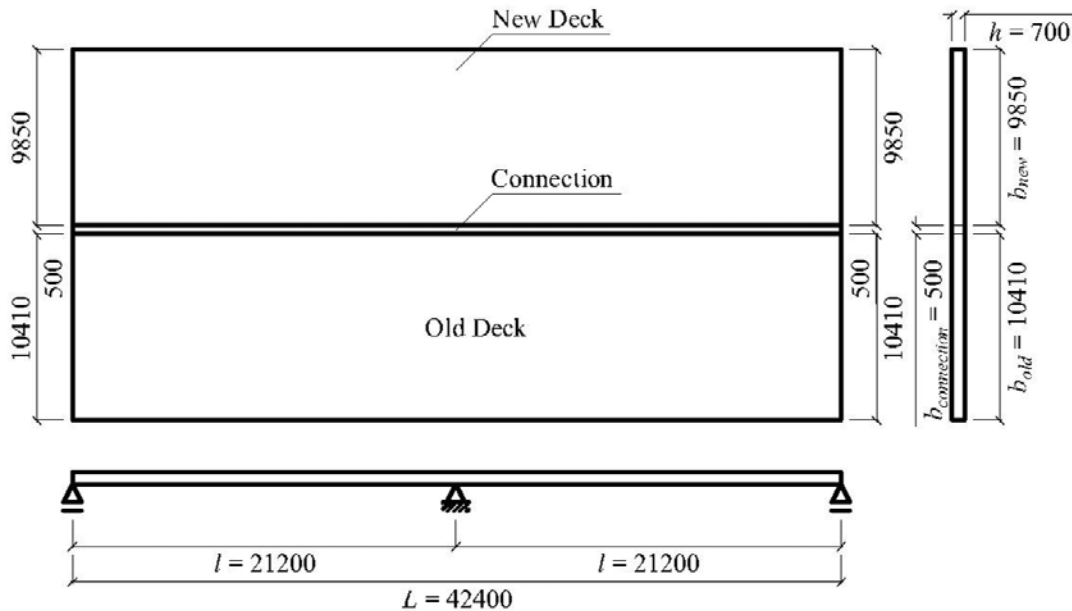


Figure 31: Sketch of Simplified Model 2 (Decks in North).

### 7.4.2 Imposed Deformation Calculated by Realistic Model 2 and Simplified Model 2

The distributions of imposed deformation along the deck are calculated by both Realistic Model 2 and Simplified Model 2. The imposed deformation of Simplified Model 2 is calculated basing on the data shown in Appendix A9.3.3, Appendix A9.3.6 and Appendix A11.3. The imposed deformation of Realistic Model 2 is calculated in a similar way as that of Simplified Model 2, where the difference is that the dimensions of Realistic Model 2 are not constant but expressed into a function of  $x$ , see Appendix A8.

As a result, the imposed deformation in Realistic Model 1 is a function of  $x$  as well. For simplicity, here only summarized the results of the calculation.

### 7.4.2.1 In-plane Imposed Deformation in Old Deck

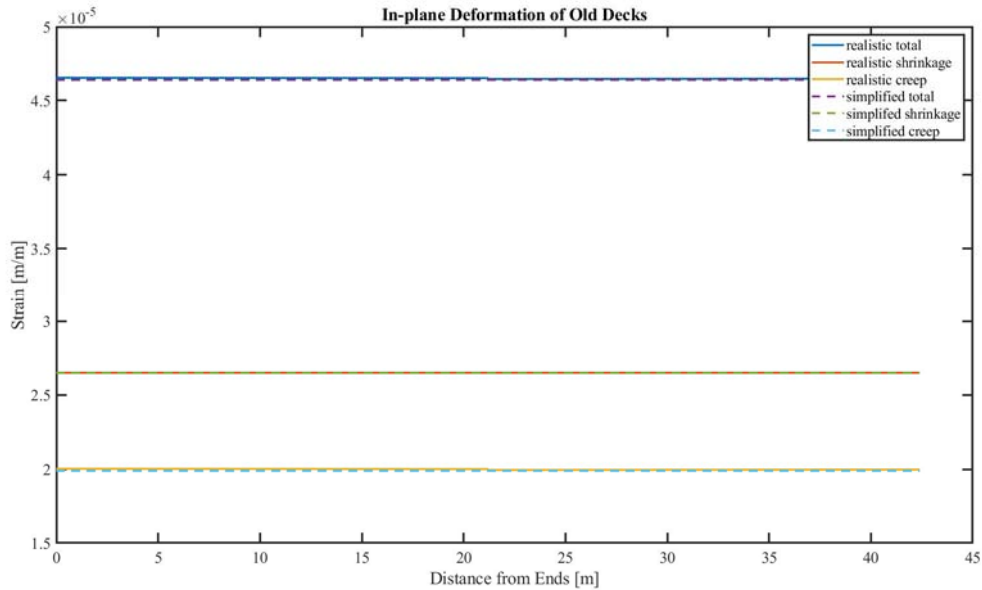


Figure 32: In-plane Imposed Deformation in Realistic Model 2 (Old Deck).

### 7.4.2.2 In-plane Imposed Deformation in Connection

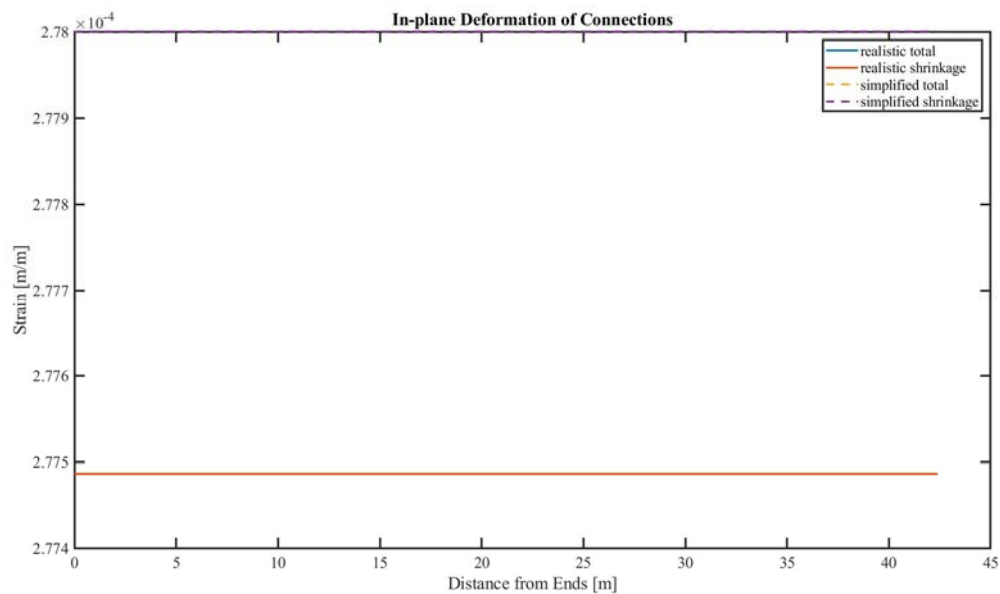


Figure 33: In-plane Imposed Deformation in Realistic Model 2 (Connection).

Since the imposed deformation due to thermal contraction is constant, see Appendix A3, it has no impact on proving the usability of simplified models and, therefore, is not taken into account in Figure 89.

### 7.4.2.3 In-plane Imposed Deformation in New Deck

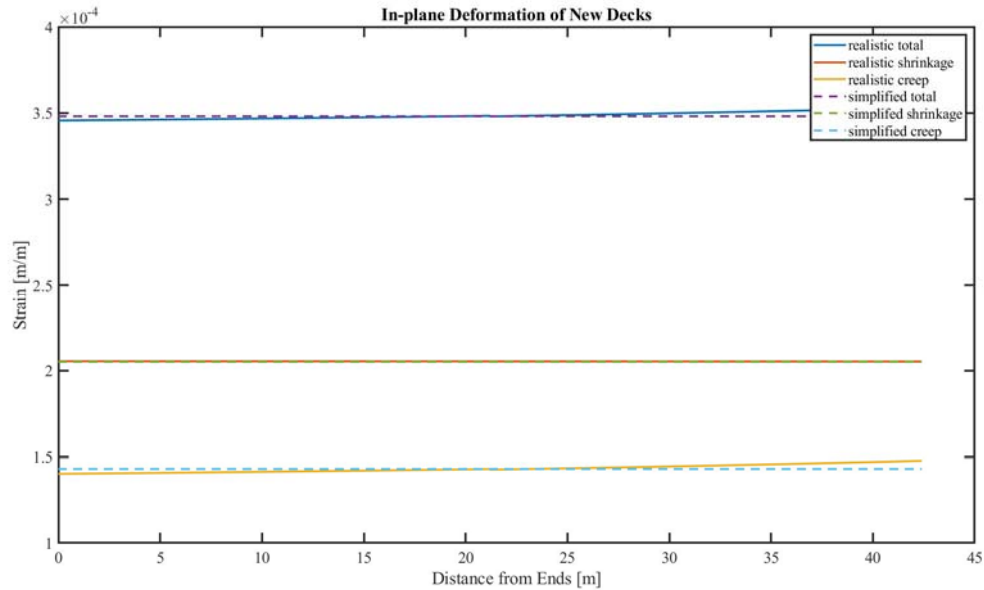


Figure 34: In-plane Imposed Deformation in Realistic Model 2 (New Deck).

### 7.4.3 Data of Mean Imposed Deformation

The mean imposed deformation calculated by both Realistic Model 2 and Simplified Model 2 are shown in Table 11. According to Table 11, the mean imposed deformation of Realistic Model 2 is close to those of Simplified Model 2. As a result, simplified models with mean width can be used in the following calculation.

Name of Data		Simplified Model		Reallistic Model	
Old Decks					
imposed deformation	$\Delta \varepsilon$	4.64E-05	m/m	4.64E-05	m/m
shrinkage strain	$\Delta \varepsilon_{cs}(t)$	2.65E-05	m/m	2.65E-05	m/m
creep strain	$\Delta \varepsilon_{cc}(t)$	1.99E-05	m/m	2.00E-05	m/m
Connection					
imposed deformation	$\Delta \varepsilon$	3.90E-04	m/m	3.90E-04	m/m
shrinkage strain	$\Delta \varepsilon_{cs}(t)$	2.77E-04	m/m	2.78E-04	m/m
thermal strain	$\Delta \varepsilon_{thermal}$	1.12E-04	m/m	1.12E-04	m/m
New Decks					
imposed deformation	$\Delta \varepsilon$	3.50E-04	m/m	3.47E-04	m/m
shrinkage strain	$\Delta \varepsilon_{cs}(t)$	2.05E-04	m/m	2.05E-04	m/m
creep strain	$\Delta \varepsilon_{cc}(t)$	1.45E-04	m/m	1.42E-04	m/m

Table 11: Summary of Mean Imposed Deformation Calculated in Section 7.4.

## 7.5 Conclusion

According to Section 7.3.3 and Section 7.4.3, the mean imposed deformation calculated basing on realistic models and simplified models are close. It means that, although the magnitude of imposed deformation is related to the dimension of structure, using mean dimensions has no impact on the mean imposed deformation.

So, Simplified Model 1 and Simplified Model 2, representing the south part and the north part of widened deck KW03.01, are used, see Figure 35 and Figure 36.

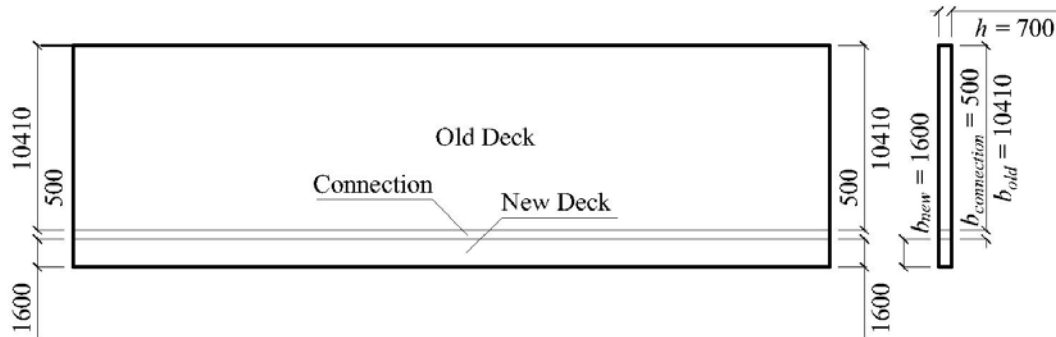


Figure 35: Sketch of Simplified Model 1 (Decks in South).

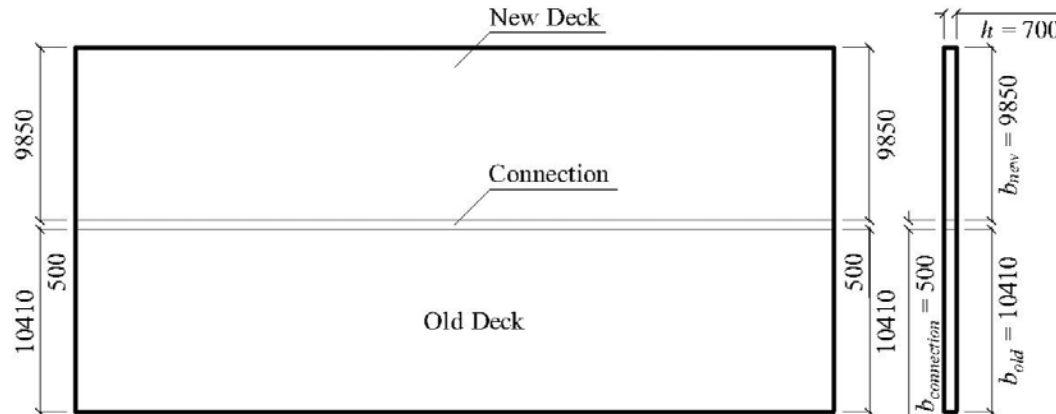


Figure 36: Sketch of Simplified Model 2 (Decks in North).

## 8 Mechanics for Structural Analysis

### 8.1 General

In addition to the models used in the simple approach, the mechanics used to calculate stress resulting from imposed deformation has to be determined as well. The mechanics used in the simple approach is a mechanics of composited cross-section with Bernoulli's rule.

At the beginning, the impact of shear deformation is not taken into account (Breugel, 2013, pp. 179 - 183). For simplicity, this mechanics without the impact of shear deformation is referred to as Mechanics 1. The introduction of Mechanics 1 is shown in Appendix A12. As shown in Appendix A12, equivalent loads of imposed deformation, normal force  $N$  and bending moment  $M$ , are applied to the cross-section of the composited cross-section to calculate the strain and stress resulting from imposed deformation. This causes problem when there are three or more layers, see Section 8.2 and Section 8.3.

To solve the problem, shear deformation has to be taken into account. Therefore, another mechanics basing on plate theory is studied (Blaauwendraad, 2006, pp. 13 - 25). For simplicity, this mechanics is referred to as Mechanics 2. The introduction of Mechanics 2 is shown in Appendix A13. As shown in Appendix A13, deformation of plate is simplified into nodal displacement which is the product of stiffness matrix and nodal forces. The stiffness matrix is the summation of normal stiffness matrix and shear stiffness matrix, where normal stiffness matrix is about normal deformation and shear stiffness matrix is about shear deformation.

### 8.2 Disadvantage of Mechanics 1

In a three-layer structure, suppose the stiffness of mid-layer is zero, it is expected that the deformation in the bottom-layer would not be transferred to the top-layer due to the extremely soft mid-layer. Therefore, the strain and stress resulting from imposed deformation in top-layer are zero. However, this is not the case according to Mechanics 1, see Figure 37 and Figure 38. Detailing information of the calculation is shown in Appendix A14.3. For the convenience of reading, here only summarized the results of the calculation.

Suppose there is imposed deformation applied to the bottom layer only, according to Mechanics 1, the equivalent bending moment is always non-zero. It means, according to Mechanics 1, the three-layer structure can be taken as a beam, where the top- and bottom-layer are the flanges while the mid-layer is the web. The stiffness of web has almost no impact on the bending resistance of the beam. Similarly, the stiffness of mid-layer has almost no impact on the stress in top- and bottom-layer.

As a result, according to Mechanics 1, the deformation in the bottom-layer is always transferred to the top-layer even if the mid-layer is 'soft'. It means, in terms of the widened deck KW03.01, Mechanics 1 would give unreliable results suppose the stiffness of connection decreases due to cracking. Therefore, to check whether the mid-layer of model used in the simple approach is 'soft' or not, an improved mechanics taking shear deformation into account is introduced. For simplicity, it is referred to as Mechanics 2.

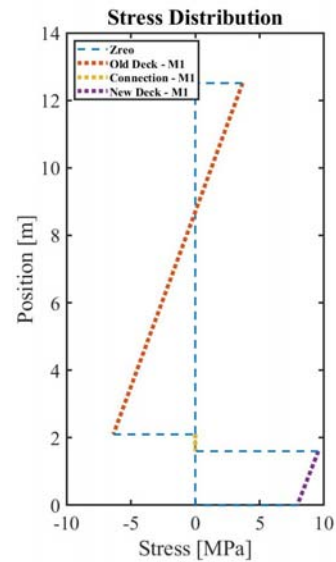
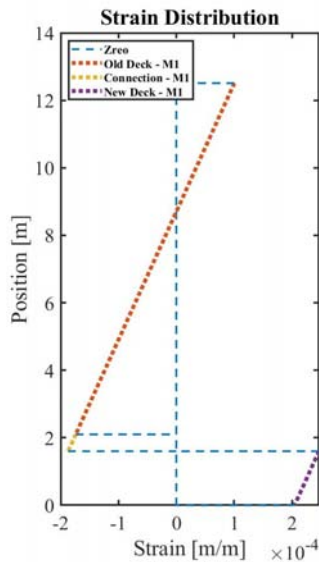


Figure 37: Strain Distribution Calculated by Mechanics 1 (M1).      Figure 38: Stress Distribution Calculated by Mechanics 1 (M1).

*\*It is expected that the strain and stress resulting from imposed deformation in top-layer are zero. However, the strain and stress calculated by Mechanics 1 (M1) are non-zero.*

### 8.3 Advantage of Mechanics 2

The reason of Mechanics 1 being unreliable is that it does not take shear deformation into account. As an improved alternative to Mechanics 1, an improved mechanics taking shear deformation into account is introduced. For simplicity, it is referred to as Mechanics 2. The detailing introduction of Mechanics 2 are shown in Appendix A13. For the convenience of reading, here provided the brief introduction to the difference between Mechanics 1 and Mechanics 2:

#### Mechanics 1:

In this mechanics, it is assumed that, when a composited cross-section is subjected to mechanical load and/or imposed deformation, the in-plane curvatures of the composited cross-section is uniform. It means the composited cross-section remains flat when it is deformed.

Equivalent loads of imposed deformation, normal force  $N$  and bending moment  $M$ , are applied to the cross-section of composited cross-section to calculate the strain and stress resulting from imposed deformation. The disadvantage of Mechanics 1 is that, with normal force  $N$  and bending moment  $M$  only, shear deformation is neglected.

#### Mechanics 2:

Mechanics 2 is basing on plate theory. According to Mechanics 2, deformation of plate is simplified into nodal displacement which is the product of stiffness matrix and nodal forces. When a composited structure subjected to imposed deformation is analyzed by Mechanics 2, the layers of the composited cross-section are spit which makes the layers free to deform. Then deformation compatibility is restored so that the deformed layers are able to be connected.

Since the stiffness matrix and nodal forces in the layers could be different, the in-plane curvature of each layer could be different. It means the composited cross-section will not remain flat when it deforms due to imposed deformation. The advantage of Mechanics 2 is that, with shear stiffness taken into account, the shear deformation is taken into account.

Calculation is carried out to the same three-layer structure mentioned in Section 8.2, see Figure 39 and Figure 40. Detailing information of the calculation is shown in Appendix A14.3. For the convenience of reading, here only summarized the results of the calculation. As a result, according to Mechanics 2, the deformation in the bottom-layer cannot be transferred to the top-layer if the elastic modulus applied to mid-layer is close to zero.

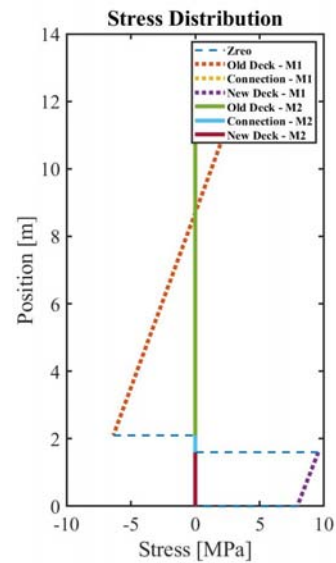
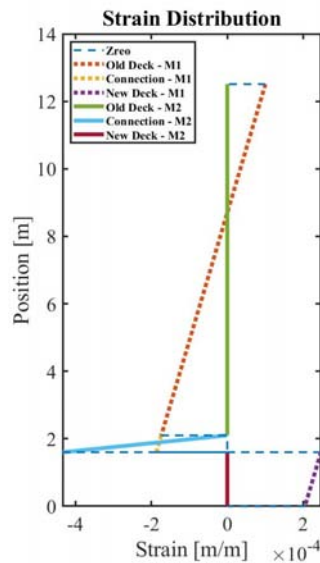


Figure 39: Strain Distribution Calculated by Mechanics 2 (M2).      Figure 40: Stress Distribution Calculated by Mechanics 2 (M2).

\*It is expected that the strain and stress resulting from imposed deformation in top-layer are zero. The strain and stress calculated by Mechanics 2 (M2) suit the expectation.

### 8.4 Conclusion

As for three-layer models, suppose the normal stiffness of mid-layer is relatively small, Mechanics 2 would be preferred which is able to give more reliable results than Mechanics 1. However, according to Appendix A19.4, in terms of widened deck KW03.01, There is no advantage of Mechanics 2 unless the elastic modulus of concrete in connections decrease to about 40% or less. According to Appendix A19.3, the elastic modulus of concrete in south and north decreases to 96% and 99% respectively due to cracking, which are much larger than 40%. Therefore, both Mechanics 1 and Mechanics 2 are capable to calculate the stress resulting from imposed deformation in widened deck KW03.01.

## 9 Calculation

### 9.1 General

With models and mechanics determined, see Chapter 7 and Chapter 8, the simple approach is carried out to calculate the stress resulting from imposed deformation and the compressive stress in concrete consumed by the stress resulting from imposed deformation. The final results of the simple approach are used to check the results of calculation carried out by SCIA.

In the simple approach, the calculation consists of two steps. In first step, calculation is carried out without cracking taken into account. The aim of the first step is to determine cracked area of widened deck KW03.01 when it is subjected to combined actions, where combined actions are the imposed deformation and prestressing forces. The cracked area is taken as the parts of widened deck KW03.01 where tensile stress resulting from combined actions exceeds the cracking strength of concrete. According to the calculation of first step, only connections are cracked, see Appendix A19.2. In second step, to take cracking into account, the normal stiffness of connections is re-evaluated by the expressions shown in Appendix A16 basing on the magnitudes of tensile deformation. Then, the stress resulting from imposed deformation and the compressive stress in concrete consumed by the stress resulting from imposed deformation are calculated as the final results of the simple approach.

The final results of the simple approach are used to check the results of calculation carried out by SCIA. The calculation carried out by SCIA is linear elastic. The inputs of the calculation, for example the magnitude of imposed deformation and material properties are constant, which are calculated by engineers instead of SCIA basing on the time history of constructions. During the calculation carried out by SCIA, 4-nodes Mindlin element are used where the mesh size is 250 mm.

### 9.2 Results of SCIA and the Simple Approach

The aim of this thesis is to provide a simple approach to check whether the prestress consumption in widened deck KW03.01 is reliable or not which is calculated by FEM software called SCIA. According to Chapter 7, Simplified Model 1 and Simplified Model 2 with mean dimensions are used in the simple approach. According to Chapter 8 and Appendix A19.4, both Mechanics 1 and Mechanics 2 without the impact of cracking is capable to calculate the stress resulting from imposed deformation in widened deck KW03.01.

In Appendix A19.4, to estimate the area which is possible to be cracked, calculation without cracking is first carried out. As shown in Appendix A15, if connections are made at time  $\Delta t_{II-III} = 28$  days, connections will be the only area which are possible to be cracked. Then re-calculation with the impact of cracking is carried out to investigate the stiffness of layers in widened deck KW03.01, see Appendix A19. As shown in Appendix A19, both Mechanics 1 and Mechanics 2 give sufficiently accurate results.

Now that models and mechanics used in the simple approach have been determined, calculations are carried out to the widened deck KW03.01 for the stress resulting from imposed deformation and the prestress consumption in proportion, where prestress consumption in proportion is the ratio of stress resulting from imposed deformation and compressive stress resulting from prestressing.

The stress resulting from imposed deformation calculated by SCIA are shown in Figure 41 and Figure 43, while those calculated by the simple approach are shown in Figure 42 and Figure 45. Figure 42 and Figure 45 are also shown in Appendix A19.2. The magnitudes of stress in each layer are shown in the tables next to the figures. As shown in the tables, although there are large prestress consumption in both SCIA and simple approach, the stress resulting from imposed deformation and prestress consumption in proportion calculated by SCIA are smaller than those calculated by the simple approach. Therefore, investigation is carried out to check the source of difference, see Section 9.3.

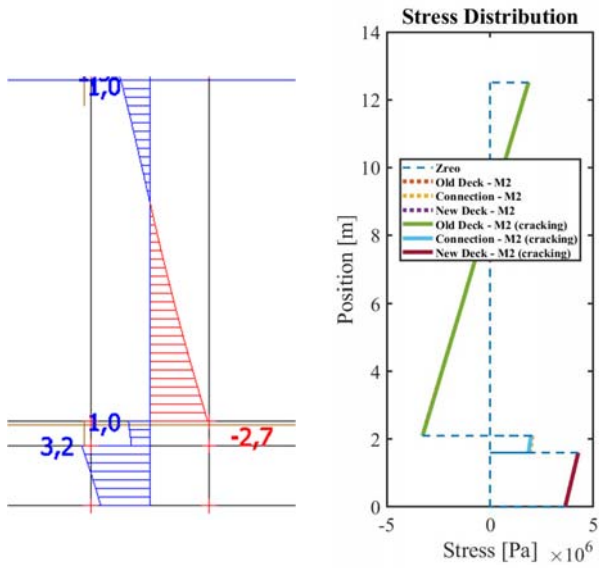


Figure 41: Stress Calculated by SCIA in South.

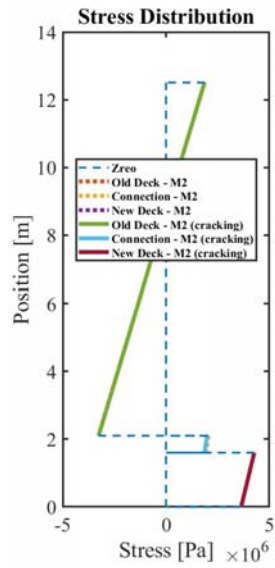


Figure 42: Stress Calculated by Mechanics 2 (M2) with and without Cracking in South.

	SCIA		Simple Approach	
Old Deck	1 MPa	15%	1.9 MPa	26%
	-2.7 MPa	-40%	-3.3 MPa	-46%
Connection	1 MPa		2.1 MPa	
	0.9 MPa		1.9 MPa	
New Deck	3.2 MPa	40%	4.3 MPa	51%
	2.3 MPa	29%	3.6 MPa	44%

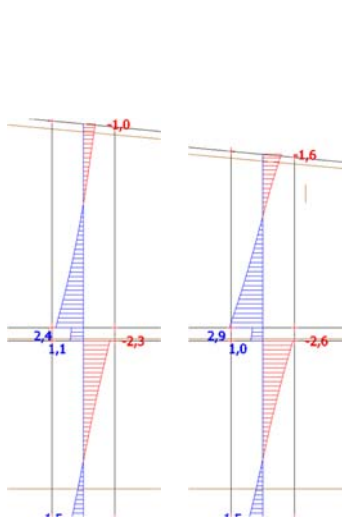


Figure 43: Stress Calculated by SCIA in North at Axis 1-2.

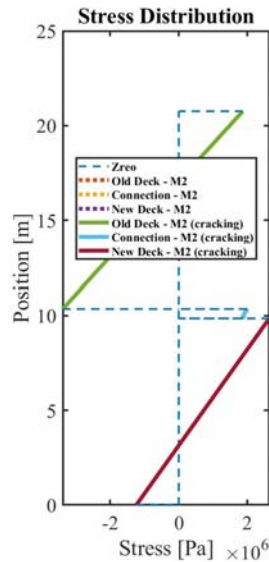


Figure 44: Stress Calculated by Mechanics 2 (M2) with and without Cracking in North at Axis 1-2.

	SCIA (Axis 1-2)		Simple Approach	
Old Deck	1.5 MPa	22%	1.9 MPa	26%
	-2.3 MPa	-34%	-3.4 MPa	-47%
Connection	1.1 MPa		2.0 MPa	
	1 MPa		1.9 MPa	
New Deck	2.4 MPa	41%	2.7 MPa	41%
	-1 MPa	-17%	-1.2 MPa	-19%

	SCIA (Axis 2-3)		Simple Approach	
Old Deck	1.5 MPa	22%	1.87 MPa	26%
	-2.6 MPa	-38%	-3.4 MPa	-47%
Connection	1 MPa		1.98 MPa	
	0.9 MPa		1.85 MPa	
New Deck	2.9 MPa	40%	2.65 MPa	41%
	-1.6 MPa	-22%	-1.2 MPa	-19%

## 9.3 Sources of Different Stress Resulting from Imposed Deformation and Prestress Consumption in Proportion

### 9.3.1 Models and Mechanics

Models used in SCIA and the simple approach are different. In the simple approach, simplified models with mean dimensions are used, see Section 7.5. However, in SCIA, realistic models are used, see Appendix A2.2.

In addition to the dimensions of models, the mechanics in SCIA and the simple approach are different as well. On one hand, the mechanics of FEM is different from the mechanics of composited cross-section mentioned in Appendix A12 and Appendix A13. On the other hand, it is assumed that the deformation of models are fully restrained in the simple approach, but not in SCIA. As a result, it is expected that the results of the simple approach would be larger than those of SCIA.

### 9.3.2 Elastic Modulus

The elastic modulus of concrete applied to models in SCIA and the simple approach are different. For simplicity, hereby only summarized the situation in the south part of widened deck KW03.01, see Table 12. The elastic modulus of concrete applied in SCIA is shown in Appendix A2.6, while those applied in the simple approach is shown in Appendix A19.2. The evaluation of other elastic modulus are shown in Expression 6 to Expression 10.

elastic modulus of concrete		SCIA	Simple Approach
Old Deck	$E_{cm}(t)$	13.4 GPa	23.4 GPa
Connection	$E_{cm}(t)$	5.1 GPa	9.7 GPa
New Deck	$E_{cm}(t)$	15.8 GPa	17.9 GPa

Table 12: Elastic Modulus of Concrete in South.

#### old deck (uncracked – SCIA)

$$E_{cm}(t) = \frac{E_{cm}}{1 + 0.8 \cdot \varphi(t, t_0)} = \frac{34.08}{1 + 0.8 \times 1.93} = 13.40 \text{ GPa} \quad (6)$$

#### connection (cracked – SCIA)

$$E_f = (3.10 + 670 \cdot \rho) \times 10^3 = (3.10 + 670 \times 2.99 \times 10^{-3}) \times 10^3 = 5.11 \text{ GPa} \quad (7)$$

where:

$$\rho \text{ is the reinforcement ratio} \\ = 2094 \text{ mm}^2 / (1000 \times 700) \text{ mm}^2 = 2.99 \times 10^{-3}$$

#### new deck (uncracked – SCIA)

$$E_{cm}(t) = \frac{E_{cm}}{1 + 0.8 \cdot \varphi(t, t_0)} = \frac{36.28}{1 + 0.8 \times 1.62} = 15.80 \text{ GPa} \quad (8)$$

#### old deck (uncracked – simple approach)

$$E_{cm}(t) = \frac{E_{cm}}{1 + 0.8 \cdot \varphi(t, t_0)} = \frac{34.00}{1 + 0.8 \times 0.57} = 23.40 \text{ GPa} \quad (9)$$

#### new deck (uncracked – simple approach)

$$E_{cm}(t) = \frac{E_{cm}}{1 + 0.8 \cdot \varphi(t, t_0)} = \frac{36.00}{1 + 0.8 \times 1.26} = 17.89 \text{ GPa} \quad (10)$$

According to Expression 6 to Expression 10, the creep factor  $\varphi(t, t_0)$  evaluated in SCIA are larger than those evaluated in the simple approach. Besides, in SCIA and the simple approach, the expressions to evaluate the elastic

modulus of concrete in connections are different as well. According to Appendix A2.6 and Appendix A19.2, only connections are expected to be cracked. As for the calculation carried out by SCIA, expressions from NEN 6720 are used evaluate the elastic modulus of concrete, see Expression 7. However, in terms of widened deck KW03.01 where in-plane loads are taken into account, the expressions introduced in Appendix A16 are recommended to evaluate the elastic modulus of concrete. For detailing information, see Appendix A21.

### 9.3.3 Imposed Deformation

Although the sources of imposed deformation taken into account in SCIA and the simple approach are same, the imposed deformation applied to models in SCIA and the simple approach are different. For simplicity, hereby only summarized the situation in the south part of widened deck KW03.01, see Table 13.

elastic modulus of concrete		SCIA	Simple Approach
Old Deck	$\Delta\varepsilon$	6.1E-05 m/m	4.6E-05 m/m
Connection	$\Delta\varepsilon$	4.6E-04 m/m	3.9E-04 m/m
New Deck	$\Delta\varepsilon$	4.9E-04 m/m	4.4E-04 m/m

Table 13: Imposed Deformation in South.

The detailing information of imposed deformation is shown in Table 14 and Table 15. According to Table 14 and Table 15, difference of imposed deformation between SCIA and the simple approach is mainly from creep. imposed deformation caused by creep in SCIA is much larger than that in the simple approach. The reason is that the creep in SCIA is calculated with a larger prestressing stress. The thickness of deck is denoted as  $h$ . According to the data file of SCIA, when calculating creep, the prestressing stress at cross-section  $h = 550$  mm is used. However, in the simple approach, the prestressing stress at cross-section  $h = 700$  mm is used. With similar prestressing force, a smaller cross-section results in larger prestressing stress and, therefore, more creep.

Old Deck		$t = 40515$ days	$t = 4015$ days	final
drying shrinkage	$\varepsilon_{cd}(t)$	2.07E-04 m/m	1.80E-04 m/m	<b>2.70E-05 m/m</b>
autogenous shrinkage	$\varepsilon_{ca}(t)$	5.12E-05 m/m	5.12E-05 m/m	<b>0.00E+00 m/m</b>
creep	$\varepsilon_{cc}(t)$	4.62E-04 m/m	4.27E-04 m/m	<b>3.50E-05 m/m</b>
creep factor ( $t_0 = 7$ days)		<b>1.93</b>	<b>1.79</b>	
Connection		$t = 36500$ days	$t = 1$ days	final
drying shrinkage	$\varepsilon_{cd}(t)$	2.06E-04 m/m	0.00E+00 m/m	<b>2.06E-04 m/m</b>
autogenous shrinkage	$\varepsilon_{ca}(t)$	5.12E-05 m/m	0.00E+00 m/m	<b>5.12E-05 m/m</b>
thermal deformation	$\varepsilon_{ct}(t)$		2.00E-04 m/m	<b>2.00E-04 m/m</b>
New Deck		$t = 36500$ days	$t = 28$ days	final
drying shrinkage	$\varepsilon_{cd}(t)$	1.83E-04 m/m	1.10E-05 m/m	<b>1.72E-04 m/m</b>
autogenous shrinkage	$\varepsilon_{ca}(t)$	7.16E-05 m/m	4.13E-05 m/m	<b>3.03E-05 m/m</b>
creep	$\varepsilon_{cc}(t)$	4.16E-04 m/m	1.30E-04 m/m	<b>2.86E-04 m/m</b>
creep factor ( $t_0 = 7$ days)	$\phi(t, t_0)$	<b>1.63</b>	<b>0.51</b>	

Table 14: Imposed Deformation in South (SCIA).

old deck		$t = 40515$ days	$t = 4044$ days	final
drying shrinkage	$\varepsilon_{cd}(t)$	1.99E-04 m/m	1.72E-04 m/m	<b>2.65E-05 m/m</b>
autogenous shrinkage	$\varepsilon_{ca}(t)$	5.12E-05 m/m	5.12E-05 m/m	<b>0.00E+00 m/m</b>
creep	$\varepsilon_{cc}(t)$	2.69E-04 m/m	2.49E-04 m/m	<b>1.99E-05 m/m</b>
creep factor ( $t_0 = 3$ days)	$\phi(t, t_0)$	<b>2.26</b>	<b>2.09</b>	
creep factor ( $t_0 = 7$ days)		<b>1.93</b>	<b>1.79</b>	
creep factor ( $t_0 = 28$ days)		<b>1.49</b>	<b>1.37</b>	
connection		$t = 36472$ days	$t = 1$ days	final
drying shrinkage	$\varepsilon_{cd}(t)$	2.26E-04 m/m	0.00E+00 m/m	<b>2.26E-04 m/m</b>
autogenous shrinkage	$\varepsilon_{ca}(t)$	5.12E-05 m/m	0.00E+00 m/m	<b>5.12E-05 m/m</b>
thermal deformation	$\varepsilon_{ct}(t)$		1.12E-04 m/m	<b>1.12E-04 m/m</b>
new deck		$t = 36500$ days	$t = 29$ days	final
drying shrinkage	$\varepsilon_{cd}(t)$	1.82E-04 m/m	8.87E-06 m/m	<b>1.74E-04 m/m</b>
autogenous shrinkage	$\varepsilon_{ca}(t)$	7.16E-05 m/m	4.18E-05 m/m	<b>2.98E-05 m/m</b>
creep	$\varepsilon_{cc}(t)$	3.41E-04 m/m	1.07E-04 m/m	<b>2.34E-04 m/m</b>
creep factor ( $t_0 = 7$ days)	$\phi(t, t_0)$	<b>1.65</b>	<b>0.52</b>	

Table 15: Imposed Deformation in South (Simple Approach).

### 9.3.4 Contribution of Each Source

According to Section 9.3.1 to Section 9.3.3 different models and mechanics, different elastic modulus of concrete and different imposed deformation used in SCIA and the simple approach, which are referred to as sources of different stress resulting from imposed deformation and different prestress consumption calculated by SCIA and the simple approach. For simplicity, the stress resulting from imposed deformation is referred to as resulting stress.

To investigate the contribution of each source, resulting stress are calculated in steps with different models, mechanics, elastic modulus of concrete and imposed deformation, see Table 16. By comparing the results of Step 0 and Step 1, contribution of different models and mechanics is investigated. By comparing the results of Step 1 and Step 2, contribution of different elastic modulus of concrete is investigated. By comparing the results of Step 2 and Step 3, contribution of different imposed deformation is investigated.

	Models	Mechanics	Elastic Modulus of Concrete	Imposed Deformation
Step 0	SCIA	SCIA	SCIA	SCIA
Step 1	Simple Approach	Simple Approach	SCIA	SCIA
Step 2	Simple Approach	Simple Approach	Simple Approach	SCIA
Step 3	Simple Approach	Simple Approach	Simple Approach	Simple Approach

Table 16: Models, Mechanics, Elastic Modulus of Concrete and Imposed Deformation Used in Each Step.

The stress resulting from imposed deformation calculated in each step are shown in Table 17 to Table 19. According to Table 17 to Table 19, from Step 0 to Step 3, the difference of models and mechanics contributes about 20% to the difference of resulting stress, while the difference of elastic modulus of concrete contributes about 80%.

The resulting stress calculated in Step 1 is larger than that calculated in Step 0. It means using models and mechanics from the simple approach increases resulting stress, which suits the expectation in Section 9.3.1. In addition, the contribution of different imposed deformation shown in Step 3 is always small in connections. The reason is that,

according to Section 9.3.3, difference of imposed deformation between SCIA and the simple approach is mainly from creep, while there is no creep in connections.

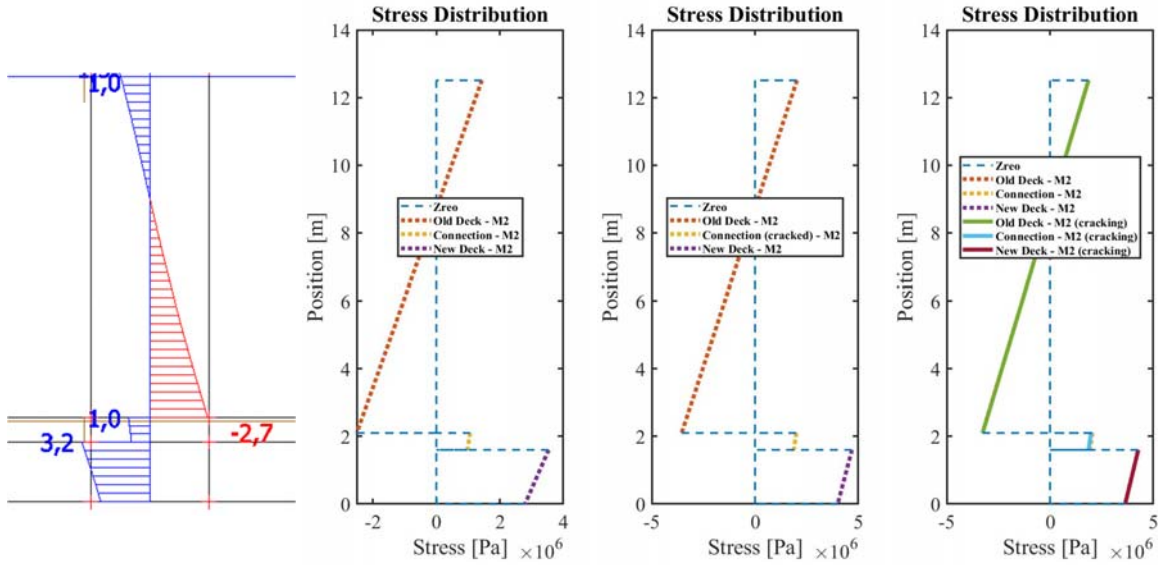


Figure 46: Stress Resulting from Imposed Deformation from Step 0 to Step 3 in South.

	Step 0		Step 1		Step 2		Step 3	
Old Deck	1 MPa	0%	1.4 MPa	42%	2.0 MPa	58%	1.9 MPa	-16%
	-2.7 MPa	0%	-2.5 MPa	-22%	-3.6 MPa	122%	-3.3 MPa	-33%
Connection	1 MPa	0%	1.1 MPa	7%	2.0 MPa	93%	2.1 MPa	7%
	0.9 MPa	0%	1.0 MPa	8%	1.9 MPa	92%	1.9 MPa	5%
New Deck	3.2 MPa	0%	3.5 MPa	23%	4.7 MPa	77%	4.3 MPa	-28%
	2.3 MPa	0%	2.8 MPa	29%	4.0 MPa	71%	3.6 MPa	-22%

Table 17: Stress Resulting from Imposed Deformation from Step 0 to Step 3 in South and Contribution to Difference in Each Step.

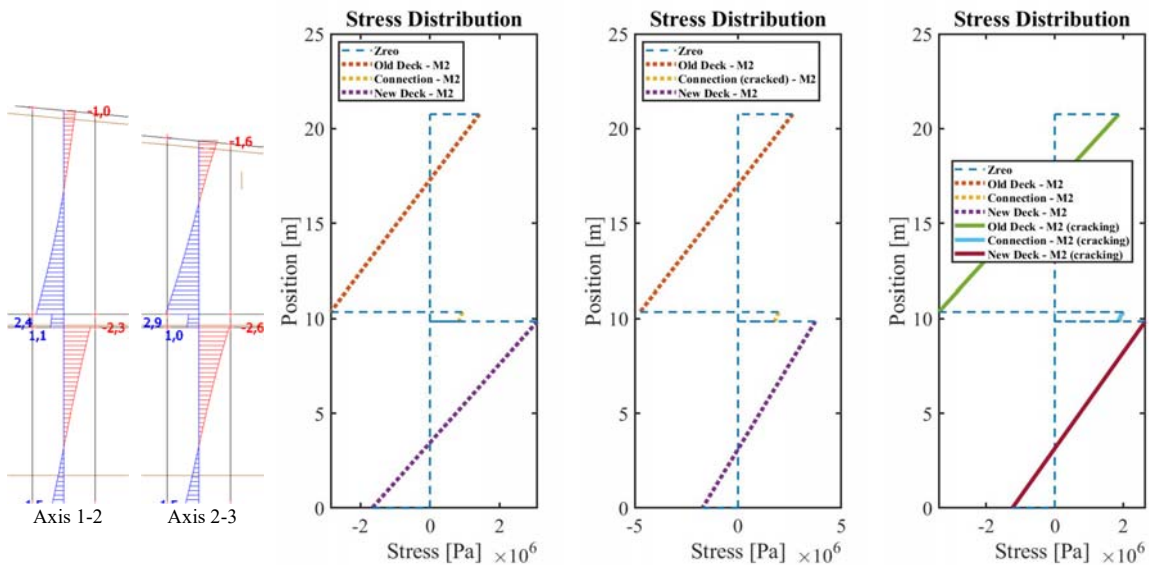


Figure 47: Stress Resulting from Imposed Deformation from Step 0 to Step 3 in North.

	Step 0		Step 1		Step 2		Step 3	
Old Deck	1.5 MPa	<b>0%</b>	1.4 MPa	<b>-7%</b>	2.7 MPa	<b>107%</b>	1.9 MPa	<b>-68%</b>
	-2.3 MPa	<b>0%</b>	-2.9 MPa	<b>23%</b>	-4.7 MPa	<b>77%</b>	-3.4 MPa	<b>-55%</b>
Connection	1.1 MPa	<b>0%</b>	0.9 MPa	<b>-21%</b>	2.0 MPa	<b>121%</b>	2.0 MPa	<b>2%</b>
	1 MPa	<b>0%</b>	0.8 MPa	<b>-21%</b>	1.8 MPa	<b>121%</b>	1.9 MPa	<b>9%</b>
New Deck	2.4 MPa	<b>0%</b>	3.1 MPa	<b>51%</b>	3.8 MPa	<b>49%</b>	2.7 MPa	<b>-81%</b>
	-1 MPa	<b>0%</b>	-1.7 MPa	<b>92%</b>	-1.7 MPa	<b>8%</b>	-1.2 MPa	<b>-67%</b>

Table 18: Stress Resulting from Imposed Deformation from Step 0 to Step 3 in North and Contribution to Difference in Each Step (Axis 1-2).

	Step 0		Step 1		Step 2		Step 3	
Old Deck	1.5 MPa	<b>0%</b>	1.4 MPa	<b>-7%</b>	2.7 MPa	<b>107%</b>	1.9 MPa	<b>-68%</b>
	-2.6 MPa	<b>0%</b>	-2.9 MPa	<b>12%</b>	-4.7 MPa	<b>88%</b>	-3.4 MPa	<b>-63%</b>
Connection	1 MPa	<b>0%</b>	0.9 MPa	<b>-8%</b>	2.0 MPa	<b>108%</b>	2.0 MPa	<b>2%</b>
	0.9 MPa	<b>0%</b>	0.8 MPa	<b>-7%</b>	1.8 MPa	<b>107%</b>	1.9 MPa	<b>8%</b>
New Deck	2.9 MPa	<b>0%</b>	3.1 MPa	<b>22%</b>	3.8 MPa	<b>78%</b>	2.7 MPa	<b>-129%</b>
	-1.6 MPa	<b>0%</b>	-1.7 MPa	<b>50%</b>	-1.7 MPa	<b>50%</b>	-1.2 MPa	<b>-400%</b>

Table 19: Stress Resulting from Imposed Deformation from Step 0 to Step 3 in North and Contribution to Difference in Each Step (Axis 2-3).

It has to be mentioned that, although the creep in old decks is small in magnitude, the difference of creep in proportion between SCIA and the simple approach is large. As a result, difference of imposed deformation in proportion between SCIA and the simple approach is large, which results in large contribution to the difference of resulting stress in old decks.

Besides, when it comes to new decks in north, see Table 18 and Table 19, the contribution of different models and mechanics can be equal to or even larger than the contribution of different elastic modulus of concrete. The reason is that, for other parts of widened deck KW03.01, the cross-section of simplified models used in the simple approach is same as those at Axis 1-2 and Axis 2-3 in SCIA, but not for new deck in north. As a result, the contribution of different models is large in new deck in north.

## 9.4 Discussion

### 9.4.1 General

According to Section 9.2, although there are large prestress consumption in both SCIA and simple approach, the stress resulting from imposed deformation and prestress consumption in proportion calculated by SCIA are smaller than those calculated by the simple approach. The sources of the differences and the contribution of each source are investigated in Section 9.3. Basing on these investigation, hereby provided a discussion on improving the calculation carried out by SCIA and reducing prestress consumption.

### 9.4.2 Improving the Calculation Carried out by SCIA

As shown in Section 9.3.2, when evaluating the elastic modulus of concrete, the creep factors  $\varphi(t, t_0)$  evaluated in SCIA are larger than those evaluated in the simple approach. In general, there are two things related to creep factor  $\varphi(t, t_0)$ . On one hand, since imposed deformation is a long-term load, creep factor is used to evaluate the elastic modulus of concrete, see Expression 6 to Expression 10. On the other hand, since imposed deformation includes the deformation due to creep, creep factor is used to calculate imposed deformation, see Table 14 and Table 15.

When evaluating the elastic modulus of concrete, factor  $t_0$  represents the timing when the long-term load is applied. As for widened deck KW03.01, factor  $t_0$  is time  $t = t_{IV}$  when connections get hard enough to produce imposed deformation.

However, when calculating the imposed deformation, or to be specific the deformation due to creep, factor  $t_0$  represents the timing when the creep begins. As for widened deck KW03.01, factor  $t_0$  should be the timing when prestressing is applied.

According to Section 6.1, connections are made after new decks being prestressed. It means the imposed deformation is applied to widened deck KW03.01 after prestressing. Therefore, the factor  $t_0$  used to evaluate the creep factor  $\varphi(t, t_0)$  for elastic modulus of concrete should be different from that used to evaluate the creep factor  $\varphi(t, t_0)$  for imposed deformation. However, in SCIA, same factor  $t_0$  is used to evaluate the creep factor  $\varphi(t, t_0)$  for elastic modulus of concrete and imposed deformation.

As shown in Section 9.3.2, different elastic modulus of concrete contributes about 80% to the difference of stress resulting from imposed deformation. Therefore, it is expected that evaluating elastic modulus of concrete with proper factor  $t_0$  and creep factor  $\varphi(t, t_0)$  as mentioned above would improve the calculation of SCIA and make the results of SCIA more reliable.

In addition to factor  $t_0$  and creep factor  $\varphi(t, t_0)$ , in SCIA and the simple approach, expressions to evaluate the elastic modulus of cracked concrete are different as well. As for SCIA, the elastic modulus of connections is constant and evaluated as if the connections are fully cracked, see Expression 7. However, in the simple approach, the elastic modulus of cracked concrete is evaluating as a function of imposed deformation, see Appendix A16.

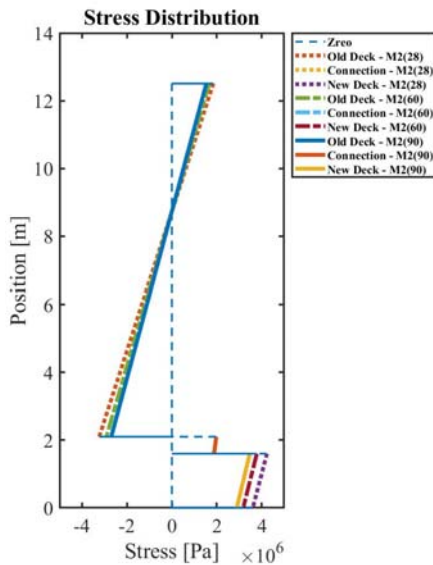
According to Section 4.1, imposed deformation may result in not fully developed crack pattern. Therefore, it is expected that using expressions shown in Appendix A16 to evaluate the elastic modulus of cracked concrete would improve the calculation of SCIA and make the results of SCIA more reliable as well.

### 9.4.3 Reducing Prestress Consumption

Prestress consumption is the compressive stress in concrete which is consumed by the tensile stress resulting from imposed deformation. According to Section 9.2, although the stress resulting from imposed deformation and prestress consumption in proportion calculated by SCIA are smaller than those calculated by the simple approach, there are large prestress consumption in both SCIA and simple approach. So, it is ensured that the prestress consumption in widened deck KW03.01 would be large at time  $t_\infty$ .

As shown in Appendix A20.3, neither increasing nor decreasing the prestressing force in new decks would help reduce prestress consumption. It is more practical to reduce prestress consumption by making connection as late as possible, see Appendix A15. However, as shown in Appendix A15, suppose the tensile strength of concrete is neglected, new decks are always cracked no matter when connections are made. Therefore, making connections later can only help decrease prestress consumption but not avoid cracking.

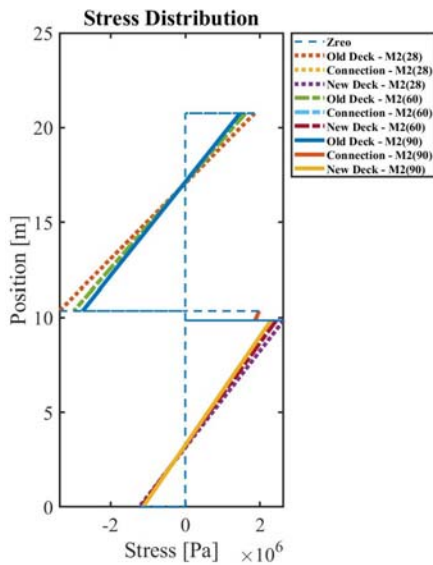
To be specific, stress resulting from imposed deformation in south and north are calculated with three different timing to make connection,  $\Delta t_{II-III} = 28$  days,  $\Delta t_{II-III} = 60$  days and  $\Delta t_{II-III} = 90$  days. For simplicity, hereby only shown the results of the calculation, see Figure 48 and Figure 49. The change of resulting stress due to later timing to make connections are shown in the tables next to the figures, where positive means increasing while negative means decreasing.



	$\Delta t_{II-III} = 28$ days	$\Delta t_{II-III} = 60$ days	$\Delta t_{II-III} = 90$ days
Old Deck	1.85 MPa	1.66 MPa	1.54 MPa
	-3.24 MPa	-2.92 MPa	-2.7 MPa
Connection	1.98 MPa	1.98 MPa	1.98 MPa
	1.89 MPa	1.88 MPa	1.86 MPa
New Deck	4.23 MPa	3.78 MPa	3.47 MPa
	3.60 MPa	3.18 MPa	2.89 MPa

	$\Delta t_{II-III} = 28$ days	$\Delta t_{II-III} = 60$ days	$\Delta t_{II-III} = 90$ days
Old Deck	0.0 %	-10.3 %	-16.8 %
	0.0 %	-9.9 %	-16.7 %
Connection	0.0 %	0.0 %	0.0 %
	0.0 %	-0.5 %	-1.6 %
New Deck	0.0 %	-10.6 %	-18.0 %
	0.0 %	-11.7 %	-19.7 %

Figure 48: Stress Resulting from Imposed Deformation in South with Different Timing to Make Connection.



	$\Delta t_{II-III} = 28$ days	$\Delta t_{II-III} = 60$ days	$\Delta t_{II-III} = 90$ days
Old Deck	1.86 MPa	1.61 MPa	1.47 MPa
	-3.36 MPa	-2.98 MPa	-2.74 MPa
Connection	1.98 MPa	1.97 MPa	1.97 MPa
	1.85 MPa	1.87 MPa	1.88 MPa
New Deck	2.63 MPa	2.43 MPa	2.29 MPa
	-1.23 MPa	-1.18 MPa	-1.13 MPa

	$\Delta t_{II-III} = 28$ days	$\Delta t_{II-III} = 60$ days	$\Delta t_{II-III} = 90$ days
Old Deck	0.0 %	-13.4 %	-21.0 %
	0.0 %	-11.3 %	-18.5 %
Connection	0.0 %	-0.5 %	-0.5 %
	0.0 %	1.1 %	1.6 %
New Deck	0.0 %	-7.6 %	-12.9 %
	0.0 %	-4.1 %	-8.1 %

Figure 49: Stress Resulting from Imposed Deformation in North with Different Timing to Make Connection.

## 10 Conclusions

There is a project called 'Approach Ring South, Groningen', where the viaduct of main roadway N7 over the Laan Corpus den Hoorn in Groningen was widened (Herepoort, 2019). The viaduct deck is called KW03.01. For simplicity, the existing decks of KW03.01 being widened are referred to as old decks, while the newly casted decks to widened existing decks are referred to as new decks.

After new decks being prestressed, old decks and new decks are connected. Since the concrete in new decks is younger than that in old decks, it is expected that the deformation of new decks would be larger and restrained by the old decks. As a result, imposed deformation is produced, see Section 4.2. Due to the tensile stress resulting from imposed deformation, the compressive stress in concrete resulting from prestressing is consumed. For the convenience of reading, the consumed compressive stress in concrete is referred to as prestress consumption.

A software called SCIA is used to calculate the prestress consumption in new decks. According to SCIA, the maximum prestress consumption in new decks are 40% and 41% respectively in south and north. To check whether the prestress consumption in widened deck KW03.01 is reliable or not, a simple approach is introduced.

To take into account the cracking at connections between old decks and new decks, three-layer models representing old decks, new decks and connections are used in the simple approach. The realistic dimensions of widened deck KW03.01 are variable, see Section 4.2. For simplicity, in the simple approach, the dimensions of models are simplified to the mean values of realistic dimensions. It is proved that a simplification of using mean thickness and width has almost no impact on the magnitude of imposed deformation, see Chapter 7.

The mechanics used in the simple approach is a mechanics of composited cross-section with Bernoulli's rule. At the beginning of investigation, the impact of shear deformation is not taken into account. For simplicity, it is referred to as Mechanics 1. The disadvantage of Mechanics 1 is that stress resulting from imposed deformation calculated by Mechanics 1 is not reliable when the mid-layer (connection) of model is 'soft', see Section 8.2 and Section 8.3. Therefore, to check whether the mid-layer (connection) of model is 'soft' or not, an improved mechanics taking shear deformation into account is introduced. For simplicity, it is referred to as Mechanics 2.

According to the stress resulting from imposed deformation calculated by Mechanics 1 and Mechanics 2, it is proved that Mechanics 2 is preferred when the mid-layer (connection) is 'soft'. As for widened deck KW03.01, the mid-layer (connection) would be taken as 'soft' when the normal stiffness of mid-layer (connection) decreasing to 40% or less due to cracking.

However, as for widened deck KW03.01, the normal stiffness of connection in south and north decrease to 96% and 99% due to cracking respectively, which are much larger than 40%, see Appendix A19.3. Therefore, as for widened deck KW03.01, Mechanics 1 and Mechanics 2 give same results and both of them can be used in the simple approach. In the end, Mechanics 2 is chosen.

According to the simple approach, the maximum prestress consumption in new decks are 51% and 40% respectively in south and north. Compared with the results of SCIA, 40% and 41%, it is proved that prestress consumption about 40% or more at time  $t_{\infty}$  in new decks are reliable. However, it does not mean there is no problem in calculation carried out by SCIA. The problem is that the input of SCIA is not evaluated properly, see Section 9.3. When evaluating elastic modulus of concrete, the factor  $t_0$  of creep factor  $\varphi(t, t_0)$  was taken as the starting date of old decks and new decks being build, while it should be the date when connections being made. When evaluating creep, to simplify the evaluation, stress in concrete at cross-section  $h = 550$  mm was used, while it should be that at cross-section  $h = 700$  mm.

In addition, as shown in Appendix A20.3, neither increasing nor decreasing the prestressing force in new decks would help reduce prestress consumption. It is more practical to reduce prestress consumption by making connection as late as possible, see Appendix A15. However, as shown in Appendix A15, suppose the tensile strength of concrete is neglected, new decks are always cracked no matter when connections are made. Therefore, making connections later can only help decrease prestress consumption but not avoid cracking.

## 11 Recommendations

### 11.1 General

The difference in the calculations carried out by SCIA and the simple approach are investigated, where the simple approach is carried out to check the prestress consumption calculated by SCIA. According to Section 9.3 the calculation carried out by SCIA has to be improved. Some recommendations to improve the calculation carried out by SCIA has been shown in Section 9.4.2. For the convenience of reading, hereby provides recommendations to improve the calculation carried out by SCIA again, together with recommendations on checking the results of SCIA.

### 11.2 About Models

As shown in Chapter 7, when a deck with variable dimensions is subjected to combined actions, it is proper to use simplified models with mean dimensions to calculate the stress resulting from combined actions. With simplified models, mechanics of composited cross-section can be easily used such as those introduced in Appendix A12 and Appendix A13.

### 11.3 About Factor $t_0$ and Creep Factor $\varphi(t, t_0)$ to Evaluate Elastic Modulus of Concrete and Imposed Deformation

As shown in Section 9.4.2, the factor  $t_0$  used to evaluate the creep factor  $\varphi(t, t_0)$  for elastic modulus of concrete should be different from that used to evaluate the creep factor  $\varphi(t, t_0)$  for imposed deformation.

When evaluating the elastic modulus of concrete, factor  $t_0$  represents the timing when the long-term load is applied. As for widened deck KW03.01, factor  $t_0$  is time  $t = t_{IV}$  when connections get hard enough to produce imposed deformation.

However, when calculating the imposed deformation, or to be specific the deformation due to creep, factor  $t_0$  represents the timing when the creep begins. As for widened deck KW03.01, factor  $t_0$  should be the timing when prestressing is applied.

### 11.4 About Expressions to Evaluate Elastic Modulus of Cracked Concrete

According to Section 4.1, imposed deformation may result in not fully developed crack pattern. Therefore, it is expected that using expressions shown in Appendix A16 to evaluate the elastic modulus of cracked concrete would improve the calculation and make the results of calculation more reliable.

### 11.5 About Mechanics Used during Calculation

As for widened deck KW03.01, since it is almost impossible for the stiffness of connections to decrease to 40% or less, to calculate the stress resulting from imposed deformation and the compressive stress in concrete consumed by the stress, it is more effective to use Mechanics 1 to check the results of SCIA, see Appendix A12. However, for other projects, Since it is unknown whether there is large shear deformation or not before carrying out a calculation, it is suggested to use Mechanics 2 for a more reliable solution, see Appendix A14.

### 11.6 About Reducing Prestress Consumption

In addition, as shown in Appendix A20.3, neither increasing nor decreasing the prestressing force in new decks would help reduce prestress consumption. It is more practical to reduce prestress consumption by making connection as late as possible, see Appendix A15. However, as shown in Appendix A15, suppose the tensile strength of concrete is neglected, new decks are always cracked no matter when connections are made. Therefore, making connections later can only help decrease prestress consumption but not avoid cracking.

## 12 References

- A. S. G. Bruggeling, W. A. de Bruijn. (1985). *Theorie en praktijk van het gewapend beton*.
- A.M. Neville, J.J. Brooks. (2010). *Concrete Technology*. PEARSON.
- Blaauwendraad, P. J. (2006). *Plate analysis, theory and application*. Delft University of Technology.
- Breguel, K. v. (1980). *Relaxation of young concrete*. Delft University of Technology.
- Breguel, E. (2013). *Concrete Structure under Imposed Thermal and Shrinkage Deformation*.
- Bruggeling, A. S. (1970). *Structural Concrete: Science into Practice*. HERON.
- CEN. (2001). *EuroCode 1: Actions on structures - Part 1-1: General actions - Densities, self-weight, imposed loads for buildings*. European Committee for Standardization.
- CEN. (2003). *Eurocode 1: Actions on structures: Part 1-3: Snow Loads*. European Committee for Standardization.
- CEN. (2005). *Eurocode 1: Actions on structures: Part 1-4: Wind Loads*. European Committee for Standardization.
- CEN. (2005). *Eurocode 1: Actions on structures: Part 1-6: Actions during execution*. European Committee for Standardization.
- H.W.Reinhardt. (2014, 4). Aspects of Imposed Deformation in Concrete Structures a Condensed Overview. *Structural Concrete*, pp. 454–460.
- Herepoort, C. (2007). *Aera Data: Calculation*. Combinatie Herepoort.
- Herepoort, C. (2007). *Area Data: Drawing*. Combinatie Herepoort.
- Herepoort, C. (2019). *Final Design - Reuse of Widened Deck KW03.01*. Combinatie Herepoort.
- Noakowski, P. (1978). *Die Bewehrung von Stahlbetonbautenlen bei Zwangsbeanspruchung infolge Temperatur*. Deutscher Ausschuss für Stahlbeton 296.
- Normalisatie, N. (1995). *TGB 1990 Regulations for Concrete Structure Requirements and Calculation Methods*. Technische Grondslagen voor Bouwconstructies.
- Rehm, G. (1961). *Über die Grundlagen des Verbundes Zwischen Stahl und Beton*. Deutscher Ausschuss für Stahlbeton.
- S.Y.Gu. (2008). *Analysis of Thermal Effects in Concrete Structures*. Tongji University.
- Scholten, F. (1989). *Bruggenbouwmethode Schreck*. Delft University of Technology.
- Veen, C. v. (1985). *Trekkracht van  $\tau$ - $\delta$  relatie tot overdrachtslengte*. Delft University of Technology.
- Veen, C. v. (1990). *Cryogenic bond stress-slip relationship*. Delft University of Technology.

## A1 Examples of Imposed Deformation Resulting in Tensile Stress

According to Section 4.1, hereby summarized three examples which shows that imposed deformation can result in tensile stress. Figure 50 (Breugel, 2013, p. 115) and Figure 52 (Breugel, 2013, p. 119) are about imposed strain while Figure 51 (Breugel, 2013, p. 116) is about imposed curvature. It is also shown in following examples that in addition to imposed deformation only, a member or structure might be subjected to imposed deformation and mechanical loads at the same time.

Figure 50 (Breugel, 2013, p. 115) shows a rectangular reservoir containing a cooled liquid. The horizontal liquid load results in tensile stresses in the walls. For part of the reservoir is in the soil and the response to the cooling is more rapid for the wall than for the slab, the walls will be shortened relatively to the slab. However, the wall is connected to the slab, making the shortening of the walls restrained and causing additional tensile stresses in the wall.

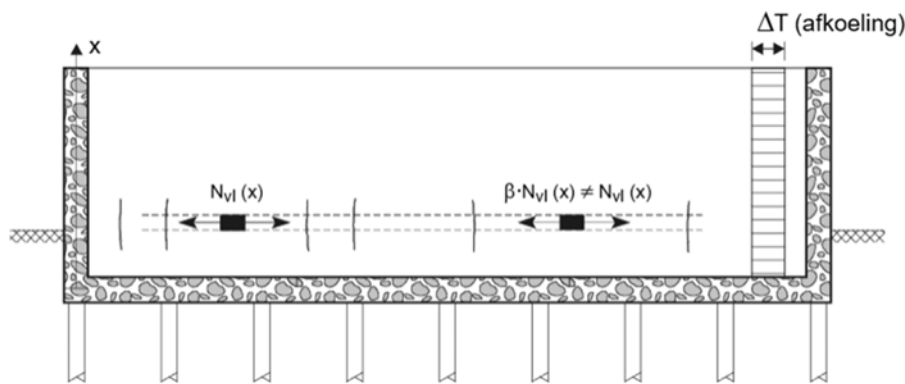


Figure 50: Rectangular Reservoir Containing a Cooled Liquid.

Figure 51 (Breugel, 2013, p. 116) shows a cylindrical reservoir containing a heated liquid. The heated water makes the inner surface of the wall swelling relatively to the outer surface. If the deformation is free, the wall will be bent. To make the deformation constitutive, an imposed curvature is introduced to the wall. And due to the liquid load, there is a hoop force inside the wall, which gives an additional tensile stress in circumferential direction.

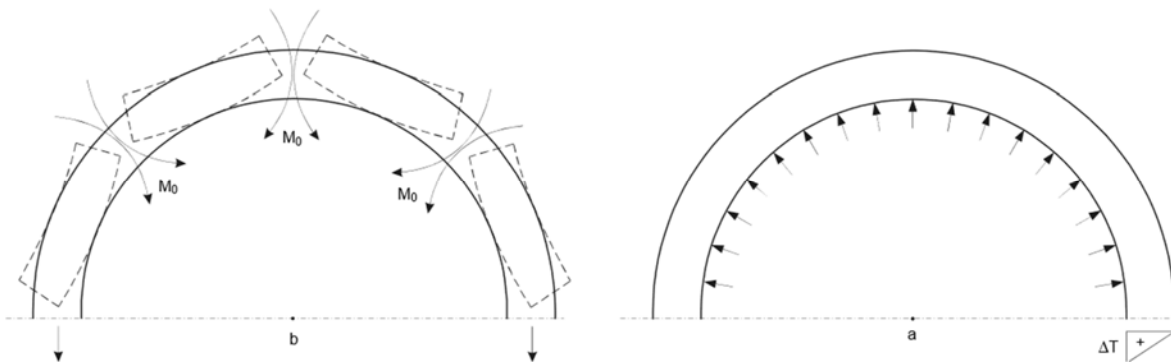


Figure 51: Cylindrical Reservoir Containing a Heated Liquid.

Figure 52 (Breugel, 2013, p. 119) shows a beam subjected to distributed load and cooling. For the ends of the beam are fixed, the shortening of the beam is fully restrained, causing a tensile stress in the longitudinal direction. And due to the distributed load, a moment is introduced to the cross-section of the beam.

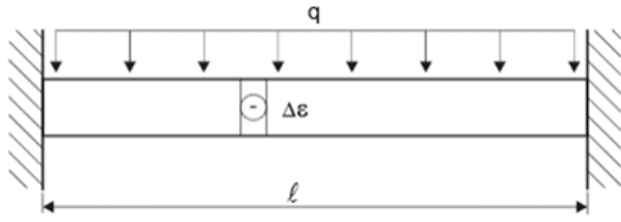


Figure 52: Beam Subjected to Distributed Load and Cooling.

## A2 Data of Calculation Carried out by SCIA

### A2.1 General

During the structure design of the widened deck KW03.01, FEM software called SCIA is used to calculate the stress resulting from imposed deformation and the compressive stress in concrete resulting from prestressing. The tensile stress resulting from imposed deformation consumes the compressive stress in concrete which results from prestressing. For simplicity, the compressive stress in concrete being consumed is referred to as prestress consumption.

The calculation carried out by SCIA is linear elastic. The inputs of the calculation, for example the magnitude of imposed deformation and material properties are constant, which are calculated by engineers instead of SCIA basing on the time history of constructions. During the calculation carried out by SCIA, 4-nodes Mindlin element are used where the mesh size is 250 mm.

### A2.2 Stress Resulting from Imposed Deformation at Time $t = 40515$ days

Stress resulting from imposed deformation calculated by SCIA is shown in *Figure 53*. As shown in *Figure 53*, realistic models are used in SCIA. As shown in Chapter 7, the thickness of the simplified models is  $h = 700$  mm, which is equal to those in realistic models at mid-span. Therefore, to make the stress calculated by SCIA and simple approach comparable, stress at mid-span is summarized, see Table 20.

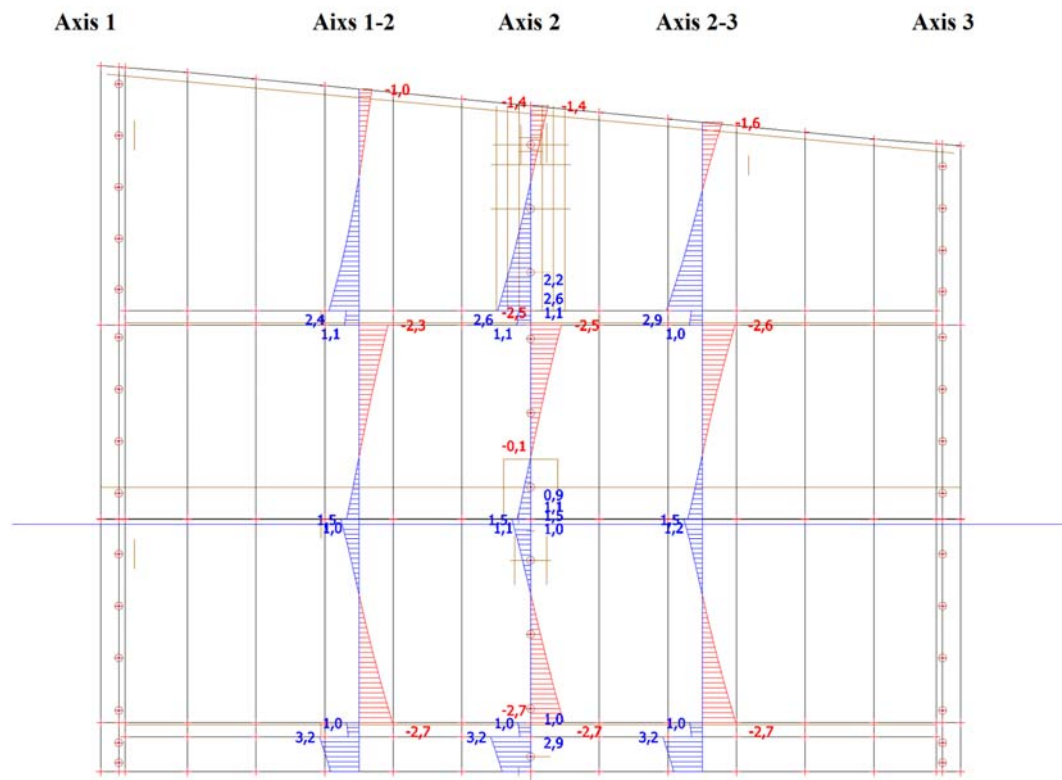


Figure 53: Stress Resulting from Imposed Deformation Calculated by SCIA.

	South	North (Axis 1-2)	North (Axis 2-3)
Old Deck	1.2 MPa	1.5 MPa	1.5 MPa
	-2.7 MPa	-2.3 MPa	-2.6 MPa
Connection	1.0 MPa	1.1 MPa	1.0 MPa
	0.9 MPa	1.0 MPa	0.9 MPa
New Deck	3.2 MPa	2.4 MPa	2.9 MPa
	2.3 MPa	-1.0 MPa	-1.6 MPa

Table 20: Stress Resulting from Imposed Deformation Calculated by SCIA.

### A2.3 Stress Resulting from Prestressing at Time $t = 40515$ days

The compressive stress in concrete resulting from prestressing calculated by SCIA is shown in Table 21 to Table 23. As shown in Figure 53, mid-span is referred to as Axis 1-2 and Axis 2-3.

Bestaand dek	$t = \infty$				$t = 0$		
	dikte [mm]	hoh ka- bels [mm]	A [mm <sup>2</sup> ]	$F_{pw}$ [kN]	$\sigma_c =$ $F_{pw}/A$ [N/mm <sup>2</sup> ]	$F_{pm0}$ [kN]	$\sigma_c =$ $F_{pm0}/A$ [N/mm <sup>2</sup> ]
as 3	550	400	220000	1897	8,62	2233	10,15
veld as 2-3	700	400	280000	1897	6,78	2233	7,98
as 2	850	400	340000	1897	5,58	2233	6,57
veld as 1-2	700	400	280000	1897	6,78	2233	7,98
as 1	550	400	220000	1897	8,62	2233	10,15

Table 21: Stress Resulting from Prestressing in Old Decks.

Uitbreiding zuid	$t = \infty$				$t = 0$		
	dikte [mm]	hoh ka- bels [mm]	A [mm <sup>2</sup> ]	$F_{pw}$ [kN]	$\sigma_c =$ $F_{pw}/A$ [N/mm <sup>2</sup> ]	$F_{pm0}$ [kN]	$\sigma_c =$ $F_{pm0}/A$ [N/mm <sup>2</sup> ]
as 3	550	583	320833,3	3297	10,28	3693	11,51
veld as 2-3	700	583	408333,3	3297	8,07	3693	9,04
as 2	850	583	495833,3	3297	6,65	3693	7,45
veld as 1-2	700	583	408333,3	3297	8,07	3693	9,04
as 1	550	583	320833,3	3297	10,28	3693	11,51

Table 22: Stress Resulting from Prestressing in South New Deck.

Uitbreiding noord	$t = \infty$				$t = 0$		
	dikte [mm]	hoh ka- bels [mm]	A [mm <sup>2</sup> ]	$F_{pw}$ [kN]	$\sigma_c =$ $F_{pw}/A$ [N/mm <sup>2</sup> ]	$F_{pm0}$ [kN]	$\sigma_c =$ $F_{pm0}/A$ [N/mm <sup>2</sup> ]
as 3	550	565	310750	3297	10,61	3693	11,88
veld as 2-3	700	642	449400	3297	7,34	3693	8,22
as 2	850	719	611150	3297	5,39	3693	6,04
veld as 1-2	700	796	557200	3297	5,92	3693	6,63
as 1	550	873	480150	3297	6,87	3693	7,69

Table 23: Stress Resulting from Prestressing in North New Deck.



	$M_{d,6.10a}$	$\sigma_{d,6.10a}$	$M_{d,6.10b}$	$\sigma_{d,6.10b}$
6X	-2036 kN·m/m	24.8 MPa	-1995 kN·m/m	24.3 MPa
8X	1161 kN·m/m	14.2 MPa	1283 kN·m/m	15.6 MPa
4X	-2158 kN·m/m	26.3 MPa	-2076 kN·m/m	25.3 MPa
5X	-1453 kN·m/m	17.7 MPa	-1391 kN·m/m	17.0 MPa
7X	1123 kN·m/m	13.7 MPa	1196 kN·m/m	14.6 MPa
11X	810 kN·m/m	9.9 MPa	882 kN·m/m	10.8 MPa

Table 25: Out-of-plane Moment and Normal Stress in New Decks.

## A2.6 Input Data

### A2.6.1 Material Properties

Hereby summarized the elastic modulus of concrete which are applied to the realistic models in SCIA. The evaluation of the elastic modulus of concrete is copied from the data files of structure design of widened deck KW03.01 (Herepoort, 2019).

#### 4.4.1. Elasticiteitsmodulus bestaande dek

De elasticiteitsmodulus van zowel het bestaande dek als de uitbreidingen wordt bepaald op tijdstip  $t=\infty$ .

##### Langsrichting bestaand dek C35/45:

$$E_{c,eff} = E_{cm} / (1 + X \cdot \Phi) = 34077 \text{ N/mm}^2 / (1 + (0,8 \cdot 1,93)) = 13395 \text{ N/mm}^2$$

Hierbij is  $X$  = verouderingsfactor. Volgens methode Trost is deze 0,8 bij wijziging van het statische systeem.

#### 4.6. Stijfheid stortstrook

Voor de stortstrook geldt dat de E-modulus in dwarsrichting minimaal gelijk moet zijn als het bestaande dek. Voor de langsrichting wordt dezelfde E-modulus gehanteerd (isotroop).

$$E_f = (3,10 + 670 \cdot 2,99 \cdot 10^{-3}) \cdot 10^3 = 5105 \text{ N/mm}^2 \geq 5000 \text{ N/mm}^2$$

#### 4.5.1. Elasticiteitsmodulus nieuwe dek

De elasticiteitsmodulus van zowel het bestaande dek als de uitbreidingen wordt bepaald op tijdstip  $t=\infty$ .

##### Langsrichting uitbreiding dek C45/55:

$$E_{c,eff} = E_{cm} / (1 + X \cdot \Phi) = 36283 \text{ N/mm}^2 / (1 + (0,8 \cdot 1,62)) = 15803 \text{ N/mm}^2$$

Hierbij is  $X$  = verouderingsfactor. Volgens methode Trost is deze 0,8 bij wijziging van het statische systeem.

##### Dwarsrichting uitbreiding dek:

In lijn met de bestaande dekken wordt uitgegaan van onderwapening  $\emptyset 20-150$ . Uit tabel NB-1 van NEN-EN 1992-1-1+C2:2011/NB:2011 volgt de fictieve Elasticiteitsmodulus:

$$E_{fic} = (3,10 + 670 \cdot \rho) \cdot 10^3 \geq 5000 \text{ N/mm}^2$$

Wapeningsverhouding  $\rho = 2094 \text{ mm}^2 / (1000 \cdot 700) \text{ mm}^2 = 2,99 \cdot 10^{-3}$ , waarbij 700 mm de gemiddelde dikte van het dek is.

$$E_f = (3,10 + 670 \cdot 2,99 \cdot 10^{-3}) \cdot 10^3 = 5105 \text{ N/mm}^2 \geq 5000 \text{ N/mm}^2$$

## A2.6.2 Imposed Deformation

Hereby summarized the imposed deformation which are applied to the realistic models in SCIA. The data of imposed deformation is copied from the data files of structure design of widened deck KW03.01 (Herepoort, 2019).

Resultaten krimp en kruip ten behoeve van BG9:

Bestaand dek			
$t = \infty$	40515 dagen		
Kruip			
$\phi_0(t, t_0)$	1,93 -		
$\sigma_c$	8,56 N/mm <sup>2</sup>		
$\varepsilon(t, t_0)$	4,62E-04	64,1 %	
Krimp			
$\varepsilon_{cd}(t)$	2,07E-04	28,8 %	
$\Delta\varepsilon_{ca}(t)$	5,12E-05	7,1 %	
Krimp+Kruip	7,20E-04	100,0 %	
$\Delta T_s(t)$	72 °C		
In Scia: $\Delta T_s(t) - \Delta T_s(t)$ -6,1 °C			
t = 11 jaar 4015 dagen			
Kruip			
$\phi_0(t, t_0)$	1,79 -		
$\sigma_c$	8,56 N/mm <sup>2</sup>		
$\varepsilon(t, t_0)$	4,27E-04	64,9 %	
Krimp			
$\varepsilon_{cd}(t)$	1,80E-04	27,3 %	
$\Delta\varepsilon_{ca}(t)$	5,12E-05	7,8 %	
Krimp+Kruip	6,58E-04	100,0 %	
$\Delta T_s(t)$	66 °C		
In Scia: $\Delta T_s(t) - \Delta T_s(t)$ -6,1 °C			
Uitbreiding dek zuid			
$t = \infty$	36500 dagen		
Kruip			
$\phi_0(t, t_0)$	1,63 -		
$\sigma_c$	9,71 N/mm <sup>2</sup>		
$\varepsilon(t, t_0)$	4,16E-04	62,1 %	
Krimp			
$\varepsilon_{cd}(t)$	1,83E-04	27,3 %	
$\Delta\varepsilon_{ca}(t)$	7,16E-05	10,7 %	
Krimp+Kruip	6,71E-04	100,0 %	
$\Delta T_s(t)$	67 °C		
In Scia: $\Delta T_s(t) - \Delta T_s(t)$ -48,9 °C			
t = 28 dagen			
Kruip			
$\phi_0(t, t_0)$	0,51 -		
$\sigma_c$	9,71 N/mm <sup>2</sup>		
$\varepsilon(t, t_0)$	1,30E-04	71,3 %	
Krimp			
$\varepsilon_{cd}(t)$	1,10E-05	6,0 %	
$\Delta\varepsilon_{ca}(t)$	4,13E-05	22,6 %	
Krimp+Kruip	1,83E-04	100,0 %	
$\Delta T_s(t)$	18 °C		
In Scia: $\Delta T_s(t) - \Delta T_s(t)$ -43,8 °C			
Stortstrook			
$t = \infty$	36500 dagen		
Kruip			
$\phi_0(t, t_0)$	1,92 -		
$\sigma_c$	0 N/mm <sup>2</sup>		
$\varepsilon(t, t_0)$	0,00E+00	0,0 %	
Krimp			
$\varepsilon_{cd}(t)$	2,06E-04	80,1 %	
$\varepsilon_{ca}(t)$	5,12E-05	19,9 %	
Krimp+Kruip	2,57E-04	100,0 %	
$\Delta T_s(t)$	26 °C		
Hydratatiekrimp			
$\Delta T_{th}$	20 °C		
$\varepsilon_{free}$	2,00E-03		
In Scia: $\Delta T_s(t) + \Delta T_{th}$ -45,7 °C			

### A3 Calculation of Thermal Deformation

The hardening process of concrete is the result of a chemical-physical reaction of cement and water. This is an exothermic reaction, which is a reaction during which heat is liberated (Breugel, 2013, p. 136). Due to this liberated heat, the temperature of the concrete rises and the concrete expands. After the exothermic reaction, the temperature of the concrete drops and the concrete shrinks. Suppose that the concrete in hardening process is connected to another existing concrete during the hardening, imposed deformation would occur due to the temperature decrement and the restraint from the connection. The strain increment  $\Delta\varepsilon_{thermal}$  caused by a temperature decrement  $\Delta T$  is as follows:

$$\Delta\varepsilon_{thermal} = \alpha_c \cdot \Delta T \cdot \psi(t, t_0) = 1.12 \times 10^{-4} \quad (11)$$

where:

- $\alpha_c$  is the thermal expansion coefficient of concrete  
=  $10 \times 10^{-6} / ^\circ\text{C}$
- $\psi(t, t_0)$  is the relaxation factor for hardening concrete  
= 0.2

In principle, the thermal expansion coefficient of concrete is a function of the thermal expansion coefficient of the components. For example, the thermal expansion coefficient of water is about five times larger than that of concrete. So, in the early stage of hardening, due to the presence of water, the thermal expansion coefficient of concrete is dominated by water (Breugel, 2013, p. 150). However, in the early stage of hardening, the stiffness of concrete is low but the relaxation of concrete is high (Breugel, 2013, p. 165). Therefore, the resulting stresses of thermal expansion in the early stage of hardening can be neglected. For a practical purpose, it is justified to adopt a constant thermal expansion coefficient to the concrete which represents the situation in the late stage of hardening (Breugel, 2013, p. 150).

As shown in Section 6.2, the concrete in old decks and connections is C35 while that in new decks is C45. Substitute the data from Table 26 into Expression 17 to calculate the magnitude of elastic modulus of concrete C35 and C45 from time  $t = 0.2$  days to time  $t = 28$  days. The results are shown in Figure 55 and Figure 56. Setting the elastic modulus of concrete  $E_{cm}(t)$  corresponding to time  $t = 28$  days as 100%, the elastic modulus of concrete C35 and C45 are expressed into proportion, see Figure 57 and Figure 58.

As shown in Figure 57 and Figure 58, the elastic modulus at time  $t = 1$  day takes about 70% of that at time  $t = 28$  days. So, it is assumed that  $\Delta t_{III-IV} = 1$  day which means it takes one day for the concrete in connections to get stiff enough to produce imposed deformation.

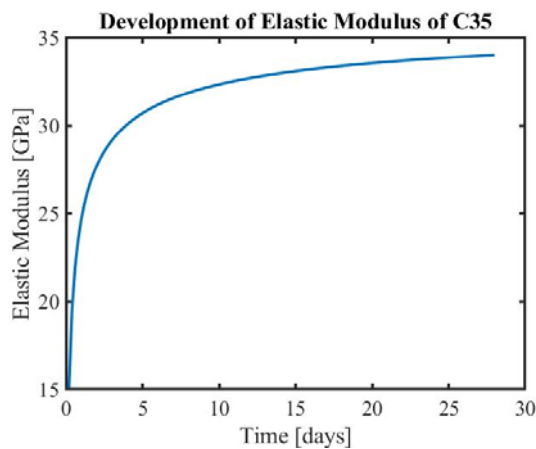


Figure 55: Development of Elastic Modulus of Concrete C35.

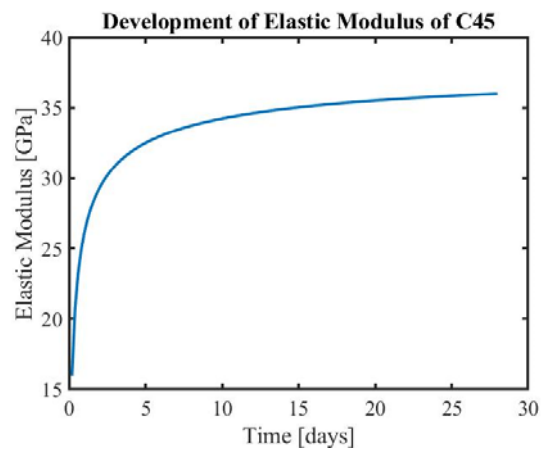


Figure 56: Development of Elastic Modulus of Concrete C45.

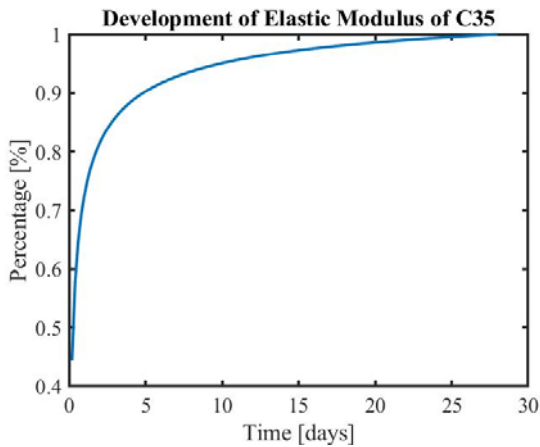


Figure 57: Development of Elastic Modulus of Concrete C35 in Proportion.

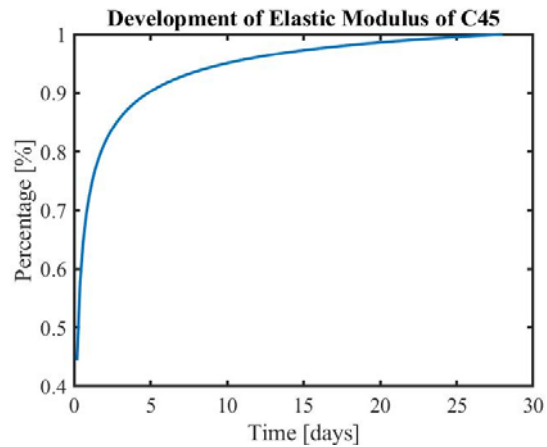


Figure 58: Development of Elastic Modulus of Concrete C45 in Proportion.

For lack of information, the temperature change during hardening in this case study is estimated according to the temperature development in a hardening concrete floor, see Figure 59 and Figure 60 (Breugel, 2013, p. 148). The thickness of the floor is 1 m. The top surface of the floor is exposed to the air while the bottom surface of the deck is based on another existing floor. In Figure 59 and Figure 60, it is shown that the maximum temperature during hardening occurs at time  $t = 1$  day and the maximum temperature in the floor at time  $t = 1$  day is  $68^{\circ}\text{C}$ .

During the construction of widened deck KW03.01, the deck was basing on formwork, of which the environment conditions were similar to those of the floor mentioned above. So, the maximum temperature in the widened deck KW03.01 during hardening is estimated to be  $68^{\circ}\text{C}$  as well. Suppose that the annual mean temperature on site is  $10^{\circ}\text{C}$ , the temperature decrement  $\Delta T$  would be  $58^{\circ}\text{C}$ .

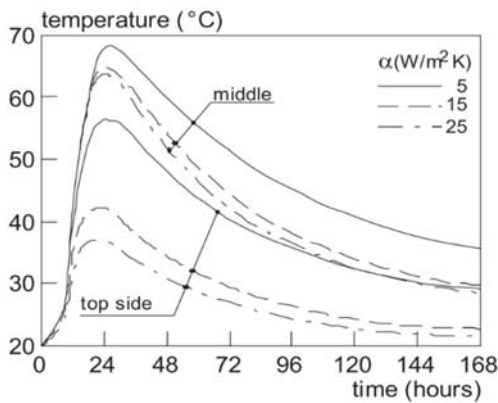


Figure 59: Temperature Development versus Time.

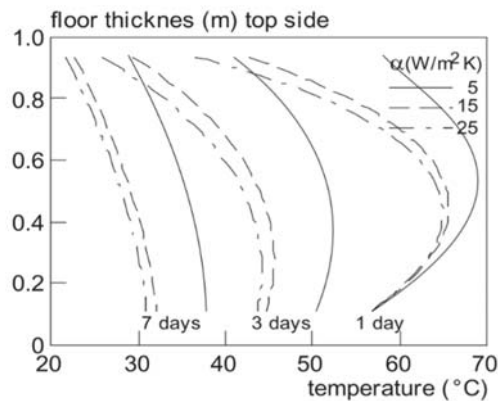


Figure 60: Temperature Development versus Height.

Relaxation has a considerable impact on the stress development in a hardening concrete. It means the resulting stress of temperature decrement  $\Delta T$  in hardening concrete is much smaller than that in a hardened concrete. During the hardening, a relatively small elastic modulus in the new concrete results in a small stiffness. When the new concrete is connected to an existing one, the resulting stress in the existing concrete is relatively small as well. Therefore, in this case study, a mathematic trick is applied, which introduces a relaxation factor  $\psi(t, t_0)$  to calculate resulting strain  $\Delta \epsilon_{thermal}$ , see Expression 11.

Expression 12 gives quite good results for the stresses in hardening concrete (Breguel, 1980). The relaxation factor calculated by Expression 12 is shown in Figure 61. Since it is assumed that the concrete get hard enough at time  $t = 1$  day (24 hours), the relaxation factor  $\psi(t, t_0)$  is estimated to be 0.2.

$$\psi(t, t_0) = e^{-\left[\left(\frac{\alpha_h(t)}{\alpha_h(t_0)} - 1\right) + 1.34 \cdot (wcr)^{1.65} \cdot t_0^{-d} \cdot (t - t_0)^n \cdot \frac{\alpha_h(t)}{\alpha_h(t_0)}\right]} \quad (12)$$

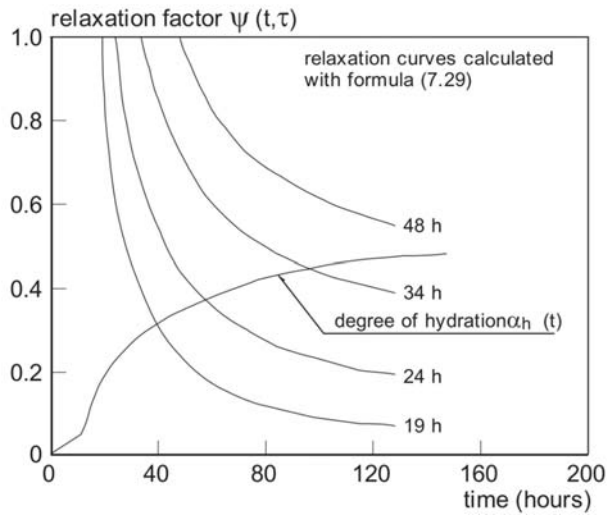


Figure 61: Relaxation Factor in Hardening Concrete.

## A4 Expressions to Evaluate the Material Properties of Concrete at Time $t$ days

The characteristic strength of concrete  $f_{ck}(t)$  at time  $t$  is evaluated as follow:

For  $3 < t < 28$  days

$$f_{ck}(t) = f_{cm}(t) - 8 \text{ [MPa]} \quad (13)$$

For  $t \geq 28$  days

$$f_{ck}(t) = f_{ck} \quad (14)$$

The compressive strength of concrete  $f_{cm}(t)$  at time  $t$  is evaluated as follow:

$$f_{cm}(t) = \beta_{cc}(t) \cdot f_{cm} \quad (15)$$

where:

- $f_{cm}$  is the compressive strength of concrete at 28 days, see Table 26
- $\beta_{cc}(t)$  is the coefficient related to time  
 $= \exp\{s[1 - (28/t)^{0.5}]\}$
- $s$  is the coefficient related to cement  
 $= 0.20$  for cement of strength Classes CEM 42.5 R, CEM 52.5 N and CEM 52.5 R (Class R)  
 $= 0.25$  for cement of strength Classes CEM 32.5 R, CEM 42.5 N (Class N)  
 $= 0.38$  for cement of strength Classes CEM 32.5 N (Class S)

The tensile strength of concrete  $f_{ctm}(t)$  at time  $t$  is evaluated as follow:

$$f_{ctm}(t) = (\beta_{cc}(t))^\alpha \cdot f_{ctm} \quad (16)$$

where:

- $f_{ctm}$  is the tensile strength of concrete at 28 days, see Table 26
- $\alpha$   
 $= 1$  for  $t < 28$  days  
 $= 2/3$  for  $t \geq 28$  days

Suppose a short-term load is applied, the elastic modulus of concrete  $E_{cm}(t)$  at time  $t$  is evaluated as follow:

$$E_{cm}(t) = \left(\frac{f_{cm}(t)}{f_{cm}}\right)^{0.3} E_{cm} \quad (17)$$

where:

- $E_{cm}$  is the elastic modulus of concrete at 28 days, see Table 26

Sterkteklassen voor beton														Vergelijking/Verklaring	
$f_{ck}$ (MPa)	12	16	20	25	30	35	40	45	50	55	60	70	80	90	
$f_{ck,cube}$ (MPa)	15	20	25	30	37	45	50	55	60	67	75	85	95	105	
$f_{cm}$ (MPa)	20	24	28	33	38	43	48	53	58	63	68	78	88	98	$f_{cm} = f_{ck} + 8 \text{ (MPa)}$
$f_{ctm}$ (MPa)	1,6	1,9	2,2	2,6	2,9	3,2	3,5	3,8	4,1	4,2	4,4	4,6	4,8	5,0	$f_{ctm} = 0,30 \times f_{ck}^{(2/3)} \leq C50/60$ $f_{ctm} = 2,12 \cdot \ln(1 + (f_{cm}/10)) > C50/60$
$f_{ak,0.05}$ (MPa)	1,1	1,3	1,5	1,8	2,0	2,2	2,5	2,7	2,9	3,0	3,1	3,2	3,4	3,5	$f_{ak,0.05} = 0,7 \times f_{ctm}$ 5 % fractiel
$f_{ak,0.95}$ (MPa)	2,0	2,5	2,9	3,3	3,8	4,2	4,6	4,9	5,3	5,5	5,7	6,0	6,3	6,6	$f_{ak,0.95} = 1,3 \times f_{ctm}$ 95 % fractiel
$E_{cm}$ (GPa)	27	29	30	31	33	34	35	36	37	38	39	41	42	44	$E_{cm} = 22[(f_{cm})/10]^{0.3}$ ( $f_{cm}$ in MPa)

Table 26: Strength and Deformation Characteristics for Concrete.

When a long-term variable load is applied to a concrete member, due to the creep or relaxation appears in the process, the concrete member performs as if its elastic modulus is decreased. For simplicity, a fictitious elastic modulus  $E_{cm}(t)$  is used to evaluate the internal forces of concrete when it is subjected to a long-term variable load (Scholten, 1989).

$$E_{cm}(t) = \frac{E_{cm}}{1 + 0.8 \cdot \varphi(t, t_0)} \quad (18)$$

where:

- $\varphi(t, t_0)$  is the creep coefficient  
 $= \varphi_0 \cdot \beta_c(t, t_0)$
- $\varphi_0$  is the notional creep coefficient  
 $= \varphi_{RH} \cdot \beta(f_{cm}) \cdot \beta(t_0)$
- $\varphi_{RH}$  is the coefficient related to the effect of relative humidity on the notional creep coefficient  
 $= 1 + \frac{1-RH/100}{0.1 \cdot \sqrt[3]{h_0}} (f_{cm} \leq 35 \text{ Mpa})$   
 $= \left[ 1 + \frac{1-RH/100}{0.1 \cdot \sqrt[3]{h_0}} \cdot \alpha_1 \right] \cdot \alpha_2 (f_{cm} > 35 \text{ Mpa})$
- $\beta(f_{cm})$  is the coefficient related to the effect of concrete strength on the notional creep coefficient  
 $= 16.8 / \sqrt{f_{cm}}$
- $\beta(t_0)$  is the coefficient related to the effect of concrete age at loading on the notional creep coefficient  
 $= \frac{1}{0.1 + t_0^{0.2}}$
- $\beta_c(t, t_0)$  is the coefficient related to the development of creep after loading  
 $= [(t - t_0) / (\beta_H + t - t_0)]^{0.3}$
- $\beta_H$  is the coefficient related to relative humidity and notional size  
 $= 1.5[1 + (0.012RH)^{18}]h_0 + 250 \leq 1500 (f_{cm} \leq 35 \text{ Mpa})$   
 $= 1.5[1 + (0.012RH)^{18}]h_0 + 250 \cdot \alpha_3 \leq 1500 \cdot \alpha_3 (f_{cm} > 35 \text{ Mpa})$
- $\alpha_1$  is the coefficient related to the influence of the concrete strength  
 $= \left( \frac{35}{f_{cm}} \right)^{0.7}$
- $\alpha_2$  is the coefficient related to the influence of the concrete strength  
 $= \left( \frac{35}{f_{cm}} \right)^{0.2}$
- $\alpha_3$  is the coefficient related to the influence of the concrete strength  
 $= \left( \frac{35}{f_{cm}} \right)^{0.5}$

## A5 Expressions to Calculate Cross-sectional Calculation at Time $t$ days

### A5.1 General

Cross-sectional calculation consists of the evaluation of cross-sectional properties and the stress resulting from the loads applied to the cross-section. Suppose there is a rectangular concrete deck with  $n$  prestressing tendons, see Figure 62, the expressions shown in this chapter would be used during cross-sectional calculation.

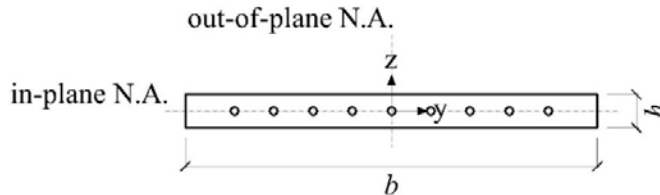


Figure 62: Cross-section.

### A5.2 Cross-sectional Properties of Concrete Deck

**cross-section area**

$$A_c = b \cdot h \quad (19)$$

where:

- $b$  is the width of cross-section
- $h$  is the height of cross-section

**out-of-plane moment of inertia**

$$I_{c,out-of-plane} = \frac{b \cdot h^3}{12} \quad (20)$$

**in-plane moment of inertia**

$$I_{c,in-plane} = \frac{h \cdot b^3}{12} \quad (21)$$

**normal stiffness**

$$EA(t) = E_{cm}(t) \cdot A_c \quad (22)$$

where:

- $E_{cm}(t)$  is the elastic modulus of concrete at time  $t$

**out-of-plane bending stiffness**

$$EI(t)_{out-of-plane} = E_{cm}(t) \cdot I_{c,out-of-plane} \quad (23)$$

**in-plane bending stiffness**

$$EI(t)_{in-plane} = E_{cm}(t) \cdot I_{c,in-plane} \quad (24)$$

### A5.3 Cross-sectional Properties of Prestressing Cables

**cross-section area of cables**

$$A_p = n \cdot \bar{A}_p \quad (25)$$

where:

- $n$  is the total number of prestressing cables

$\bar{A}_p$  is the area of cross-section per cable

**prestressing ratio**

$$\rho_p = \frac{A_p}{A_c} \quad (26)$$

**elastic modulus ratio at time  $t$**

$$\alpha_e = \frac{E_p}{E_{cm}(t)} \quad (27)$$

where:

$E_p$  is the elastic modulus of prestressing cables

**normal stiffness per cable**

$$E\bar{A} = E_p \cdot \bar{A}_p \quad (28)$$

**normal stiffness of cables**

$$EA = E_p \cdot A_p \quad (29)$$

## A5.4 Stress Resulting from Loads

There are four possible loads which could be applied to the cross-section shown in Figure 62, the normal force  $N$ , the bending moment out-of-plane  $M_{out-of-plane}$ , the bending moment in-plane  $M_{in-plane}$  and the shear force  $V$ .

Suppose the cross-section is subjected to the bending moment out-of-plane  $M_{out-of-plane}$ , the cross-section would rotate around the in-plane N.A.. Suppose the cross-section is subjected to the bending moment in-plane  $M_{in-plane}$ , the cross-section would rotate around the out-of-plane N.A..

**normal stresses at top or bottom edge of the deck**

$$\sigma_{t/b} = \frac{N}{A_c} - \frac{M_{out-of-plane} \cdot z}{I_{c,out-of-plane}} \quad (30)$$

where:

$N$  is the normal force from certain action

$M_{out-of-plane}$  is the out-of-plane moment from certain action

$z$  is the z-coordinate of top or bottom edge of cross-section

**normal stresses at right or left edge of the deck**

$$\sigma_{r/l} = \frac{N}{A_c} - \frac{M_{in-plane} \cdot y}{I_{c,in-plane}} \quad (31)$$

where:

$N$  is the normal force from certain action

$M_{in-plane}$  is the in-plane moment from certain action

$y$  is the y-coordinate of right or left edge of cross-section

**shear stresses**

$$\tau = \frac{V}{A_c} \quad (32)$$

where:

$V$  is the shear force from certain action

## A6 Expressions to Calculate the Remaining Prestressing Force in Model with Uniform Cross-section Mean Dimensions at Time $t$ days

Expressions from Eurocode *NEN-EN 1992-1-1+C2* are used to calculate the strain of creep and shrinkage and the relaxation loss. Suppose that the prestressing force is applied step by step and the cables are prestressed from both sides, the loss of the prestressing force applied at step  $\zeta$  would be expressed as follow:

### Initial prestressing force

$$\Delta P_{max,\zeta} = P_{m0,\zeta} \quad (33)$$

where:

$$P_{m0,\zeta} \quad \text{is the initial prestressing force per cable after immediate loss}$$

$$= \frac{1}{1+\alpha_e \rho_p} \cdot \Delta P_{max,\zeta}$$

$\Delta P_{max,\zeta}$  is the total prestressing force per cable

$\zeta$  is the sequence number of certain prestressing step

### elastic loss per cable

$$\Delta P_{el,mean} = A_p E_p \left[ \frac{j \cdot \Delta \sigma_{c,p}(t_p)}{E_{cm}(t_p)} \right] \quad (34)$$

where:

$$j = \frac{n-1}{2n}$$

$n$  is the total number of prestressing cables

$$\Delta \sigma_{c,p}(t_p) \quad \text{is the increment of stress in concrete when a new prestressing cable is applied}$$

$$= n \cdot P_{m0,\zeta} / A_c$$

### friction loss per cable

$$\Delta P_\mu(x) = \Delta P_{max,\zeta} [1 - e^{-\mu(\theta+kx)}] \quad (35)$$

where:

$\mu$  is the coefficient of friction  
= 0.19

$k$  is the coefficient of wobble effect  
= 0.01 rad/m

$\theta$  is the angular rotation

$R_i$  is the radius of curve  $i$  of the tendons

$x$  is the distance from certain point to the ends

### shrinkage loss of cables

$$\Delta P_{shr} = \bar{A}_p E_p \varepsilon_{cs} \quad (36)$$

where:

$\varepsilon_{cs}$  is the total shrinkage of concrete  
=  $\varepsilon_{cd}(t) + \varepsilon_{ca}(t)$

$\varepsilon_{cd}(t)$  is the drying shrinkage  
=  $[\beta_{ds}(t, t_s) - \beta_{ds}(t_p, t_s)] \cdot k_h \cdot \varepsilon_{cd,0}$

$\beta_{ds}(t, t_s)$  is the coefficient related to drying shrinkage  
=  $(t - t_s) / (t - t_s + 0.04 \sqrt{h_0^3})$

$\beta_{ds}(t_p, t_s)$  is the coefficient related to drying shrinkage

$$= (t_p - t_s) / \left( t_p - t_s + 0.04 \sqrt{h_0^3} \right)$$

- $t_s$  is the end of curing  
 $h_0$  is the notional size  
 $= 2A_c/u$   
 $u$  is the perimeter of cross-section  
 $k_h$  is the coefficient depending on the notional size  $h_0$  according to Table 27  
 $\varepsilon_{cd,0}$  is the basic drying shrinkage  
 $= 0.85[(220 + 110 \cdot \alpha_{ds1}) \cdot \exp(-\alpha_{ds2} \cdot f_{cm}/f_{cm0})] \cdot 10^{-6} \cdot \beta_{RH}$   
 $f_{cm0}$  = 10 MPa  
 $\alpha_{ds1}$  is the coefficient related to cement  
 $= 3$  for cement Class S  
 $= 4$  for cement Class N  
 $= 6$  for cement Class R  
 $\alpha_{ds2}$  is the coefficient related to cement  
 $= 0.13$  for cement Class S  
 $= 0.12$  for cement Class N  
 $= 0.11$  for cement Class R  
 $\beta_{RH}$  =  $1.55[1 - (RH/RH_0)^3]$   
 $RH_0$  = 100 %  
 $\varepsilon_{ca}(t)$  is the strain of autogenous shrinkage  
 $= [\beta_{as}(t) - \beta_{as}(t_s)] \cdot \varepsilon_{ca}(\infty)$   
 $\varepsilon_{ca}(\infty)$  =  $2.5(f_{ck} - 10) \cdot 10^{-6}$   
 $\beta_{as}(t)$  =  $1 - \exp(-0.2t^{0.5})$

$h_0$	100	200	300	>500
$k_h$	1	0.85	0.75	0.7

Table 27: Values of  $k_h$ .

#### mean creep loss per cable

$$\Delta P_{cr} = \bar{A}_p E_p \varepsilon_{cc,m}(t) \quad (37)$$

where:

- $\varepsilon_{cc,m}(t)$  is the mean strain of creep  
 $= (\varepsilon_{cc,ends}(t) + \varepsilon_{cc,mid-support}(t))/2$   
 $\varepsilon_{cc,ends}(t)$  is the strain of creep at the ends  
 $= (P_{m0}/EA(t_p) - \Delta P_\mu(0)/EA(t_p) - \Delta P_{el,mean}(t_p)/E\bar{A}) \cdot \varphi(t, t_0)$   
 $\varepsilon_{cc,mid-support}(t)$  is the strain of creep at the ends  
 $= (P_{m0}/EA(t_p) - \Delta P_\mu(l)/EA(t_p) - \Delta P_{el,mean}(t_p)/E\bar{A}) \cdot \varphi(t, t_0)$   
 $t_p$  is the timing when prestressing is applied

#### creep loss per cable at certain point

$$\Delta P_{cr} = \bar{A}_p E_p \varepsilon_{cc,x}(t) \quad (38)$$

where:

- $\varepsilon_{cc,x}(t)$  is the strain of creep at certain point  
 $= (P_{m0}/EA(t_p) - \Delta P_\mu(x)/EA(t_p) - \Delta P_{el,mean}(t_p)/E\bar{A}) \cdot \varphi(t, t_0)$   
 $x$  is the distance from certain point to the ends

$t_p$  is the timing when prestressing is applied

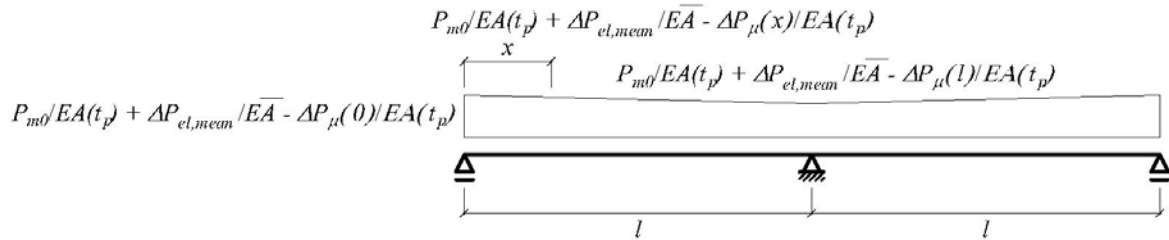


Figure 63: Distribution of Elastic Deformation.

### relaxation loss per cable

$$\Delta P_r = \bar{A}_p \cdot \Delta \sigma_{pr} \quad (39)$$

where:

$$\begin{aligned} \Delta \sigma_{pr} &= \left[ 0.39 \rho_{1000} e^{6.7\mu} \left( \frac{\Delta t}{1000} \right)^{0.75(1-\mu)} \right] \cdot 10^{-5} \cdot \sigma_{pi} \text{ for Class 1} \\ &= \left[ 0.66 \rho_{1000} e^{9.1\mu} \left( \frac{\Delta t}{1000} \right)^{0.75(1-\mu)} \right] \cdot 10^{-5} \cdot \sigma_{pi} \text{ for Class 2} \\ &= \left[ 1.98 \rho_{1000} e^{8\mu} \left( \frac{\Delta t}{1000} \right)^{0.75(1-\mu)} \right] \cdot 10^{-5} \cdot \sigma_{pi} \text{ for Class 3} \end{aligned}$$

$\Delta t$  is the hours after prestressing  
 $= 24(t - t_0) \leq 500000$

$\rho_{1000}$  the relaxation loss in % at 1000 hours after tensing and at a mean temperature of 20°C  
 $= 8\%$  for Class 1  
 $= 2.5\%$  for Class 2  
 $= 4\%$  for Class 3  
 or taken from the certificate

$\mu = \sigma_{pi} / f_{pk}$

$\sigma_{pi} = \sum_1^{\zeta} P_{m0,\zeta} / \bar{A}_p$

### total loss per cable

$$\Delta P_{\zeta,t_0-t} = \Delta P_{el,mean} + \Delta P_{\mu} + \Delta P_{cr} + \Delta P_r + \Delta P_s/n \quad (40)$$

With the prestressing loss obtained, the total remaining prestress force at time  $t$  days is the summation of remaining prestress force of each step as follow:

$$P(t) = \sum n \cdot (\Delta P_{max,\zeta} - \Delta P_{\zeta,t_0-t}) \quad (41)$$

## A7 The Impact of Prestressing Steps

### A7.1 General

The old decks are prestressed in three prestressing steps (Herepoort, 2007, p. 25), or in short the steps, while the new decks are prestressed all in 1 step (Herepoort, 2019). The increment of step  $i$  is denoted as  $\Delta P_{max,i}$ . The data of prestressing is shown in Figure 64 and Figure 65.

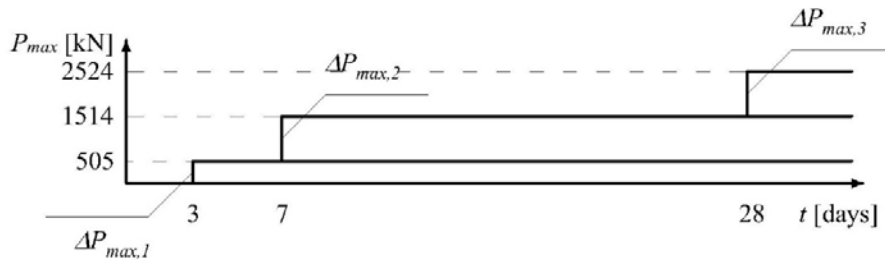


Figure 64: Prestressing Steps of Old Decks.



Figure 65: Prestressing Steps of New Decks.

When prestressing is applied in steps, to make sure that the magnitude of prestressing force being applied suits the requirement at the end of each step, the prestress loss between the steps has to be compensated. It means, suppose prestressing steps are taken into account, prestress loss between the steps has to be calculated to determine the magnitude of prestressing force in each step.

When it comes to the widened deck KW03.01, the prestressing force in old decks was applied in three steps at time  $t = 3$  days,  $t = 7$  days and  $t = 28$  days. For simplicity, impact of prestressing steps is investigated to see whether it is proper to calculate imposed deformation and remaining prestressing force as if the prestressing force is applied all in one step at time  $t = 7$  days. Suppose the imposed deformation and remaining prestressing force in three steps are same as those of applying prestressing force all in one step, the impact of prestressing steps would be taken as small. Otherwise, the impact of prestressing steps would be taken as large.

### A7.2 Results

The models used during investigation are Simplified Model 1 and Simplified Model 2, see Section 7.3.1 and Section 7.4.1. The input data is shown in Chapter 5. The material properties applied to the expressions are calculated by the input data and the expressions in Appendix A4 and Appendix A5. The imposed deformation and prestress loss in old decks are calculated by the expressions in Appendix A6.

For the convenience of reading, hereby only summarized the prestress loss calculated during investigation in percentage, see Figure 66 to Figure 69. The data of the calculation is summarized in Appendix A8.

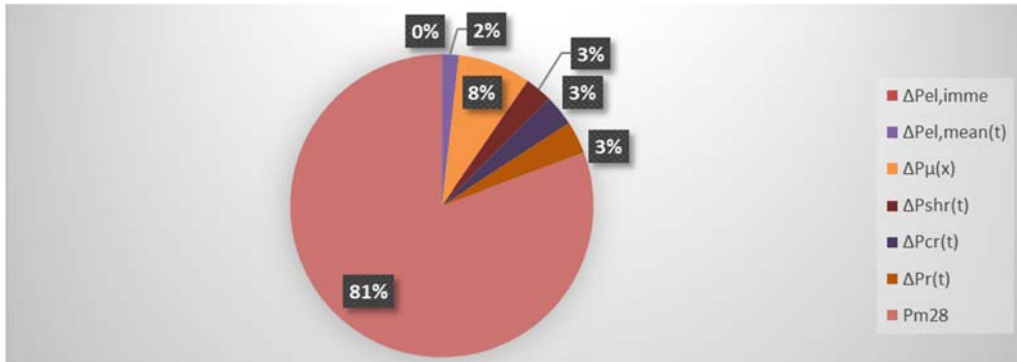


Figure 66: Prestress Loss Calculated by Three Steps at Time  $t = 4015$  days (11 years).

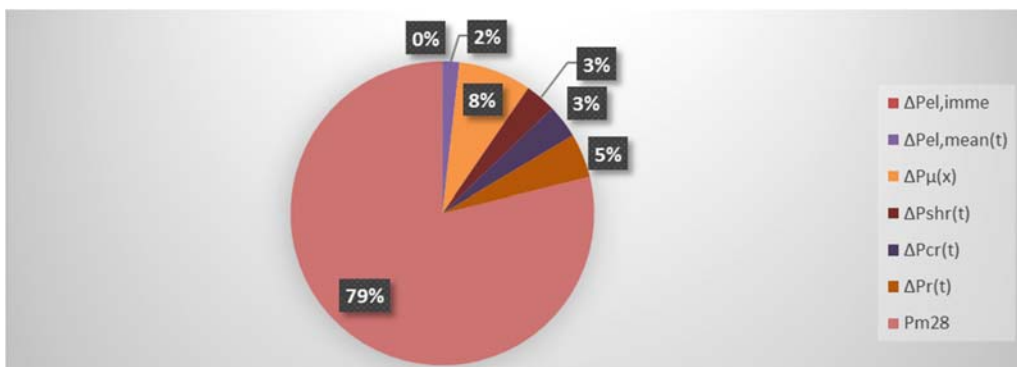


Figure 67: Prestress Loss Calculated by Time  $t = 40515$  days (111 years).

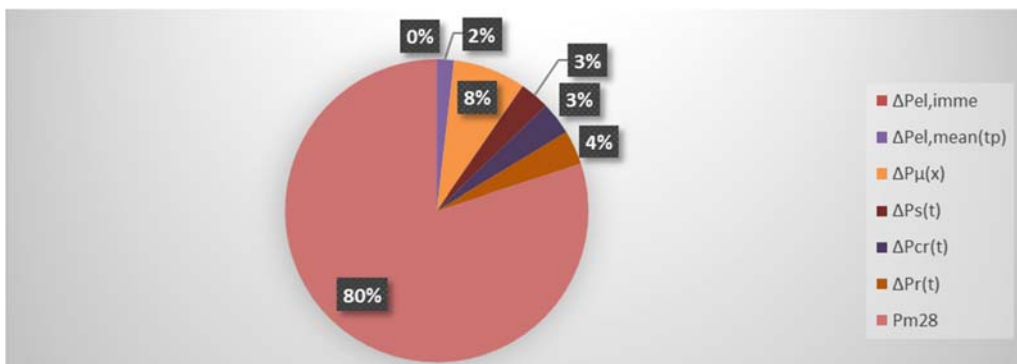


Figure 68: Prestress Loss Calculated by All in One Step at Time  $t = 4015$  days (11 years).

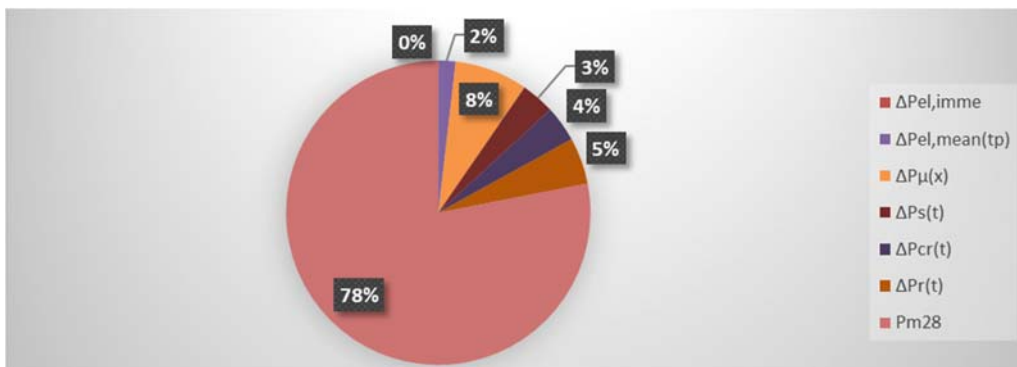


Figure 69: Prestress Loss Calculated by All in One Step at Time  $t = 40515$  days (111 years).

## A7.3 Discussion

### A7.3.1 Imposed Deformation

As shown in Section 6.1, connections were built at about  $\Delta t = 11$  years after old decks being built. As a result, to investigate the impact of prestressing steps on the imposed deformation in old decks, the imposed deformation is taken as the increment of shrinkage and creep from time  $t = 4015$  days (11 years) to time  $t = 40515$  days (111 years) approximately.

According to Figure 66 to Figure 69, the increment of shrinkage and creep from time  $t = 4015$  days (11 years) to time  $t = 40515$  days (111 years) is small. The detailing data of the increment is as follow:

#### three steps

$$\Delta \varepsilon_{shr} = \varepsilon_{shr,111} - \varepsilon_{shr,11} = 2.50 \times 10^{-4} - 2.23 \times 10^{-4} = \mathbf{2.65 \times 10^{-5}}$$

$$\Delta \varepsilon_{cr} = \varepsilon_{cr,111} - \varepsilon_{cr,11} = 2.69 \times 10^{-4} - 2.49 \times 10^{-4} = \mathbf{1.99 \times 10^{-5}}$$

#### all in one step

$$\Delta \varepsilon_{shr} = \varepsilon_{shr,111} - \varepsilon_{shr,11} = 2.56 \times 10^{-4} - 2.29 \times 10^{-4} = \mathbf{2.65 \times 10^{-5}}$$

$$\Delta \varepsilon_{cr} = \varepsilon_{cr,111} - \varepsilon_{cr,11} = 2.74 \times 10^{-4} - 2.54 \times 10^{-4} = \mathbf{2.03 \times 10^{-5}}$$

where:

$\varepsilon_{shr,t}$  is the shrinkage in old decks at time  $t$

$\varepsilon_{cr,t}$  is the creep in old decks at time  $t$

As for three steps, the coefficient  $t_0$  used to calculate creep factor  $\varphi(t, t_0)$  and the coefficient  $t_p$  used to calculate shrinkage factor  $\beta_{ts}(t_p, t_s)$  are different from those for all in one step. So, the creep  $\varepsilon_{cr,t}$  and the shrinkage  $\varepsilon_{shr,t}$  calculated by three steps and all in one step are different.

However, the imposed deformation is the increment of shrinkage and creep. The difference of increment  $\Delta \varepsilon_{cr}$  and  $\Delta \varepsilon_{shr}$  calculated by three steps and all in one step are 2% and 0% respectively. Therefore, the impact of prestressing steps on imposed deformation is small.

### A7.3.2 Remaining Prestressing Force

The widened deck is subjected to not only imposed deformation but also remaining prestressing force at time  $t = 40515$  days (111 years). As shown in Appendix A7.1, when prestressing force is applied in steps, compensation has to be made to the prestress loss between steps. Therefore, the initial prestressing force applied by three steps is larger than that applied by all in one step. The initial prestressing forces are as follow:

#### three steps

$$P_{m0} = \mathbf{2648 \text{ kN/cable}}$$

#### all in one step

$$P_{m0} = \mathbf{2524 \text{ kN/cable}}$$

According to Figure 66 to Figure 69, the remaining per cable at time  $t = 40515$  days (111 years) calculated by three steps and all in one step are as follow:

#### three steps

$$P_{m\infty} = 79\% \cdot P_{m0} = \mathbf{2092 \text{ kN/cable}}$$

#### all in one step

$$P_{m\infty} = 78\% \cdot P_{m0} = 1969 \text{ kN/cable}$$

The difference of remaining prestressing force  $P_{m\infty}$  calculated by three steps and all in one step is 6%. Therefore, the impact of prestressing steps on remaining prestressing force is small.

#### A7.4 Conclusion

The impact of prestressing steps on imposed deformation and remaining prestressing force is small. Therefore, it is proper to calculate imposed deformation and remaining prestressing force as if the prestressing force is applied all in one step at time  $t = 7$  days instead of three steps at time  $t = 3$  days,  $t = 7$  days and  $t = 28$  days.

## A8 Dimensions and Material Properties of Models Required to Calculate Prestress Loss

### A8.1 Simplified Model 1

The sketch of Simplified Model 1 has been shown in Section 7.3.1. The input data is shown in Chapter 5. The material properties applied to the expressions are calculated by the input data and the expressions in Appendix A4 and Appendix A5. The prestress loss are calculated by the expressions in Appendix A6.

Dimensions of Simplified Model 1 are shown in Table 28 to Table 30.

height of cross-section	$h$	0.70 m
width of cross-section	$b$	10.41 m
length of structure	$L$	42.40 m

Table 28: Dimensions of Old Deck in Simplified Model 1.

height of cross-section	$h$	0.70 m
width of cross-section	$b$	1.60 m
length of structure	$L$	42.40 m

Table 29: Dimensions of New Deck in Simplified Model 1.

height of cross-section	$h$	0.70 m
width of cross-section	$b$	0.50 m
length of structure	$L$	42.40 m

Table 30: Dimensions of Connection in Simplified Model 1.

Material properties of prestressing cables in old deck and new deck are shown in Table 31 and Table 32.

elastic modulus	$E_p$	1.95E+11 Pa
area of prestressing cable	$\bar{A}_p$	1.80E-03 m <sup>2</sup>
number of prestressing cable	$n$	25
area of prestressing cables	$A_p$	4.50E-02 m <sup>2</sup>
ratio of prestress	$\rho_p$	6.12E-03
eccentricity	$e_p$	0.00 m

Table 31: Material Properties of Prestressing Cables in Old Deck.

elastic modulus	$E_p$	1.95E+11 Pa
area of prestressing cable	$\bar{A}_p$	2.85E-03 m <sup>2</sup>
number of prestressing cable	$n$	3
area of prestressing cables	$A_p$	8.55E-03 m <sup>2</sup>
ratio of prestress	$\rho_p$	7.63E-03
eccentricity	$e_p$	0.00 m

Table 32: Material Properties of Prestressing Cables in New Deck.

Since the prestress in old decks is applied in three steps at time  $t = 3$  days,  $t = 7$  days and  $t = 28$  days respectively (Herepoort, 2007, p. 25), material properties of concrete in old deck at time  $t = 3$  days,  $t = 7$  days and  $t = 28$  days are required, see Table 33, Table 34 and Table 35.

characteristic strength	$f_{ck}$	3.50E+07	Pa
compression strength	$f_{cm}$	4.30E+07	Pa
elastic modulus	$E_{cm}$	3.40E+10	Pa
characteristic strength	$f_{ck}(t)$	3.50E+07	Pa
mean compression strength	$f_{cm}(t)$	5.48E+07	Pa
where:			
factor related to time	$\beta_{cc}(t)$	1.28E+00	
elastic modulus	$E_{cm}(t)$	2.91E+10	Pa

Table 33: Material Properties of Concrete in Old Deck at Time  $t = 3$  days.

characteristic strength	$f_{ck}$	3.50E+07	Pa
compression strength	$f_{cm}$	4.30E+07	Pa
elastic modulus	$E_{cm}$	3.40E+10	Pa
characteristic strength	$f_{ck}(t)$	3.35E+07	Pa
mean compression strength	$f_{cm}(t)$	3.35E+07	Pa
where:			
factor related to time	$\beta_{cc}(t)$	7.79E-01	
elastic modulus	$E_{cm}(t)$	3.15E+10	Pa

Table 34: Material Properties of Concrete in Old Deck at Time  $t = 7$  days.

characteristic strength	$f_{ck}$	3.50E+07	Pa
compression strength	$f_{cm}$	4.30E+07	Pa
elastic modulus	$E_{cm}$	3.40E+10	Pa
characteristic strength	$f_{ck}(t)$	3.50E+07	Pa
mean compression strength	$f_{cm}(t)$	4.30E+07	Pa
where:			
factor related to time	$\beta_{cc}(t)$	1.00E+00	
elastic modulus	$E_{cm}(t)$	3.20E+06	Pa

Table 35: Material Properties of Concrete in Old Deck at Time  $t = 28$  days.

Since the prestress in new deck is applied all in one step at time  $t = 7$  days, material properties of concrete in new deck at time  $t = 7$  days is required, see Table 36.

characteristic strength	$f_{ck}$	4.50E+07	Pa
compression strength	$f_{cm}$	5.30E+07	Pa
elastic modulus	$E_{cm}$	3.60E+10	Pa
characteristic strength	$f_{ck}(t)$	4.50E+07	Pa
mean compression strength	$f_{cm}(t)$	5.37E+07	Pa
where:			
factor related to time	$\beta_{cc}(t)$	1.01E+00	
elastic modulus	$E_{cm}(t)$	3.61E+10	Pa

Table 36: Material Properties of Concrete in New Deck at Time  $t = 7$  days.

## A8.2 Realistic Model 1

The sketch of Realistic Model 1 has been shown in Section 7.3.1. The input data is shown in Chapter 5. The material properties applied to the expressions are calculated by the input data and the expressions in Appendix A4 and Appendix A5. The prestress loss are calculated by the expressions in Appendix A6.

Dimensions of Realistic Model 1 are shown in Table 37 to Table 39.

height of cross-section	$h(x)$	$0.000014x + 0.55$ m
width of cross-section	$b$	10.41 m
length of structure	$L$	42.40 m

\* $x$  is the distance from certain point to the ends of the deck in [mm], see Figure 70.

Table 37: Dimensions of Old Deck in Realistic Model 1.

height of cross-section	$h(x)$	$0.000014x + 0.55$ m
width of cross-section	$b$	1.60 m
length of structure	$L$	42.40 m

\* $x$  is the distance from certain point to the ends of the deck in [mm], see Figure 70.

Table 38: Dimensions of New Deck in Realistic Model 1.

height of cross-section	$h(x)$	$0.000014x + 0.55$ m
width of cross-section	$b$	0.50 m
length of structure	$L$	42.40 m

\* $x$  is the distance from certain point to the ends of the deck in [mm], see Figure 70.

Table 39: Dimensions of Connection in Realistic Model 1.

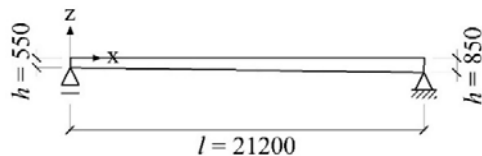


Figure 70: Side View of Half Realistic Model 1.

Material properties of prestressing cables in old deck and new deck are shown in Table 40 and Table 41.

elastic modulus	$E_p$	$1.95E+11$ Pa
area of prestressing cable	$\bar{A}_p$	$1.80E-03$ m <sup>2</sup>
number of prestressing cable	$n$	25
area of prestressing cables	$A_p$	$4.50E-02$ m <sup>2</sup>
ratio of prestress	$\rho_p$	-
eccentricity	$e_p$	0.00 m

\*The ratio of prestress is not shown because it is a function of  $x$ .

Table 40: Material Properties of Prestressing Cables in Old Deck.

elastic modulus	$E_p$	$1.95E+11$ Pa
area of prestressing cable	$\bar{A}_p$	$2.85E-03$ m <sup>2</sup>
number of prestressing cable	$n$	3
area of prestressing cables	$A_p$	$8.55E-03$ m <sup>2</sup>
ratio of prestress	$\rho_p$	-
eccentricity	$e_p$	0.00 m

\*The ratio of prestress is not shown because it is a function of  $x$ .

Table 41: Material Properties of Prestressing Cables in New Deck.

Since the prestress in old decks is applied in three steps at time  $t = 3$  days,  $t = 7$  days and  $t = 28$  days respectively (Herepoort, 2007, p. 25), material properties of concrete in old deck at time  $t = 3$  days,  $t = 7$  days and  $t = 28$  days are required, see Table 42, Table 43 and Table 44.

characteristic strength	$f_{ck}$	3.50E+07 Pa
compression strength	$f_{cm}$	4.30E+07 Pa
elastic modulus	$E_{cm}$	3.40E+10 Pa
characteristic strength	$f_{ck}(t)$	3.50E+07 Pa
mean compression strength	$f_{cm}(t)$	5.48E+07 Pa
where:		
factor related to time	$\beta_{cc}(t)$	1.28E+00
elastic modulus	$E_{cm}(t)$	2.91E+10 Pa

Table 42: Material Properties of Concrete in Old Deck at Time  $t = 3$  days.

characteristic strength	$f_{ck}$	3.50E+07 Pa
compression strength	$f_{cm}$	4.30E+07 Pa
elastic modulus	$E_{cm}$	3.40E+10 Pa
characteristic strength	$f_{ck}(t)$	3.35E+07 Pa
mean compression strength	$f_{cm}(t)$	3.35E+07 Pa
where:		
factor related to time	$\beta_{cc}(t)$	7.79E-01
elastic modulus	$E_{cm}(t)$	3.15E+10 Pa

Table 43: Material Properties of Concrete in Old Deck at Time  $t = 7$  days.

characteristic strength	$f_{ck}$	3.50E+07 Pa
compression strength	$f_{cm}$	4.30E+07 Pa
elastic modulus	$E_{cm}$	3.40E+10 Pa
characteristic strength	$f_{ck}(t)$	3.50E+07 Pa
mean compression strength	$f_{cm}(t)$	4.30E+07 Pa
where:		
factor related to time	$\beta_{cc}(t)$	1.00E+00
elastic modulus	$E_{cm}(t)$	3.20E+06 Pa

Table 44: Material Properties of Concrete in Old Deck at Time  $t = 28$  days.

Since the prestress in new deck is applied all in one step at time  $t = 7$  days, material properties of concrete in new deck at time  $t = 7$  days is required, see Table 45.

characteristic strength	$f_{ck}$	4.50E+07 Pa
compression strength	$f_{cm}$	5.30E+07 Pa
elastic modulus	$E_{cm}$	3.60E+10 Pa
characteristic strength	$f_{ck}(t)$	4.50E+07 Pa
mean compression strength	$f_{cm}(t)$	5.37E+07 Pa
where:		
factor related to time	$\beta_{cc}(t)$	1.01E+00
elastic modulus	$E_{cm}(t)$	3.61E+10 Pa

Table 45: Material Properties of Concrete in New Deck at Time  $t = 7$  days.

### A8.3 Simplified Model 2

The sketch of Simplified Model 2 has been shown in Section 7.4.1. The input data is shown in Chapter 5. The material properties applied to the expressions are calculated by the input data and the expressions in Appendix A4 and Appendix A5. The prestress loss are calculated by the expressions in Appendix A6.

Dimensions of Simplified Model 2 are shown in Table 46 to Table 48.

height of cross-section	$h$	0.70 m
width of cross-section	$b$	10.41 m
length of structure	$L$	42.40 m

Table 46: Dimensions of Old Deck in Simplified Model 2.

height of cross-section	$h$	0.70 m
width of cross-section	$b$	9.85 m
length of structure	$L$	42.40 m

Table 47: Dimensions of New Deck in Simplified Model 2.

height of cross-section	$h$	0.70 m
width of cross-section	$b$	0.50 m
length of structure	$L$	42.40 m

Table 48: Dimensions of Connection in Simplified Model 2.

Material properties of prestressing cables in old deck and new deck are shown in Table 49 and Table 50.

elastic modulus	$E_p$	1.95E+11 Pa
area of prestressing cable	$\bar{A}_p$	1.80E-03 m <sup>2</sup>
number of prestressing cable	$n$	25
area of prestressing cables	$A_p$	4.50E-02 m <sup>2</sup>
ratio of area	$\rho_p$	6.12E-03
eccentricity	$e_p$	0.00 m

Table 49: Material Properties of Prestressing Cables in Old Deck.

elastic modulus	$E_p$	1.95E+11 Pa
area of prestressing cable	$\bar{A}_p$	2.85E-03 m <sup>2</sup>
number of prestressing cable	$n$	14
area of prestressing cables	$A_p$	3.99E-02 m <sup>2</sup>
ratio of area	$\rho_p$	5.79E-03
eccentricity	$e_p$	0.00 m

Table 50: Material Properties of Prestressing Cables in New Deck.

Since the prestress in old decks is applied in three steps at time  $t = 3$  days,  $t = 7$  days and  $t = 28$  days respectively (Herepoort, 2007, p. 25), material properties of concrete in old deck at time  $t = 3$  days,  $t = 7$  days and  $t = 28$  days are required, see Table 51, Table 52 and Table 53.

characteristic strength	$f_{ck}$	3.50E+07	Pa
compression strength	$f_{cm}$	4.30E+07	Pa
elastic modulus	$E_{cm}$	3.40E+10	Pa
characteristic strength	$f_{ck}(t)$	3.50E+07	Pa
mean compression strength	$f_{cm}(t)$	5.48E+07	Pa
where:			
factor related to time	$\beta_{cc}(t)$	1.28E+00	
elastic modulus	$E_{cm}(t)$	2.91E+10	Pa

Table 51: Material Properties of Concrete in Old Deck at Time  $t = 3$  days.

characteristic strength	$f_{ck}$	3.50E+07	Pa
compression strength	$f_{cm}$	4.30E+07	Pa
elastic modulus	$E_{cm}$	3.40E+10	Pa
characteristic strength	$f_{ck}(t)$	3.35E+07	Pa
mean compression strength	$f_{cm}(t)$	3.35E+07	Pa
where:			
factor related to time	$\beta_{cc}(t)$	7.79E-01	
elastic modulus	$E_{cm}(t)$	3.15E+10	Pa

Table 52: Material Properties of Concrete in Old Deck at Time  $t = 7$  days.

characteristic strength	$f_{ck}$	3.50E+07	Pa
compression strength	$f_{cm}$	4.30E+07	Pa
elastic modulus	$E_{cm}$	3.40E+10	Pa
characteristic strength	$f_{ck}(t)$	3.50E+07	Pa
mean compression strength	$f_{cm}(t)$	4.30E+07	Pa
where:			
factor related to time	$\beta_{cc}(t)$	1.00E+00	
elastic modulus	$E_{cm}(t)$	3.20E+06	Pa

Table 53: Material Properties of Concrete in Old Deck at Time  $t = 28$  days.

Since the prestress in new deck is applied all in one step at time  $t = 7$  days, material properties of concrete in new deck at time  $t = 7$  days is required, see Table 54.

characteristic strength	$f_{ck}$	4.50E+07	Pa
compression strength	$f_{cm}$	5.30E+07	Pa
elastic modulus	$E_{cm}$	3.60E+10	Pa
characteristic strength	$f_{ck}(t)$	4.50E+07	Pa
mean compression strength	$f_{cm}(t)$	5.37E+07	Pa
where:			
factor related to time	$\beta_{cc}(t)$	1.01E+00	
elastic modulus	$E_{cm}(t)$	3.61E+10	Pa

Table 54: Material Properties of Concrete in New Deck at Time  $t = 7$  days.

## A8.4 Realistic Model 2

The sketch of Realistic Model 2 has been shown in Section 7.4.1. The input data is shown in Chapter 5. The material properties applied to the expressions are calculated by the input data and the expressions in Appendix A4 and Appendix A5. The prestress loss are calculated by the expressions in Appendix A6.

Dimensions of Simplified Model 2 are shown in Table 55 to Table 57.

height of cross-section	$h$	0.70 m
width of cross-section	$b$	10.41 m
length of structure	$L$	42.40 m

Table 55: Dimensions of Old Deck in Simplified Model 2.

height of cross-section	$h$	0.70 m
width of cross-section	$b$	$-0.000092x + 11.8$ m
width of cross-section	$b$	$0.000092x + 7.9$ m
length of structure	$L$	42.40 m

\* $x$  is the distance from certain point to the ends of the deck in [mm], see Figure 71 and Figure 72.

Table 56: Dimensions of New Deck in Simplified Model 2.

height of cross-section	$h$	0.70 m
width of cross-section	$b$	0.50 m
length of structure	$L$	42.40 m

Table 57: Dimensions of Connection in Simplified Model 2.

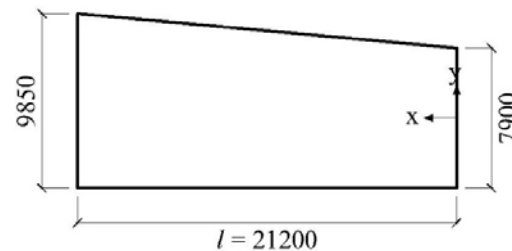
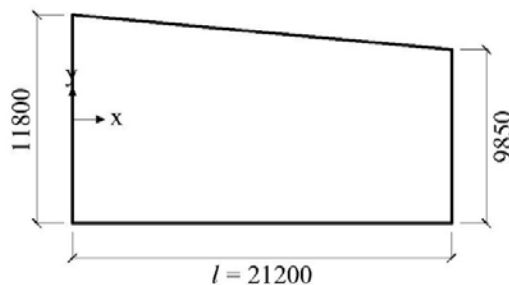


Figure 71: Sketch of Top View of Half Deck 1.

Figure 72: Sketch of Top View of Half Deck 2.

Material properties of prestressing cables in old deck and new deck are shown in Table 58 and Table 59.

elastic modulus	$E_p$	$1.95E+11$ Pa
area of prestressing cable	$\bar{A}_p$	$1.80E-03$ m <sup>2</sup>
number of prestressing cable	$n$	25
area of prestressing cables	$A_p$	$4.50E-02$ m <sup>2</sup>
ratio of area	$\rho_p$	-
eccentricity	$e_p$	0.00 m

\*The ratio of prestress is not shown because it is a function of  $x$ .

Table 58: Material Properties of Prestressing Cables in Old Deck.

elastic modulus	$E_p$	1.95E+11	Pa
area of prestressing cable	$\bar{A}_p$	2.85E-03	m <sup>2</sup>
number of prestressing cable	$n$	14	
area of prestressing cables	$A_p$	3.99E-02	m <sup>2</sup>
ratio of area	$\rho_p$	-	
eccentricity	$e_p$	0.00	m

\*The ratio of prestress is not shown because it is a function of  $x$ .

Table 59: Material Properties of Prestressing Cables in New Deck.

Since the prestress in old decks is applied in three steps at time  $t = 3$  days,  $t = 7$  days and  $t = 28$  days respectively (Herepoort, 2007, p. 25), material properties of concrete in old deck at time  $t = 3$  days,  $t = 7$  days and  $t = 28$  days are required, see Table 60, Table 61 and Table 62.

characteristic strength	$f_{ck}$	3.50E+07	Pa
compression strength	$f_{cm}$	4.30E+07	Pa
elastic modulus	$E_{cm}$	3.40E+10	Pa
characteristic strength	$f_{ck}(t)$	3.50E+07	Pa
mean compression strength	$f_{cm}(t)$	5.48E+07	Pa
where:			
factor related to time	$\beta_{cc}(t)$	1.28E+00	
elastic modulus	$E_{cm}(t)$	2.91E+10	Pa

Table 60: Material Properties of Concrete in Old Deck at Time  $t = 3$  days.

characteristic strength	$f_{ck}$	3.50E+07	Pa
compression strength	$f_{cm}$	4.30E+07	Pa
elastic modulus	$E_{cm}$	3.40E+10	Pa
characteristic strength	$f_{ck}(t)$	3.35E+07	Pa
mean compression strength	$f_{cm}(t)$	3.35E+07	Pa
where:			
factor related to time	$\beta_{cc}(t)$	7.79E-01	
elastic modulus	$E_{cm}(t)$	3.15E+10	Pa

Table 61: Material Properties of Concrete in Old Deck at Time  $t = 7$  days.

characteristic strength	$f_{ck}$	3.50E+07	Pa
compression strength	$f_{cm}$	4.30E+07	Pa
elastic modulus	$E_{cm}$	3.40E+10	Pa
characteristic strength	$f_{ck}(t)$	3.50E+07	Pa
mean compression strength	$f_{cm}(t)$	4.30E+07	Pa
where:			
factor related to time	$\beta_{cc}(t)$	1.00E+00	
elastic modulus	$E_{cm}(t)$	3.20E+06	Pa

Table 62: Material Properties of Concrete in Old Deck at Time  $t = 28$  days.

Since the prestress in new deck is applied all in one step at time  $t = 7$  days, material properties of concrete in new deck at time  $t = 7$  days is required, see Table 63.

characteristic strength	$f_{ck}$	4.50E+07	Pa
compression strength	$f_{cm}$	5.30E+07	Pa
elastic modulus	$E_{cm}$	3.60E+10	Pa
characteristic strength	$f_{ck}(t)$	4.50E+07	Pa
mean compression strength	$f_{cm}(t)$	5.37E+07	Pa
where:			
factor related to time	$\beta_{cc}(t)$	1.01E+00	
elastic modulus	$E_{cm}(t)$	3.61E+10	Pa

Table 63: Material Properties of Concrete in New Deck at Time  $t = 7$  days.

## A9 Calculation of Prestress Loss (Old Deck)

### A9.1 General

As shown in Appendix A7, to investigate whether it is proper or not to calculate imposed deformation and remaining prestressing force as if the prestressing force is applied all in one step at time  $t = 7$  days instead of three steps at time  $t = 3$  days,  $t = 7$  days and  $t = 28$  days, imposed deformation and prestress loss in old decks are calculated in Appendix A7 by both three steps and all in one step. Hereby summarized the data of the calculation carried out in Appendix A7.

The difference between three steps and all in one step is that, for three steps, prestress loss between the steps has to be compensated. Therefore the increment of prestressing force applied to old decks in each step has to be calculated, see Appendix A10.

### A9.2 All in One Step (Old Deck)

Hereby summarized the remaining prestressing force and prestress loss calculated by all in one step, see Table 64 and Table 65. The detailing data of the calculation is shown in Appendix A9.2.1 and Appendix A9.2.2. Since prestressing force is applied all in one step, the prestress loss in Table 64 and Table 65 is same as those shown in Appendix A9.2.1 and Appendix A9.2.2 respectively.

initial prestressing force per cable	$P_{m0}$	2.52E+06	N
mean elastic loss per cable	$\Delta P_{el,mean}$	4.63E+04	N
friction loss per cable	$\Delta P_{\mu}(x)$	1.96E+05	N
shrinkage loss of per cable	$\Delta P_{shr}(t)$	8.05E+04	N
creep loss of per cable	$\Delta P_{cr}(t)$	8.91E+04	N
relaxation loss per cable	$\Delta P_r(t)$	9.24E+04	N
final prestressing force per cable	$P_{m\infty}$	2.02E+06	N

Table 64: Prestress Loss and Remaining Prestressing Force Calculated by All in One Step at time  $t = 11$  years.

initial prestressing force per cable	$P_{m0}$	2.52E+06	N
mean elastic loss per cable	$\Delta P_{el,mean}$	4.63E+04	N
friction loss per cable	$\Delta P_{\mu}(x)$	1.96E+05	N
shrinkage loss of per cable	$\Delta P_{shr}(t)$	8.05E+04	N
creep loss of per cable	$\Delta P_{cr}(t)$	8.91E+04	N
relaxation loss per cable	$\Delta P_r(t)$	9.24E+04	N
final prestressing force per cable	$P_{m\infty}$	2.02E+06	N
<b>final prestressing force of cables</b>	$P_{m\infty}$	<b>4.93E+07</b>	<b>N</b>
<b>stress resulting from prestressing</b>	$\sigma_{p\infty}$	<b>6.76E+06</b>	<b>Pa</b>

Table 65: Prestress Loss and Remaining Prestressing Force Calculated by All in One Step at time  $t = 111$  years.

### A9.2.1 Calculation Related to $P_{1,7-t_\infty}$ ( $t_\infty = 11 \text{ years} + 29 \text{ days}$ )

$P_{1,7-t_\infty}$  represents the prestressing force applied all in one step from time  $t = 7$  days to  $t = 11 \text{ years} + 29$  days.

#### initial prestressing force

original increment <b>per cable</b>	$\Delta P_{max,1}$	2.52E+06	N
where:			
initial prestressing force <b>per cable</b>	$P_{m0}$	2.52E+06	N

Table 66: Immediate Loss of Step 1 from Time  $t = 7$  days to Time  $t = 11 \text{ years} + 29$  days.

#### elastic loss

mean elastic loss <b>per cable</b>	$\Delta P_{el,mean}(t)$	4.63E+04	N
where:			
factor related to number of tendon	$j$	0.48	
initial prestressing force <b>per cable</b>	$P_{m0}$	2.52E+06	N
variation of prestress	$\Delta \sigma_{el,mean}$	8.66E+06	N/m <sup>2</sup>

Table 67: Elastic Loss of Step 1 from Time  $t = 7$  days to Time  $t = 11 \text{ years} + 29$  days.

#### friction loss

friction loss <b>per cable</b>	$\Delta P_\mu(x)$	1.96E+05	N
where:			
factor of friction	$\mu$	0.19	
angular rotation	$\theta$	0.21	rad
wobble effect	$k$	0.01	rad/m

Table 68: Friction Loss of Step 1 from Time  $t = 7$  days to Time  $t = 11 \text{ years} + 29$  days.

**shrinkage loss**

shrinkage loss of <b>cables</b>	$\Delta P_{shr}(t)$	2.01E+06	N
shrinkage loss of <b>per cable</b>	$\Delta P_{shr}(t)$	8.05E+04	N
where:			
shrinkage	$\varepsilon_{cs}$	2.29E-04	m/m
final drying shrinkage	$\varepsilon_{cd}(t)$	1.78E-04	m/m
initial drying shrinkage	$\varepsilon_{cd,0}$	3.00E-04	m/m
factor related to cement	$\alpha_{ds1}$	4.00	
	$\alpha_{ds2}$	0.12	
factor	$f_{cm0}$	1.00E+07	Pa
factor	$RH_0$	100.00	%
factor	$\beta_{RH}$	0.90	
factor related to notional size	$k_h$	0.70	
factor	$\beta_{ts}(t, t_s)$	0.86	
factor	$\beta_{ts}(t_p, t_s)$	0.01	
time at the end of curing	$t_s$	1.00	days
final autogenous shrinkage	$\varepsilon_{ca}(t)$	5.12E-05	m/m
initial autogenous shrinkage	$\varepsilon_{ca}(\infty)$	6.25E-05	m/m
factor	$\beta_{as}(t)$	1.00	
factor	$\beta_{as}(t_s)$	0.18	

Table 69: Shrinkage Loss of Step 1 from Time  $t = 3$  days to Time  $t = 11$  years + 29 days.

**creep loss**

creep loss of <b>per cable</b>	$\Delta P_{cr}(t)$	8.91E+04	N
where:			
creep strain at ends	$\varepsilon_{cc,mean}(t)$	2.54E-04	m/m

Table 70: Creep Loss of Step 1 from Time  $t = 7$  days to Time  $t = 11$  years + 29 days.

**relaxation loss**

relaxation loss <b>per cable</b>	$\Delta P_r(t)$	9.24E+04	N
where:			
variation of prestress	$\Delta \sigma_{pr}$	5.13E+07	Pa
initial prestress per cable	$\sigma_{pi}$	1.40E+09	Pa
factor	$\mu$	0.75	
relaxation loss at 1000 hrs	$\rho_{1000}$	2.50	%

Table 71: Relaxation Loss of Step 1 from Time  $t = 7$  days to Time  $t = 11$  years + 29 days.

### A9.2.2 Calculation Related to $P_{1,7-t_{\infty}}$ ( $t_{\infty} = 111$ years)

$P_{1,7-t_{\infty}}$  represents the prestressing force applied in all in one step from time  $t = 7$  days to  $t = 111$  years.

#### initial prestressing force

original increment <b>per cable</b>	$\Delta P_{max,1}$	2.52E+06	N
where:			
initial prestressing force <b>per cable</b>	$P_{m0}$	2.52E+06	N

Table 72: Immediate Loss of Step 1 from Time  $t = 7$  days to Time  $t = 111$  years.

#### elastic loss

mean elastic loss <b>per cable</b>	$\Delta P_{el,mean}(t)$	4.63E+04	N
where:			
factor related to number of tendon	$j$	0.48	
initial prestressing force <b>per cable</b>	$P_{m0}$	2.52E+06	N
variation of prestress	$\Delta \sigma_{el,mean}$	8.66E+06	N/m <sup>2</sup>

Table 73: Elastic Loss of Step 1 from Time  $t = 7$  days to Time  $t = 111$  years.

#### friction loss

friction loss <b>per cable</b>	$\Delta P_{\mu}(x)$	1.96E+05	N
where:			
factor of friction	$\mu$	0.19	
angular rotation	$\theta$	0.21	rad
wobble effect	$k$	0.01	rad/m

Table 74: Friction Loss of Step 1 from Time  $t = 7$  days to Time  $t = 111$  years.

### shrinkage loss

shrinkage loss of <b>cables</b>	$\Delta P_{shr}(t)$	2.25E+06	N
shrinkage loss of <b>per cable</b>	$\Delta P_{shr}(t)$	8.98E+04	N
where:			
shrinkage	$\varepsilon_{cs}$	2.56E-04	m/m
final drying shrinkage	$\varepsilon_{cd}(t)$	2.05E-04	m/m
initial drying shrinkage	$\varepsilon_{cd,0}$	3.00E-04	m/m
factor related to cement	$\alpha_{ds1}$	4.00	
	$\alpha_{ds2}$	0.12	
factor	$f_{cm0}$	1.00E+07	Pa
factor	$RH_0$	100.00	%
factor	$\beta_{RH}$	0.90	
factor related to notional size	$k_h$	0.70	
factor	$\beta_{ts}(t, t_s)$	0.98	
factor	$\beta_{ts}(t_p, t_s)$	0.01	
time at the end of curing	$t_s$	1.00	days
final autogenous shrinkage	$\varepsilon_{ca}(t)$	5.12E-05	m/m
initial autogenous shrinkage	$\varepsilon_{ca}(\infty)$	6.25E-05	m/m
factor	$\beta_{as}(t)$	1.00	
factor	$\beta_{as}(t_s)$	0.18	

Table 75: Shrinkage Loss of Step 1 from Time  $t = 3$  days to Time  $t = 111$  years.

### creep loss

creep loss of <b>per cable</b>	$\Delta P_{cr}(t)$	9.63E+04	N
where:			
creep strain at ends	$\varepsilon_{cc,mean}(t)$	2.75E-04	m/m

Table 76: Creep Loss of Step 1 from Time  $t = 7$  days to Time  $t = 111$  years.

### relaxation loss

relaxation loss <b>per cable</b>	$\Delta P_r(t)$	1.25E+05	N
where:			
variation of prestress	$\Delta \sigma_{pr}$	6.95E+07	Pa
initial prestress per cable	$\sigma_{pi}$	1.40E+09	Pa
factor	$\mu$	0.75	
relaxation loss at 1000 hrs	$\rho_{1000}$	2.50	%

Table 77: Relaxation Loss of Step 1 from Time  $t = 7$  days to Time  $t = 111$  years.

### A9.3 Three Steps (Old Deck)

Hereby summarized the remaining prestressing force and prestress loss calculated by three steps, see Table 78 and Table 79. The detailing data of the calculation is shown in Appendix A9.3.1 to Appendix A9.3.6.

As for Table 78, mean elastic loss, friction loss and creep loss are the summation of those shown in Appendix A9.3.1 to Appendix A9.3.3 while shrinkage loss and relaxation loss are only from Appendix A9.3.3. Similarly, when it comes to Table 79, mean elastic loss, friction loss and creep loss are the summation of those shown in Appendix A9.3.4 to Appendix A9.3.6 while shrinkage loss and relaxation loss are only from Appendix A9.3.6.

initial prestressing force per cable	$P_{m0}$	2.65E+06	N
mean elastic loss per cable	$\Delta P_{el,mean}$	4.78E+04	N
friction loss per cable	$\Delta P_{\mu}(x)$	2.06E+05	N
shrinkage loss of per cable	$\Delta P_s(t)$	7.83E+04	N
creep loss of per cable	$\Delta P_{cr}(t)$	8.72E+04	N
relaxation loss per cable	$\Delta P_r(t)$	9.23E+04	N
final prestressing force per cable	$P_{m\infty}$	2.14E+06	N

Table 78: Prestress Loss and Remaining Prestressing Force Calculated by Three Steps at time  $t = 11$  years.

initial prestressing force per cable	$P_{m0}$	2.65E+06	N
mean elastic loss per cable	$\Delta P_{el,mean}$	4.78E+04	N
friction loss per cable	$\Delta P_{\mu}(x)$	2.06E+05	N
shrinkage loss of per cable	$\Delta P_s(t)$	8.76E+04	N
creep loss of per cable	$\Delta P_{cr}(t)$	9.42E+04	N
relaxation loss per cable	$\Delta P_r(t)$	1.25E+05	N
final prestressing force per cable	$P_{m\infty}$	2.09E+06	N
<b>final prestressing force of cables</b>	<b><math>P_{m\infty}</math></b>	<b>5.22E+07</b>	<b>N</b>
<b>stress resulting from prestressing</b>	<b><math>\sigma_{p\infty}</math></b>	<b>7.16E+06</b>	<b>Pa</b>

Table 79: Prestress Loss and Remaining Prestressing Force Calculated by Three Steps at time  $t = 111$  years.

### A9.3.1 Calculation Related to $P_{1,3-t_\infty}$ ( $t_\infty = 11 \text{ years} + 29 \text{ days}$ )

$P_{1,3-t_\infty}$  represents the prestressing force applied in the first of three steps, or in short Step 1, from  $t = 3$  days to  $t = 11$  years.

#### initial prestressing force

original increment <b>per cable</b>	$\Delta P_{max,1}$	5.05E+05	N
where:			
initial prestressing force <b>per cable</b>	$P_{m0}$	5.05E+05	N

Table 80: Immediate Loss of Step 1 from Time  $t = 3$  days to Time  $t = 11$  years + 29 days.

#### elastic loss

mean elastic loss <b>per cable</b>	$\Delta P_{el,mean}(t)$	1.00E+04	N
where:			
factor related to number of tendon	$j$	0.48	
initial prestressing force <b>per cable</b>	$P_{m0}$	5.05E+05	N
variation of prestress	$\Delta \sigma_{el,mean}$	1.73E+06	N/m <sup>2</sup>

Table 81: Elastic Loss of Step 1 from Time  $t = 3$  days to Time  $t = 11$  years + 29 days.

#### friction loss

friction loss <b>per cable</b>	$\Delta P_\mu(x)$	3.93E+04	N
where:			
factor of friction	$\mu$	0.19	
angular rotation	$\theta$	0.21	rad
wobble effect	$k$	0.01	rad/m

Table 82: Friction Loss of Step 1 from Time  $t = 3$  days to Time  $t = 11$  years + 29 days.

**shrinkage loss**

shrinkage loss of <b>cables</b>	$\Delta P_{shr}(t)$	2.02E+06	N
shrinkage loss of <b>per cable</b>	$\Delta P_{shr}(t)$	8.10E+04	N
where:			
shrinkage	$\epsilon_{cs}$	2.31E-04	m/m
final drying shrinkage	$\epsilon_{cd}(t)$	1.80E-04	m/m
initial drying shrinkage	$\epsilon_{cd,0}$	3.00E-04	m/m
factor related to cement	$\alpha_{ds1}$	4.00	
	$\alpha_{ds2}$	0.12	
factor	$f_{cm0}$	1.00E+07	Pa
factor	$RH_0$	100.00	%
factor	$\beta_{RH}$	0.90	
factor related to notional size	$k_h$	0.70	
factor	$\beta_{ts}(t, t_s)$	0.86	
factor	$\beta_{ts}(t_p, t_s)$	0.00	
time at the end of curing	$t_s$	1.00	days
final autogenous shrinkage	$\epsilon_{ca}(t)$	5.12E-05	m/m
initial autogenous shrinkage	$\epsilon_{ca}(\infty)$	6.25E-05	m/m
factor	$\beta_{as}(t)$	1.00	
factor	$\beta_{as}(t_s)$	0.18	

Table 83: Shrinkage Loss of Step 1 from Time  $t = 3$  days to Time  $t = 11$  years + 29 days.

**creep loss**

creep loss of <b>per cable</b>	$\Delta P_{cr}(t)$	2.26E+04	N
where:			
creep strain at ends	$\epsilon_{cc,mean}(t)$	6.44E-05	m/m

Table 84: Creep Loss of Step 1 from Time  $t = 3$  days to Time  $t = 11$  years + 29 days.

**relaxation loss**

relaxation loss <b>per cable</b>	$\Delta P_r(t)$	6.06E+02	N
where:			
variation of prestress	$\Delta \sigma_{pr}$	3.36E+05	Pa
initial prestress per cable	$\sigma_{pi}$	2.81E+08	Pa
factor	$\mu$	0.15	
relaxation loss at 1000 hrs	$\rho_{1000}$	2.50	%

Table 85: Relaxation Loss of Step 1 from Time  $t = 3$  days to Time  $t = 11$  years + 29 days.

### A9.3.2 Calculation Related to $P_{2,7-t_\infty}$ ( $t_\infty = 11 \text{ years} + 29 \text{ days}$ )

$P_{2,7-t_\infty}$  represents the prestressing force applied in the second of three steps, or in short Step 2, from time  $t = 7$  days to  $t = 11$  years.

#### initial prestressing force

original increment <b>per cable</b>	$\Delta P_{max,2}$	1.05E+06	N
where:			
initial prestressing force <b>per cable</b>	$P_{m0}$	1.05E+06	N

Table 86: Immediate Loss of Step 2 from Time  $t = 7$  days to Time  $t = 11 \text{ years} + 29 \text{ days}$ .

#### elastic loss

mean elastic loss <b>per cable</b>	$\Delta P_{el,mean}(t)$	1.92E+04	N
where:			
factor related to number of tendon	$j$	0.48	
initial prestressing force <b>per cable</b>	$P_{m0}$	1.05E+06	N
variation of prestress	$\Delta \sigma_{el,mean}$	3.60E+06	N/m <sup>2</sup>

Table 87: Elastic Loss of Step 2 from Time  $t = 7$  days to Time  $t = 11 \text{ years} + 29 \text{ days}$ .

#### friction loss

friction loss <b>per cable</b>	$\Delta P_\mu(x)$	8.15E+04	N
where:			
factor of friction	$\mu$	0.19	
angular rotation	$\theta$	0.21	rad
wobble effect	$k$	0.01	rad/m

Table 88: Friction Loss of Step 2 from Time  $t = 7$  days to Time  $t = 11 \text{ years} + 29 \text{ days}$ .

**shrinkage loss**

shrinkage loss of <b>cables</b>	$\Delta P_{shr}(t)$	2.01E+06	N
shrinkage loss of <b>per cable</b>	$\Delta P_{shr}(t)$	8.05E+04	N
where:			
shrinkage	$\varepsilon_{cs}$	2.29E-04	m/m
final drying shrinkage	$\varepsilon_{cd}(t)$	1.78E-04	m/m
initial drying shrinkage	$\varepsilon_{cd,0}$	3.00E-04	m/m
factor related to cement	$\alpha_{ds1}$	4.00	
	$\alpha_{ds2}$	0.12	
factor	$f_{cm0}$	1.00E+07	Pa
factor	$RH_0$	100.00	%
factor	$\beta_{RH}$	0.90	
factor related to notional size	$k_h$	0.70	
factor	$\beta_{ts}(t, t_s)$	0.86	
factor	$\beta_{ts}(t_p, t_s)$	0.01	
time at the end of curing	$t_s$	1.00	days
final autogenous shrinkage	$\varepsilon_{ca}(t)$	5.12E-05	m/m
initial autogenous shrinkage	$\varepsilon_{ca}(\infty)$	6.25E-05	m/m
factor	$\beta_{as}(t)$	1.00	
factor	$\beta_{as}(t_s)$	0.18	

Table 89: Shrinkage Loss of Step 2 from Time  $t = 7$  days to Time  $t = 11$  years + 29 days.

**creep loss**

creep loss of <b>per cable</b>	$\Delta P_{cr}(t)$	3.70E+04	N
where:			
creep strain at ends	$\varepsilon_{cc,mean}(t)$	1.06E-04	m/m

Table 90: Creep Loss of Step 2 from Time  $t = 7$  days to Time  $t = 11$  years + 29 days.

**relaxation loss**

relaxation loss <b>per cable</b>	$\Delta P_r(t)$	1.00E+04	N
where:			
variation of prestress	$\Delta \sigma_{pr}$	5.57E+06	Pa
initial prestress per cable	$\sigma_{pi}$	8.41E+08	Pa
factor	$\mu$	0.45	
relaxation loss at 1000 hrs	$\rho_{1000}$	2.50	%

Table 91: Relaxation Loss of Step 2 from Time  $t = 7$  days to Time  $t = 11$  years + 29 days.

### A9.3.3 Calculation Related to $P_{3,28-t_\infty}$ ( $t_\infty = 11 \text{ years} + 29 \text{ days}$ )

$P_{3,28-t_\infty}$  represents the prestressing force applied in the third of three steps, or in short Step 3, from time  $t = 28$  days to  $t = 11$  years.

#### initial prestressing force

original increment <b>per cable</b>	$\Delta P_{max,3}$	1.09E+06	N
where:			
initial prestressing force <b>per cable</b>	$P_{m0}$	1.09E+06	N

Table 92: Immediate Loss of Step 3 from Time  $t = 28$  days to Time  $t = 11$  years + 29 days.

#### elastic loss

mean elastic loss <b>per cable</b>	$\Delta P_{el,mean}(t)$	1.88E+04	N
where:			
factor related to number of tendon	$j$	0.48	
initial prestressing force <b>per cable</b>	$P_{m0}$	1.11E+06	N
variation of prestress	$\Delta \sigma_{el,mean}$	3.75E+06	N/m <sup>2</sup>

Table 93: Elastic Loss of Step 3 from Time  $t = 28$  days to Time  $t = 11$  years + 29 days.

#### friction loss

friction loss <b>per cable</b>	$\Delta P_\mu(x)$	8.51E+04	N
where:			
factor of friction	$\mu$	0.19	
angular rotation	$\theta$	0.21	rad
wobble effect	$k$	0.01	rad/m

Table 94: Friction Loss of Step 3 from Time  $t = 28$  days to Time  $t = 11$  years + 29 days.

### shrinkage loss

shrinkage loss of <b>cables</b>	$\Delta P_{shr}(t)$	1.96E+06	N
shrinkage loss of <b>per cable</b>	$\Delta P_{shr}(t)$	7.83E+04	N
where:			
shrinkage	$\varepsilon_{cs}$	2.23E-04	m/m
final drying shrinkage	$\varepsilon_{cd}(t)$	1.72E-04	m/m
initial drying shrinkage	$\varepsilon_{cd,0}$	3.00E-04	m/m
factor related to cement	$\alpha_{ds1}$	4.00	
	$\alpha_{ds2}$	0.12	
factor	$f_{cm0}$	1.00E+07	Pa
factor	$RH_0$	100.00	%
factor	$\beta_{RH}$	0.90	
factor related to notional size	$k_h$	0.70	
factor	$\beta_{ts}(t, t_s)$	0.86	
factor	$\beta_{ts}(t_p, t_s)$	0.04	
time at the end of curing	$t_s$	1.00	days
final autogenous shrinkage	$\varepsilon_{ca}(t)$	5.12E-05	m/m
initial autogenous shrinkage	$\varepsilon_{ca}(\infty)$	6.25E-05	m/m
factor	$\beta_{as}(t)$	1.00	
factor	$\beta_{as}(t_s)$	0.18	

Table 95: Shrinkage Loss of Step 3 from Time  $t = 28$  days to Time  $t = 11$  years + 29 days.

### creep loss

creep loss of <b>per cable</b>	$\Delta P_{cr}(t)$	2.79E+04	N
where:			
creep strain at ends	$\varepsilon_{cc,mean}(t)$	7.94E-05	m/m

Table 96: Creep Loss of Step 3 from Time  $t = 28$  days to Time  $t = 11$  years + 29 days.

### relaxation loss

relaxation loss <b>per cable</b>	$\Delta P_r(t)$	9.23E+04	N
where:			
variation of prestress	$\Delta \sigma_{pr}$	5.13E+07	Pa
initial prestress per cable	$\sigma_{pi}$	1.40E+09	Pa
factor	$\mu$	0.75	
relaxation loss at 1000 hrs	$\rho_{1000}$	2.50	%

Table 97: Relaxation Loss of Step 3 from Time  $t = 28$  days to Time  $t = 11$  years + 29 days.

### A9.3.4 Calculation Related to $P_{1,3-t_\infty}$ ( $t_\infty = 111$ years)

$P_{1,3-t_\infty}$  represents the prestressing force applied in the first of three steps, or in short Step 1, from time  $t = 3$  days to  $t = 111$  years.

#### immediate loss

original increment <b>per cable</b>	$\Delta P_{max,1}$	5.05E+05	N
where:			
initial prestressing force <b>per cable</b>	$P_{m0}$	5.05E+05	N

Table 98: Immediate Loss of Step 1 from Time  $t = 3$  days to Time  $t = t_\infty$  days.

#### elastic loss

mean elastic loss <b>per cable</b>	$\Delta P_{el,mean}(t)$	1.00E+04	N
where:			
factor related to number of tendon	$j$	0.48	
initial prestressing force <b>per cable</b>	$P_{m0}$	5.05E+05	N
variation of prestress	$\Delta \sigma_{el,mean}$	1.73E+06	N/m <sup>2</sup>

Table 99: Elastic Loss of Step 1 from Time  $t = 3$  days to Time  $t = t_\infty$  days.

#### friction loss

friction loss <b>per cable</b>	$\Delta P_\mu(x)$	3.93E+04	N
where:			
factor of friction	$\mu$	0.19	
angular rotation	$\theta$	0.21	rad
wobble effect	$k$	0.01	rad/m

Table 100: Friction Loss of Step 1 from Time  $t = 3$  days to Time  $t = t_\infty$  days.

**shrinkage loss**

shrinkage loss of <b>cables</b>	$\Delta P_{shr}(t)$	2.26E+06	N
shrinkage loss of <b>per cable</b>	$\Delta P_{shr}(t)$	9.03E+04	N
where:			
shrinkage	$\varepsilon_{cs}$	2.57E-04	m/m
final drying shrinkage	$\varepsilon_{cd}(t)$	2.06E-04	m/m
initial drying shrinkage	$\varepsilon_{cd,0}$	3.00E-04	m/m
factor related to cement	$\alpha_{ds1}$	4.00	
	$\alpha_{ds2}$	0.12	
factor	$f_{cm0}$	1.00E+07	Pa
factor	$RH_0$	100.00	%
factor	$\beta_{RH}$	0.90	
factor related to notional size	$k_h$	0.70	
factor	$\beta_{is}(t, t_s)$	0.98	
factor	$\beta_{is}(t_p, t_s)$	0.00	
time at the end of curing	$t_s$	1.00	days
final autogenous shrinkage	$\varepsilon_{ca}(t)$	5.12E-05	m/m
initial autogenous shrinkage	$\varepsilon_{ca}(\infty)$	6.25E-05	m/m
factor	$\beta_{as}(t)$	1.00	
factor	$\beta_{as}(t_s)$	0.18	

Table 101: Shrinkage Loss of Step 1 from Time  $t = 3$  days to Time  $t = t_\infty$  days.

**creep loss**

creep loss of <b>per cable</b>	$\Delta P_{cr}(t)$	2.44E+04	N
where:			
creep strain	$\varepsilon_{cc}(t)$	6.95E-05	m/m

Table 102: Creep Loss of Step 1 from Time  $t = 3$  days to Time  $t = t_\infty$  days.

**relaxation loss**

relaxation loss <b>per cable</b>	$\Delta P_r(t)$	1.72E+03	N
where:			
variation of prestress	$\Delta \sigma_{pr}$	9.56E+05	Pa
initial prestress per cable	$\sigma_{pi}$	2.81E+08	Pa
factor	$\mu$	0.15	
relaxation loss at 1000 hrs	$\rho_{1000}$	2.50	%

Table 103: Relaxation Loss of Step 1 from Time  $t = 3$  days to Time  $t = t_\infty$  days.

### A9.3.5 Calculation Related to $P_{2,7-t_\infty}$ ( $t_\infty = 111$ years)

$P_{2,7-t_\infty}$  represents the prestressing force applied in the second of three steps, or in short Step 2, from time  $t = 7$  days to  $t = 111$  years.

#### immediate loss

original increment <b>per cable</b>	$\Delta P_{max,2}$	1.05E+06	N
where:			
initial prestressing force <b>per cable</b>	$P_{m0}$	1.05E+06	N

Table 104: Immediate Loss of Step 2 from Time  $t = 7$  days to Time  $t = t_\infty$  days.

#### elastic loss

mean elastic loss <b>per cable</b>	$\Delta P_{el,mean}(t)$	1.92E+04	N
where:			
factor related to number of tendon	$j$	0.48	
initial prestressing force <b>per cable</b>	$P_{m0}$	1.05E+06	N
variation of prestress	$\Delta \sigma_{el,mean}$	3.60E+06	N/m <sup>2</sup>

Table 105: Elastic Loss of Step 2 from Time  $t = 7$  days to Time  $t = t_\infty$  days.

#### friction loss

friction loss <b>per cable</b>	$\Delta P_\mu(x)$	8.15E+04	N
where:			
factor of friction	$\mu$	0.19	
angular rotation	$\theta$	0.21	rad
wobble effect	$k$	0.01	rad/m

Table 106: Friction Loss of Step 2 from Time  $t = 7$  days to Time  $t = t_\infty$  days.

**shrinkage loss**

shrinkage loss of <b>cables</b>	$\Delta P_{shr}(t)$	2.25E+06	N
shrinkage loss of <b>per cable</b>	$\Delta P_{shr}(t)$	8.98E+04	N
where:			
shrinkage	$\varepsilon_{cs}$	2.56E-04	m/m
final drying shrinkage	$\varepsilon_{cd}(t)$	2.05E-04	m/m
initial drying shrinkage	$\varepsilon_{cd,0}$	3.00E-04	m/m
factor related to cement	$\alpha_{ds1}$	4.00	
	$\alpha_{ds2}$	0.12	
factor	$f_{cm0}$	1.00E+07	Pa
factor	$RH_0$	100.00	%
factor	$\beta_{RH}$	0.90	
factor related to notional size	$k_h$	0.70	
factor	$\beta_{is}(t, t_s)$	0.98	
factor	$\beta_{is}(t_p, t_s)$	0.01	
time at the end of curing	$t_s$	1.00	days
final autogenous shrinkage	$\varepsilon_{ca}(t)$	5.12E-05	m/m
initial autogenous shrinkage	$\varepsilon_{ca}(\infty)$	6.25E-05	m/m
factor	$\beta_{as}(t)$	1.00	
factor	$\beta_{as}(t_s)$	0.18	

Table 107: Shrinkage Loss of Step 2 from Time  $t = 7$  days to Time  $t = t_\infty$  days.

**creep loss**

creep loss of <b>per cable</b>	$\Delta P_{cr}(t)$	4.00E+04	N
where:			
creep strain	$\varepsilon_{cc}(t)$	1.14E-04	m/m

Table 108: Creep Loss of Step 2 from Time  $t = 7$  days to Time  $t = t_\infty$  days.

**relaxation loss**

relaxation loss <b>per cable</b>	$\Delta P_r(t)$	1.97E+04	N
where:			
variation of prestress	$\Delta \sigma_{pr}$	1.09E+07	Pa
initial prestress per cable	$\sigma_{pi}$	8.41E+08	Pa
factor	$\mu$	0.45	
relaxation loss at 1000 hrs	$\rho_{1000}$	2.50	%

Table 109: Relaxation Loss of Step 2 from Time  $t = 7$  days to Time  $t = t_\infty$  days.

### A9.3.6 Calculation Related to $P_{3,28-t_\infty}$ ( $t_\infty = 111$ years)

$P_{3,28-t_\infty}$  represents the prestressing force applied in the third of three steps, or in short Step 3, from time  $t = 28$  days to  $t = 111$  years.

#### immediate loss

original increment <b>per cable</b>	$\Delta P_{max,3}$	1.09E+06	N
where:			
initial prestressing force <b>per cable</b>	$P_{m0}$	1.09E+06	N

Table 110: Immediate Loss of Step 3 from Time  $t = 28$  days to Time  $t = t_\infty$  days.

#### elastic loss

mean elastic loss <b>per cable</b>	$\Delta P_{el,mean}(t)$	1.86E+04	N
where:			
factor related to number of tendon	$j$	0.48	
initial prestressing force <b>per cable</b>	$P_{m0}$	1.09E+06	N
variation of prestress	$\Delta \sigma_{el,mean}$	3.75E+06	N/m <sup>2</sup>

Table 111: Elastic Loss of Step 3 from Time  $t = 28$  days to Time  $t = t_\infty$  days.

#### friction loss

friction loss <b>per cable</b>	$\Delta P_\mu(x)$	8.51E+04	N
where:			
factor of friction	$\mu$	0.19	
angular rotation	$\theta$	0.21	rad
wobble effect	$k$	0.01	rad/m

Table 112: Friction Loss of Step 3 from Time  $t = 28$  days to Time  $t = t_\infty$  days.

**shrinkage loss**

shrinkage loss of <b>cables</b>	$\Delta P_{shr}(t)$	2.19E+06	N
shrinkage loss of <b>per cable</b>	$\Delta P_{shr}(t)$	8.76E+04	N
where:			
shrinkage	$\varepsilon_{cs}$	2.50E-04	m/m
final drying shrinkage	$\varepsilon_{cd}(t)$	1.99E-04	m/m
initial drying shrinkage	$\varepsilon_{cd,0}$	3.00E-04	m/m
factor related to cement	$\alpha_{ds1}$	4.00	
	$\alpha_{ds2}$	0.12	
factor	$f_{cm0}$	1.00E+07	Pa
factor	$RH_0$	100.00	%
factor	$\beta_{RH}$	0.90	
factor related to notional size	$k_h$	0.70	
factor	$\beta_{is}(t, t_s)$	0.98	
factor	$\beta_{is}(t_p, t_s)$	0.04	
time at the end of curing	$t_s$	1.00	days
final autogenous shrinkage	$\varepsilon_{ca}(t)$	5.12E-05	m/m
initial autogenous shrinkage	$\varepsilon_{ca}(\infty)$	6.25E-05	m/m
factor	$\beta_{as}(t)$	1.00	
factor	$\beta_{as}(t_s)$	0.18	

Table 113: Shrinkage Loss of Step 3 from Time  $t = 28$  days to Time  $t = t_\infty$  days.

**creep loss**

creep loss of <b>per cable</b>	$\Delta P_{cr}(t)$	2.98E+04	N
where:			
creep strain	$\varepsilon_{cc}(t)$	8.49E-05	m/m

Table 114: Creep Loss of Step 3 from Time  $t = 28$  days to Time  $t = t_\infty$  days.

**relaxation loss**

relaxation loss <b>per cable</b>	$\Delta P_r(t)$	1.25E+05	N
where:			
variation of prestress	$\Delta \sigma_{pr}$	6.95E+07	Pa
initial prestress per cable	$\sigma_{pi}$	1.40E+09	Pa
factor	$\mu$	0.75	
relaxation loss at 1000 hrs	$\rho_{1000}$	2.50	%

Table 115: Relaxation Loss of Step 3 from Time  $t = 28$  days to Time  $t = t_\infty$  days.

## A10 Calculation of Increment of Prestressing Force Applied in Each Step (Old Deck)

### A10.1 Calculation of $\Delta P_{1,3-7}$ (Old Deck)

$\Delta P_{1,3-7}$  represents the prestress loss of Step 1 which appears between Step 1 and Step 2 from time  $t = 3$  days to  $t = 7$  days. As shown in Appendix A7.1, prestressing force in old deck at the end of Step 1 is  $P_1 = 505$  kN. Therefore, the original increment of prestressing force in Step 1 is as follow:

$$\Delta P_{max,1} = 505 \text{ kN}$$

Then  $\Delta P_{1,3-7}$  is as follow:

$$\Delta P_{1,3-7} = \Delta P_{el,mean} + \Delta P_{\mu} + \Delta P_{cr} + \Delta P_r + \Delta P_{shr}/n = 40 \text{ kN} \quad (42)$$

#### initial prestressing force

original increment <b>per cable</b>	$\Delta P_{max,1}$	5.05E+05 N
where:		
initial prestressing force <b>per cable</b>	$P_{m0}$	5.05E+05 N

Table 116: Immediate Loss of Step 1 from Time  $t = 3$  days to Time  $t = 7$  days.

#### elastic loss

mean elastic loss <b>per cable</b>	$\Delta P_{el,mean}(t)$	1.00E+04 N
where:		
factor related to number of tendon	$j$	0.48
initial prestressing force <b>per cable</b>	$P_{m0}$	5.05E+05 N
variation of prestress	$\Delta \sigma_{el,mean}$	1.73E+06 N/m <sup>2</sup>

Table 117: Elastic Loss of Step 1 from Time  $t = 3$  days to Time  $t = 7$  days.

#### friction loss

friction loss <b>per cable</b>	$\Delta P_{\mu}(\theta)$	2.01E+04 N
where:		
factor of friction	$\mu$	0.19
angular rotation	$\theta$	0.21 rad
wobble effect	$k$	0.01 rad/m

Table 118: Friction Loss of Step 1 from Time  $t = 3$  days to Time  $t = 7$  days.

**shrinkage loss**

shrinkage loss of <b>cables</b>	$\Delta P_{shr}(t)$	1.37E+05	N
shrinkage loss of <b>per cable</b>	$\Delta P_{shr}(t)$	<b>5.47E+03</b>	N
where:			
shrinkage	$\varepsilon_{cs}$	1.56E-05	m/m
final drying shrinkage	$\varepsilon_{cd}(t)$	1.23E-06	m/m
initial drying shrinkage	$\varepsilon_{cd,0}$	3.00E-04	m/m
factor related to cement	$\alpha_{ds1}$	4.00	
	$\alpha_{ds2}$	0.12	
factor	$f_{cm0}$	1.00E+07	Pa
factor	$RH_0$	100.00	%
factor	$\beta_{RH}$	0.90	
factor related to notional size	$k_h$	0.70	
factor	$\beta_{ts}(t, t_s)$	0.01	
factor	$\beta_{ts}(t_p, t_s)$	0.00	
time at the end of curing	$t_s$	1.00	days
final autogenous shrinkage	$\varepsilon_{ca}(t)$	1.44E-05	m/m
initial autogenous shrinkage	$\varepsilon_{ca}(\infty)$	6.25E-05	m/m
factor	$\beta_{as}(t)$	0.41	
factor	$\beta_{as}(t_s)$	0.18	

Table 119: Shrinkage Loss of Step 1 from Time  $t = 3$  days to Time  $t = 7$  days.

**creep loss**

creep loss of <b>per cable</b>	$\Delta P_{cr}(t)$	<b>4.29E+03</b>	N
where:			
creep strain at ends	$\varepsilon_{cc,mean}(t)$	1.22E-05	m/m

Table 120: Creep Loss of Step 1 from Time  $t = 3$  days to Time  $t = 7$  days.

**relaxation loss**

relaxation loss <b>per cable</b>	$\Delta P_r(t)$	<b>7.39E+00</b>	N
where:			
variation of prestress	$\Delta \sigma_{pr}$	4.11E+03	Pa
initial prestress per cable	$\sigma_{pi}$	2.81E+08	Pa
factor	$\mu$	0.15	
relaxation loss at 1000 hrs	$\rho_{1000}$	2.50	%

Table 121: Relaxation Loss of Step 1 from Time  $t = 3$  days to Time  $t = 7$  days.

## A10.2 Calculation of $\Delta P_{1,3-28}$ (Old Deck)

$\Delta P_{1,3-28}$  represents the prestress loss of Step 1 which appears between Step 1 and Step 3 from time  $t = 3$  days to  $t = 28$  days. As shown in Appendix A7.1, prestressing force in old deck at the end of Step 1 is  $P_1 = 505$  kN. Therefore, the original increment of prestressing force in Step 1 is as follow:

$$\Delta P_{max,1} = 505 \text{ kN}$$

Then  $\Delta P_{1,3-28}$  is as follow:

$$\Delta P_{1,3-28} = \Delta P_{el,mean} + \Delta P_{\mu} + \Delta P_{cr} + \Delta P_r + \Delta P_{shr}/n = 51 \text{ kN} \quad (43)$$

### initial prestressing force

original increment <b>per cable</b>	$\Delta P_{max,1}$	5.05E+05 N
where:		
initial prestressing force <b>per cable</b>	$P_{m0}$	5.05E+05 N

Table 122: Immediate Loss of Step 1 from Time  $t = 3$  days to Time  $t = 28$  days.

### elastic loss

mean elastic loss <b>per cable</b>	$\Delta P_{el,mean}(t)$	1.00E+04 N
where:		
factor related to number of tendon	$j$	0.48
initial prestressing force <b>per cable</b>	$P_{m0}$	5.05E+05 N
variation of prestress	$\Delta \sigma_{el,mean}$	1.73E+06 N/m <sup>2</sup>

Table 123: Elastic Loss of Step 1 from Time  $t = 3$  days to Time  $t = 28$  days.

### friction loss

friction loss <b>per cable</b>	$\Delta P_{\mu}(\theta)$	2.01E+04 N
where:		
factor of friction	$\mu$	0.19
angular rotation	$\theta$	0.21 rad
wobble effect	$k$	0.01 rad/m

Table 124: Friction Loss of Step 1 from Time  $t = 3$  days to Time  $t = 28$  days.

**shrinkage loss**

shrinkage loss of <b>cables</b>	$\Delta P_{shr}(t)$	3.24E+05	N
shrinkage loss of <b>per cable</b>	$\Delta P_{shr}(t)$	<b>1.30E+04</b>	<b>N</b>
where:			
shrinkage	$\varepsilon_{cs}$	3.70E-05	m/m
final drying shrinkage	$\varepsilon_{cd}(t)$	7.49E-06	m/m
initial drying shrinkage	$\varepsilon_{cd,0}$	3.00E-04	m/m
factor related to cement	$\alpha_{ds1}$	4.00	
	$\alpha_{ds2}$	0.12	
factor	$f_{cm0}$	1.00E+07	Pa
factor	$RH_0$	100.00	%
factor	$\beta_{RH}$	0.90	
factor related to notional size	$k_h$	0.70	
factor	$\beta_{ts}(t, t_s)$	0.04	
factor	$\beta_{ts}(t_p, t_s)$	0.00	
time at the end of curing	$t_s$	1.00	days
final autogenous shrinkage	$\varepsilon_{ca}(t)$	2.95E-05	m/m
initial autogenous shrinkage	$\varepsilon_{ca}(\infty)$	6.25E-05	m/m
factor	$\beta_{as}(t)$	0.65	
factor	$\beta_{as}(t_s)$	0.18	

Table 125: Shrinkage Loss of Step 1 from Time  $t = 3$  days to Time  $t = 28$  days.

**creep loss**

creep loss of <b>per cable</b>	$\Delta P_{cr}(t)$	<b>7.40E+03</b>	<b>N</b>
where:			
creep strain at ends	$\varepsilon_{cc,end}(t)$	2.11E-05	m/m

Table 126: Creep Loss of Step 1 from Time  $t = 3$  days to Time  $t = 7$  days.

**relaxation loss**

relaxation loss <b>per cable</b>	$\Delta P_r(t)$	<b>2.37E+01</b>	<b>N</b>
where:			
variation of prestress	$\Delta \sigma_{pr}$	1.32E+04	Pa
initial prestress per cable	$\sigma_{pi}$	2.81E+08	Pa
factor	$\mu$	0.15	
relaxation loss at 1000 hrs	$\rho_{1000}$	2.50	%

Table 127: Relaxation Loss of Step 1 from Time  $t = 3$  days to Time  $t = 7$  days.

### A10.3 Calculation of $\Delta P_{2,7-28}$ (Old Deck)

$\Delta P_{2,7-28}$  represents the prestress loss of Step 2 which appears between Step 2 and Step 3 from time  $t = 7$  days to  $t = 28$  days. As shown in Appendix A7.1, prestressing force in old deck at the end of Step 2 is  $P_2 = 1514$  kN. Therefore, the original increment of prestressing force in Step 2 is as follow:

$$\Delta P_{max,2} = P_2 - P_1 + \Delta P_{1,3-7} = 1049 \text{ kN}$$

Then  $\Delta P_{2,7-28}$  is as follow:

$$\Delta P_{2,7-28} = \Delta P_{el,mean} + \Delta P_{\mu} + \Delta P_{cr} + \Delta P_r + \Delta P_s/n = 86 \text{ kN} \quad (44)$$

#### initial prestressing force

original increment <b>per cable</b>	$\Delta P_{max,2}$	1.05E+06 N
where:		
initial prestressing force <b>per cable</b>	$P_{m0}$	1.05E+06 N

Table 128: Immediate Loss of Step 2 from Time  $t = 7$  days to Time  $t = 28$  days.

#### elastic loss

mean elastic loss <b>per cable</b>	$\Delta P_{el,mean}(t)$	1.92E+04 N
where:		
factor related to number of tendon	$j$	0.48
initial prestressing force <b>per cable</b>	$P_{m0}$	1.05E+06 N
variation of prestress	$\Delta \sigma_{el,mean}$	3.60E+06 N/m <sup>2</sup>

Table 129: Elastic Loss of Step 2 from Time  $t = 7$  days to Time  $t = 28$  days.

#### friction loss

friction loss <b>per cable</b>	$\Delta P_{\mu}(\theta)$	4.18E+04 N
where:		
factor of friction	$\mu$	0.19
angular rotation	$\theta$	0.21 rad
wobble effect	$k$	0.01 rad/m

Table 130: Friction Loss of Step 2 from Time  $t = 7$  days to Time  $t = 28$  days.

**shrinkage loss**

shrinkage loss of <b>cables</b>	$\Delta P_{shr}(t)$	3.14E+05	N
shrinkage loss of <b>per cable</b>	$\Delta P_{shr}(t)$	<b>1.25E+04</b>	N
where:			
shrinkage	$\varepsilon_{cs}$	3.57E-05	m/m
final drying shrinkage	$\varepsilon_{cd}(t)$	6.25E-06	m/m
initial drying shrinkage	$\varepsilon_{cd,0}$	3.00E-04	m/m
factor related to cement	$\alpha_{ds1}$	4.00	
	$\alpha_{ds2}$	0.12	
factor	$f_{cm0}$	1.00E+07	Pa
factor	$RH_0$	100.00	%
factor	$\beta_{RH}$	0.90	
factor related to notional size	$k_h$	0.70	
factor	$\beta_{ts}(t, t_s)$	0.04	
factor	$\beta_{ts}(t_p, t_s)$	0.01	
time at the end of curing	$t_s$	1.00	days
final autogenous shrinkage	$\varepsilon_{ca}(t)$	2.95E-05	m/m
initial autogenous shrinkage	$\varepsilon_{ca}(\infty)$	6.25E-05	m/m
factor	$\beta_{as}(t)$	0.65	
factor	$\beta_{as}(t_s)$	0.18	

Table 131: Shrinkage Loss of Step 2 from Time  $t = 7$  days to Time  $t = 28$  days.

**creep loss**

creep loss of <b>per cable</b>	$\Delta P_{cr}(t)$	<b>1.15E+04</b>	N
where:			
creep strain at ends	$\varepsilon_{cc,end}(t)$	3.28E-05	m/m

Table 132: Creep Loss of Step 2 from Time  $t = 7$  days to Time  $t = 28$  days.

**relaxation loss**

relaxation loss <b>per cable</b>	$\Delta P_r(t)$	<b>1.15E+03</b>	N
where:			
variation of prestress	$\Delta \sigma_{pr}$	6.42E+05	Pa
initial prestress per cable	$\sigma_{pi}$	8.41E+08	Pa
factor	$\mu$	0.45	
relaxation loss at 1000 hrs	$\rho_{1000}$	2.50	%

Table 133: Relaxation Loss of Step 2 from Time  $t = 7$  days to Time  $t = 28$  days.

#### A10.4 Increment of Prestressing Force Applied in Each Step

As shown in Appendix A7.1, prestressing force in old deck at the end of Step 1 is  $P_1 = 505$  kN. Therefore, the original increment of prestressing force in Step 1 is as follow:

$$\Delta P_{max,1} = 505 \text{ kN}$$

As shown in Appendix A7.1, prestressing force in old deck at the end of Step 2 is  $P_2 = 1514$  kN. Prestress loss between Step 1 and Step 2 has to be compensated. The compensation is as follow:

$$\Delta P_{1,3-7} = 40 \text{ kN}$$

Therefore, the original increment of prestressing force in Step 2 is as follow:

$$\Delta P_{max,2} = P_2 - P_1 + \Delta P_{1,3-7} = 1049 \text{ kN}$$

As shown in Appendix A7.1, prestressing force in old deck at the end of Step 3 is  $P_3 = 2524$  kN. Prestress loss between Step 2 and Step 3 has to be compensated. The compensation is as follow:

$$(\Delta P_{1,3-28} - \Delta P_{r,1,3-28}) - (\Delta P_{1,3-7} - \Delta P_{r,1,3-7}) + (\Delta P_{2,7-28} - \Delta P_{shr,2,7-28}) = 84 \text{ kN}$$

Therefore, the original increment of prestressing force in Step 3 is as follow:

$$\Delta P_{max,3} = P_3 - P_2 + (\Delta P_{1,3-28} - \Delta P_{r,1,3-28}) - (\Delta P_{1,3-7} - \Delta P_{r,1,3-7}) + (\Delta P_{2,7-28} - \Delta P_{shr,2,7-28}) = 1094 \text{ kN}$$

## A11 Calculation of Prestress Loss (New Deck)

### A11.1 General

As shown in Appendix A7, the prestressing force is applied all in one step at time  $t = 7$  days. Imposed deformation and prestress loss in new decks are calculated by all in one step.

The models used during investigation are Simplified Model 1 and Simplified Model 2, see Section 7.3.1 and Section 7.4.1. The input data is shown in Chapter 5. The material properties applied to the expressions are calculated by the input data and the expressions in Appendix A4 and Appendix A5. The imposed deformation and prestress loss in old decks are calculated by the expressions in Appendix A6. Hereby summarized the data of the calculation.

### A11.2 All in One Step (New Deck - South)

Hereby summarized the remaining prestressing force and prestress loss calculated by all in one step, see Table 134 and Table 135. The detailing data of the calculation is shown in Appendix A11.2.1 and Appendix A11.2.2. Since prestressing force is applied all in one step, the prestress loss in Table 134 and Table 135 are same as those shown in Appendix A11.2.1 and Appendix A11.2.2 respectively.

initial prestressing force per cable	$P_{m0}$	3.96E+06	N
mean elastic loss per cable	$\Delta P_{el,mean}$	5.88E+04	N
friction loss per cable	$\Delta P_{\mu}(x)$	2.70E+05	N
shrinkage loss of per cable	$\Delta P_{shr}(t)$	3.38E+03	N
creep loss of per cable	$\Delta P_{cr}(t)$	5.97E+04	N
relaxation loss per cable	$\Delta P_r(t)$	5.14E+04	N
final prestressing force per cable	$P_{m\infty}$	3.51E+06	N

Table 134: Prestress Loss and Remaining Prestressing Force Calculated by All in One Step at time  $t = 11$  years + 29 days.

initial prestressing force per cable	$P_{m0}$	3.96E+06	N
mean elastic loss per cable	$\Delta P_{el,mean}$	5.88E+04	N
friction loss per cable	$\Delta P_{\mu}(x)$	2.70E+05	N
shrinkage loss of per cable	$\Delta P_{shr}(t)$	1.41E+05	N
creep loss of per cable	$\Delta P_{cr}(t)$	1.90E+05	N
relaxation loss per cable	$\Delta P_r(t)$	1.90E+05	N
final prestressing force per cable	$P_{m\infty}$	3.11E+06	N
<b>final prestressing force of cables</b>	<b><math>P_{m\infty}</math></b>	<b>9.32E+06</b>	<b>N</b>
<b>stress resulting from prestressing</b>	<b><math>\sigma_{p\infty}</math></b>	<b>8.32E+06</b>	<b>Pa</b>

Table 135: Prestress Loss and Remaining Prestressing Force Calculated by All in One Step at time  $t = 111$  years.

### A11.2.1 Calculation Related to $P_{1,7-t_{\infty}}$ ( $t_{\infty} = 11 \text{ years} + 29 \text{ days}$ )

$P_{1,7-t_{\infty}}$  represents the prestressing force applied all in one step from time  $t = 7$  days to  $t = 11 \text{ years} + 29$  days.

#### immediate loss

original increment <b>per cable</b>	$\Delta P_{max}$	3.96E+06	N
where:			
initial prestressing force <b>per cable</b>	$P_{m0}$	3.96E+06	N

Table 136: Immediate Loss from Time  $t = 7$  days to Time  $t = t_{\infty}$  days.

#### elastic loss

mean elastic loss <b>per cable</b>	$\Delta P_{el,mean}(t)$	5.88E+04	N
where:			
factor related to number of tendon	$j$	0.33	
initial prestressing force <b>per cable</b>	$P_{m0}$	3.96E+06	N
variation of prestress	$\Delta \sigma_{el,mean}$	1.06E+07	N/m <sup>2</sup>

Table 137: Elastic Loss from Time  $t = 7$  days to Time  $t = t_{\infty}$  days.

#### friction loss

friction loss <b>per cable</b>	$\Delta P_{\mu}(x)$	2.70E+05	N
where:			
factor of friction	$\mu$	0.19	
angular rotation	$\theta$	0.16	rad
wobble effect	$k$	0.01	rad/m

Table 138: Friction Loss from Time  $t = 7$  days to Time  $t = t_{\infty}$  days.

**shrinkage loss**

shrinkage loss of <b>cables</b>	$\Delta P_{shr}(t)$	8.45E+04	N
shrinkage loss of <b>per cable</b>	$\Delta P_{shr}(t)$	3.38E+03	N
where:			
shrinkage	$\varepsilon_{cs}$	5.07E-05	m/m
final drying shrinkage	$\varepsilon_{cd}(t)$	8.87E-06	m/m
initial drying shrinkage	$\varepsilon_{cd,0}$	2.66E-04	m/m
factor related to cement	$\alpha_{ds1}$	4.00	
	$\alpha_{ds2}$	0.12	
factor	$f_{cm0}$	1.00E+07	Pa
factor	$RH_0$	100.00	%
factor	$\beta_{RH}$	0.90	
factor related to notional size	$k_h$	0.70	
factor	$\beta_{ts}(t, t_s)$	0.06	
factor	$\beta_{ts}(t_p, t_s)$	0.01	
time at the end of curing	$t_s$	1.00	days
final autogenous shrinkage	$\varepsilon_{ca}(t)$	4.18E-05	m/m
initial autogenous shrinkage	$\varepsilon_{ca}(\infty)$	8.75E-05	m/m
factor	$\beta_{as}(t)$	0.66	
factor	$\beta_{as}(t_s)$	0.18	

Table 139: Shrinkage Loss from Time  $t = 7$  days to Time  $t = t_\infty$  days.

**creep loss**

creep loss of <b>per cable</b>	$\Delta P_{cr}(t)$	5.97E+04	N
where:			
creep strain	$\varepsilon_{cc}(t)$	1.07E-04	m/m

Table 140: Creep Loss from Time  $t = 7$  days to Time  $t = t_\infty$  days.

**relaxation loss**

relaxation loss <b>per cable</b>	$\Delta P_r(t)$	5.14E+04	N
where:			
variation of prestress	$\Delta \sigma_{pr}$	1.80E+07	Pa
initial prestress per cable	$\sigma_{pi}$	1.39E+09	Pa
factor	$\mu$	0.75	
relaxation loss at 1000 hrs	$\rho_{1000}$	2.50	%

Table 141: Relaxation Loss from Time  $t = 7$  days to Time  $t = t_\infty$  days.

### A11.2.2 Calculation Related to $P_{1,7-t_{\infty}}$ ( $t_{\infty} = 111$ years)

$P_{1,7-t_{\infty}}$  represents the prestressing force applied all in one step from time  $t = 7$  days to  $t = 111$  years.

#### immediate loss

original increment <b>per cable</b>	$\Delta P_{max}$	3.96E+06	N
where:			
initial prestressing force <b>per cable</b>	$P_{m0}$	3.96E+06	N

Table 142: Immediate Loss from Time  $t = 7$  days to Time  $t = t_{\infty}$  days.

#### elastic loss

mean elastic loss <b>per cable</b>	$\Delta P_{el,mean}(t)$	5.88E+04	N
where:			
factor related to number of tendon	$j$	0.33	
initial prestressing force <b>per cable</b>	$P_{m0}$	3.96E+06	N
variation of prestress	$\Delta \sigma_{el,mean}$	1.06E+07	N/m <sup>2</sup>

Table 143: Elastic Loss from Time  $t = 7$  days to Time  $t = t_{\infty}$  days.

#### friction loss

friction loss <b>per cable</b>	$\Delta P_{\mu}(x)$	2.70E+05	N
where:			
factor of friction	$\mu$	0.19	
angular rotation	$\theta$	0.16	rad
wobble effect	$k$	0.01	rad/m

Table 144: Friction Loss from Time  $t = 7$  days to Time  $t = t_{\infty}$  days.

**shrinkage loss**

shrinkage loss of <b>cables</b>	$\Delta P_{shr}(t)$	4.24E+05	N
shrinkage loss of <b>per cable</b>	$\Delta P_{shr}(t)$	1.41E+05	N
where:			
shrinkage	$\varepsilon_{cs}$	2.54E-04	m/m
final drying shrinkage	$\varepsilon_{cd}(t)$	1.82E-04	m/m
initial drying shrinkage	$\varepsilon_{cd,0}$	2.66E-04	m/m
factor related to cement	$\alpha_{ds1}$	4.00	
	$\alpha_{ds2}$	0.12	
factor	$f_{cm0}$	1.00E+07	Pa
factor	$RH_0$	100.00	%
factor	$\beta_{RH}$	0.90	
factor related to notional size	$k_h$	0.70	
factor	$\beta_{ts}(t, t_s)$	0.99	
factor	$\beta_{ts}(t_p, t_s)$	0.01	
time at the end of curing	$t_s$	1.00	days
final autogenous shrinkage	$\varepsilon_{ca}(t)$	7.16E-05	m/m
initial autogenous shrinkage	$\varepsilon_{ca}(\infty)$	8.75E-05	m/m
factor	$\beta_{as}(t)$	1.00	
factor	$\beta_{as}(t_s)$	0.18	

Table 145: Shrinkage Loss from Time  $t = 7$  days to Time  $t = t_\infty$  days.

**creep loss**

creep loss of <b>per cable</b>	$\Delta P_{cr}(t)$	1.90E+05	N
where:			
creep strain	$\varepsilon_{cc}(t)$	3.41E-04	m/m

Table 146: Creep Loss from Time  $t = 7$  days to Time  $t = t_\infty$  days.

**relaxation loss**

relaxation loss <b>per cable</b>	$\Delta P_r(t)$	1.90E+05	N
where:			
variation of prestress	$\Delta \sigma_{pr}$	6.65E+07	Pa
initial prestress per cable	$\sigma_{pi}$	1.39E+09	Pa
factor	$\mu$	0.75	
relaxation loss at 1000 hrs	$\rho_{1000}$	2.50	%

Table 147: Relaxation Loss from Time  $t = 7$  days to Time  $t = t_\infty$  days.

### A11.3 All in One Step (New Deck - North)

Hereby summarized the remaining prestressing force and prestress loss calculated by all in one step, see Table 148 and Table 149. The detailing data of the calculation is shown in Appendix A11.2.1 and Appendix A11.2.2. Since prestressing force is applied all in one step, the prestress loss in Table 148 and Table 149 are same as those shown in Appendix A11.2.1 and Appendix A11.2.2 respectively.

initial prestressing force per cable	$P_{m0}$	3.96E+06	N
mean elastic loss per cable	$\Delta P_{el,mean}$	6.21E+04	N
friction loss per cable	$\Delta P_{\mu}(x)$	2.70E+05	N
shrinkage loss of per cable	$\Delta P_{shr}(t)$	1.48E+04	N
creep loss of per cable	$\Delta P_{cr}(t)$	3.48E+04	N
relaxation loss per cable	$\Delta P_r(t)$	5.14E+04	N
final prestressing force per cable	$P_{m\infty}$	3.52E+06	N

Table 148: Prestress Loss and Remaining Prestressing Force Calculated by All in One Step at time  $t = 11$  years + 29 days.

initial prestressing force per cable	$P_{m0}$	3.96E+06	N
mean elastic loss per cable	$\Delta P_{el,mean}$	6.21E+04	N
friction loss per cable	$\Delta P_{\mu}(x)$	2.70E+05	N
shrinkage loss of per cable	$\Delta P_{shr}(t)$	1.41E+05	N
creep loss of per cable	$\Delta P_{cr}(t)$	1.15E+05	N
relaxation loss per cable	$\Delta P_r(t)$	1.90E+05	N
final prestressing force per cable	$P_{m\infty}$	3.18E+06	N
<b>final prestressing force of cables</b>	$P_{m\infty}$	<b>4.45E+07</b>	<b>N</b>
<b>stress resulting from prestressing</b>	$\sigma_{p\infty}$	<b>6.45E+06</b>	<b>Pa</b>

Table 149: Prestress Loss and Remaining Prestressing Force Calculated by All in One Step at time  $t = 111$  years.

### A11.3.1 Calculation Related to $P_{1,7-t_{\infty}}$ ( $t_{\infty} = 11 \text{ years} + 29 \text{ days}$ )

$P_{1,7-t_{\infty}}$  represents the prestressing force applied all in one step from time  $t = 7$  days to  $t = 11 \text{ years} + 29$  days.

#### immediate loss

original increment <b>per cable</b>	$\Delta P_{max}$	3.96E+06	N
where:			
initial prestressing force <b>per cable</b>	$P_{m0}$	3.96E+06	N

Table 150: Immediate Loss from Time  $t = 7$  days to Time  $t = t_{\infty}$  days.

#### elastic loss

mean elastic loss <b>per cable</b>	$\Delta P_{el,mean}(t)$	6.21E+04	N
where:			
factor related to number of tendon	$j$	0.46	
initial prestressing force <b>per cable</b>	$P_{m0}$	3.96E+06	N
variation of prestress	$\Delta \sigma_{el,mean}$	8.03E+06	N/m <sup>2</sup>

Table 151: Elastic Loss from Time  $t = 7$  days to Time  $t = t_{\infty}$  days.

#### friction loss

friction loss <b>per cable</b>	$\Delta P_{\mu}(x)$	2.70E+05	N
where:			
factor of friction	$\mu$	0.19	
angular rotation	$\theta$	0.16	rad
wobble effect	$k$	0.01	rad/m

Table 152: Friction Loss from Time  $t = 7$  days to Time  $t = t_{\infty}$  days.

**shrinkage loss**

shrinkage loss of <b>cables</b>	$\Delta P_{shr}(t)$	3.71E+05	N
shrinkage loss of <b>per cable</b>	$\Delta P_{shr}(t)$	1.48E+04	N
where:			
shrinkage	$\varepsilon_{cs}$	4.77E-05	m/m
final drying shrinkage	$\varepsilon_{cd}(t)$	5.83E-06	m/m
initial drying shrinkage	$\varepsilon_{cd,0}$	2.66E-04	m/m
factor related to cement	$\alpha_{ds1}$	4.00	
	$\alpha_{ds2}$	0.12	
factor	$f_{cm0}$	1.00E+07	Pa
factor	$RH_0$	100.00	%
factor	$\beta_{RH}$	0.90	
factor related to notional size	$k_h$	0.70	
factor	$\beta_{ts}(t, t_s)$	0.04	
factor	$\beta_{ts}(t_p, t_s)$	0.01	
time at the end of curing	$t_s$	1.00	days
final autogenous shrinkage	$\varepsilon_{ca}(t)$	4.18E-05	m/m
initial autogenous shrinkage	$\varepsilon_{ca}(\infty)$	8.75E-05	m/m
factor	$\beta_{as}(t)$	0.66	
factor	$\beta_{as}(t_s)$	0.18	

Table 153: Shrinkage Loss from Time  $t = 7$  days to Time  $t = t_\infty$  days.

**creep loss**

creep loss of <b>per cable</b>	$\Delta P_{cr}(t)$	3.48E+04	N
where:			
creep strain	$\varepsilon_{cc}(t)$	6.25E-05	m/m

Table 154: Creep Loss from Time  $t = 7$  days to Time  $t = t_\infty$  days.

**relaxation loss**

relaxation loss <b>per cable</b>	$\Delta P_r(t)$	5.14E+04	N
where:			
variation of prestress	$\Delta \sigma_{pr}$	1.80E+07	Pa
initial prestress per cable	$\sigma_{pi}$	1.39E+09	Pa
factor	$\mu$	0.75	
relaxation loss at 1000 hrs	$\rho_{1000}$	2.50	%

Table 155: Relaxation Loss from Time  $t = 7$  days to Time  $t = t_\infty$  days.

### A11.3.2 Calculation Related to $P_{1,7-t_{\infty}}$ ( $t_{\infty} = 111$ years)

$P_{1,7-t_{\infty}}$  represents the prestressing force applied all in one step from time  $t = 7$  days to  $t = 111$  years.

#### immediate loss

original increment <b>per cable</b>	$\Delta P_{max}$	3.96E+06	N
where:			
initial prestressing force <b>per cable</b>	$P_{m0}$	3.96E+06	N

Table 156: Immediate Loss from Time  $t = 7$  days to Time  $t = t_{\infty}$  days.

#### elastic loss

mean elastic loss <b>per cable</b>	$\Delta P_{el,mean}(t)$	6.21E+04	N
where:			
factor related to number of tendon	$j$	0.46	
initial prestressing force <b>per cable</b>	$P_{m0}$	3.96E+06	N
variation of prestress	$\Delta \sigma_{el,mean}$	8.03E+06	N/m <sup>2</sup>

Table 157: Elastic Loss from Time  $t = 7$  days to Time  $t = t_{\infty}$  days.

#### friction loss

friction loss <b>per cable</b>	$\Delta P_{\mu}(x)$	2.70E+05	N
where:			
factor of friction	$\mu$	0.19	
angular rotation	$\theta$	0.16	rad
wobble effect	$k$	0.01	rad/m

Table 158: Friction Loss from Time  $t = 7$  days to Time  $t = t_{\infty}$  days.

**shrinkage loss**

shrinkage loss of <b>cables</b>	$\Delta P_{shr}(t)$	1.97E+06	N
shrinkage loss of <b>per cable</b>	$\Delta P_{shr}(t)$	1.41E+05	N
where:			
shrinkage	$\varepsilon_{cs}$	2.53E-04	m/m
final drying shrinkage	$\varepsilon_{cd}(t)$	1.81E-04	m/m
initial drying shrinkage	$\varepsilon_{cd,0}$	2.66E-04	m/m
factor related to cement	$\alpha_{ds1}$	4.00	
	$\alpha_{ds2}$	0.12	
factor	$f_{cm0}$	1.00E+07	Pa
factor	$RH_0$	100.00	%
factor	$\beta_{RH}$	0.90	
factor related to notional size	$k_h$	0.70	
factor	$\beta_{ts}(t, t_s)$	0.98	
factor	$\beta_{ts}(t_p, t_s)$	0.01	
time at the end of curing	$t_s$	1.00	days
final autogenous shrinkage	$\varepsilon_{ca}(t)$	7.16E-05	m/m
initial autogenous shrinkage	$\varepsilon_{ca}(\infty)$	8.75E-05	m/m
factor	$\beta_{as}(t)$	1.00	
factor	$\beta_{as}(t_s)$	0.18	

Table 159: Shrinkage Loss from Time  $t = 7$  days to Time  $t = t_\infty$  days.

**creep loss**

creep loss of <b>per cable</b>	$\Delta P_{cr}(t)$	1.15E+05	N
where:			
creep strain	$\varepsilon_{cc}(t)$	2.08E-04	m/m

Table 160: Creep Loss from Time  $t = 7$  days to Time  $t = t_\infty$  days.

**relaxation loss**

relaxation loss <b>per cable</b>	$\Delta P_r(t)$	1.90E+05	N
where:			
variation of prestress	$\Delta \sigma_{pr}$	6.65E+07	Pa
initial prestress per cable	$\sigma_{pi}$	1.39E+09	Pa
factor	$\mu$	0.75	
relaxation loss at 1000 hrs	$\rho_{1000}$	2.50	%

Table 161: Relaxation Loss from Time  $t = 7$  days to Time  $t = t_\infty$  days.

## A12 Mechanics 1

### A12.1 General

In Mechanics 1, it is assumed that, when a composited cross-section is subjected to mechanical load and/or imposed deformation, the in-plane curvatures of the composited cross-section is uniform. It means the composited cross-section remains flat when it is deformed.

Equivalent loads of imposed deformation, normal force  $N$  and bending moment  $M$ , are applied to the cross-section of composited cross-section to calculate the strain and stress resulting from imposed deformation. The disadvantage of Mechanics 1 is that, with normal force  $N$  and bending moment  $M$  only, shear deformation is neglected.

Suppose there is a composited cross-section with three layers, see Figure 73, the expressions to calculate the resulting strain and stress are shown in this chapter.

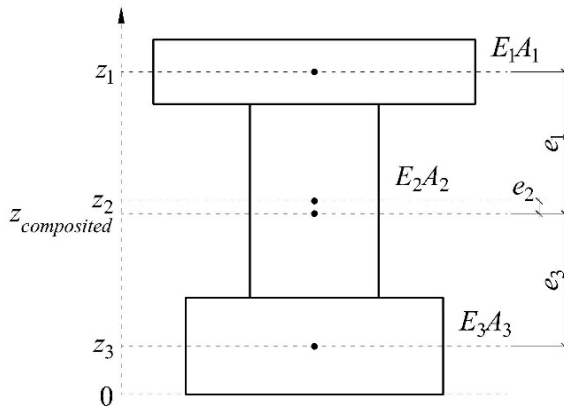


Figure 73: Composited Cross-section.

### A12.2 Properties of Cross-section

#### normal stiffness of composited cross-section

$$(EA)_{composited} = \sum_{i=1}^n E_i A_i \quad (45)$$

#### bending stiffness of composited cross-section

$$(EI)_{composited} = \sum_{i=1}^n E_i I_i + \sum_{i=1}^n E_i A_i \cdot e_i^2 \quad (46)$$

where:

- $e_i$  is the eccentricity of gravity of certain layer  
 $= z_i - z_{composited}$
- $z_i$  is the position of gravity of certain layer
- $z_{composited}$  is the position of gravity of composited cross-section  
 $= \frac{\sum_{i=1}^n E_i A_i \cdot z_i}{(EA)_{composited}}$

### A12.3 Response under ‘Imposed Deformation’

Suppose that the Layer  $i$  is subjected to the imposed deformation  $\Delta\varepsilon$ , to calculate the response of the composited cross-section, a standard procedure would be used as follow:

1. Split the composited cross-section, making the Layer  $i$  free to deform. After that, an external normal force  $N_i^*$  is applied to Layer  $i$ , see Figure 74.

$$N_i^* = \Delta\varepsilon \cdot (EA)_i \quad (47)$$

2. After the external normal force  $N_i^*$  is applied, the layers are again connected to each other. Then, another external force  $N^{**}$  is applied to the composited cross-section at same position with same magnitude but reverse sign.

$$N^{**} = -N_i^* \quad (48)$$

By moving the external normal force  $N^{**}$  to the neutral axis of the composited cross-section, a compensating moment  $M^{**}$  is obtained, see Figure 74.

$$M^{**} = N^{**} \cdot e_i \quad (49)$$

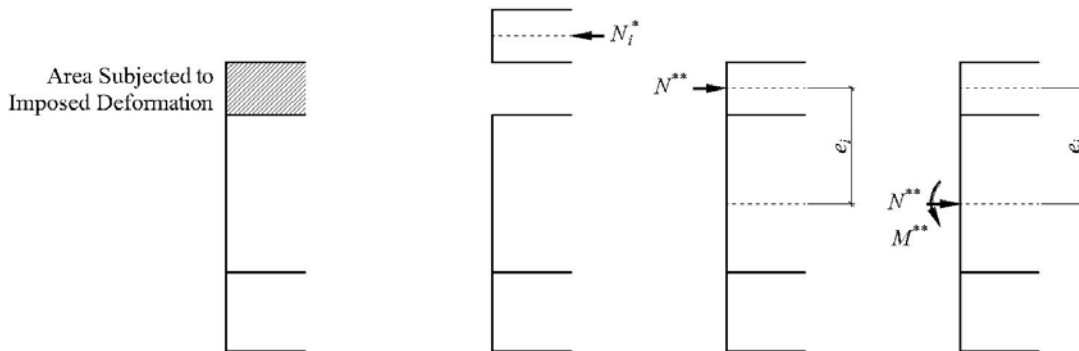


Figure 74: External Normal Force  $N_i^*$ , External Normal Force  $N^{**}$  and Compensating Moment  $M^{**}$ .

3. In the end, the equivalent loads of imposed deformation applied to the composited cross-section is a superposition of external normal force  $N_i^*$ , external normal force  $N^{**}$  and compensating moment  $M^{**}$ . The external normal force  $N_i^*$  is applied to the Layer  $i$  which is subjected to the imposed deformation  $\Delta\varepsilon$ , while the external normal force  $N^{**}$  and compensating moment  $M^{**}$  are applied to the whole cross-section, see Figure 75.

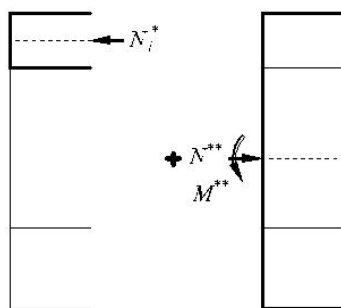


Figure 75: Superposition.

4. Use the expressions introduced in A12.4 to calculate the resulting strain and stress in cross-section under external normal force  $N_i^*$ , external normal force  $N^{**}$  and compensating moment  $M^{**}$  respectively. Then the response of composited cross-section under imposed deformation is a superposition of the resulting strain and stress of the equivalent loads.

## A12.4 Response under ‘Mechanical Load’

### strain at certain point under external normal force

$$\varepsilon_{N,i} = \varepsilon \quad (50)$$

where:

- $\varepsilon$  is the strain of composited cross-section  
=  $N/(EA)_{\text{composited}}$
- $N$  is the external normal force applied to the composited cross-section

### strain at certain point under external moment

$$\varepsilon_{M,i} = \kappa \cdot e_i \quad (51)$$

where:

- $\kappa$  is the curvature for composited cross-section  
=  $M/(EI)_{\text{composited}}$
- $M$  is the external moment applied to the composited cross-section
- $e_i$  is the eccentricity from certain point to the gravity of composited cross-section

### stress at certain point under external normal force

$$\sigma_{N,i} = E_i A_i \cdot \varepsilon_{N,i} \quad (52)$$

where:

- $\varepsilon_{N,i}$  is the strain due to normal force at certain point

### stress at certain point under external moment

$$\sigma_{M,i} = E_i A_i \cdot \varepsilon_{M,i} \quad (53)$$

where:

- $\varepsilon_{M,i}$  is the strain due to moment at certain point

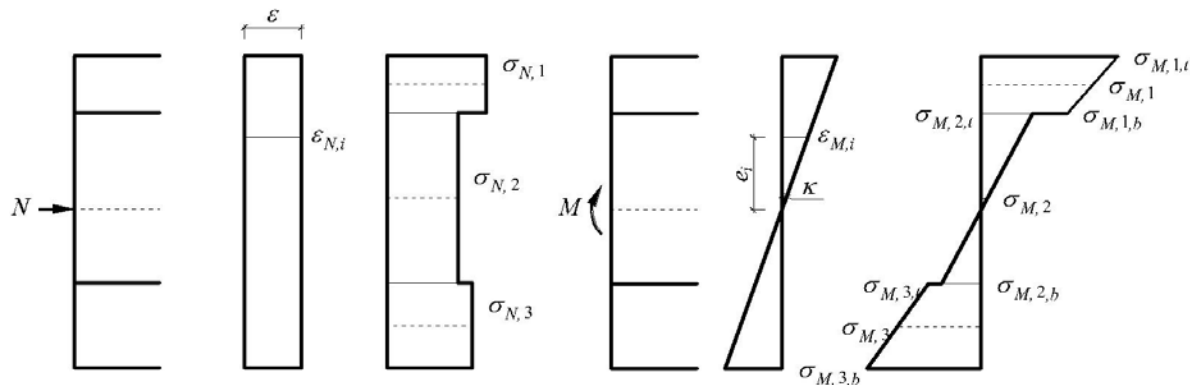


Figure 76: Sketch of Strain and Stress.

## A13 Mechanics 2

### A13.1 General

Mechanics 2 is basing on plate theory. According to Mechanics 2, deformation of plate is simplified into nodal displacement which is the product of stiffness matrix and nodal forces. When a composited structure subjected to imposed deformation is analyzed by Mechanics 2, the layers of the composited cross-section are spit which makes the layers free to deform. Then deformation compatibility is restored so that the deformed layers are able to be connected.

Since the stiffness matrix and nodal forces in the layers could be different, the in-plane curvature of each layer could be different. It means the composited cross-section will not remain flat when it deforms due to imposed deformation. The advantage of Mechanics 2 is that, with shear stiffness taken into account, the shear deformation is taken into account.

Suppose there is a three-layer composited deck and the layers subject to different imposed deformation, see Figure 77, the expressions to calculate the resulting strain and stress are shown in this chapter.

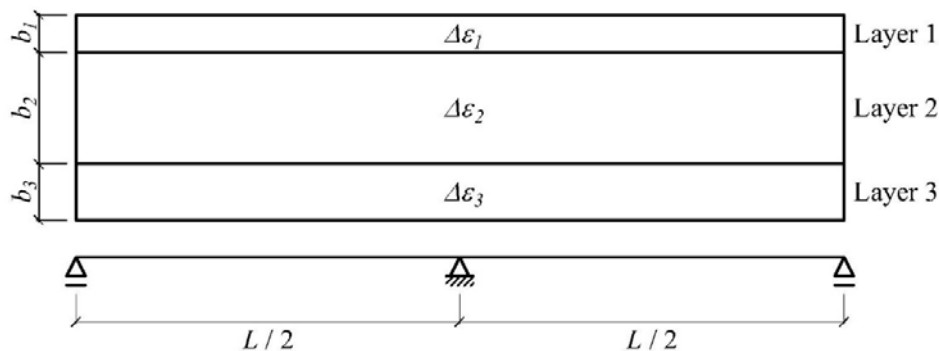


Figure 77: Top and Side View of Composited Deck.

### A13.2 Split Layers and Deformation Compatibility

As shown in Figure 78, the composited cross-section is split into three free layers. Suppose different imposed deformation,  $\Delta\varepsilon_1$ ,  $\Delta\varepsilon_2$  and  $\Delta\varepsilon_3$ , are applied to the split layers, the deformed shapes of the layers would be different. The differences between the deformed shapes, or in short the gaps, make the deformed layers unable to be re-connected.

To re-connect the layers, the gaps have to be closed, or in other words the compatibility of deformation has to be restored, see Figure 79. Since the magnitudes of imposed deformation are known, the deformation required to restore compatibility can be calculated and, therefore, equilibrium about deformation is made. Then, by describing the required deformation into nodal displacement which is the product of stiffness matrix and nodal forces, nodal forces to restore compatibility can be calculated by solving the equilibrium. Finally, with nodal forces calculated, strain and stress resulting from imposed deformation can be calculated.

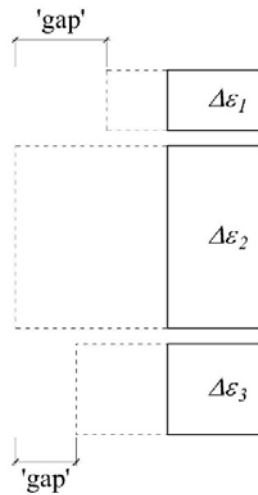


Figure 78: 'Gaps' due to Free Deformation.

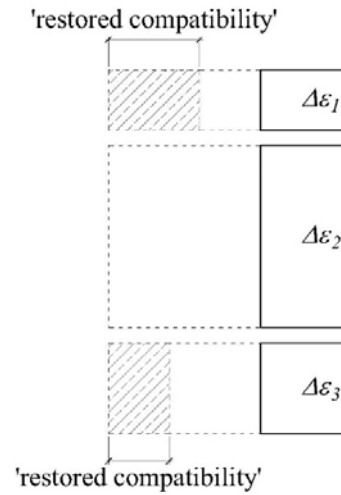


Figure 79: 'Restored Compatibility'.

### A13.3 General Elasticity Matrices

In an arbitrary plate, the in-plane strain  $\varepsilon_{xx}$ ,  $\varepsilon_{yy}$  and  $\gamma$  are presented into nodal displacement  $u_x$  and  $u_y$ , while the in-plane stresses  $n_{xx}$ ,  $n_{yy}$  and  $n_{xy}$  in a plate are presented into in-plane nodal forces  $F_x$  and  $F_y$  (Blaauwendraad, 2006, pp. 13 - 25). With the relation between in-plane strain and stress, the general relation between nodal displacement and forces is established, of which matrix form is referred to as general elasticity matrices, see Expression 54 and Expression 55.

**Normal stiffness:**

$$\begin{bmatrix} F_{x1} \\ F_{y1} \\ F_{x2} \\ F_{y2} \\ F_{x3} \\ F_{y3} \\ F_{x4} \\ F_{y4} \end{bmatrix} = \frac{E_{cm}(t)}{2} \cdot \begin{bmatrix} \beta & 0 & -\beta & 0 & 0 & 0 & 0 & 0 \\ 0 & \alpha & 0 & 0 & 0 & -\alpha & 0 & 0 \\ -\beta & 0 & \beta & 0 & 0 & 0 & 0 & 0 \\ 0 & 0 & 0 & \alpha & 0 & 0 & 0 & -\alpha \\ 0 & 0 & 0 & 0 & \beta & 0 & -\beta & 0 \\ 0 & -\alpha & 0 & 0 & 0 & \alpha & 0 & 0 \\ 0 & 0 & 0 & 0 & -\beta & 0 & \beta & 0 \\ 0 & 0 & 0 & -\alpha & 0 & 0 & 0 & \alpha \end{bmatrix} \cdot \begin{bmatrix} u_{x1} \\ u_{y1} \\ u_{x2} \\ u_{y2} \\ u_{x3} \\ u_{y3} \\ u_{x4} \\ u_{y4} \end{bmatrix}$$

or in short:

$$\mathbf{f}_n = \frac{E_{cm}(t)}{2} \cdot \mathbf{E}_n \cdot \mathbf{u} \quad (54)$$

where:

- $E_{cm}(t)$  is the elastic modulus of concrete at time  $t$
- $\alpha = L/b$
- $\beta = b/L$
- $L$  is the length of a rectangular plate
- $b$  is the width of a rectangular plate
- $\mathbf{f}_n$  is the vector of nodal forces related to normal deformation
- $\mathbf{E}_n$  is the general elasticity matrix related to normal deformation
- $\mathbf{u}$  is the vector of nodal displacement

\*There are four corners, or in another word nodes, in a rectangular plate.  $F_{xi}$  and  $F_{yi}$  are the nodal forces in longitudinal and transverse direction at the  $i$ -th node, while  $u_{xi}$  and  $u_{yi}$  are the nodal displacement in longitudinal and transverse direction at the  $i$ -th node.

Shear stiffness:

$$\begin{pmatrix} F_{x1} \\ F_{y1} \\ F_{x2} \\ F_{y2} \\ F_{x3} \\ F_{y3} \\ F_{x4} \\ F_{y4} \end{pmatrix} = \frac{E}{8(1+\nu)} \cdot \begin{bmatrix} \alpha & 1 & \alpha & -1 & -\alpha & 0 & -\alpha & -1 \\ 1 & \beta & 1 & -\beta & -1 & \beta & -1 & -\beta \\ \alpha & 1 & \alpha & -1 & -\alpha & 0 & -\alpha & -1 \\ -1 & -\beta & -1 & \beta & 1 & -\beta & 1 & \beta \\ -\alpha & -1 & -\alpha & 1 & \alpha & -1 & \alpha & 1 \\ 1 & \beta & 1 & -\beta & -1 & \beta & -1 & -\beta \\ \alpha & -1 & -\alpha & 1 & \alpha & -1 & \alpha & 1 \\ -1 & -\beta & -1 & \beta & 1 & -\beta & 1 & \beta \end{bmatrix} \cdot \begin{pmatrix} u_{x1} \\ u_{y1} \\ u_{x2} \\ u_{y2} \\ u_{x3} \\ u_{y3} \\ u_{x4} \\ u_{y4} \end{pmatrix}$$

or in short:

$$\mathbf{f}_v = \frac{E_{cm}(t)}{8(1+\nu)} \cdot \mathbf{E}_v \cdot \mathbf{u} \quad (55)$$

where:

- $\nu$  is the Poison's ratio of concrete, which is taken as zero for simplicity
- $\mathbf{f}_v$  is the vector of nodal forces related to shear deformation
- $\mathbf{E}_v$  is the general elasticity matrix related to shear deformation

Then the general elasticity matrix  $\mathbf{E}$  related to both normal and shear deformation is defined as the summation of those related to normal deformation and shear deformation, see Expression 56.

$$\mathbf{E} = \frac{E_{cm}(t)}{2} \cdot \mathbf{E}_n + \frac{E_{cm}(t)}{8(1+\nu)} \cdot \mathbf{E}_v \quad (56)$$

### A13.4 Specific Elasticity Matrix

When it comes to the response of a specific composited deck subjected to imposed deformation, a specific elasticity matrix  $\mathbf{E}_i$  is required which is derived basing on the general elasticity matrix  $\mathbf{E}$ . Take half of the deck shown in Figure 77 as an example. According to the supports shown in Figure 77, the split layers with in-plane supports of half of the deck is determined as shown in Figure 80. Substitute the elastic modulus of concrete of Layer  $i$  into Expression 56 and extract the elements from general elasticity matrix  $\mathbf{E}$  which are related to unrestrained nodal displacement according to the in-plane supports shown in Figure 80, the relation between nodal forces and displacement in Layer  $i$  is derived, see Expression 57 and Expression 58.

$$\begin{pmatrix} F_{y,2i-1,i} \\ F_{x,2i,i} \\ F_{y,2i,i} \\ F_{x,2i+2,i} \\ F_{y,2i+2,i} \end{pmatrix} = \begin{bmatrix} a_{22} & a_{23} & a_{24} & a_{27} & a_{28} \\ a_{32} & a_{33} & a_{34} & a_{37} & a_{38} \\ a_{42} & a_{43} & a_{44} & a_{47} & a_{48} \\ a_{72} & a_{73} & a_{74} & a_{77} & a_{78} \\ a_{82} & a_{83} & a_{84} & a_{87} & a_{88} \end{bmatrix} \cdot \begin{pmatrix} u_{y,2i-1,i} \\ u_{x,2i,i} \\ u_{y,2i,i} \\ u_{x,2i+2,i} \\ u_{y,2i+2,i} \end{pmatrix}$$

or in short:

$$\mathbf{f}_i = \mathbf{E}_i \cdot \mathbf{u}_i \quad (57)$$

where:

- $F_{x,l,i}$  is the nodal force in longitudinal direction at Node  $l$  in Layer  $i$
- $F_{y,l,i}$  is the nodal force in transverse direction at Node  $l$  in Layer  $i$
- $u_{x,l,i}$  is the nodal displacement in longitudinal direction at Node  $l$  in Layer  $i$
- $u_{y,l,i}$  is the nodal displacement in transverse direction at Node  $l$  in Layer  $i$
- $l$  is the serial number of nodes in Layer  $i$ , see Figure 80
- $\mathbf{f}_i$  is the vector of nodal forces in Layer  $i$
- $\mathbf{u}_i$  is the vector of nodal displacement in Layer  $i$
- $a_{jk}$  is the element in the general elasticity matrix  $\mathbf{E}$  of Layer  $i$  at the  $j$ -th row and  $k$ -th column

$E_i$  is the specific elasticity matrix of Layer  $i$

$$\begin{bmatrix} u_{y,2i-1,i} \\ u_{x,2i,i} \\ u_{y,2i,i} \\ u_{x,2i+2,i} \\ u_{y,2i+2,i} \end{bmatrix} = \begin{bmatrix} b_{11,i} & b_{12,i} & b_{13,i} & b_{14,i} & b_{15,i} \\ b_{21,i} & b_{22,i} & b_{23,i} & b_{24,i} & b_{25,i} \\ b_{31,i} & b_{32,i} & b_{33,i} & b_{34,i} & b_{35,i} \\ b_{41,i} & b_{42,i} & b_{43,i} & b_{44,i} & b_{45,i} \\ b_{51,i} & b_{52,i} & b_{53,i} & b_{54,i} & b_{55,i} \end{bmatrix} \cdot \begin{bmatrix} F_{y,2i-1,i} \\ F_{x,2i,i} \\ F_{y,2i,i} \\ F_{x,2i+2,i} \\ F_{y,2i+2,i} \end{bmatrix}$$

or in short:

$$\mathbf{u}_i = \mathbf{E}_i^{-1} \cdot \mathbf{f}_i \quad (58)$$

where:

$b_{jk,i}$  is the element in the inverse matrix  $\mathbf{E}_i^{-1}$  of Layer  $i$  at the  $j$ -th row and  $k$ -th column

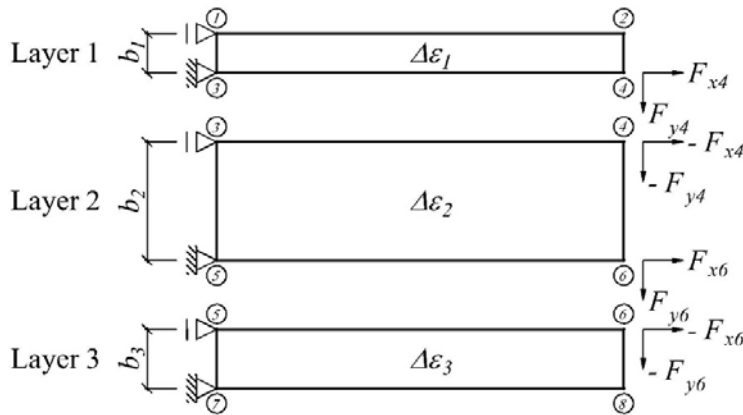


Figure 80: Sketch of Split Deck.

Suppose the internal forces between layers are represented by the nodal forces shown in Figure 80, the nodal displacement in the layers would be derived as follow:

**Layer 1**

$$\begin{bmatrix} u_{y,1,1} \\ u_{x,2,1} \\ u_{y,2,1} \\ u_{x,4,1} \\ u_{y,4,1} \end{bmatrix} = \begin{bmatrix} b_{14,1} & b_{15,1} \\ b_{24,1} & b_{25,1} \\ b_{34,1} & b_{35,1} \\ b_{44,1} & b_{45,1} \\ b_{54,1} & b_{55,1} \end{bmatrix} \cdot \begin{bmatrix} F_{x,4,1} \\ F_{y,4,1} \end{bmatrix} = \begin{bmatrix} b_{14,1} & b_{15,1} \\ b_{24,1} & b_{25,1} \\ b_{34,1} & b_{35,1} \\ b_{44,1} & b_{45,1} \\ b_{54,1} & b_{55,1} \end{bmatrix} \cdot \begin{bmatrix} F_{x,4} \\ F_{y,4} \end{bmatrix}$$

or in short:

$$\mathbf{u}_1 = \mathbf{B}_1 \cdot \mathbf{f}_1 \quad (59)$$

where:

$\mathbf{B}_1$  is the columns extracted from inverse matrix  $\mathbf{E}_1^{-1}$  of Layer 1 related to the nodal forces in

**Layer 2**

$$\begin{bmatrix} u_{y,3,2} \\ u_{x,4,2} \\ u_{y,4,2} \\ u_{x,6,2} \\ u_{y,6,2} \end{bmatrix} = \begin{bmatrix} b_{12,2} & b_{13,2} & b_{14,2} & b_{15,2} \\ b_{22,2} & b_{23,2} & b_{24,2} & b_{25,2} \\ b_{32,2} & b_{33,2} & b_{34,2} & b_{35,2} \\ b_{42,2} & b_{43,2} & b_{44,2} & b_{45,2} \\ b_{52,2} & b_{53,2} & b_{54,2} & b_{55,2} \end{bmatrix} \cdot \begin{bmatrix} F_{x,4,2} \\ F_{y,4,2} \\ F_{x,6,2} \\ F_{y,6,2} \end{bmatrix} = \begin{bmatrix} b_{12,2} & b_{13,2} & b_{14,2} & b_{15,2} \\ b_{22,2} & b_{23,2} & b_{24,2} & b_{25,2} \\ b_{32,2} & b_{33,2} & b_{34,2} & b_{35,2} \\ b_{42,2} & b_{43,2} & b_{44,2} & b_{45,2} \\ b_{52,2} & b_{53,2} & b_{54,2} & b_{55,2} \end{bmatrix} \cdot \begin{bmatrix} -F_{x,4} \\ -F_{y,4} \\ F_{x,6} \\ F_{y,6} \end{bmatrix}$$

or in short:

$$\mathbf{u}_2 = \mathbf{B}_2 \cdot \mathbf{f}_2 \quad (60)$$

where:

$\mathbf{B}_2$  is the columns extracted from inverse matrix  $\mathbf{E}_2^{-1}$  of Layer 2 related to the nodal forces in Layer 3

$$\begin{bmatrix} u_{y,5,3} \\ u_{x,6,3} \\ u_{y,6,3} \\ u_{x,8,3} \\ u_{y,8,3} \end{bmatrix} = \begin{bmatrix} b_{12,3} & b_{13,3} \\ b_{22,3} & b_{23,3} \\ b_{32,3} & b_{33,3} \\ b_{42,3} & b_{43,3} \\ b_{52,3} & b_{53,3} \end{bmatrix} \cdot \begin{bmatrix} F_{x,6,3} \\ F_{y,6,3} \end{bmatrix} = \begin{bmatrix} b_{14,1} & b_{15,1} \\ b_{24,1} & b_{25,1} \\ b_{34,1} & b_{35,1} \\ b_{44,1} & b_{45,1} \\ b_{54,1} & b_{55,1} \end{bmatrix} \cdot \begin{bmatrix} -F_{x,6} \\ -F_{y,6} \end{bmatrix}$$

or in short:

$$\mathbf{u}_3 = \mathbf{B}_3 \cdot \mathbf{f}_3 \quad (61)$$

where:

$\mathbf{B}_3$  is the columns extracted from inverse matrix  $\mathbf{E}_3^{-1}$  of Layer 3 related to the nodal forces in

### A13.5 Restore Compatibility

The split layers are free to deform subjected to imposed deformation. To make the layers able to be connected, the compatibility of deformation has to be restored. As for the layers shown in Figure 80, the deformed shape of layers subjected to imposed deformation and internal forces ought to be compatible.

#### Longitudinal Deformation Compatibility between Layer 1 and Layer 2

$$(\Delta\varepsilon_2 - \Delta\varepsilon_1) \cdot \frac{L}{2} = u_{x,4,1} - u_{x,4,2} \quad (62)$$

#### Transverse Deformation Compatibility between Layer 1 and Layer 2

$$u_{y,4,1} = u_{y,4,2} - u_{y,3,2} \quad (63)$$

#### Longitudinal Deformation Compatibility between Layer 2 and Layer 3

$$(\Delta\varepsilon_3 - \Delta\varepsilon_2) \cdot \frac{L}{2} = u_{x,6,2} - u_{x,6,3} \quad (64)$$

#### Transverse Deformation Compatibility between Layer 2 and Layer 3

$$u_{y,6,2} = u_{y,6,3} - u_{y,5,3} \quad (65)$$

Substitute Expression 59 to 61 into Expression 62 to 65 to solve the internal forces  $F_{x,4}$  and  $F_{x,6}$ . Then substitute the solved internal forces  $F_{x,4}$  and  $F_{x,6}$  back into Expression 59 to 61 to solve the nodal displacement to restore compatibility.

### A13.6 In-plane Strain and Stress Resulting from Imposed Deformation

The in-plane strain and stress resulting from imposed deformation in longitudinal direction are calculated by the solved nodal displacement to restore compatibility. The expressions used during the calculation are as follow:

$$\begin{bmatrix} \varepsilon_{xx,2,1} \\ \varepsilon_{xx,4,1} \\ \varepsilon_{xx,4,2} \\ \varepsilon_{xx,6,2} \\ \varepsilon_{xx,6,3} \\ \varepsilon_{xx,8,3} \end{bmatrix} = \frac{L}{2} \cdot \begin{bmatrix} u_{x,2,1} \\ u_{x,4,1} \\ u_{x,4,2} \\ u_{x,6,2} \\ u_{x,6,3} \\ u_{x,8,3} \end{bmatrix}$$

or in short:

$$\mathbf{e}_{xx} = \frac{L}{2} \cdot \mathbf{u}_x \quad (66)$$

where:

$\varepsilon_{xx,l,i}$  is the strain in longitudinal direction at Node  $l$  in Layer  $i$

$$\begin{bmatrix} \sigma_{xx,2,1} \\ \sigma_{xx,4,1} \\ \sigma_{xx,4,2} \\ \sigma_{xx,6,2} \\ \sigma_{xx,6,3} \\ \sigma_{xx,8,3} \end{bmatrix} = \frac{L}{2} \cdot \begin{bmatrix} 1 & 1 & 1 & 1 & 1 & 1 \\ \frac{1}{E_{cm,1}(t)} & \frac{1}{E_{cm,1}(t)} & \frac{1}{E_{cm,2}(t)} & \frac{1}{E_{cm,2}(t)} & \frac{1}{E_{cm,3}(t)} & \frac{1}{E_{cm,3}(t)} \end{bmatrix} \cdot \begin{bmatrix} u_{x,2,1} \\ u_{x,4,1} \\ u_{x,4,2} \\ u_{x,6,2} \\ u_{x,6,3} \\ u_{x,8,3} \end{bmatrix}$$

or in short:

$$\boldsymbol{\sigma}_{xx} = \frac{L}{2} \cdot \mathbf{E}_{cm}^T \cdot \mathbf{u}_x \quad (67)$$

where:

$\sigma_{xx,l,i}$  is the stress in longitudinal direction at Node  $l$  in Layer  $i$

$E_{cm,i}(t)$  is the elastic modulus of concrete in Layer  $i$  at time  $t$

## A14 Comparison of Mechanics 1 and Mechanics 2

### A14.1 General

To show the limitation of Mechanics 1 and the advantage of Mechanics 2, a series of calculations carried out to a three-layer model. The dimensions of the three-layer model used in the calculations are same. However, the material properties and imposed deformation applied to the models are different, or in short the conditions are different. Both Mechanics 1 and Mechanics 2 are used during the calculations. Although the conditions are **NOT** the real case, the calculations under different conditions are able to show the limitation of Mechanics 1 and the advantage of Mechanics 2 in a more clear way, because the resulting strain and stress are easy to be predicted under the conditions.

Since it is impossible to check the results calculated by Mechanics 2 under all the possible conditions, the extreme conditions mentioned above are also used to prove that Mechanics 2 is applicable in this thesis. Suppose the strain and stress resulting imposed deformation, or in short the resulting strain and stress, calculated by Mechanic 2 suits the expectations under all the conditions, Mechanics 2 would be taken as applicable in this thesis. Otherwise, the mechanics would be taken as inapplicable. Hereby summarized the conditions.

$$\text{Conditions 1: } \Delta \epsilon_{new} = \Delta \epsilon_{old} = \mathbf{0}, E_{cm,connection}(t) \approx \mathbf{0}$$

Under Conditions 1, imposed deformation is assumed only applied to the connection, while the elastic modulus of connection is assumed to be zero approximately.

The aim to give calculation under Conditions 1 is to check whether the mechanics are applicable or not when the imposed deformation is applied to an extremely soft layer.

In expectation, since the connection is so soft, the imposed deformation would hardly result in any strain and stress in the old and new decks.

$$\text{Conditions 2: } \Delta \epsilon_{old} = \Delta \epsilon_{connection} = \mathbf{0}, E_{cm,connection}(t) \approx \mathbf{0}$$

Under Conditions 2, imposed deformation is assumed only applied to the new deck, while the elastic modulus of connection is assumed to be zero approximately.

The aim to give calculation under Conditions 2 is to check whether the mechanics are applicable or not when the connection is too soft to transfer the imposed deformation from one side to the other side.

In expectation, since the connection is too soft, the imposed deformation in the new deck would not be transferred to the old one. So, the imposed deformation would hardly result in any strain and stress in the old deck.

$$\text{Conditions 3: } \Delta \epsilon_{old} = \Delta \epsilon_{connection} = \mathbf{0}, E_{cm,connection}(t) = E_{cm,old}(t)$$

Under Conditions 3, imposed deformation is assumed only applied to the new deck, while the elastic modulus of old deck and connection are assumed to be same.

The aim to give calculation under Conditions 3 is to check whether the mechanics are applicable or not when two adjacent layers share same material properties.

In expectation, the connection and old deck would perform as a single layer.

$$\text{Conditions 4: } \Delta \epsilon_{old} = \Delta \epsilon_{connection} = \mathbf{0}, E_{cm,connection}(t) = E_{cm,old}(t) = \mathbf{1.2 Pa} \sim \mathbf{36.6 GPa}$$

Under Conditions 4, imposed deformation is assumed only applied to the new deck, while the elastic modulus of old deck and connection are assumed to be same. A series of elastic modulus are applied to old deck and connection.

As shown in Section 31, the limitation of Mechanics 1 is expected to be neglecting shear deformation. The aim to give calculation under Conditions 4 is to check whether the difference of elastic modulus is the only reason of Mechanics 1 and Mechanics 2 giving different results or not, or in other words is to check whether the difference of elastic modulus is the only source of shear deformation or not.

Suppose Mechanics 1 and Mechanics 2 give similar results, the difference of elastic modulus would not be the only source of considerable shear deformation but also the number of layers. Otherwise, the difference of elastic modulus is enough to be the source of shear deformation.

## A14.2 Conditions 1

### A14.2.1 Aim and Expectation

In Conditions 1, it is assumed that the imposed deformation is only applied to the connection while the elastic modulus of connection is zero. The aim to give calculation under Conditions 1 is to check whether the mechanics are applicable or not when the imposed deformation is applied to an extremely soft layer. It is expected that the resulting strain would be non-zero and positive only in the connection, while the resulting stress would be zero in the whole widened deck KW03.01, see Figure 81 and Figure 84.

### A14.2.2 Input Data

As shown in Appendix A13, the expressions in Mechanics 2 contains elastic modulus in denominators. So, the elastic modulus of connection during calculation is assumed to be  $1 \times 10^{-9}$  GPa, which is close but not equal to zero. The material properties and imposed deformation applied in Conditions 1 are shown in Table 162 and Table 163.

elastic modulus in <b>Old Deck</b>	$E_{cm}(t)$	3.66E+01	GPa
elastic modulus in <b>Connection</b>	$E_{cm}(t)$	1.00E-09	GPa
elastic modulus in <b>New Deck</b>	$E_{cm}(t)$	3.87E+01	GPa

Table 162: Material Properties Applied under Conditions 1.

imposed deformation in <b>Old Deck</b>	$\Delta\varepsilon$	0	m/m
imposed deformation in <b>Connection</b>	$\Delta\varepsilon$	3.89E-04	m/m
imposed deformation in <b>New Deck</b>	$\Delta\varepsilon$	0	m/m

\*The structure will be shortened if it is subjected to the imposed deformation in Table 163, suppose it is free to deform.

Table 163: Imposed Deformation Applied under Conditions 1.

### A14.2.3 Results

The resulting strain and stress calculated by Mechanics 1 only are shown in Figure 82 and Figure 85 respectively, while those calculated by both Mechanics 1 and Mechanics 2 are shown in Figure 83 and Figure 86 respectively.

Since the stiffness of connection is not zero exactly, non-zero stresses are obtained by both Mechanics 1 (M1) and Mechanics 2 (M2). However, with a power of  $-10$ , the stresses are almost zero. So, both the stress distribution calculated by both Mechanics 1 (M1) and Mechanics 2 (M2) suit the expectation.

In general, the shortening of the connection is restrained by the old deck and new deck. Since the stiffness of connection is assumed close to zero but not zero, non-zero stresses are obtained. Therefore, the parts in old deck and new deck, which are close to the connection, are in compression. However, with a power of  $-10$ , the stresses can be taken as zero approximately.

According to Mechanics 1, under Conditions 1, the in-plane curvature of deformed deck is uniform. The zero-point of stress appears in the old deck, see Figure 85, making the whole new deck in compression. However, according to Mechanics 2, under Conditions 1, the in-plane curvature of deformed deck is variable. So, part of the old deck and new deck are in tension, see Figure 83 and Figure 86.

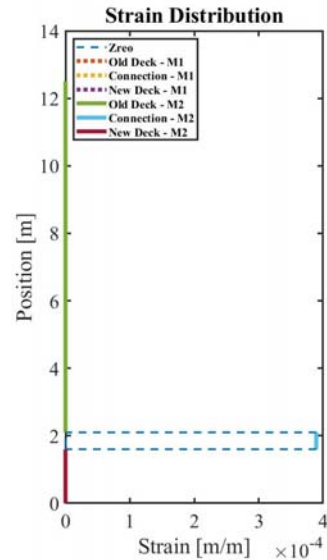
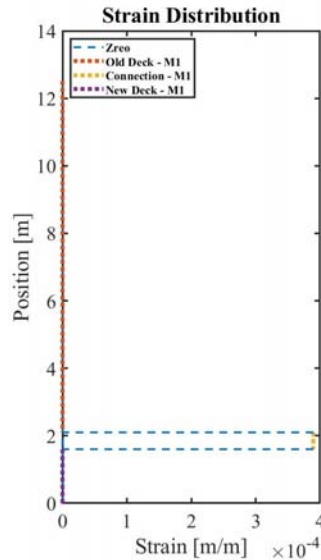
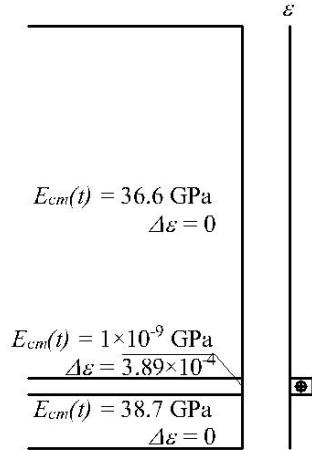


Figure 81: Material Properties, Imposed Deformation and the Sketch of Expectation (Strain) under Conditions 1.

Figure 82: Strain Distribution Calculated by Mechanics 1 (M1) under Conditions 1.

Figure 83: Strain Distribution Calculated by Mechanics 1 (M1) and Mechanics 2 (M2) under Conditions 1.

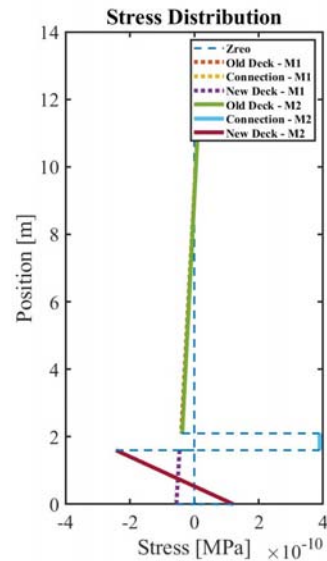
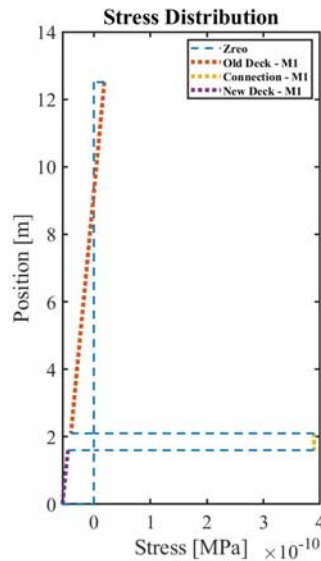
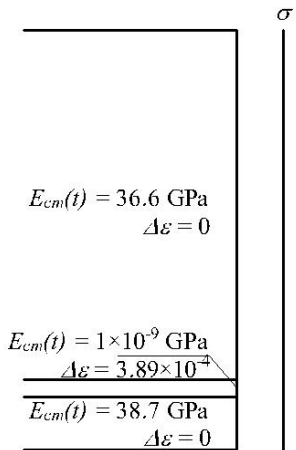


Figure 84: Material Properties, Imposed Deformation and the Sketch of Expectation (Stress) under Conditions 1.

Figure 85: Stress Distribution Calculated by Mechanics 1 (M1) under Conditions 1.

Figure 86: Stress Distribution Calculated by Mechanics 1 (M1) and Mechanics 2 (M2) under Conditions 1.

### A14.2.4 Conclusion

Under Conditions 1, although the resulting stress calculated by Mechanics 1 and Mechanics 2 are not same, since both the results calculated by Mechanics 1 and Mechanics 2 suit the expectation, both of them are applicable when the imposed deformation is applied to an extremely soft layer.

## A14.3 Conditions 2

### A14.3.1 Aim and Expectation

In Conditions 2, it is assumed that the imposed deformation is only applied to the new deck while the elastic modulus of connection is set to be zero. The aim to give calculation under Conditions 2 is to check whether the mechanics are applicable or not when the connection is too soft to transfer the imposed deformation from one side to the other side. It is expected that the resulting strain would be non-zero and negative only in connection, while the resulting stress would be close to zero in the whole widened deck KW03.01, see Figure 87 and Figure 90.

### A14.3.2 Input Data

Similar to Mechanics 1, the elastic modulus of connection during calculation is set to be  $1 \times 10^{-9}$  GPa, which is close but not equal to zero. The material properties and imposed deformation applied in Conditions 2 are shown in Table 162 and Table 163.

elastic modulus in <b>Old Deck</b>	$E_{cm}(t)$	3.66E+01	GPa
elastic modulus in <b>Connection</b>	$E_{cm}(t)$	1.00E-09	GPa
elastic modulus in <b>New Deck</b>	$E_{cm}(t)$	3.87E+01	GPa

Table 164: Material Properties Applied in Conditions 2.

imposed deformation in <b>Old Deck</b>	$\Delta\varepsilon$	0	m/m
imposed deformation in <b>Connection</b>	$\Delta\varepsilon$	0	m/m
imposed deformation in <b>New Deck</b>	$\Delta\varepsilon$	4.34E-04	m/m

\*The structure will be shortened if it is subjected to the imposed deformation in Table 165, suppose it is free to deform.

Table 165: Imposed Deformation Applied in Conditions 2.

## 12.1.1 Results

The resulting strain and stress calculated by Mechanics 1 only are shown in Figure 88 and Figure 91 respectively, while those calculated by both Mechanics 1 and Mechanics 2 are shown in Figure 89 and Figure 92 respectively.

Under Conditions 2, results calculated by Mechanics 1 does not suit the expectation while those calculated by Mechanics 2 do. The strain and stress distribution in the old deck and new deck calculated by Mechanics 1 are non-zero which is different from the expectation.

In general, the shortening of the new deck should be restrained by the connection. However, the connection is too soft to give a strong restrain to the new deck. So, the new deck is almost free to deform instead of being in tension.

According to Mechanics 1, under Conditions 2, the in-plane curvature of deformed deck is uniform. The zero-point of strain and stress appears in the old deck, making the strain and stress in old deck and new deck non-zero, see Figure 88 and Figure 91.

According to Mechanics 2, the in-plane curvature of deformed deck is variable. The strain calculated by Mechanics 2 is the deformation to restore compatibility. The connection is too soft and too easy to deform so that hardly any deformation is required in new deck to restore deformation compatibility. Therefore, the strain distribution is almost zero in new deck calculated by Mechanics 2, see Figure 89.

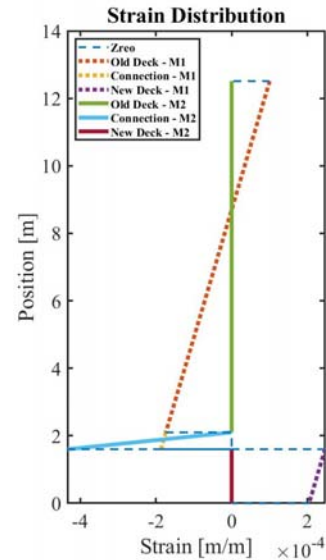
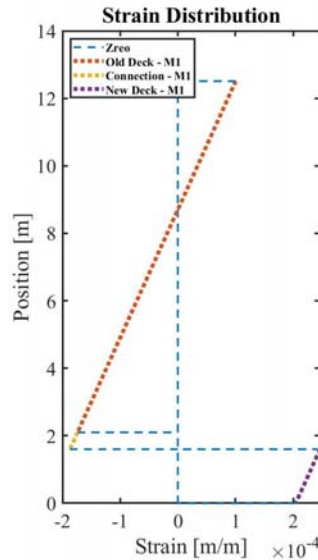
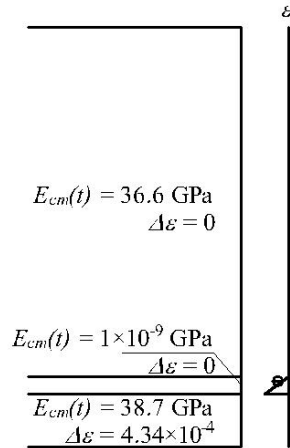


Figure 87: Material Properties, Imposed Deformation and the Sketch of Expectation (Strain) under Conditions 2.

Figure 88: Strain Distribution Calculated by Mechanics 1 (M1) under Conditions 2.

Figure 89: Strain Distribution Calculated by Mechanics 1 (M1) and Mechanics 2 (M2) under Conditions 2.

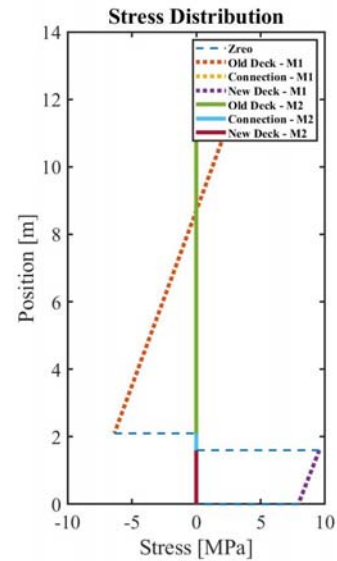
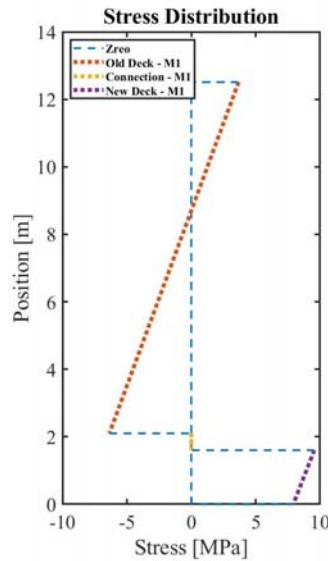
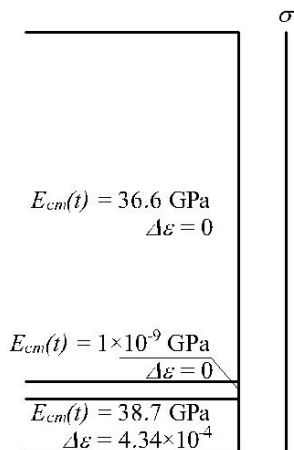


Figure 90: Material Properties, Imposed Deformation and the Sketch of Expectation (Stress) under Conditions 2.

Figure 91: Stress Distribution Calculated by Mechanics 1 (M1) under Conditions 2.

Figure 92: Stress Distribution Calculated by Mechanics 1 (M1) and Mechanics 2 (M2) under Conditions 2.

### A14.3.3 Conclusion

Under Conditions 2, Mechanics 1 is not applicable because it makes the imposed deformation transferred from one side to the other side when the connection not stiff enough produce imposed deformation. However, since the results calculated by Mechanics 2 suits the expectation, Mechanics 2 is applicable when the connection is too soft to transfer the imposed deformation from one side to the other side.

## A14.4 Conditions 3

### A14.4.1 Aim and Expectation

A reliable mechanics should be able to predict the deformation of the two-layer model with a three-layer model, by applying same material properties to two adjacent layers. So, in Conditions 3, it is assumed that the imposed deformation is only applied to the new deck while the elastic modulus of old deck and connection are assumed to be same.

The aim to give calculation under Conditions 3 is to check whether the mechanics are applicable or not when two adjacent layers share same material properties. It is expected that the in-plane curvature in old deck and connection would be uniform. Since the shortening of new deck is restrained by connection, the part of old deck and connection close to new deck would be in compression, while the new deck would be in tension, see Figure 93 and Figure 96.

### 12.1.2 Input Data

The material properties and imposed deformation applied in Conditions 3 are shown in Table 166 and Table 167.

elastic modulus in <b>Old Deck</b>	$E_{cm}(t)$	3.66E+01	GPa
elastic modulus in <b>Connection</b>	$E_{cm}(t)$	3.66E+01	GPa
elastic modulus in <b>New Deck</b>	$E_{cm}(t)$	3.87E+01	GPa

Table 166: Material Properties Applied in Conditions 3.

imposed deformation in <b>Old Deck</b>	$\Delta\varepsilon$	0	m/m
imposed deformation in <b>Connection</b>	$\Delta\varepsilon$	0	m/m
imposed deformation in <b>New Deck</b>	$\Delta\varepsilon$	4.34E-04	m/m

\*The structure will be shortened if it is subjected to the imposed deformation in Table 167, suppose it is free to deform.

Table 167: Imposed Deformation Applied in Conditions 3.

### 12.1.3 Results

The resulting strain and stress calculated by Mechanics 1 only are shown in Figure 94 and Figure 97 respectively, while those calculated by both Mechanics 1 and Mechanics 2 are shown in Figure 95 and Figure 98 respectively.

Both the results calculated by Mechanics 1 and Mechanics 2 suit the expectation. The old deck and the connection perform as a single layer. Since the shortening of new deck is restrained by connection, the part of old deck and connection close to new deck is in compression, while the new deck is in tension.

In general, the shortening of the new deck is restrained by the connection. Therefore, the part in new deck, which are close to the connection, is in tension. According to both Mechanics 1 and Mechanics 2, the in-plane curvature in the old deck and connection is uniform, see Figure 94 and Figure 97.

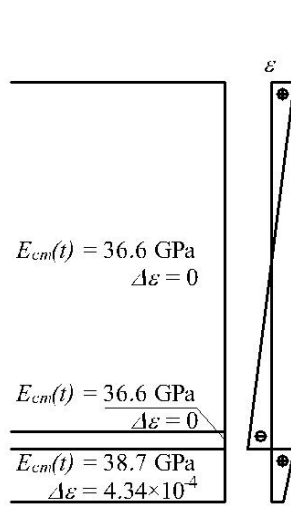


Figure 93: Material Properties, Imposed Deformation and the Sketch of Expectation (Strain) under Conditions 3.

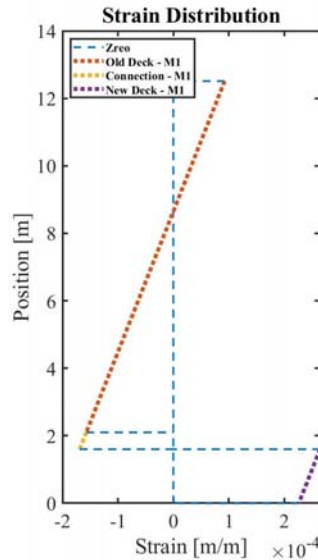


Figure 94: Strain Distribution Calculated by Mechanics 1 (M1) under Conditions 3.

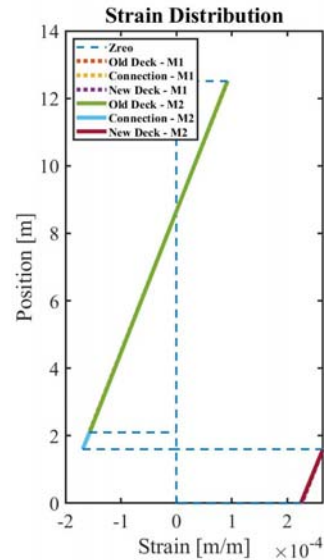


Figure 95: Strain Distribution Calculated by Mechanics 1 (M1) and Mechanics 2 (M2) under Conditions 3.

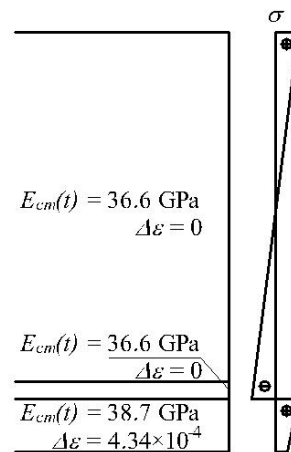


Figure 96: Material Properties, Imposed Deformation and the Sketch of Expectation (Stress) under Conditions 3.

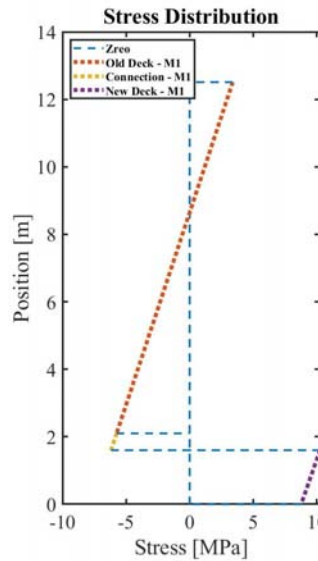


Figure 97: Stress Distribution Calculated by Mechanics 1 (M1) under Conditions 3.

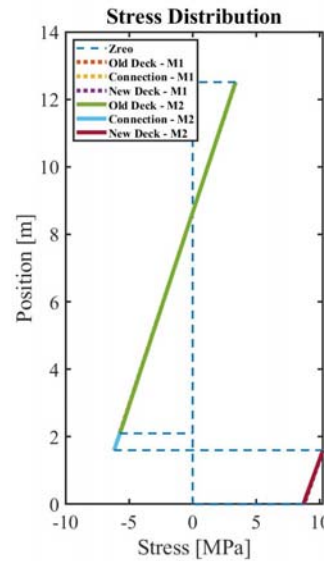


Figure 98: Stress Distribution Calculated by Mechanics 1 (M1) and Mechanics 2 (M2) under Conditions 3.

### A14.4.2 Conclusion

Since both the results calculated by Mechanics 1 and Mechanics 2 suit the expectation, both Mechanics 1 and Mechanics 2 are applicable when two adjacent layers share same material properties. In other words, both Mechanics 1 and Mechanics 2 are able to predict the deformation of the two-layer model with a three-layer model, by applying same material properties to two adjacent layers.

## A14.5 Conditions 4

### A14.5.1 Aim and Expectation

In Conditions 4, it is assumed that the imposed deformation is only applied to the new deck while the elastic modulus of old deck and connection are assumed to be same.

As shown in Section A14.3 and A14.4, the results calculated by Mechanics 1 suit the expectation under Conditions 3 but not under Conditions 2. As shown in Chapter 8.2, the limitation of Mechanics 1 is expected to be neglecting shear deformation. So, the aim to give calculation under Conditions 4 is to study, to what extent, the shear deformation is neglectable.

The calculations carried out under Conditions 3 and Conditions 4 are same except for the magnitude of elastic modulus applied to new deck and connection. To show the impact of elastic modulus on the shear deformation, a series of elastic modulus are applied to old deck and connection.

Suppose Mechanics 1 and Mechanics 2 give similar results, the difference of elastic modulus would not be the only source of considerable shear deformation but also the number of layers. Otherwise, the difference of elastic modulus is enough to be the source of shear deformation.

### A14.5.2 Input Data

A series of elastic modulus are applied to old deck and connection. The material properties and imposed deformation applied in Conditions 3 are shown in Table 168 and Table 169.

elastic modulus in <b>Old Deck</b>	$E_{cm}(t)$	1.20E-09~3.66E+01	GPa
elastic modulus in <b>Connection</b>	$E_{cm}(t)$	1.20E-09~3.66E+01	GPa
elastic modulus in <b>New Deck</b>	$E_{cm}(t)$	3.87E+01	GPa

Table 168: Material Properties Applied in Conditions 4.

imposed deformation in <b>Old Deck</b>	$\Delta\varepsilon$	0	m/m
imposed deformation in <b>Connection</b>	$\Delta\varepsilon$	0	m/m
imposed deformation in <b>New Deck</b>	$\Delta\varepsilon$	4.34E-04	m/m

\*The structure will be shortened if it is subjected to the imposed deformation in Table 168, suppose it is free to deform.

Table 169: Imposed Deformation Applied in Conditions 4.

### A14.5.3 Results

A series of stress distribution corresponding to different elastic modulus of old deck and concrete in connection are calculated. The calculation is carried out by both Mechanics 1 and Mechanics 2. The colour in the image represents the mean strain resulting from the imposed deformation applied to old deck, connection and old deck.

Take the strain resulting from imposed deformation as an example. As shown in Section A14.4, one elastic modulus applied to the old deck and connection is corresponding to one strain distribution calculated by Mechanics 1 and Mechanics 2 respectively. Then a series of elastic modulus applied to the old deck and connection is corresponding to is corresponding to a series of strain distribution calculated by Mechanics 1 and Mechanics 2 respectively.

By taking the position in cross-section, the elastic modulus of concrete and the strain resulting from imposed deformation as x-, y- and z-axis respectively, the 3D images of the strain distribution calculated by Mechanics 1 and Mechanics 2 are plotted respectively, see Figure 100 and Figure 102.

In other words, Figure 100 and Figure 102 are a series of Figure 94 and Figure 97 placed one by one according to the elastic modulus applied to old deck and connection. To show the difference between Figure 100 and Figure 102, the

y-view of the 3D image is plotted, see Figure 103 and Figure 104. In Figure 103 and Figure 104, the red line and green represent the strain distribution in old deck and connection when the elastic modulus of concrete applied to old deck and connection is 0.06 GPa and 1.2 Pa respectively.

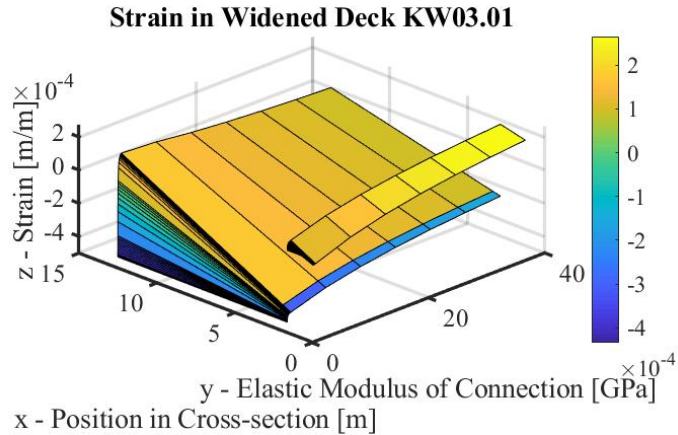
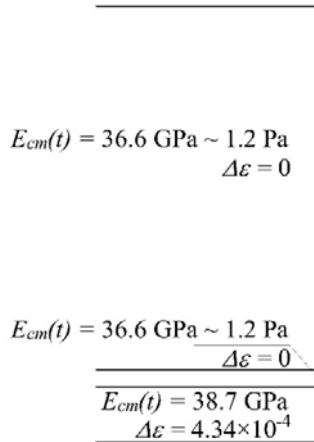


Figure 99: Material Properties and Imposed Deformation in the South Part ( $\Delta t_{II-III} = 28 \text{ days}$ ).

Figure 100: Three-Dimensional Image of Strain Resulting from All Imposed Deformation in Conditions 4.

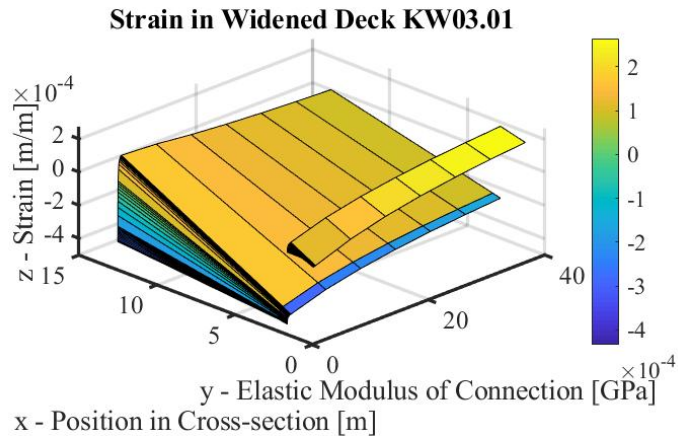
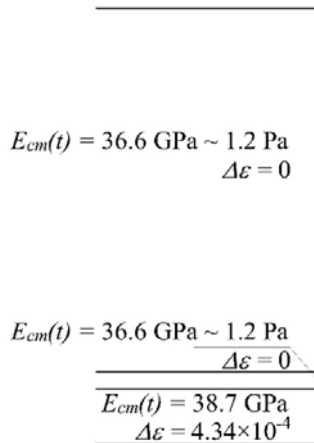


Figure 101: Material Properties and Imposed Deformation in the South Part ( $\Delta t_{II-III} = 28 \text{ days}$ ).

Figure 102: Three-Dimensional Image of Strain Resulting from All Imposed Deformation in Conditions 4.

The both in-plane curvature in the old deck and the connection calculated by Mechanics 1 and Mechanics 2 are uniform. It is proved again that both Mechanics 1 and Mechanics 2 are able to predict the deformation of the two-layer model with a three-layer model, by applying same material properties to two adjacent layers.

However, when the elastic modulus of concrete applied to old deck and connection is smaller than 0.06 GPa, the difference between resulting strain calculated by Mechanics 1 and Mechanics 2 becomes obvious, see the parts between red line and green line in Figure 103 and Figure 104. It means, in two-layer model, the limitation of Mechanics 1, neglecting the shear deformation, becomes obvious when the stiffness of a layer is much smaller than that of the other.

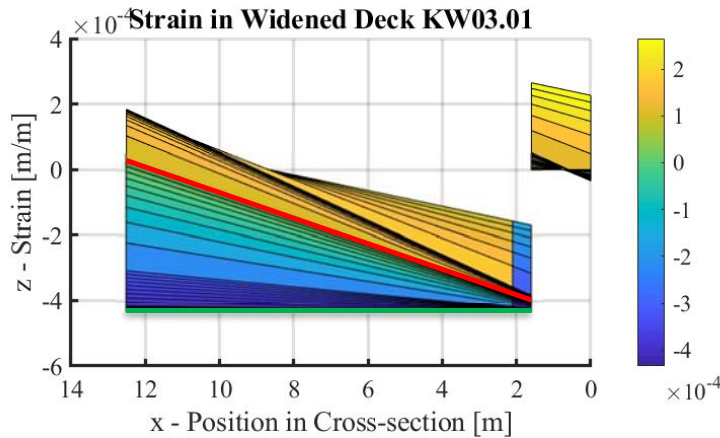


Figure 103: Y-View of Figure 100.

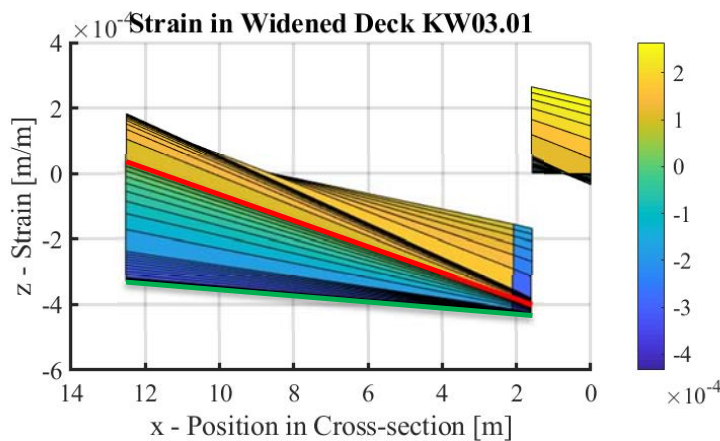


Figure 104: Y-View of Figure 102.

#### A14.5.4 Conclusion

According to the results under Condition 1 to Condition 4, whether the shear deformation is neglectable or not depends on various factors: the number of layers, the elastic modulus and the imposed deformation applied to the layers. Suppose the shear deformation is not neglectable, Mechanics 2 is preferred to give more reliable results. However, when a two-layer model is applied, the shear deformation is neglectable in most cases, because the elastic modulus of concrete would not be in the situation as low as shown in Figure 103 and Figure 104.

#### A14.6 Conclusion

According to Section A14.2, Section A14.3 and Section A14.4, the advantage of Mechanics 2 is that it takes shear deformation into account. As a result, the results of Mechanics 1 and Mechanics 2 are close only if there is no impact of shear deformation, otherwise the results of mechanics 2 is more reliable. Since it is unknown whether there is large shear deformation or not before carrying out a calculation, it is suggested to use Mechanics 2 for a more reliable solution.

## A15 Impact of Timing to Make Connection on the Resulting Stress

### A15.1 General

It is expected that different timing to make connection would result in different in-plane strain and stress distribution at time  $t = t_{\infty}$ . To investigate the impact of timing to make connection on the stress resulting from imposed deformation, stress resulting from imposed deformation is calculated with a series of timing to make connection. For simplicity, the impact of cracking is not taken into account. The mechanics used during the calculations are shown in Appendix A12 and Appendix A13. Results of the calculations are investigated to see whether it is possible to find a critical timing to make connection which is the earliest one resulting in no prestress consumption in old decks and new decks at time  $t = t_{\infty}$ .

According to Appendix A12 and Appendix A13, stress resulting from imposed deformation is calculated basing on split layers which are first free to deform. The deformation of the layers are calculated with time  $t = t_{\infty}$  ( $t_{\infty} = 111$  years). Then mechanical loads are applied to the deformed layers as internal load to restore the deformation compatibility so that the layers can be reassembled.

Before the layers being reassembled, the compressive stress resulting from prestressing are calculated with time  $t = t_{\infty}$  ( $t_{\infty} = 111$  years). To restore deformation compatibility, additional deformation is applied to the layers. The compressive stress resulting from prestressing would be decreased due to the shortening of the layers while increased due to the elongation of the layers. For simplicity, the impact of additional deformation due to imposed deformation, or in other words the impact of imposed deformation, on the compressive stress is neglected. Therefore, the prestress consumption in proportion is the ratio of the stress resulting from imposed deformation and prestressing, where prestressing force is calculated as a constant with time  $t = t_{\infty}$  ( $t_{\infty} = 111$  years).

### A15.2 Time History of Construction

As shown in Section 6.1, connections in widened deck KW03.01 are made at time  $\Delta t_{II-III} = 28$  days after new decks being built. To investigate the impact of timing to make connection, instead of time  $\Delta t_{II-III} = 28$  days, a series of new timing to make connection are applied from time  $\Delta t_{II-III} = 7$  days to time  $\Delta t_{II-III} = 50$  years.

The models used during investigation are Simplified Model 1 and Simplified Model 2, see Section 7.3.1 and Section 7.4.1. The input data is shown in Chapter 5. The material properties applied to the expressions are calculated by the input data and the expressions in Appendix A4 and Appendix A5. The imposed deformation and prestress loss in old decks are calculated by the expressions in Appendix A6. For the convenience of reading, the imposed deformation in old decks, new decks and connections are denoted as  $\Delta \varepsilon_{old}$ ,  $\Delta \varepsilon_{new}$  and  $\Delta \varepsilon_{connection}$ . For the simplicity, here only summarized the data of time history of construction, see Table 170 and Table 171.

time of old deck being built	$t_I$	0 years
time of new deck being built	$t_{II}$	11 years
time of connection being built after new deck being built	$\Delta t_{II-III}$	7 ~ 18250 days
connected age of <b>connection</b>	$\Delta t_{III-IV}$	1 days
target time after new deck being built	$\Delta t_{II-V}$	36500 days

Table 170: Basic Data of Time History of Construction.

time of connection being stiff after new deck being built	$\Delta t_{II-IV}$	8 ~ 18251	days
connected age of <b>old deck</b>	$\Delta t_{I-IV}$	4023 ~ 22266	days
connected age of <b>new deck</b>	$\Delta t_{II-IV}$	8 ~ 18251	days
target age of <b>old deck</b>	$\Delta t_{I-V}$	40515	days
target age of <b>connection</b>	$\Delta t_{III-V}$	36451 ~ 18250	days
target age of <b>new deck</b>	$\Delta t_{II-V}$	36500	days

\*The data in Table 170 is evaluated basing on the data in Table 171.

Table 171: Other Data of Time History of Construction.

Prestress is taken into account, which is constant and uniformly distributed in old decks and new decks. The calculation of compressive stress resulting from prestressing at time  $t = t_{\infty}$  has been introduced in Appendix A9.3, Appendix A11.2 and Appendix A11.3. For simplicity, hereby only summarized the results of the calculation, see Table 172.

<b>South:</b>			
prestress in <b>old deck</b>	$\sigma_{old,prestressing}$	7.16E+06	Pa
prestress in <b>new deck</b>	$\sigma_{new,prestressing}$	8.32E+06	m/m
<b>North:</b>			
prestress in <b>old deck</b>	$\sigma_{old,prestressing}$	7.16E+06	m/m
prestress in <b>new deck</b>	$\sigma_{new,prestressing}$	6.45E+06	m/m

Table 172: Compressive Stress Resulting from Prestressing at time  $t = t_{\infty}$  ( $t_{\infty} = 111$  years).

### A15.3 Results (Making Connection at Time $\Delta t_{II-III} = 7 \sim 18250$ days)

With the new time history of construction shown in Appendix A15.2, the stress resulting from imposed deformation are calculated as a function of  $\Delta t_{II-III}$ . Mechanics 2 is used during the calculation. The final resulting stress shown in Figure 106 and Figure 108 is the summation of the resulting stress and the compressive stress resulting from prestressing, while the prestress consumption in proportion is the ratio of them.

According to Figure 106 and Figure 108, in new decks, the maximum compressive stress appears when connections are made at time  $\Delta t_{II-III} \approx 4000$  days. Suppose only in-plane loads are taken into account, the old decks and new decks are always in compression while the connections are always in tension. Suppose out-of-plane loads are also taken into account, as shown in Appendix A2.5, the maximum tensile stress resulting from out-of-plane loads in cross-section at mid-span varies from  $\sigma_d = 9.9$  MPa to  $\sigma_d = 15.6$  MPa, which is always larger than the maximum compressive stress resulting from in-plane loads shown in Figure 106 and Figure 108. As a result, suppose the tensile strength of concrete is neglected, new decks are always cracked no matter when connections are made.

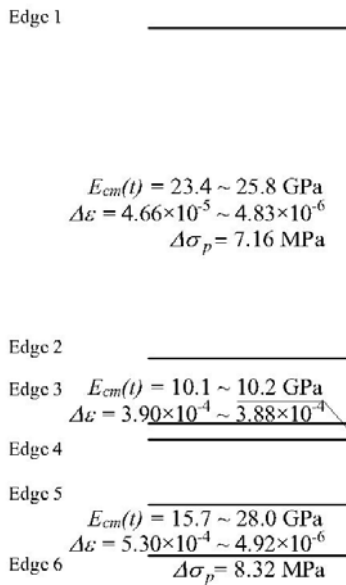


Figure 105: Sketch of Edges in the South Part.

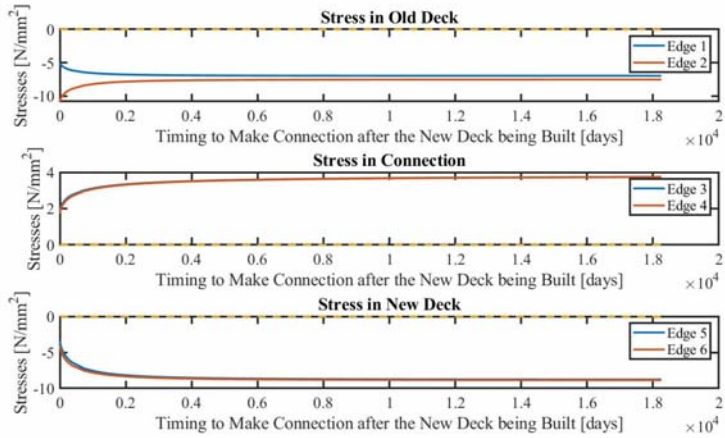


Figure 106: Final Resulting Stress in the South Part without Cracking.

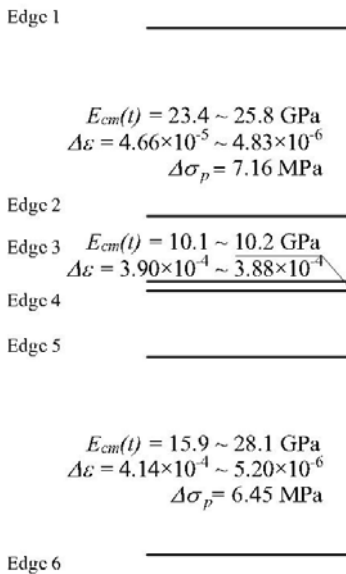


Figure 107: Sketch of Edges in the North Part.

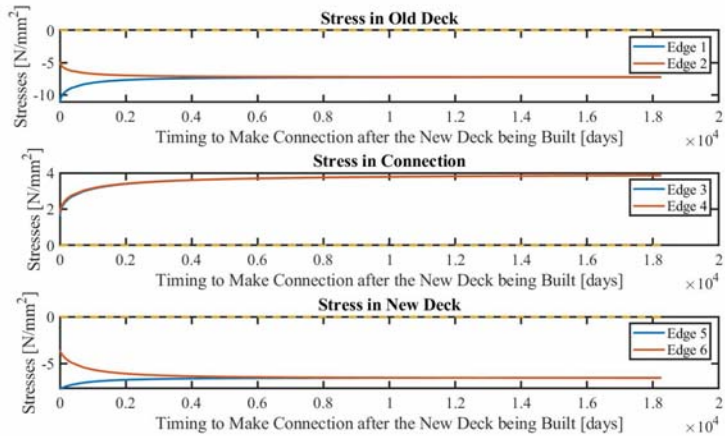


Figure 108: Final Resulting Stress in the North Part without Cracking.

### A15.4 Results (Making Connection at Time $t = 7\sim 90$ days)

Since either no prestress consumption or minimum prestress consumption is practical, see Appendix A15.4, the investigation has to zoom in to a practical period. Therefore, the final resulting stress when connections are made before 90 days are investigated, see Figure 110 and Figure 112.

As shown in Figure 110 and Figure 112, suppose the connection is made at 90 days or earlier, the timing to make connection would have significant impact on the magnitude of final resulting stress. In terms of prestress consumption, to save prestress, connection should be made as late as possible.

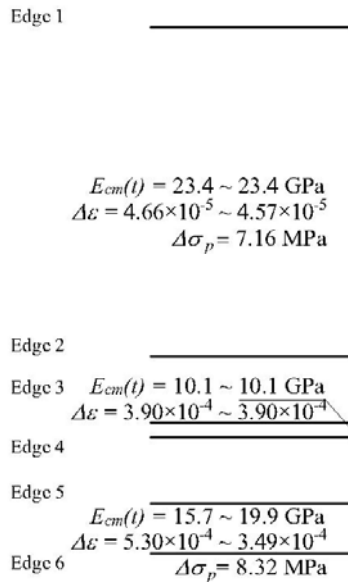


Figure 109: Sketch of Edges in the South Part.

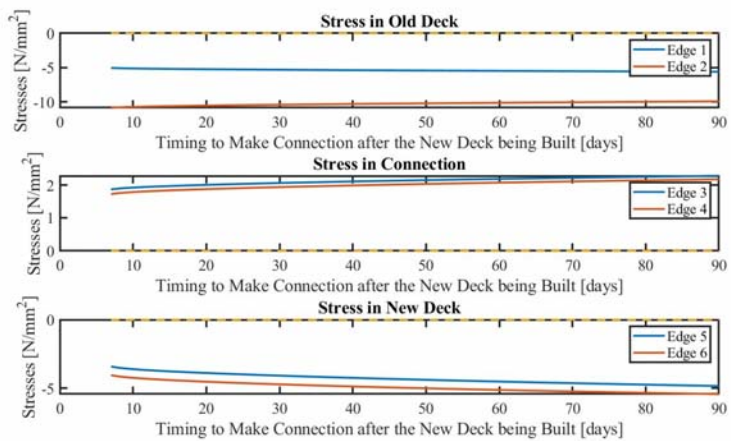


Figure 110: Final resulting Stress in the South Part without Cracking (7~90 days).

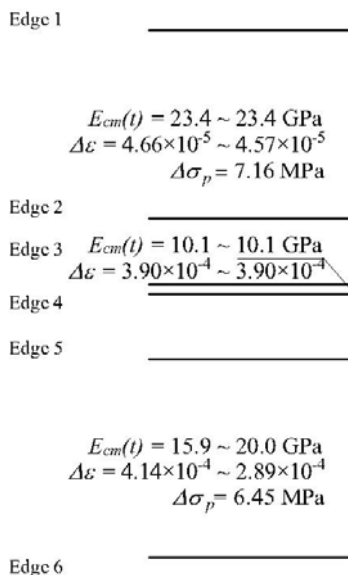


Figure 111: Sketch of Edges in the North Part.

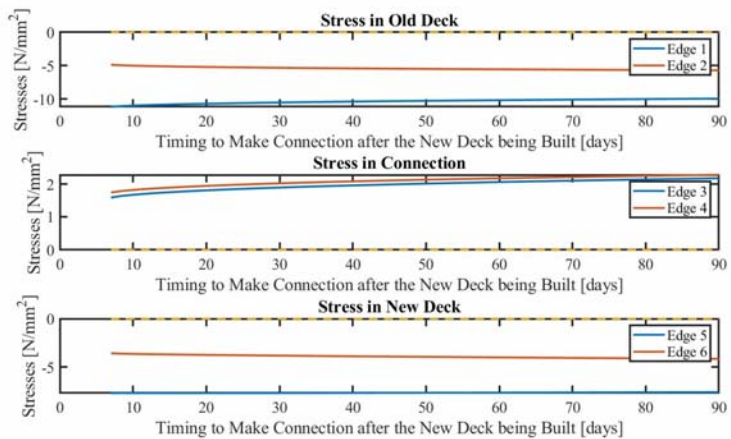


Figure 112: Final resulting Stress in the North Part without Cracking (7~90 days).

### A15.5 Prestress Consumption without Cracking

As shown in Appendix A15.1, the prestress consumption in proportion is the ratio of the stress resulting from imposed deformation and prestressing, where prestressing force is calculated as a constant with time  $t = t_{\infty}$  ( $t_{\infty} = 111$  years). The results of the calculation are shown in Figure 110 and Figure 112. When the stress resulting from imposed deformation is tensile stress, the ratio would be positive. Otherwise, the ratio would be negative.

In general, a later timing to make connection results in less prestress consumption. As shown in Figure 114 and Figure 116, the maximum prestress consumption in proportion occurs when the connection is made at time  $\Delta t_{II-III} = 7$  days. The values of the maximum prestress consumption in proportion are shown in Table 173. It is shown that the maximum prestress consumption appears at the new deck in south when connections are made at time  $\Delta t_{II-III} = 7$  days, where 58.8% of compressive stress resulting from prestress is consumed due to imposed deformation.

South	Old	29.5 %
	New	58.8 %
North	Old	30.0 %
	New	44.5 %

Table 173: Ratio between Maximum Tensile Stress and Prestress.

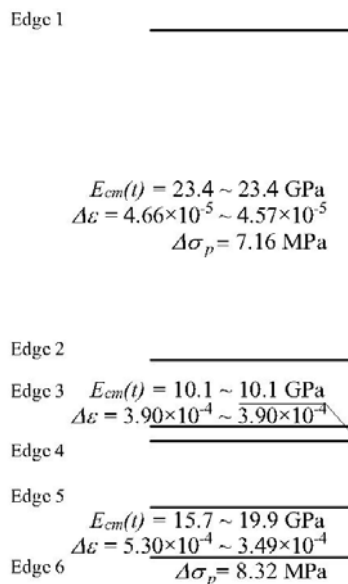


Figure 113: Sketch of Edges in the South Part.

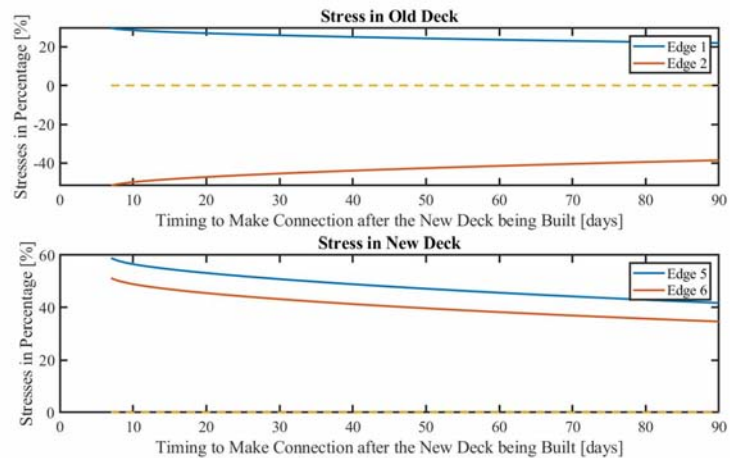


Figure 114: Consumption of Prestress in the South Part without Cracking (7~90 days).

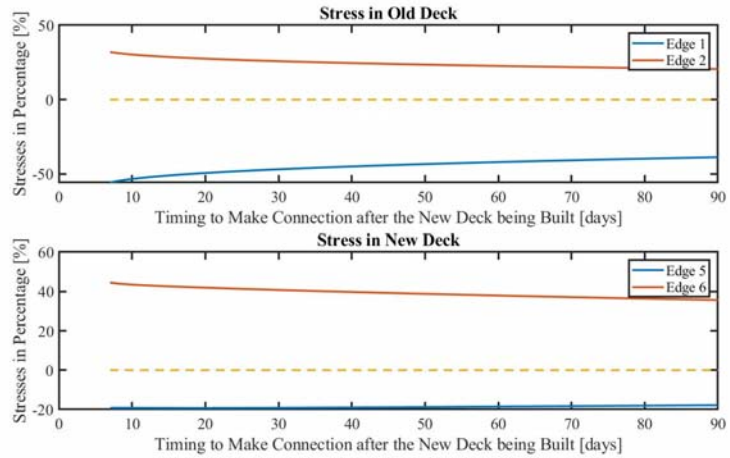
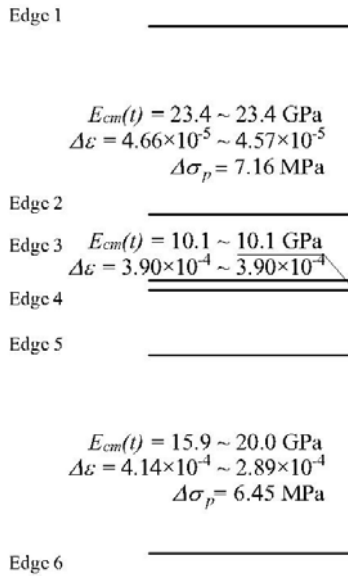


Figure 115: Sketch of Edges in the North Part.

Figure 116: Consumption of Prestress in the North Part without Cracking (7~90 days).

### A15.6 Examples

To be specific, hereby shown final resulting stress when connections are made at time  $\Delta t_{II-III} = 7$  days,  $\Delta t_{II-III} = 14$  days and time  $\Delta t_{II-III} = 28$  days.

#### Example 1: south part (connection made at time $t = 7$ days)

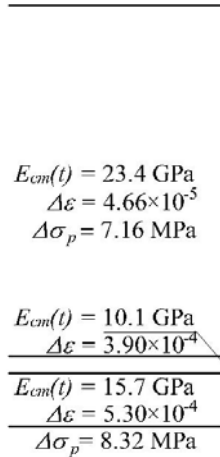


Figure 117: Material Properties and Imposed Deformation in South ( $\Delta t_{II-III} = 7$  days).

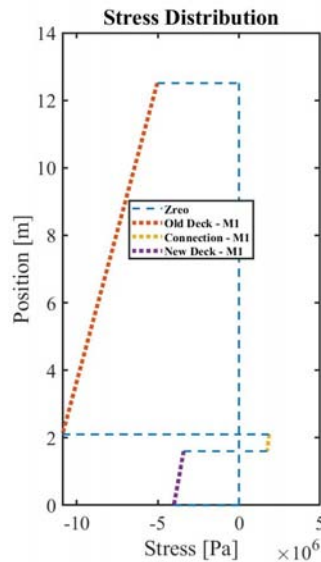


Figure 118: Stress Calculated by Mechanics 1 (M1) in South ( $\Delta t_{II-III} = 7$  days).

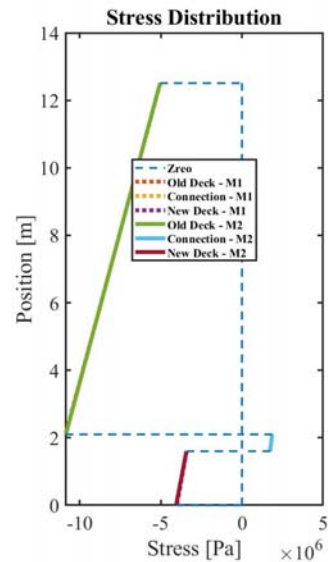


Figure 119: Stress Calculated by Mechanics 1 (M1) and Mechanics 2 (M2) in South ( $\Delta t_{II-III} = 7$  days).

#### Example 2: south part (connection made at time $t = 14$ days)

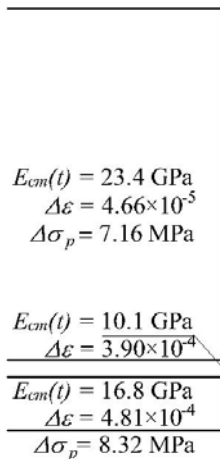


Figure 120: Material Properties and Imposed Deformation in South ( $\Delta t_{II-III} = 14$  days).

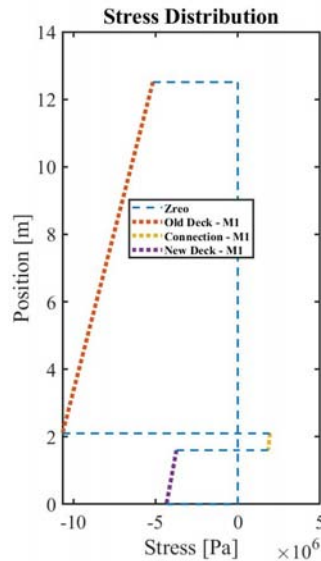


Figure 121: Stress Calculated by Mechanics 1 (M1) in South ( $\Delta t_{II-III} = 14$  days).

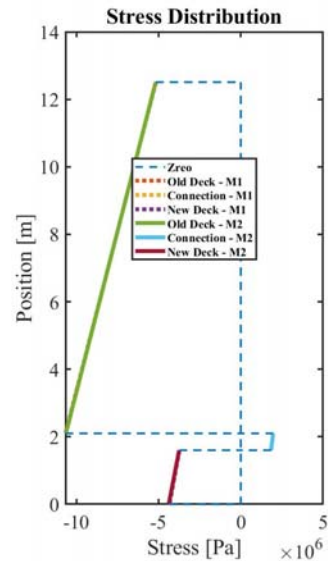


Figure 122: Stress Calculated by Mechanics 1 (M1) and Mechanics 2 (M2) in South ( $\Delta t_{II-III} = 14$  days).

**Example 3: south part (connection made at time  $t = 28$  days)**

$E_{cm}(t) = 23.4 \text{ GPa}$ $\Delta\varepsilon = 4.64 \times 10^{-5}$ $\Delta\sigma_p = 7.16 \text{ MPa}$
$E_{cm}(t) = 10.1 \text{ GPa}$ $\Delta\varepsilon = 3.90 \times 10^{-4}$
$E_{cm}(t) = 17.9 \text{ GPa}$ $\Delta\varepsilon = 4.37 \times 10^{-4}$ $\Delta\sigma_p = 8.32 \text{ MPa}$

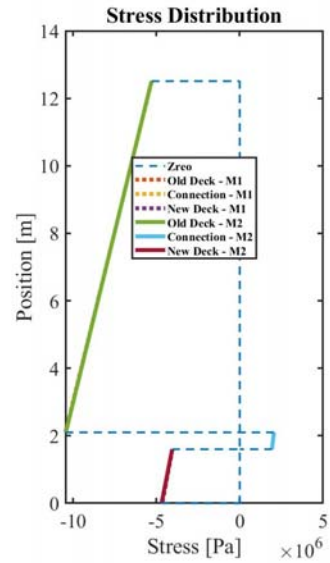
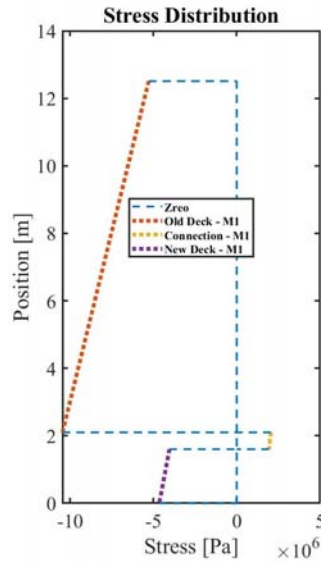


Figure 123: Material Properties and Imposed Deformation in South ( $\Delta t_{II-III} = 28$  days).

Figure 124: Stress Calculated by Mechanics 1 (M1) in South ( $\Delta t_{II-III} = 28$  days).

Figure 125: Stress Calculated by Mechanics 1 (M1) and Mechanics 2 (M2) in South ( $\Delta t_{II-III} = 28$  days).

**Example 4: north part (connection made at time  $t = 7$  days)**

$E_{cm}(t) = 23.4 \text{ GPa}$ $\Delta\varepsilon = 4.66 \times 10^{-5}$ $\Delta\sigma_p = 7.16 \text{ MPa}$
$E_{cm}(t) = 10.1 \text{ GPa}$ $\Delta\varepsilon = 3.90 \times 10^{-4}$
$E_{cm}(t) = 15.9 \text{ GPa}$ $\Delta\varepsilon = 4.14 \times 10^{-4}$ $\Delta\sigma_p = 6.45 \text{ MPa}$

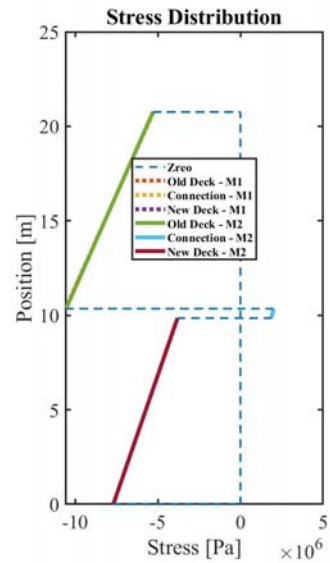
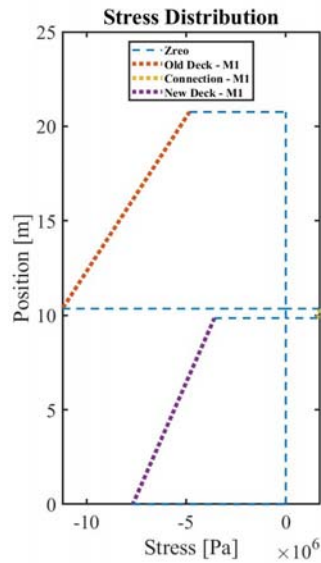


Figure 126: Material Properties and Imposed Deformation in North ( $\Delta t_{II-III} = 7$  days).

Figure 127: Stress Calculated by Mechanics 1 (M1) in North ( $\Delta t_{II-III} = 7$  days).

Figure 128: Stress Calculated by Mechanics 1 (M1) and Mechanics 2 (M2) in North ( $\Delta t_{II-III} = 7$  days).

**Example 5: north part (connection made at time  $t = 14$  days)**

$E_{cm}(t) = 23.4 \text{ GPa}$ $\Delta\varepsilon = 4.66 \times 10^{-5}$ $\Delta\sigma_p = 7.16 \text{ MPa}$
$E_{cm}(t) = 10.1 \text{ GPa}$ $\Delta\varepsilon = 3.90 \times 10^{-4}$
$E_{cm}(t) = 17.0 \text{ GPa}$ $\Delta\varepsilon = 3.81 \times 10^{-4}$ $\Delta\sigma_p = 6.45 \text{ MPa}$

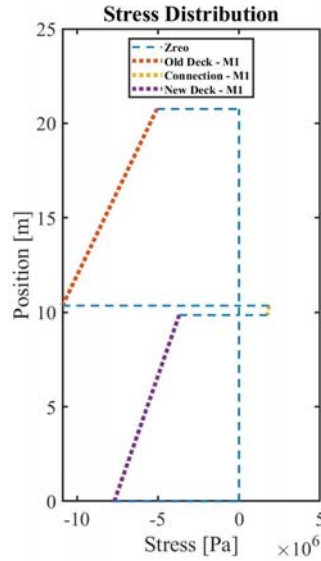


Figure 129: Material Properties and Imposed Deformation in North ( $\Delta t_{II-III} = 14$  days).

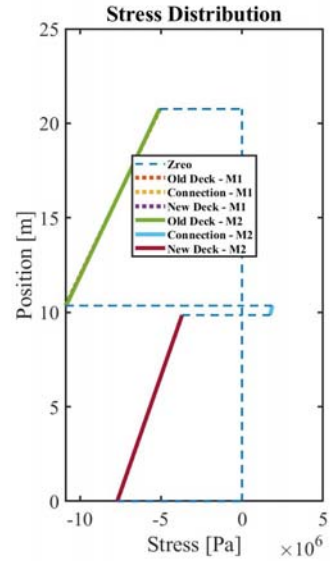


Figure 130: Stress Calculated by Mechanics 1 (M1) in North ( $\Delta t_{II-III} = 14$  days).

Figure 131: Stress Calculated by Mechanics 1 (M1) and Mechanics 2 (M2) in North ( $\Delta t_{II-III} = 14$  days).

**Example 6: north part (connection made at time  $t = 28$  days)**

$E_{cm}(t) = 23.4 \text{ GPa}$ $\Delta\varepsilon = 4.64 \times 10^{-5}$ $\Delta\sigma_p = 7.16 \text{ MPa}$
$E_{cm}(t) = 10.1 \text{ GPa}$ $\Delta\varepsilon = 3.90 \times 10^{-4}$
$E_{cm}(t) = 18.1 \text{ GPa}$ $\Delta\varepsilon = 3.50 \times 10^{-4}$ $\Delta\sigma_p = 6.45 \text{ MPa}$

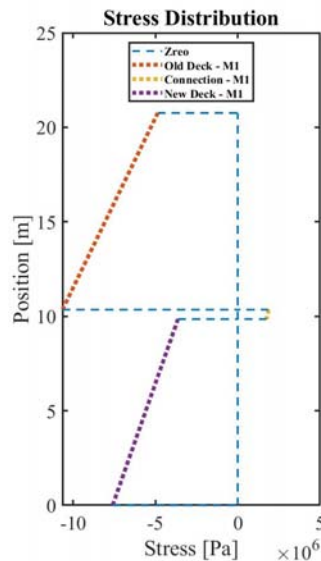


Figure 132: Material Properties and Imposed Deformation in North ( $\Delta t_{II-III} = 28$  days).

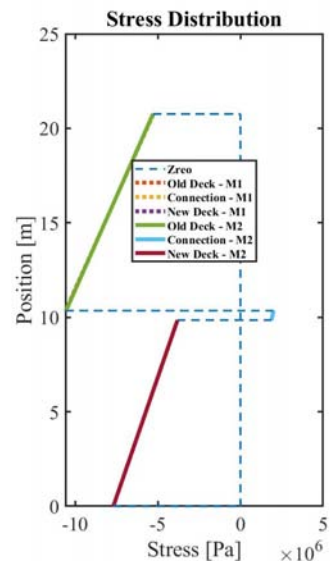


Figure 133: Stress Calculated by Mechanics 1 (M1) in North ( $\Delta t_{II-III} = 28$  days).

Figure 134: Stress Calculated by Mechanics 1 (M1) and Mechanics 2 (M2) in North ( $\Delta t_{II-III} = 28$  days).

\*The final resulting stress calculated by Mechanics 1 (M1) and Mechanics 2 (M2) are almost same.

## A15.7 Discussion

In general, the final resulting stress in widened deck KW03.01 calculated by Mechanics 1 and Mechanics 2 are almost same when cracking is not taken into account. The reason is that the stiffness of connections are not small enough. The results calculated by Mechanics 1 and Mechanics 2 are different only when the stiffness of connection is extremely small, see Appendix A19. However, such a small stiffness will not appear if cracking is not taken into account.

When a long-term variable load is applied to a concrete member, due to the creep or relaxation appears in the process, the concrete member performs as if its elastic modulus is decreased. For simplicity, a fictitious elastic modulus  $E_{cm}(t)$  is used to evaluate the internal forces in concrete when it is subjected to a long-term variable load, see Expression 18 (Scholten, 1989).

According to Expression 18, small elastic modulus are applied to the model. As a result, the tensile stress resulting from imposed deformation is much smaller than the compressive stress from prestress, making old decks and new decks always be in compression.

If connections are made at earlier timing, imposed deformation will be  $\Delta\varepsilon_{old} \ll \Delta\varepsilon_{connection} \ll \Delta\varepsilon_{new}$ .  $\Delta\varepsilon_{old} \ll \Delta\varepsilon_{connection}$  because the concrete in old decks is much older than in connections. The deformation of old deck mainly appears before connections being made which is not restrained. Therefore, the imposed deformation in old decks is much smaller than that in connections.  $\Delta\varepsilon_{connection} \ll \Delta\varepsilon_{new}$  because new decks are prestressed but not connections. Creep due to prestressing provides additional shortening to new decks, while there is no creep in connections.

If connections are made at later timing, imposed deformation will be  $\Delta\varepsilon_{old} \ll \Delta\varepsilon_{connection} \leq \Delta\varepsilon_{new}$  or  $\Delta\varepsilon_{old} \ll \Delta\varepsilon_{new} \leq \Delta\varepsilon_{connection}$ . The reason of  $\Delta\varepsilon_{old} \ll \Delta\varepsilon_{new}$  has been mentioned above. There are two reasons of  $\Delta\varepsilon_{connection}$  getting close to even exceeding  $\Delta\varepsilon_{new}$ . First, creep of new decks mostly appears in earlier ages. Suppose the connections are made at later timing, the shortening due to creep would mostly be free, resulting in hardly any imposed deformation in new decks. Second, dimensions of new decks are larger than those of connections. So, the shortening due to shrinkage in new deck is smaller than that in connections. For both reasons, a later timing to make connection results in  $\Delta\varepsilon_{connection}$  getting close to even exceeding  $\Delta\varepsilon_{new}$ .

## A15.8 Conclusion

Either no prestress consumption or minimum prestress consumption is practical because the minimum prestress consumption appears when the connection is made at time  $\Delta t_{II-III} \approx 4000$  days or later. Suppose only in-plane loads are taken into account, the old decks and new decks are always in compression while the connections are always in tension. Suppose out-of-plane loads are also taken into account, the maximum tensile stress resulting from out-of-plane loads in cross-section at mid-span is always larger than the maximum compressive stress resulting from in-plane loads. As a result, suppose the tensile strength of concrete is neglected, new decks are always cracked no matter when connections are made.

## A16 Relation between Mean Normal Stiffness and Imposed deformation in a Tensile Member

### A16.1 Bond Stress – Slip Relationship

Bond stress – slip relationship is starting point from which the models used in the books are developed (Bruggeling, 1970, p. 53) (Veen C. v., 1990, p. 22). The bond stress – slip relationship is obtained by a pull-out test (Rehm, 1961, p. 138), see Figure 135. With curve-fitting, the experiment data of bond stress – slip relationship is expressed into an exponential curve (Noakowski, 1978, p. 153):

$$\tau_b = a \cdot \delta^b \quad (68)$$

where:

- $\tau_b$  is the bond stress from pull-out test
- $\delta$  is the slip from 'Pull-out Test'
- $a$  is the bond strength  
=  $0.38 f_{ccm}$
- $b$  is the factor related to the shape of  $\tau_b - \delta$  diagram  
= 0.18

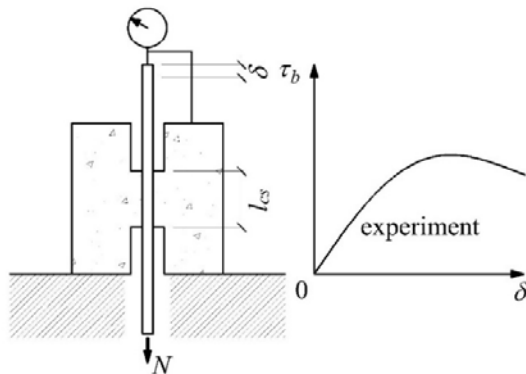


Figure 135: Bond Stress - Slip Curve Obtained by a Pull-out Test.

### A16.2 Primary Cracks Only

#### A16.2.1 Stress Distribution

Transition length  $l_{st}$  is the minimum distance at which cracks occur, or in other words transfer length (Veen C. v., 1990, p. 25). Area inside the transition length on both sides of the cracks is called transition zone. Take half of the transition zone in a tensile member as an independent member, see Figure 136. The force balance in the element is derived basing on Figure 136, see Expression 69.

The tensile force in cross-section  $\sigma_{s0} \cdot A_s + \sigma_{c0} \cdot A_c$  is balanced by the tensile force  $\sigma_{s,cr} \cdot A_s$  in rebar at crack. For the force balance in rebar, the tensile force in rebar  $A_s \cdot (\sigma_{s,cr} - \sigma_{s0})$  is transferred to the concrete by bond within transition zone. So, a distance of  $l_{st}$  beginning from the crack is necessary for the concrete stress increasing from zero to a value equal to tensile strength  $\sigma_{cr}$ . And, therefore, transition length  $l_{st}$  is the minimum distance at which cracks occur (Veen C. v., 1990, p. 23).

$$\sigma_{s,cr} \cdot A_s = \sigma_{s0} \cdot A_s + \sigma_{c0} \cdot A_c \quad (69)$$

where:

- $\sigma_{s,cr}$  is the stress in rebar, or in short the steel stress, at crack
- $\sigma_{s0}$  is the stress in rebar, or in short the steel stress, at the ends of transition zone
- $\sigma_{c0}$  is the stress in concrete, or in short the concrete stress, at the ends of transition zone  
=  $\sigma_{cr}$
- $\sigma_{cr}$  is the *cracking strength* of concrete  
=  $0.6f_{ccm}$  (A. S. G. Bruggeling, W. A. de Bruijn, 1985)
- $A_s$  is the area of cross-section of rebar
- $A_c$  is the area of cross-section of concrete

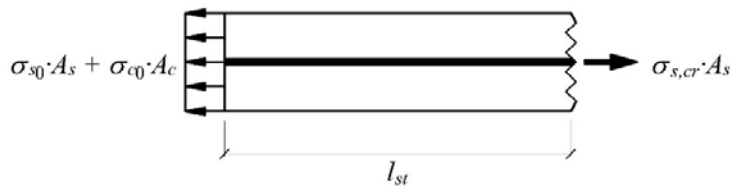


Figure 136: Force Balance in Half Transition Zone.

Let the  $x$ -axis begins at a distance of  $l_{st}$  from crack and points to the crack, see Figure 137. Suppose the strain in rebar and concrete at certain point is same when the concrete at this point is not cracked, the deformation compatibility at point  $x = 0$  m would be derived into Expression 70.

$$\varepsilon_{s0} = \varepsilon_{c0} \quad (70)$$

where:

- $\varepsilon_{s0}$  is the strain in rebar, or in short the steel strain, at point  $x = 0$  m  
=  $\sigma_{s0}/E_s$
- $E_s$  is the elastic modulus of rebar
- $\varepsilon_{c0}$  is the strain in concrete, or in short the concrete strain, at point  $x = 0$  m  
=  $\sigma_{c0}/E_c$
- $E_c$  is the elastic modulus of concrete

Solve Expression 69 and Expression 70 to derive the expressions of steel stresses  $\sigma_{s,cr}$  and  $\sigma_{s0}$  in primary cracks, see Expression 71 and Expression 72.

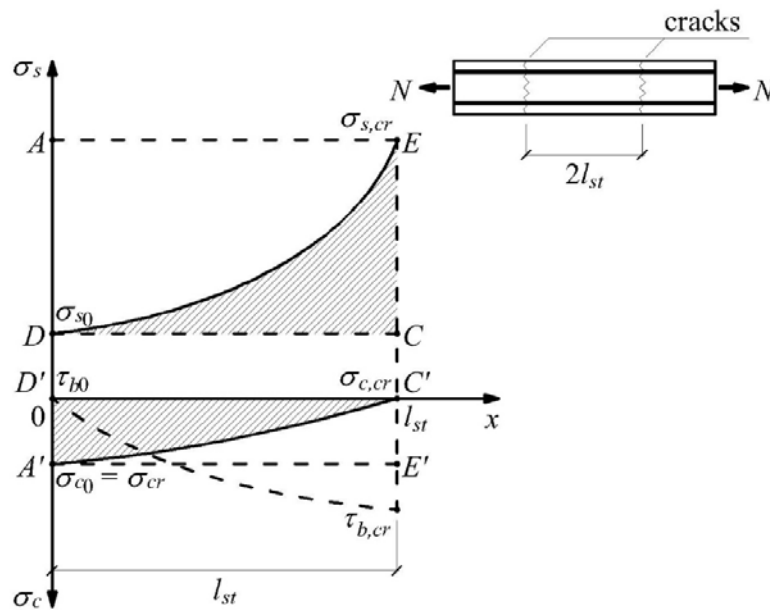
$$\sigma_{s,cr} = \sigma_{cr} \cdot \left( \alpha_e + \frac{1}{\rho_{eff}} \right) \quad (71)$$

where:

- $\alpha_e$  is the elastic modulus ratio  
=  $E_s/E_c$
- $\rho_{eff}$  is the effective reinforcement ratio  
=  $A_s/A_{c,eff}$

$$\sigma_{s0} = \alpha_e \cdot \sigma_{cr} \quad (72)$$

It is generally assumed that the Bond Stress-Slip Relationship is valid for each element  $dx$  and the bond strength  $a$  and the factor  $b$  related to the shape of  $\tau_b - \delta$  diagram are constants inside transition zone (Veen C. v., 1990, p. 24). The distribution of steel stress, concrete stress and bond stress are shown in Figure 137 (Bruggeling, 1970, p. 35).



\* $\sigma_{s,cr}$ ,  $\sigma_{c,cr}$  and  $\tau_{b,cr}$  represent the steel stress, concrete stress and bond stress at cracks, while  $\sigma_{s0}$ ,  $\sigma_{c0}$  and  $\tau_{b0}$  represent the steel stress, concrete stress and bond stress at the ends of transition zone.

Figure 137: Sketch of Stress Distribution in Transition Zone (Primary Cracks Only).

## A16.2.2 Shape Factors for Primary Cracks

Basing on Figure 137, shape factors are introduced to express the distribution of steel stress and concrete stress in transition zone. The magnitude of the shape factors is dependent only on the factor  $b$  in the exponential curve of the bond stress – slip relationship (Veen C. v., 1985, pp. 263 - 344) (Noakowski, 1978, p. 153). Therefore, the definition and magnitudes of the shape factors when there are primary cracks only are as follow:

**Shape factor of steel stress:**

$$S\sigma_s = \frac{\text{shadow area CDE}}{\text{area CDAE}} = \frac{\int_0^{l_{st}} \sigma_s(x) \cdot dx}{(\sigma_{s,cr} - \sigma_{s0}) \cdot l_{st}} = \frac{1 - b}{2} \quad (73)$$

**Shape factor of concrete stress:**

$$S\sigma_c = \frac{\text{shadow area C'D'E'}}{\text{area C'D'A'E'}} = \frac{\int_0^{l_{st}} \sigma_c(x) \cdot dx}{\sigma_{c0} \cdot l_{st}} = \frac{1 + b}{2} \quad (74)$$

**Shape factor of bond stress**

$$S\tau_b = \frac{\int_0^{l_{st}} \tau_b(x) \cdot dx}{\tau_{b,cr} \cdot l_{st}} = \frac{1 - b}{1 + b} \quad (75)$$

## A16.2.3 Slip at Crack and Transition Length

Take the rebar in half of the transition zone as an independent element. As shown in Appendix A16.2.1, the tensile force  $A_s \cdot (\sigma_{s,cr} - \sigma_{s0})$  is transferred to the concrete by the bond within transition zone, see Figure 138. Basing on Figure 138, the force balance in rebar derived, see Expression 76.

$$(\sigma_{s,cr} - \sigma_{s0}) \cdot \frac{1}{4} \pi \phi^2 = \tau_{bm} \cdot l_{st} \cdot \pi \phi \quad (76)$$

where:

$\varnothing$  is the diameter of rebar  
 $\tau_{bm}$  is the mean bond stress  
 $= S\tau_b \cdot \tau_{b,cr}$

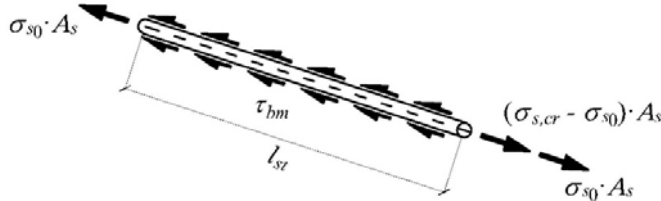


Figure 138: Force Balance in Rebar within Half Transition Zone.

According to the pull-out test shown in Appendix A16.1, the extra elongation of the rebar and the shortening of the concrete within transition zone, or in short the slip at crack, is denoted as  $\delta_{cr}$ . Substitute Expression 68 into Expression 76 to derive the relation between transition length  $l_{st}$  and slip  $\delta_{cr}$  at crack, see Expression 77. Therefore, the slip at crack  $\delta_{cr}$  is expressed into Expression 78.

$$l_{st} = \frac{\sigma_{s,cr} \cdot \varnothing}{4(1 + \alpha_e \cdot \rho_{eff}) \cdot S\tau_b \cdot \tau_{b,cr}} \quad (77)$$

where:

$\tau_{b,cr}$  is the bond stress at crack when there are primary cracks only  
 $= a \cdot \delta_{cr}^b$

$$\delta_{cr} = (\varepsilon_{sm} - \varepsilon_{cm}) \cdot l_{st} \quad (78)$$

where:

$\varepsilon_{sm}$  is the mean steel strain inside transition zone when there are primary cracks only  
 $= S\sigma_s \cdot (\sigma_{s,cr} - \sigma_{s0})/E_s + \sigma_{s0}/E_s$

$\varepsilon_{cm}$  is the mean concrete strain inside transition zone when there are primary cracks only  
 $= S\sigma_c \cdot \sigma_{cr}/E_s$

Solve Expression 77 and Expression 78 to calculate the transition length  $l_{st}$  and the slip  $\delta_{cr}$  at crack. The results are shown by Expression 79 and Expression 80.

$$\delta_{cr} = \left( \frac{1+b}{2} \cdot \frac{\varnothing}{4} \cdot \frac{1}{a \cdot E_s} \cdot \frac{\sigma_{s,cr}^2}{1 + \alpha_e \cdot \rho_{eff}} \right)^{\frac{1}{1+b}} \quad (79)$$

$$l_{st} = 2 \cdot \frac{\delta_{cr} \cdot E_s}{(1-b) \cdot \sigma_{s,cr}} \quad (80)$$

#### A16.2.4 Mean Normal Stiffness inside Transition Zone

If a reinforced concrete member is cracked, the concrete will be broken but not the rebar. Since the crack width is small compared with the length of transition, the mean strain of the cracked member inside transition zone can be represented by the mean steel strain at same position, see Expression 81.

$$\varepsilon_{sm} = S\sigma_s \cdot \frac{\sigma_{s,cr} - \sigma_{s0}}{E_s} + \frac{\sigma_{s0}}{E_s} = \frac{1}{E_s} (S\sigma_s \cdot \sigma_{s,cr} + S\sigma_c \cdot \sigma_{s0}) \quad (81)$$

where:

$\varepsilon_{sm}$  is the mean steel strain when there are primary cracks only

By substituting Expression 71 and Expression 72 into Expression 81 and replacing  $\sigma_{s0}/E_s$  with  $\varepsilon_{s0}$ , the expression of mean steel stress inside the transition zone when there are primary cracks only is derived, see Expression 82. It means, when a new crack is about to occur, the mean steel strain inside the transition zone is  $X$  times larger than that outside the transition zone.

As shown in Figure 139, when a new crack is about to occur, the tensile forces both inside and outside the transition zone are equal to cracking force  $N_{cr}$ . Therefore, in this case, the mean normal stiffness outside the transition zone is  $X$  times larger than that inside the transition zone, see Expression 83.

$$\varepsilon_{sm} = X \cdot \varepsilon_{s0} \quad (82)$$

where:

$X$  is a constant describing the increase of deformation  
 $= \left[ S\sigma_s \cdot \left( 1 + \frac{1}{\alpha_e \cdot \rho_{eff}} \right) + S\sigma_c \right]$

$S\sigma_s$  is the shape factor of steel stress when there are primary cracks only, see Expression 73

$S\sigma_c$  is the shape factor of concrete stress when there are primary cracks only, see Expression 7494

$$(EA)_{cr,1} = \frac{(EA)_0}{X} \quad (83)$$

where:

$(EA)_{cr,1}$  is the mean normal stiffness inside the transition zone when there are primary cracks only

$(EA)_0$  is the mean normal stiffness outside the transition zone  
 $= E_s \cdot A_s + E_{cm}(t) \cdot A_c$

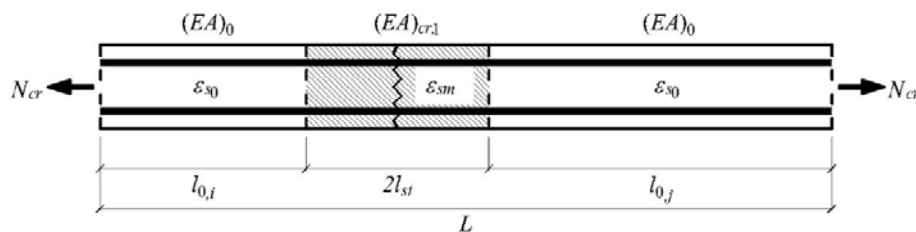


Figure 139: Force Balance in Cracked Tensile Member when a New Crack is about to Occur (Primary Cracks Only).

### A16.2.5 Mean Normal Stiffness of Cracked Tensile Member (Primary Cracks Only)

Simplify the cracked tensile member into a series of springs, see Figure 140. The mean normal stiffness inside  $(EA)_{cr,1}$  and that outside the transition zone  $(EA)_0$  in Figure 140 are evaluated by Expression 82 and Expression 83. Suppose that there are  $n$  primary cracks occurred, the elasticity of springs would be derived as follow:

$$k_{cr,1} = \frac{(EA)_{cr,1}}{l_{cr,1}} = \frac{(EA)_0}{X \cdot l_{cr,1}} \quad (84)$$

where:

$k_{cr,1}$  is the elasticity of spring which represents the part of tensile member inside the transition zone

$l_{cr,1}$  is the length of spring with elasticity  $k_{cr,1}$   
 $= 2n \cdot l_{st}$

$$k_0 = \frac{(EA)_0}{L - l_{cr,1}} \quad (85)$$

where:

$k_0$  is the elasticity of spring which represents the part of tensile member outside the transition zone

$L$  is the total length of the tensile member

Expression 86 shows the relation between the elasticity of combined springs and those of single springs. By substituting Expression 84 and Expression 85 into Expression 86, the expression of elasticity of combined springs  $k_m$  is derived, see Expression 87.

$$\frac{1}{k_m} = \frac{1}{k_0} + \frac{1}{k_{cr,1}} \quad (86)$$

where:

$k_m$  is the elasticity of spring which represents the whole tensile member

$$k_m = \frac{(EA)_0}{(X - 1) \cdot 2n \cdot l_{st} + L} \quad (87)$$

Basing on the relation between the mean normal stiffness and the mean elasticity shown in Expression 88, the expression of mean normal stiffness of the whole tensile member is derived, also see Expression 88

$$(EA)_m = k_m \cdot L = \frac{(EA)_0}{\Omega} \quad (88)$$

where:

$\Omega$  is a constant describing the decrease of mean normal stiffness  
 $= [(X - 1) \cdot 2n \cdot l_{st} + L] / L$

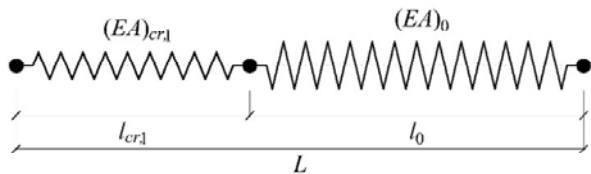


Figure 140: Spring Form of Tensile Member (Primary Cracks Only).

## A16.3 Primary and Secondary Cracks

### A16.3.1 Stress Distribution

When secondary cracks occur, the stress distribution inside the transition zone is different from that when there are primary cracks only (Veen C. v., 1990, p. 27). The bold lines in Figure 141 and Figure 142 represent the distribution of stresses when  $b = 0$  and  $b = 1$ . As shown in Figure 141 and Figure 142, the distribution of steel strain when secondary cracks occur is different from that when there are primary cracks only.

The shape factor of steel stress when secondary cracks occur is 1.5 times and 2 times of that when there are primary cracks only respectively in Figure 141 and Figure 142 (Veen C. v., 1990, p. 28). Then the expressions of mean steel strain in Figure 141 and Figure 142 are derived, see Expression 89 and Expression 90.

$$\varepsilon_{sm} = \frac{1}{E_s} [ \sigma_{s0} + 1.5 \cdot (\sigma_{s,cr} - \sigma_{s0}) \cdot S\sigma_s ] \quad (89)$$

where:

$\varepsilon_{sm}$  is the steel strain inside transition zone when secondary cracks occur  
 $S\sigma_s$  is the shape factor of steel stress when there are primary cracks only and  $b = 0$

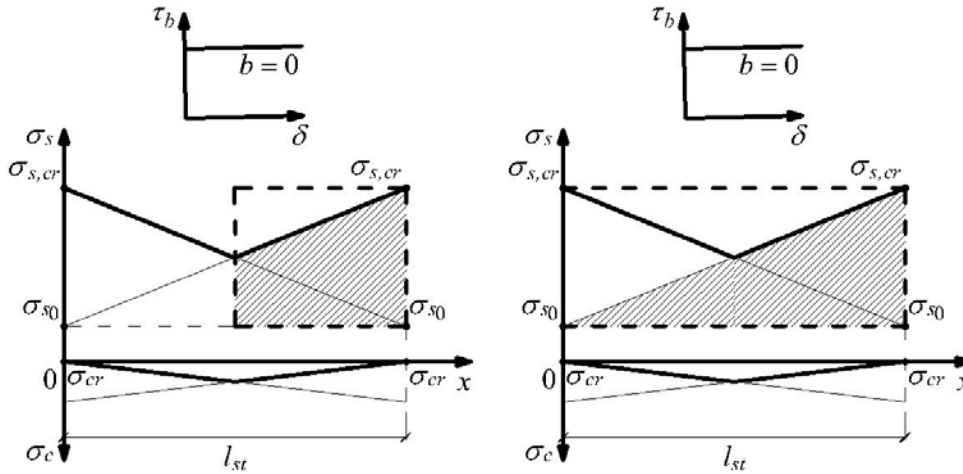


Figure 141: Sketch of Shape Factor in Transition Zone when  $b = 0$  (Secondary and Primary Cracks).

$$\varepsilon_{sm} = \frac{1}{E_s} \left[ \sigma_{s0} + 2 \cdot (\sigma_{s,cr} - \sigma_{s0}) \cdot S\sigma_s \right] \quad (90)$$

where:

- $\varepsilon_{sm}$  is the steel strain inside transition zone when secondary cracks occur
- $S\sigma_s$  is the shape factor of steel stress when there are primary cracks only and  $b = 1$

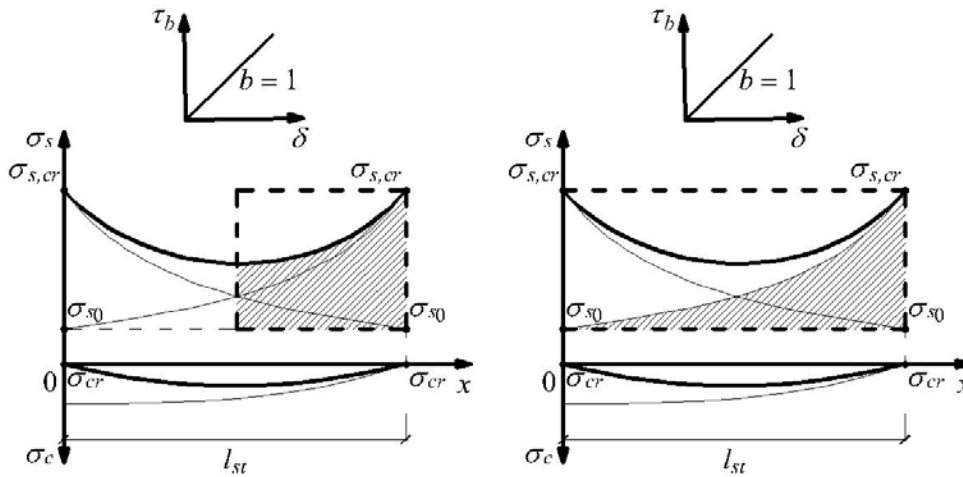


Figure 142: Sketch of Shape Factor in Transition Zone when  $b = 1$  (Secondary and Primary Cracks).

### A16.3.2 Shape Factors for Primary and Secondary Cracks

Assumed that the relation between the factor  $b$  and the shape factor of steel stress is linear for  $0 \leq b \leq 1$ , Expression 89 and Expression 90 would be derived into Expression 91. Substitute Expression 73 into Expression 91, Expression 92 is derived.

$$\varepsilon_{sm} = \frac{1}{E_s} \left[ \sigma_{s0} + \frac{3+b}{2} \cdot (\sigma_{s,cr} - \sigma_{s0}) \cdot S\sigma_s \right] \quad (91)$$

$$\varepsilon_{sm} = \frac{1}{E_s} \left[ \frac{(3+b)(1-b)}{4} \cdot \sigma_{s,cr} + \frac{(1+b)^2}{4} \cdot \sigma_{s0} \right] \quad (92)$$

Compare Expression 92 with Expression 81, the shape factors of steel stress and concrete stress when secondary cracks occur are as follow:

**Shape factor of steel stress:**

$$S\sigma_s = \frac{(3+b)(1-b)}{4} \quad (93)$$

**Shape factor of concrete stress:**

$$S\sigma_c = \frac{(1+b)^2}{4} \quad (94)$$

### A16.3.3 Idealized Crack Pattern

An idealized crack pattern is introduced when it comes to the fully developed cracks (Veen C. v., 1990, p. 29) (Bruggeling, 1970, p. 57), see Figure 143. In the idealized crack pattern, the crack distance varies from  $l_{st}$  to  $2l_{st}$ , and the mean strain in transition zone  $\varepsilon_{sm,3}$  when fully developed cracks occur is derived as follow:

$$\varepsilon_{sm,3} = \frac{2\varepsilon_{sm,1} + \varepsilon_{sm,1+2}}{3} = \frac{1}{E_s} \left[ \frac{(7+b)(1-b)}{12} \cdot \sigma_{s,cr} + \frac{(1+b)(5+b)}{4} \cdot \sigma_{s0} \right] \quad (95)$$

where:

$\varepsilon_{sm,1}$  is the mean steel strain between primary cracks, see Expression 81

$\varepsilon_{sm,1+2}$  is the mean steel strain between primary and secondary cracks when secondary cracks occur, see Expression 92

Compare Expression 95 with Expression 81, the shape factors of steel stress and concrete stress between primary cracks where secondary crack occurs, or in short between primary cracks, are as follow:

**Shape factor of steel stress**

$$S\sigma_s = \frac{(7+b)(1-b)}{12} \quad (96)$$

**Shape factor of concrete stress**

$$S\sigma_c = \frac{(1+b)(5+b)}{4} \quad (97)$$

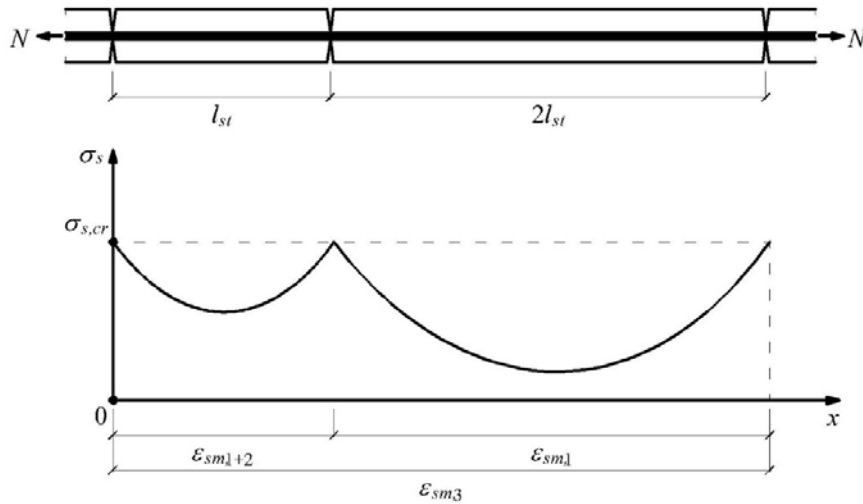


Figure 143: Sketch of Stress Distribution in Transition Zone (Idealize Crack Pattern).

To make sure that the idealized crack pattern is able to form when fully developed cracks occur, the distance between primary cracks ought to be  $3l_{st}$ , while a secondary cracks ought to occur in between two primary cracks at a distance of  $l_{st}$  from one of them, as shown in Figure 143. It means, in this thesis, the position of the cracks are predicted basing on the ideal crack pattern shown in Figure 143. Basing on this prediction, the mean normal stiffness between primary cracks is derived, see Appendix A16.3.4.

### A16.3.4 Mean Normal Stiffness of Idealized Crack Pattern

When a reinforced concrete member is cracked, the concrete will be broken but not the rebar. Since the crack width is small compared with the length of transition, the mean strain of the cracked member between primary cracks where secondary crack occurs, or in short in idealized crack pattern, can be represented by the mean steel strain at same position, see Expression 91 and/or Expression 92.

By substituting Expression 71 and Expression 72 into Expression 92 and replacing  $\sigma_{s0}/E_s$  with  $\epsilon_{s0}$ , the expression of mean steel stress between primary cracks is derived, see Expression 98. It means, when a new crack is about to occur, the mean steel strain between primary cracks is  $\Psi$  times larger than that outside the transition zone.

As shown in Figure 144, when a new secondary crack is about to occur, the tensile forces both inside and outside the transition zone are equal to cracking force  $N_{cr}$ . Therefore, in this case, the mean normal stiffness outside the transition zone is  $\Psi$  times larger than that between primary cracks, see Expression 99.

$$\epsilon_{sm} = \Psi \cdot \epsilon_{s0} \tag{98}$$

where:

$\Psi$  is a constant describing the increase of deformation

$$= \left[ S\sigma_s \cdot \left( 1 + \frac{1}{\alpha_e \cdot \rho_{eff}} \right) + S\sigma_c \right]$$

$S\sigma_s$  is the shape factor of steel stress of idealized crack pattern, see Expression 96

$S\sigma_c$  is the shape factor of concrete stress of idealized crack pattern, see Expression 97

$$(EA)_{cr,3} = \frac{(EA)_0}{\Psi} \tag{99}$$

where:

$(EA)_{cr,3}$  is the mean normal stiffness of idealized crack pattern

$(EA)_0$  is the mean normal stiffness outside the transition zone  
 $= E_s \cdot A_s + E_c \cdot A_c$

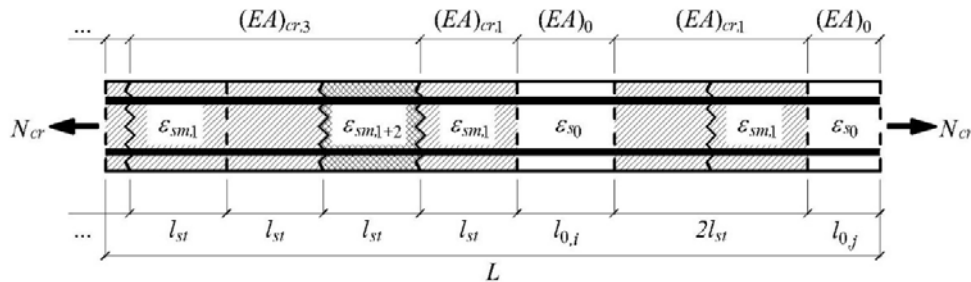


Figure 144: Force Balance in Cracked Tensile Member when a New Crack is about to Occur (Primary and Secondary Cracks).

### A16.3.5 Mean Normal Stiffness of Cracked Tensile Member

The mean normal stiffness of cracked tensile member when secondary cracks occur is related to the final cracked pattern. For simplification, this part is introduced in A16.5. Before that, the final crack pattern has to be determined, see A16.4.

## A16.4 Crack Pattern

### A16.4.1 Formation Process of Crack Pattern

The mean normal stiffness of cracked tensile member when secondary cracks occur is related to the final cracked pattern. To obtain the idealized crack pattern, a concept of formation process of crack pattern related to imposed deformation  $\Delta\varepsilon$  has to be introduced, see Figure 145. In general, there are for important timing during the formation process of crack pattern, which divides the process into four stages:

- $\Delta\varepsilon_I$  the imposed deformation which results in tensile strain in tensile member
- $\Delta\varepsilon_{II}$  the imposed deformation when primary cracks occur, which is referred to as cracking strain  $\varepsilon_{cr}$
- $\Delta\varepsilon_{III}$  the imposed deformation when secondary cracks occur, which is referred to as partially developed cracking strain  $\varepsilon_{pdc}$
- $\Delta\varepsilon_{IV}$  the imposed deformation when fully developed cracks occur, which is referred to as fully developed cracking strain  $\varepsilon_{fdc}$

#### Stage 1:

$\Delta\varepsilon_I < \Delta\varepsilon \leq \Delta\varepsilon_{II}$ : the tensile member is in tension but not cracked, which results in a linear deformation

#### Stage 2:

$\Delta\varepsilon_{II} < \Delta\varepsilon \leq \Delta\varepsilon_{III}$ : primary cracks occur due to imposed deformation and reach their maximum at  $\Delta\varepsilon = \Delta\varepsilon_{III}$

#### Stage 3:

$\Delta\varepsilon_{III} < \Delta\varepsilon \leq \Delta\varepsilon_{IV}$ : secondary cracks occur due to imposed deformation and reach their maximum at  $\Delta\varepsilon = \Delta\varepsilon_{IV}$

#### Stage 4:

$\Delta\varepsilon_{IV} < \Delta\varepsilon$ : all the cracks are developed into fully developed cracks

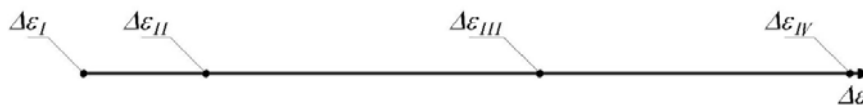


Figure 145: Formation process of Crack Pattern.

#### A16.4.2 Crack Pattern when $\Delta\varepsilon_{II} < \Delta\varepsilon \leq \Delta\varepsilon_{III}$ (Stage 2)

In Stage 2, primary cracks occur. As shown in Appendix A16.3.3, the position of primary cracks can be predicted due to the idealized crack pattern. To make sure that the idealized crack pattern is able to form when fully developed cracks occur, the distance between primary cracks ought to be  $3l_{st}$ .

It means that, when primary cracks are not at their maximum, the primary cracks occur one by one at positions randomly as the imposed deformation increases with certain distances which are the integral multiple of  $3l_{st}$ , see Figure 146. When the maximum is obtained, all the primary cracks have a distance of  $3l_{st}$  from the neighbour ones, see Figure 147. Basing on Figure 147, the maximum number of primary crack  $n_{max}$  is calculated as follow:

$$n_{max} = \text{ROUNDDOWN}\left(\frac{L}{3l_{st}}, 0\right) \quad (100)$$

where:

$L$  is the length of the tensile member

\*  $\text{ROUNDDOWN}(x, 0)$  is a function calculating the maximum integer which is smaller than  $x$ .

When primary cracks occur, the tensile member is divided into several segments by the cracks. Independent from the number of primary cracks, the summation of elongation in each segment ought to equal to the total elongation of the tensile member. Therefore, suppose that the  $(n + 1)$  - th primary cracks is about to occur when a imposed deformation  $\Delta\varepsilon$  is applied to the tensile member, an equation of deformation would be made as follow:

$$\delta_{total} = \delta_{cr,1} + \delta_0 \quad (101)$$

where:

$\delta_{total}$  is the total elongation of the tensile member

$\delta_{cr,1}$  is the total elongation of inside the transition zone

$$= \varepsilon_{sm} \cdot 2n \cdot l_{st}$$

$n$  is the number of primary cracks which have already occurred

$\varepsilon_{sm}$  is the mean steel strain inside the transition zone

$$= X \cdot \varepsilon_{s0}$$

$\varepsilon_{s0}$  is the steel strain outside the transition zone, see Expression 72

$\delta_0$  is the total elongation outside the transition zone

$$= \varepsilon_{s0} \cdot (L - 2n \cdot l_{st})$$

Resulting from Expression 101, the relation between the number of primary cracks which have already occurred and the magnitude of imposed deformation is as follow:

$$n = \frac{(\Delta\varepsilon - \varepsilon_{s0}) \cdot L}{(X - 1) \cdot \varepsilon_{s0} \cdot 2l_{st}} \quad (102)$$

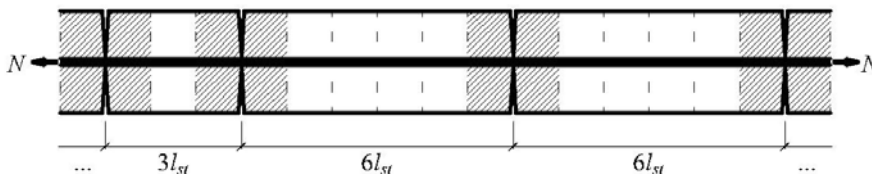


Figure 146: Crack Pattern when Primary Cracks are not at Their Maximum.

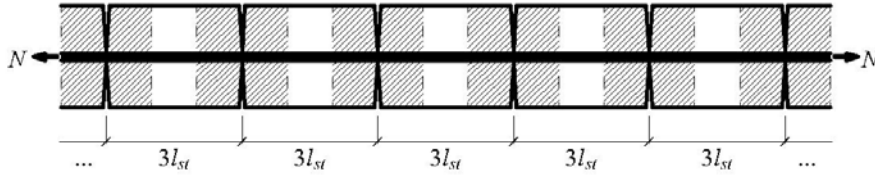


Figure 147: Crack Pattern when Primary Cracks are at Their Maximum.

\*The shadowed parts in Figure 146 and Figure 147 represent the transition zone in the tensile member.

### A16.4.3 Crack Pattern when $\Delta\varepsilon_{III} < \Delta\varepsilon \leq \Delta\varepsilon_{IV}$ (Stage 3)

In Stage 3, primary cracks have reach their maximum while secondary cracks occur. As shown in Appendix A16.3.3, the position of secondary cracks can be predicted due to the idealized crack pattern. To make sure that the idealized crack pattern is able to form when fully developed cracks occur, a secondary cracks ought to occur in between two primary cracks at a distance of  $l_{st}$  from one of them, as shown in Figure 143.

It means that, before secondary cracks occur, the tensile member has been divided by primary cracks into segments with a length of  $3l_{st}$ , see Figure 147. When the secondary cracks are not at their maximum, some of these segments are divided by the secondary cracks into idealized crack pattern, see Figure 148. When the maximum is obtained, the all the segments are divided into idealized crack pattern by the secondary cracks, see Figure 149. Basing on Figure 149, the maximum number of secondary crack  $m_{max}$  is calculated as follow:

$$m_{max} = \begin{cases} \text{ROUNDDOWN}\left(\frac{L}{3l_{st}}, 0\right) - 1, & \text{MOD}(L, 3l_{st}) < 1 \\ \text{ROUNDDOWN}\left(\frac{L}{3l_{st}}, 0\right), & \text{MOD}(L, 3l_{st}) \geq 1 \end{cases} \quad (103)$$

\*MOD(x,y) is a function calculating the remainder of x/y.

When secondary cracks occur, some of the segments in Figure 147 change into idealized crack pattern. Independent from the number of primary cracks, the summation of elongation in each segment and idealized crack pattern ought to equal to the total elongation of the tensile member. Therefore, suppose that the  $(m + 1)$  - th secondary cracks is about to occur when a imposed deformation  $\Delta\varepsilon$  is applied to the tensile member, an equation of deformation would be made as follow:

$$\delta_{total} = \delta_{cr,3} + \delta_{cr,1} + \delta_0 \quad (104)$$

where:

- $\delta_{cr,3}$  is the total elongation of the idealized crack pattern  
 $= \varepsilon_{sm,3} \cdot 3m \cdot l_{st}$
- $m$  is the number of secondary cracks which have already occurred
- $\varepsilon_{sm,3}$  is the mean steel strain of idealized crack pattern  
 $= \Psi \cdot \varepsilon_{s0}$
- $\delta_{cr,1}$  is the total elongation of remained segments  
 $= \varepsilon_{sm,1} \cdot 2(n_{max} - m) \cdot l_{st}$
- $n_{max}$  is the maximum number of primary cracks
- $\varepsilon_{sm,1}$  is the mean steel strain inside the transition zone  
 $= X \cdot \varepsilon_{s0}$
- $\varepsilon_{s0}$  is the steel strain outside the transition zone, see Expression 72
- $\delta_0$  is the total elongation outside the transition zone  
 $= \varepsilon_{s0} \cdot (L - m \cdot l_{st} - 2n \cdot l_{st})$

Resulting from Expression 104, the relation between the number of secondary cracks which have already occurred and the magnitude of imposed deformation is as follow:

$$m = \frac{(X - 1) \cdot 2n \cdot l_{st} \cdot \varepsilon_{s0} - (\Delta\varepsilon - \varepsilon_{s0}) \cdot L}{(2X - 3\Psi + 1) \cdot \varepsilon_{s0} \cdot l_{st}} \quad (105)$$

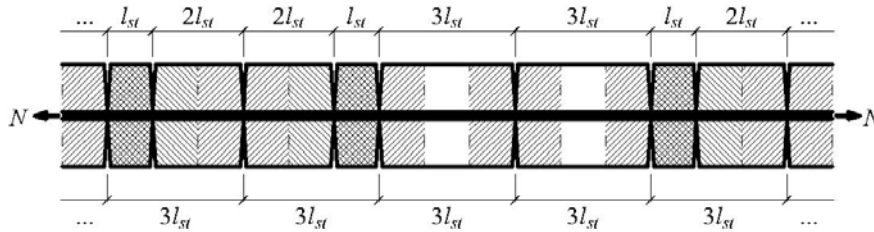


Figure 148: Crack Pattern when Secondary Cracks are not at Their Maximum.

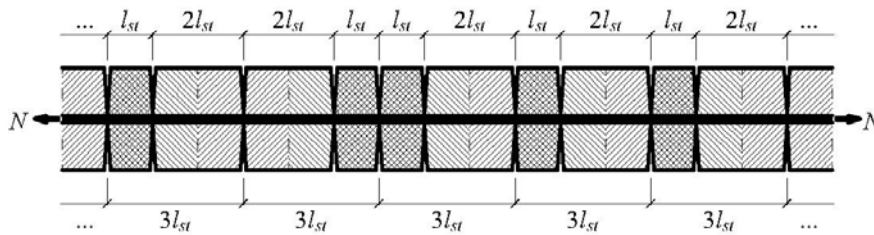


Figure 149: Crack Pattern when Secondary Cracks are at Their Maximum.

## A16.5 Mean Normal Stiffness of Cracked Tensile Member (Primary and Secondary Cracks)

As shown in Appendix A16.4, the relations between the number of primary or secondary cracks and the magnitude of imposed deformation are derived. Simplify the cracked tensile member into a series of springs, see Figure 150. The mean normal stiffness of tensile member with idealized crack pattern  $(EA)_{cr,3}$ , segments shown in Figure 147  $(EA)_{cr,1}$  and that outside the transition zone  $(EA)_0$  in Figure 150 are evaluated by Expression 99, Expression 82 and Expression 83 respectively. Suppose that there are  $m$  secondary cracks occurred, the elasticity of springs would be derived as follow:

$$k_{cr,3} = \frac{(EA)_{cr,3}}{l_{cr,3}} = \frac{(EA)_0}{\Psi \cdot l_{cr,3}} \quad (106)$$

where:

- $k_{cr,3}$  is the elasticity of spring which represents the part of tensile member with idealized crack pattern
- $l_{cr,3}$  is the length of spring with elasticity  $k_{cr,3}$   
 $= 3m \cdot l_{st}$

$$k_{cr,1} = \frac{(EA)_{cr,1}}{l_{cr,1}} = \frac{(EA)_0}{X \cdot l_{cr,1}} \quad (107)$$

where:

- $k_{cr,1}$  is the elasticity of spring which represents the segments shown in Figure 147
- $l_{cr,1}$  is the length of spring with elasticity  $k_{cr,1}$   
 $= 2(n - m) \cdot l_{st}$

$$k_0 = \frac{(EA)_0}{L - l_{cr,3} - l_{cr,1}} \quad (108)$$

where:

$k_0$  is the elasticity of spring which represents the part of tensile member outside the transition zone  
 $L$  is the total length of the tensile member

Expression 109 shows the relation between the elasticity of combined springs and those of single springs. By substituting Expression 106, Expression 107 and Expression 108 into Expression 109, the expression of elasticity of combined springs  $k_m$  is derived, see Expression 110.

$$\frac{1}{k_m'} = \frac{1}{k_0} + \frac{1}{k_{cr,1}} + \frac{1}{k_{cr,3}} \quad (109)$$

where:

$k_m'$  is the elasticity of spring which represents the whole tensile member

$$k_m' = \frac{(EA)_0}{L - (m + 2n_{max}) \cdot l_{st} + 2(n_{max} - m) \cdot X \cdot l_{st} + 3m \cdot \Psi \cdot l_{st}} \quad (110)$$

Basing on the relation between the mean normal stiffness and the mean elasticity shown in Expression 111, the expression of mean normal stiffness of the whole tensile member is derived, also see Expression 111.

$$(EA)_{m'} = k_m' \cdot L = \frac{(EA)_0}{\Omega'} \quad (111)$$

where:

$\Omega'$  is a constant describing the decreasing of mean normal stiffness  
 $= [L - (m + 2n_{max}) \cdot l_{st} + 2(n_{max} - m) \cdot X \cdot l_{st} + 3m \cdot \Psi \cdot l_{st}]/L$

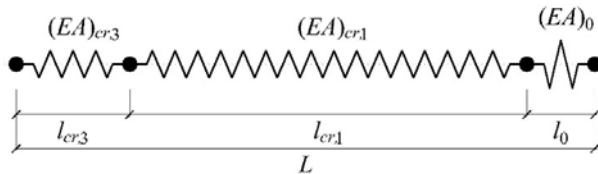


Figure 150: Spring Form of Tensile Member (Primary and Secondary Cracks).

## A16.6 Conclusion

According to Expression 102 and Expression 105, the number of cracks is a function of imposed deformation, while, according to Expression 88 and Expression 111, the mean normal stiffness is a function of the number of cracks. The expressions describing the relation between mean normal stiffness and imposed deformation are complex. For simplicity, here only summarized the derivation of the expressions:

### Primary cracks only:

By substituting Expression 102 into Expression 88, relation between mean normal stiffness and imposed deformation is derived.

### Secondary cracks occur:

By substituting Expression 105 into Expression 111, relation between mean normal stiffness and imposed deformation is established.

In addition, to show the reliability of the relation derived here, an example is given in Appendix A17.

## A17 Calculation of Mean Normal Stiffness

### A17.1 General

A calculation is carried out here to prove that the relation between mean normal stiffness and imposed deformation derived in Appendix A16 is capable to describe the behavior of a cracked tensile member when *imposed deformation* is applied. Suppose the diagram of equivalent normal force and imposed deformation calculated here suits the schematised  $N - \epsilon$  diagram, see Figure 2, the relation between mean normal stiffness and imposed deformation derived in Appendix A16 would be taken reliable.

### A17.2 Input Data

#### A17.2.1 Dimensions

The dimensions of the model are summarized in Table 28. It is the model of a concrete tensile member which is reinforced. Two rows of reinforcement  $6\Phi 25$  in longitudinal direction is applied. The basic dimensions of reinforcement are summarized in Table 175. Substitute the data from Table 175 into Expressions 118 to 122, the dimensions of effective area is evaluated, see Table 176.

height of cross-section	$h$	0.70 m
width of cross-section	$b$	0.50 m
length of total	$L$	42.40 m
area of cross-section	$A_c$	0.35 m <sup>2</sup>

Table 174: Dimensions of the Connection.

diameter of rebar	$\Phi_s$	25 mm
area of rebar	$A_s$	491 mm <sup>2</sup>
spacing	$s$	83 mm
cover	$c$	55 mm

Table 175: Basic Dimensions of Reinforcement.

effective area of concrete per rebar	$A_{c,eff}$	28125 mm <sup>2</sup>
where:		
width of effective area ( $< s$ )	$b_{eff}$	83.33 mm
height of effective area ( $< h/2$ )	$h_{eff}$	337.50 mm
effective reinforcement ratio	$\rho_{eff}$	0.0175

Table 176: Dimensions of Effective Area.

#### A17.2.2 Material Properties and Imposed Deformation

To calculate the diagram of equivalent normal force and imposed deformation which shows the development process of crack pattern, a series of imposed deformation  $\Delta\epsilon$  is applied to the tensile member. The magnitude of *imposed deformation* is as follow:

$$\Delta\epsilon = 0.0 \times 10^{-4} \sim 5 \times 10^{-4} \quad (112)$$

The basic data of material properties and environmental conditions of are shown in Table 177. In this calculation, the *imposed deformation* is applied to the tensile member at time  $t = 36500$  days. The material properties at time  $t = 36500$  days are shown in Table 35. Substitute time  $t = 36500$  days into Expressions 13 to 17, the material properties of concrete at time  $t = 36500$  days are evaluated.

Environment	relative humidity	RH	75 %
Cement (CEM III/B)	coefficient related to cement	$s$	0.25
Concrete (C35/45)	characteristic strength	$f_{ck}$	35 MPa
	gravity	$\gamma_c$	25 kN/m <sup>3</sup>
	compressive strength	$f_{cm}$	43 MPa
	Tensile strength	$f_{ctm}$	3.2 MPa
	elastic modulus	$E_{cm}$	34 GPa
	poisson's ratio	$\nu$	0.2
	coefficient of thermal expansion	$\alpha_c$	0.00001 /°C
Reinforcement – Top (B500)	elastic modulus	$E_s$	210 GPa
	ratio of elastic modulus	$\alpha_e$	5.74
	diameter of rebar	$\Phi_s$	25 mm
	spacing	$s$	100 mm
	cover	$c$	55 mm
Reinforcement – Bottom (B500)	elastic modulus	$E_s$	210 GPa
	ratio of elastic modulus	$\alpha_e$	5.74
	diameter of rebar	$\Phi_s$	25 mm
	spacing	$s$	100 mm
	cover	$c$	55 mm

Table 177: Basic Data of Material Properties and Environmental Conditions.

characteristic strength	$f_{ck}$	3.50E+07 Pa
compression strength	$f_{cm}$	4.30E+07 Pa
elastic modulus	$E_{cm}$	3.40E+10 Pa
characteristic strength	$f_{ck}(t)$	3.50E+07 Pa
mean compression strength	$f_{cm}(t)$	5.48E+07 Pa
where:		
factor related to time	$\beta_{cc}(t)$	1.28
elastic modulus	$E_{cm}(t)$	3.66E+10 Pa

Table 178: Material Properties of Concrete at Time  $t = 36500$  days.

### A17.3 Expressions of Equivalent Normal Force

According to Appendix A16.4.1, there are four stages during the formation process of crack pattern. The expressions of equivalent normal force  $N$  are different in different stages.

Expression 100 and Expression 103 are the expressions of the maximum number of primary and secondary cracks respectively. By substituting Expression 100 back to Expression 102 and solving the equation, the imposed deformation  $\Delta\varepsilon = \varepsilon_{pdc}$  is evaluated which results in the maximum primary cracks. Similarly, by substituting Expression 103 back to Expression 105 and solving the equation, the imposed deformation  $\Delta\varepsilon = \varepsilon_{fdc}$  is evaluated which results in the maximum secondary cracks.

Then substitute  $\Delta\varepsilon = \varepsilon_{pdc}$  and  $\Delta\varepsilon = \varepsilon_{fdc}$  into the relations between mean normal stiffness and imposed deformation which have been established, the mean normal stiffness  $(EA)_{pdc}$  and  $(EA)_{fdc}$  are evaluated when the tensile member is subjected to  $\Delta\varepsilon = \varepsilon_{pdc}$  and  $\Delta\varepsilon = \varepsilon_{fdc}$  respectively.

Suppose a tensile member is subjected to a imposed deformation  $\Delta\varepsilon$ , the expressions of equivalent normal force  $N$  are as follow:

$$\Delta\varepsilon_I < \Delta\varepsilon \leq \Delta\varepsilon_{II}(\varepsilon_{cr}):$$

$$N = \Delta\varepsilon \cdot (EA)_0 \quad (113)$$

where:

$\Delta\varepsilon$  is the imposed deformation  
 $(EA)_0$  is the mean normal stiffness of uncrack tensile member  
 $= E_s \cdot A_s + E_{cm}(t) \cdot A_c$

$$\Delta\varepsilon_{II}(\varepsilon_{cr}) < \Delta\varepsilon \leq \Delta\varepsilon_{III}(\varepsilon_{pdc}):$$

$$N = \Delta\varepsilon \cdot (EA)_m \quad (114)$$

where:

$(EA)_m$  is the mean normal stiffness of tensile member with primary cracks only, see Expression 88

$$\Delta\varepsilon_{III}(\varepsilon_{pdc}) < \Delta\varepsilon \leq \Delta\varepsilon_{IV}(\varepsilon_{fdc}):$$

$$N = \Delta\varepsilon \cdot (EA)_m' \quad (115)$$

where:

$(EA)_m'$  is the mean normal stiffness of tensile member with primary and secondary cracks, see Expression 111

$$\Delta\varepsilon_{IV}(\varepsilon_{fdc}) < \Delta\varepsilon:$$

$$N = \varepsilon_{fdc} \cdot (EA)_{fdc} + (\Delta\varepsilon - \varepsilon_{fdc}) \cdot (EA)_s \quad (116)$$

where:

$\varepsilon_{fdc}$  is the strain when secondary cracks are at their maximum  
 $(EA)_{fdc}$  is the mean normal stiffness of tensile member subjected to  $\varepsilon_{fdc}$   
 $(EA)_s$  is the mean normal stiffness rebars  
 $= E_s \cdot A_s$

The cracking strain  $\varepsilon_{cr}$  at time  $t$  is evaluated as follow:

$$\varepsilon_{cr} = \frac{\sigma_{cr}}{E_{cm}(t)} = 0.53 \times 10^{-4} \quad (117)$$

where:

$\sigma_{cr}$  is the cracking strength of concrete  
 $0.6 \times f_{ctm}$   
 $f_{ctm}$  is the tensile strength of concrete at time  $t = 28$  days

## A17.4 Results

Basing on the data shown in Appendix A17.2, substitute Expression 112 into relation between mean normal stiffness and imposed deformation derived in Appendix A16, a series of equivalent normal forces  $N$  are calculated. Plot the equivalent normal forces  $N$  and their corresponding imposed deformation, the  $N - \Delta\varepsilon$  diagram of the tensile member is obtained, see Figure 151.

As shown in Figure 151, the dashed lines in purple, green and light blue represent the cracking strain  $\varepsilon_{cr}$ , partially developed strain  $\varepsilon_{pdc}$  and fully developed strain  $\varepsilon_{fdc}$  respectively. The diagram is divided into four parts which are corresponding to the formation process introduced in Appendix A16.4.1.

It is shown that the variance of equivalent normal force during the development process of crack pattern is small. It means the impact of cracking on the equivalent normal force is not significant from the view of whole tensile member.

During calculation, the constants which describing the increasing of deformation  $\chi$  and  $\psi$  are 5.09 and 5.90. It means, suppose the primary cracks are at their maximum and no secondary cracks occurs, the deformation of the transition zones 5.09 times larger than that when it is not cracked. And, suppose the tensile member is fully cracked with an idealized crack pattern shown in Figure 143, the deformation of the transition zones 5.90 times larger than that when it is not cracked.

However, the total length of the connection  $L$  is much longer than that of transition zones of a single crack  $2l_{st}$ . As results, the increment of deformation due to a single crack gives hardly any difference to the deformation of whole tensile member. And, therefore, the decrement of equivalent normal force is small. In the end, the  $N - \delta \epsilon$  diagram is approximately an horizontal line, when the tensile member is not fully cracked, see Figure 151.

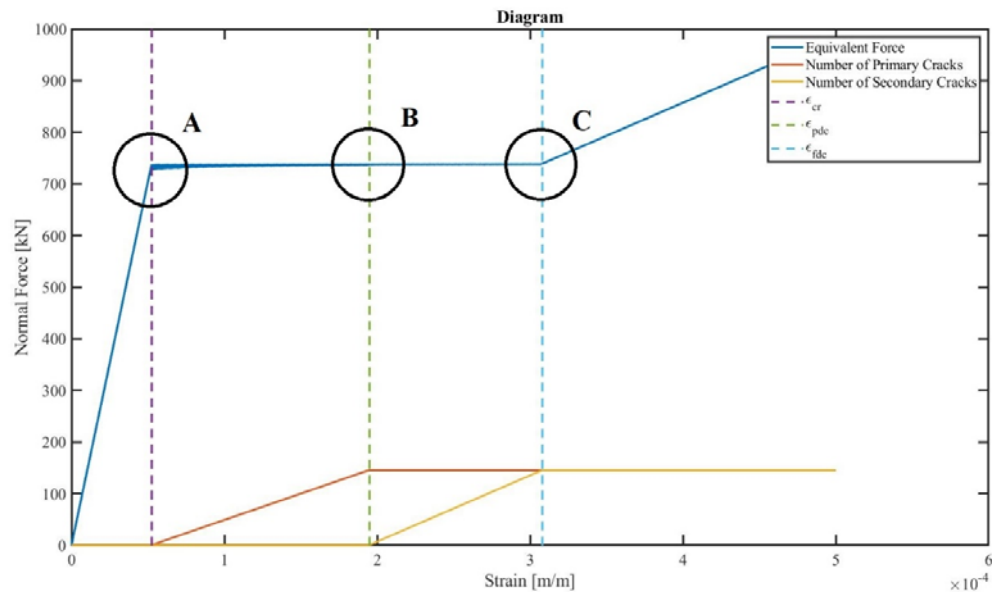


Figure 151:  $N - \delta$  Diagram of Connection in the South Part of Widened Deck KW03.01.

In addition, it is shown that, from  $\Delta \epsilon = \epsilon_{cr}$  to  $\Delta \epsilon = \epsilon_{fdc}$ , the variance of equivalent normal force is getting smaller. Details A, Details B and Details C are shown in Figure 152, Figure 153 and Figure 154.

As shown in Figure 152, Figure 153 and Figure 154, the equivalent normal force varies as the *imposed deformation* increases. It reaches its maximum when a new crack is about to occur and drops to its minimum after a new crack occurs. The diagram between a minimum and a maximum is linear, because it is assumed that the mean normal stiffness of the tensile member is constant during this process.

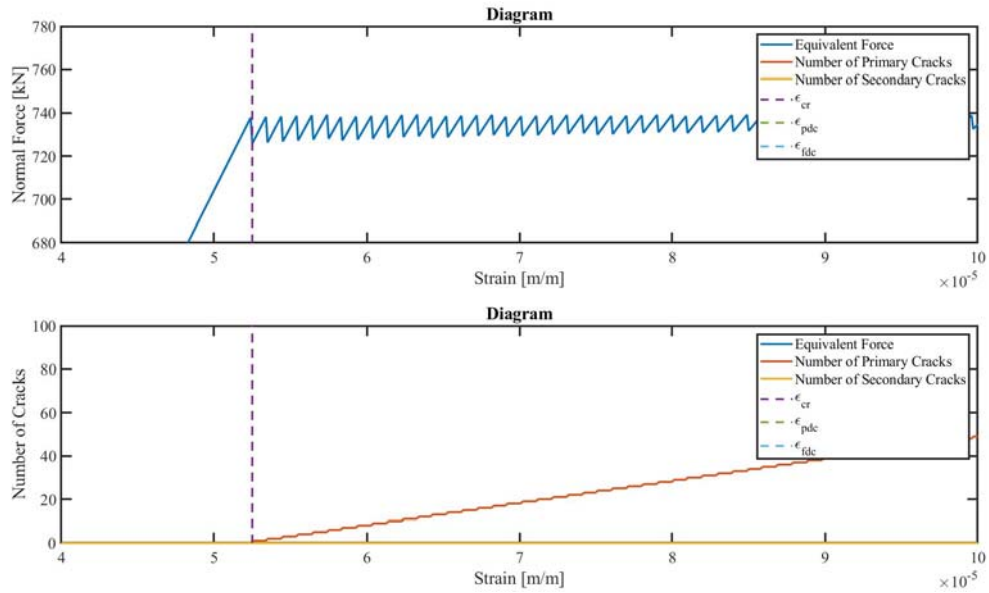


Figure 152: Details A.

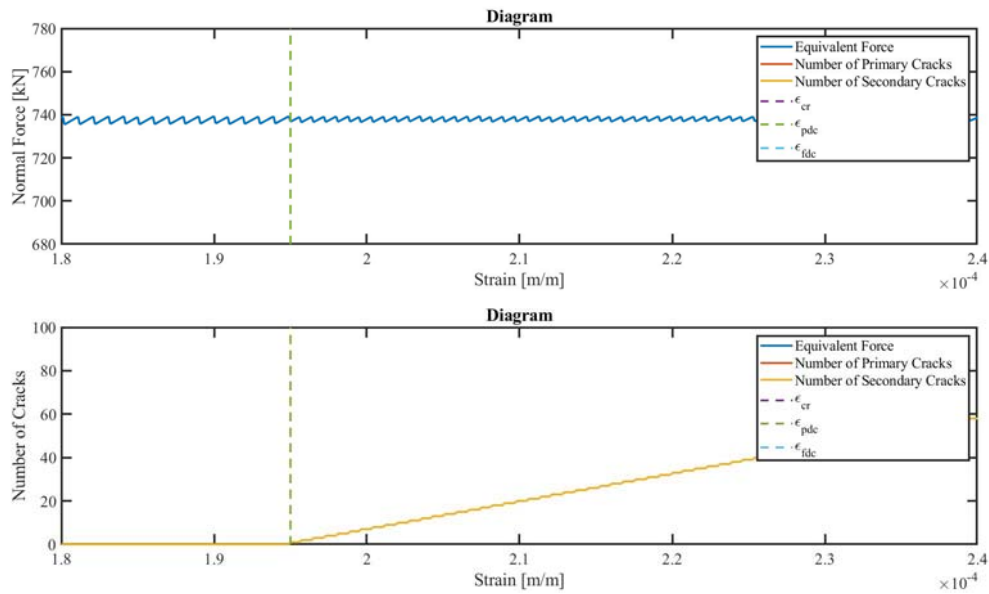


Figure 153: Details B.

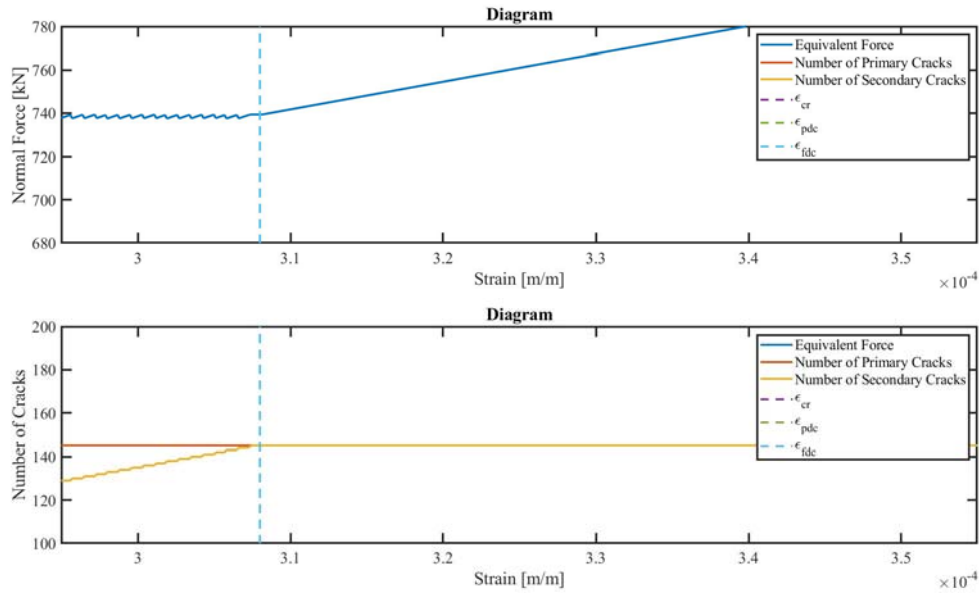


Figure 154: Details C.

### A17.5 Conclusion

According to Figure 151, suppose a tensile member is much longer than the transition zone of single crack, the impact of cracking on the equivalent normal force is neglectable. However, it is proved that the decrement of normal stiffness is significant when a tensile member is cracked due to imposed deformation.

A copy of Figure 2 is shown in Figure 155. Compare Figure 151 with Figure 155, it is shown that the diagram of equivalent normal force and imposed deformation calculated here suits the schematised  $N - \epsilon$  diagram. So, the relation between mean normal stiffness and imposed deformation derived in Appendix A16 is reliable.

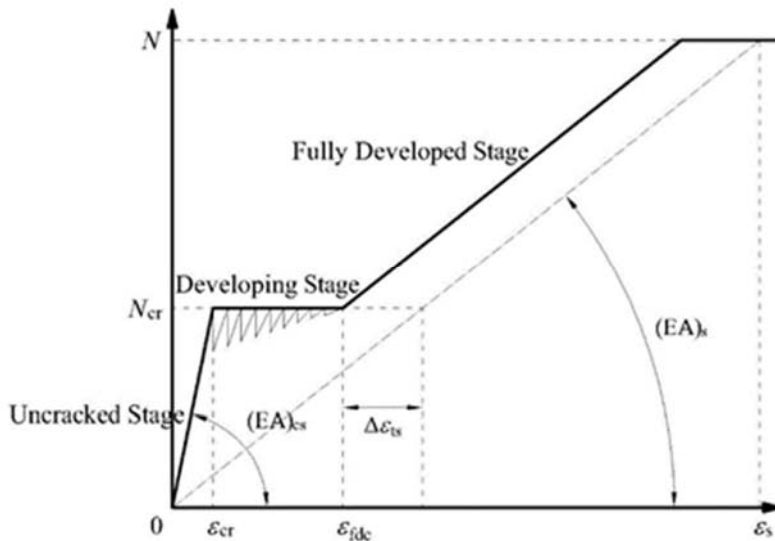


Figure 155: Sketch of  $N - \delta$  Diagram in 'Pink Book'.

## A18 Expressions to Evaluate the Effective Area of Rebar

According to Eurocode, when the calculation about cracking is carried out, the effective area surrounding the reinforcement has to be taken into account, see Figure 156. As shown in Figure 156, the cracks are concentrated in a certain part of tensile member. The cross-section of this part is taken as effective area in this thesis. The expression of the maximum width of effective area  $b_{eff,max}$  is as follow:

$$b_{eff,max} = 5 \left( c + \frac{\phi_s}{2} \right) \quad (118)$$

where:

$c$  is the cover of rebar

$\phi_s$  is the diameter of rebar

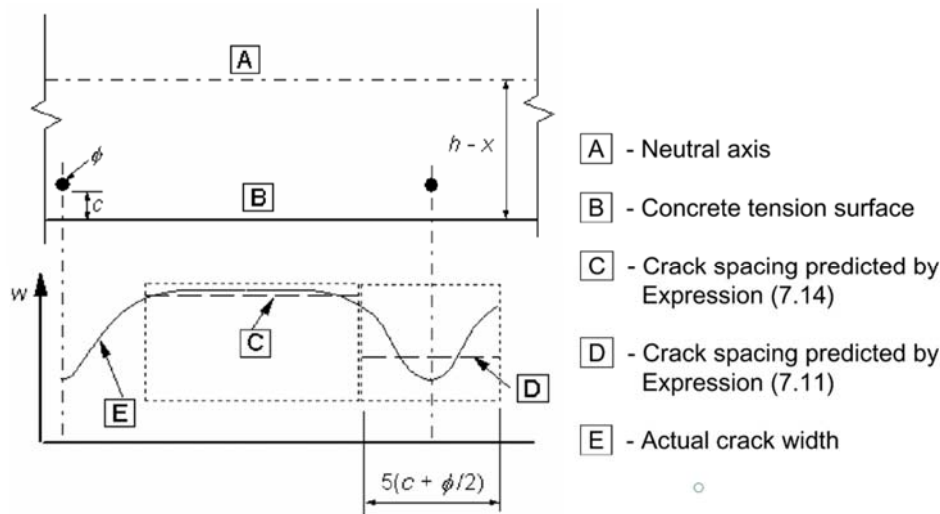


Figure 156: Effective Area in Tensile Member.

Basing on Expression 118, the effective area surrounding rebar in a tensile member is estimated, see Figure 157. The shadowed part in Figure 157 represents the effective area. The expressions of width  $b_{eff}$  and height  $h_{eff}$  of effective area are as follow:

$$b_{eff} = \text{MIN} \left[ 5 \left( c + \frac{\phi_s}{2} \right), s \right] \quad (119)$$

where:

$s$  is the spacing of rebar

$$h_{eff} = \text{MIN} \left[ c + \frac{\phi_s}{2} + 2.5 \left( c + \frac{\phi_s}{2} \right), \frac{h}{2} \right] \quad (120)$$

where:

$h$  is the height of cross-section

With the width and height of effective area evaluated, the area of effective area and the effective reinforcement ratio are evaluated as follow:

$$A_{c,eff} = b_{eff} \cdot h_{eff} \quad (121)$$

$$\rho_{s,eff} = \frac{A_s}{A_{c,eff}} \quad (122)$$

where:

$A_s$  is the cross-section area of rebar  
 $= \pi \cdot \phi_s^2 / 4$

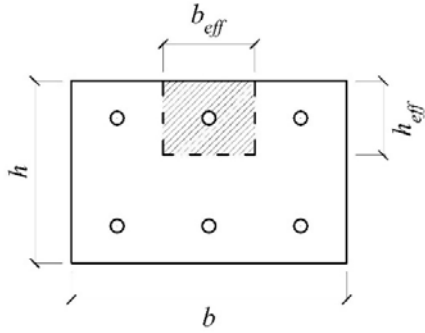


Figure 157: Sketch of Effective Area.

## A19 Impact of Cracking on Prestress Consumption in Proportion

### A19.1 General

As shown in Appendix A15, independent from the timing to make connection, only connections are in tension. Therefore, only connections are possible to be cracked. With the cracked zone estimated, calculations with the impact of cracking is carried out.

The stress at which cracking occurs in concrete is referred to as the cracking strength of concrete  $\sigma_{cr}$ , or in short the cracking strength. Suppose the tensile stress in connections resulting from combined actions exceeds the cracking strength, the connections would be taken as the cracked area to investigate the impact of cracking.

The cracking strength is often assumed to be equal to the tensile strength of concrete  $f_{ctm}(t)$  at time  $t = 28$  days (Breugel, 2013, p. 72). The expression to evaluate  $f_{ctm}(t)$  at time  $t = 28$  days is shown in Appendix A3, see Expression 16. However, an important factor to the cracking strength is the duration of load which causes cracking. Suppose a long-term load is applied, cracking strength would be smaller than that when a short-term load is applied (A. S. G. Bruggling, W. A. de Bruijn, 1985). The expression to evaluate the cracking strength  $\sigma_{cr}$  is as follow:

$$\sigma_{cr} = 0.6 \cdot f_{ctm}(t) \quad (123)$$

where:

$f_{ctm}(t)$  is the tensile strength of concrete at time  $t = 28$  days when short-term load is applied

With cracking strength, suppose the deformation applied to connections is known, the mean normal stiffness of cracked connections is available, see Appendix A16. As shown in Appendix A16, a relation is established between the mean normal stiffness of a cracked concrete tensile member and imposed deformation applied to it. According to the relation established in Appendix A16, the normal stiffness of the connections are re-evaluated when cracking is taken into account. With the re-evaluated normal stiffness in connections, the in-plane strain and stress in widened deck KW03.01 resulting from the imposed deformation are re-calculated.

The imposed deformation used to evaluate the mean normal stiffness of connections is taken as the mean strain resulting from imposed deformation when cracking is **not** taken into account. The means strain resulting from imposed deformation when cracking is not taken into account is substituted into the expressions in Appendix A16 as imposed deformation to re-evaluate the normal stiffness in connections.

The stress resulting from imposed deformation, shown in Appendix A15.6, is calculated without the impact of cracking. Hereby, to investigate the impact of cracking on the resulting strain and stress, re-calculation are carried out to Example 3 and Example 6 with cracking taken into account, see Appendix A19.2.

### A19.2 Re-calculated Examples

The stress resulting from imposed deformation and prestress consumption in proportion in widened deck KW03.01 are re-calculated. For each re-calculated example, four figures are plotted:

1. A sketch showing material properties and imposed deformation.
2. Stress resulting from imposed deformation calculated by Mechanics 1 and Mechanics 2 with cracking.
3. Stress resulting from imposed deformation calculated by Mechanics 2 with and without cracking.
4. Prestress consumption in proportion calculated by Mechanics 2 with and without cracking.

For the same reason shown in Appendix A15.1, the impact of additional deformation due to imposed deformation, or in other words the impact of imposed deformation, on the compressive stress is neglected. The compressive stress resulting from prestressing at time  $t = t_{\infty}$  in old decks and new decks is equal to those calculated in Appendix A15. As a result, to show the impact of cracking clear, hereby only shown the stress resulting from imposed deformation, where the compressive stress resulting from prestressing is excluded.

In general, due to imposed deformation, only connections are cracked. Therefore, the stiffness of connection decreases. For simplicity, the decreased stiffness is represented into a fictitious elastic modulus of concrete which is smaller than the original one, see Figure 158 and Figure 162.

As shown in Figure 159 and Figure 163, with cracking taken into account, stress resulting from imposed deformation calculated by Mechanics 1 and Mechanics 2 are almost same. As shown in Figure 160, Figure 161, Figure 164 and Figure 165, stress resulting from imposed deformation and prestress consumption in proportion calculated Mechanics 2 with and without cracking are almost same. It means, when connections are made at time  $\Delta t_{II-III} = 28$  days, although connections is cracked, the impact of cracking on stress resulting from imposed deformation is small.

**Example 3: south part (connection made at time  $\Delta t_{II-III} = 28$  days)**

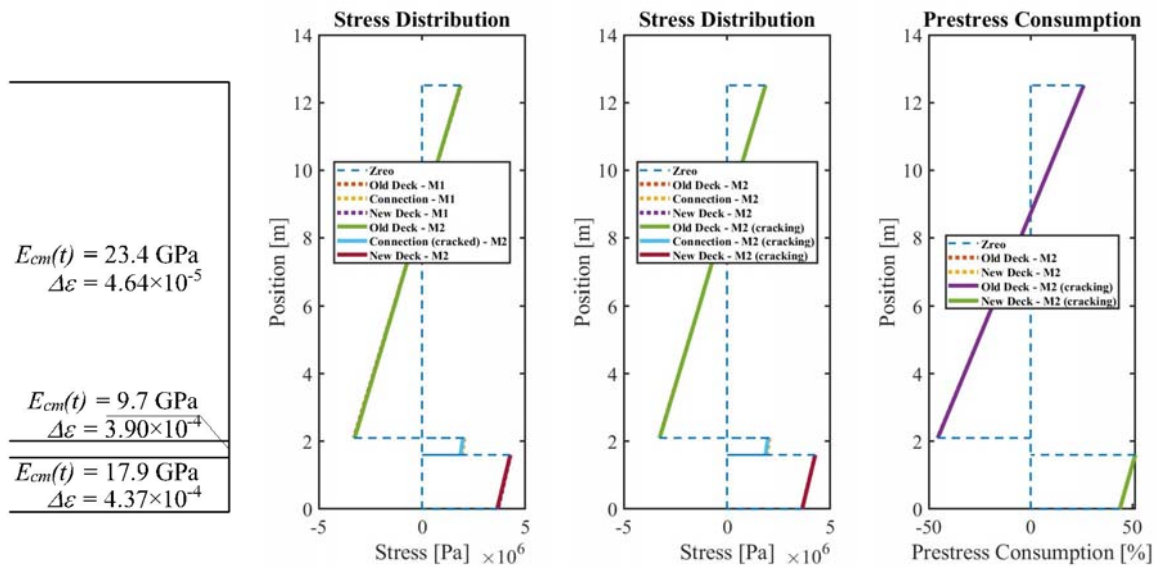


Figure 158: Material Properties and Imposed Deformation in South ( $\Delta t_{II-III} = 28$  days).

Figure 159: Stress Calculated by Mechanics 1 (M1) and Mechanics 2 (M2) in South ( $\Delta t_{II-III} = 28$  days).

Figure 160: Stress Calculated by Mechanics 2 (M2) with and without Cracking in South ( $\Delta t_{II-III} = 28$  days).

Figure 161: Prestress Consumption Calculated by Mechanics 2 (M2) with and without Cracking in South ( $\Delta t_{II-III} = 28$  days).

**Example 6: north part (connection made at time  $\Delta t_{II-III} = 28$  days)**

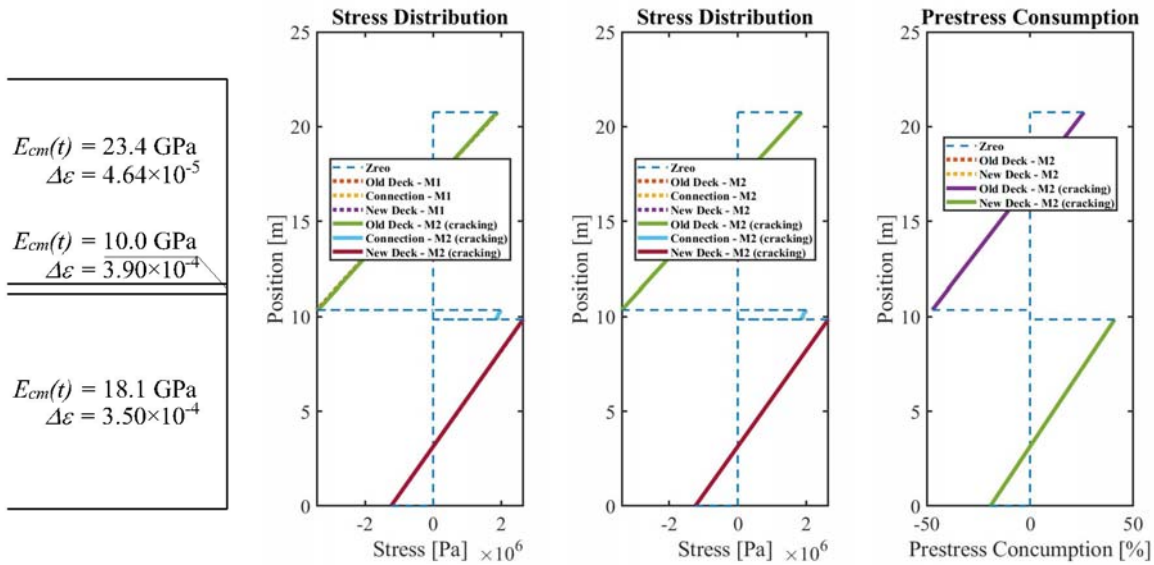


Figure 162: Material Properties and Imposed Deformation in North ( $\Delta t_{II-III} = 28$  days).

Figure 163: Stress Calculated by Mechanics 1 (M1) and Mechanics 2 (M2) in North ( $\Delta t_{II-III} = 28$  days).

Figure 164: Stress Calculated by Mechanics 2 (M2) with and without Cracking in North ( $\Delta t_{II-III} = 28$  days).

Figure 165: Prestress Consumption Calculated by Mechanics 2 (M2) with and without Cracking in North ( $\Delta t_{II-III} = 28$  days).

### A19.3 Additional Calculation

As shown in Appendix A19.2, the connections are cracked while the impact of cracking is small. To investigate the possible impact of cracking, an additional calculation is carried out to Example 3. According to Appendix A16, cracking decreases the stiffness connection. Same as the re-calculation in Appendix A19.2, the decreased stiffness is represented into a fictitious elastic modulus of concrete which is smaller than the original one. The original elastic modulus of concrete in connection is  $E_{cm}(t) = 10.1 \text{ GPa}$ . So, during the additional calculation, the fictitious elastic modulus of concrete in connection varies from  $E_{cm}(t) = 1 \text{ Pa}$  to  $E_{cm}(t) = 10.1 \text{ GPa}$ , see Figure 166 and Figure 168.

In the additional calculation, stress resulting from imposed deformation in widened deck KW03.01 is a function of elastic modulus  $E_{cm}(t)$  in connection. The resulting stress is calculated by both Mechanics 1 and Mechanics 2.

The results of additional calculation is plotted into three dimensional figures, see Figure 167 and Figure 169. As shown in Figure 167 and Figure 169, the three axis represent the position in cross-section, the elastic modulus of concrete and the stress resulting from imposed deformation respectively. In addition to Figure 167 and Figure 169, two dimensional figures are plotted as well, where the two axis represent the elastic modulus of concrete and the stress resulting from imposed deformation respectively, see Figure 170 and Figure 171.

As shown in Figure 169 and Figure 171, before the elastic modulus of concrete in connections decrease to 40%, the impact of cracking is small. As shown in Appendix A19.2, the elastic modulus of concrete in Example 3 decreases to 96.0% which is far from 40%. As a result, the impact of cracking on the stress resulting from imposed deformation in Example 3 is small. Similarly, the elastic modulus of concrete in Example 6 decreases to 99.0% which is far from 40% as well. Therefore, the impact of cracking on the stress resulting from imposed deformation in Example 6 is also small.

As shown in Figure 167 and Figure 169, before the elastic modulus of concrete in connections decrease to 40%, the stress calculated by Mechanics 1 and Mechanics 2 are almost same. However, as shown in Figure 169, when the elastic modulus of concrete in connections decrease to 40% or less, the stress in widened deck KW03.01 calculated by Mechanics 2 drop to zero, while those calculated by Mechanics 1 are non-zero in old decks and new decks.

It means, when the elastic modulus of concrete in connection is not extremely small, both Mechanics 1 and Mechanics 2 are usable. The difference between Mechanics 1 and Mechanics 2 is significant only when the elastic modulus of concrete in connection is extremely small. Also see Figure 170 and Figure 171.

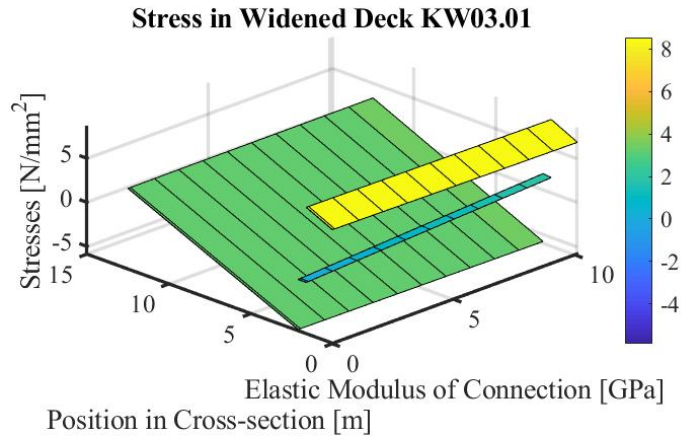
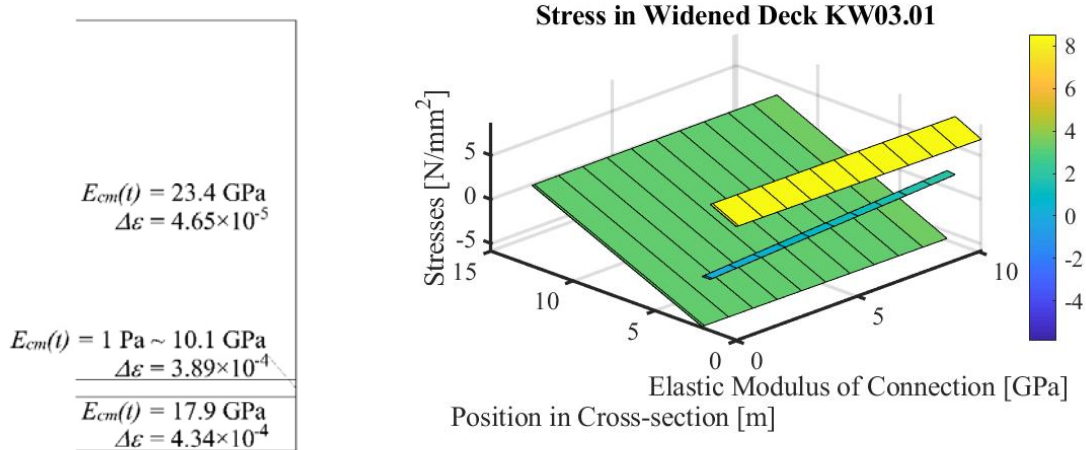


Figure 166: Material Properties and Imposed Deformation in the South Part ( $\Delta t_{II-III} = 28$  days). Figure 167: Stress Distribution in Example 3 Calculated by Mechanics 1 (M1) Corresponding to a Series of Elastic Modulus Applied to Connection.

\*The colour in the image represents the mean stress resulting from the imposed deformation applied to old deck, connection and old deck. This three-dimensional image shows the impact of decreased elastic modulus on the stress calculated by Mechanics 1.

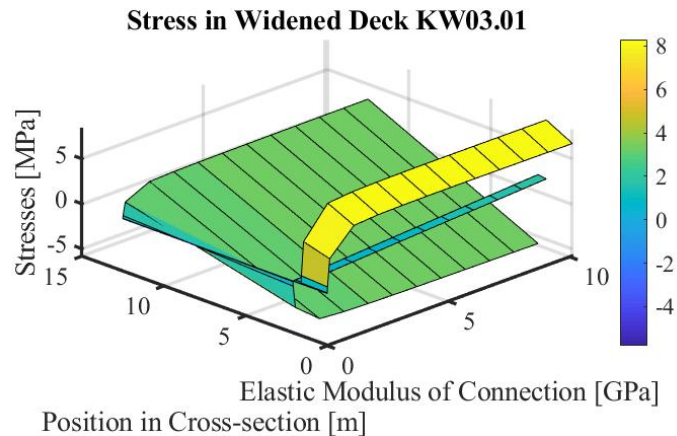
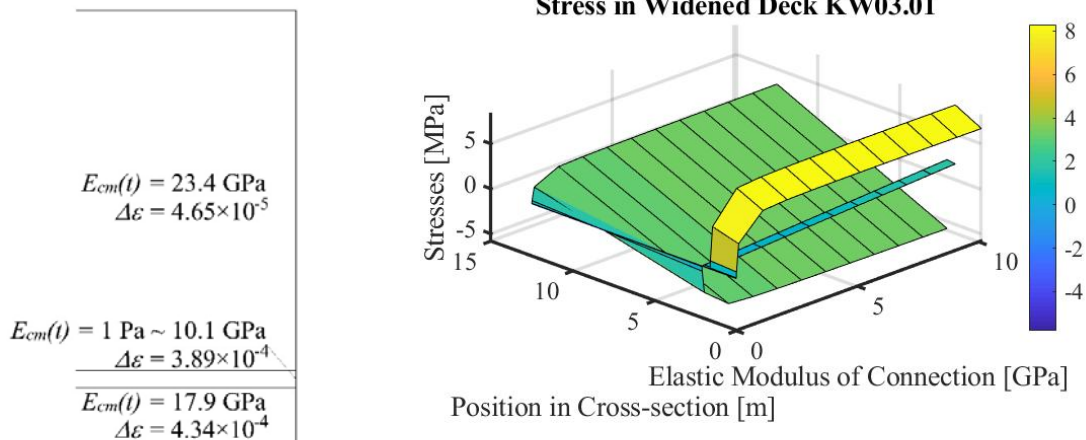


Figure 168: Material Properties and Imposed Deformation in the South Part ( $\Delta t_{II-III} = 28$  days). Figure 169: Stress Distribution in Example 3 Calculated by Mechanics 2 (M2) Corresponding to a Series of Elastic Modulus Applied to Connection.

\*The colour in the image represents the mean stress resulting from the imposed deformation applied to old deck, connection and old deck. This three-dimensional image shows the impact of decreased elastic modulus on the stress calculated by Mechanics 2.

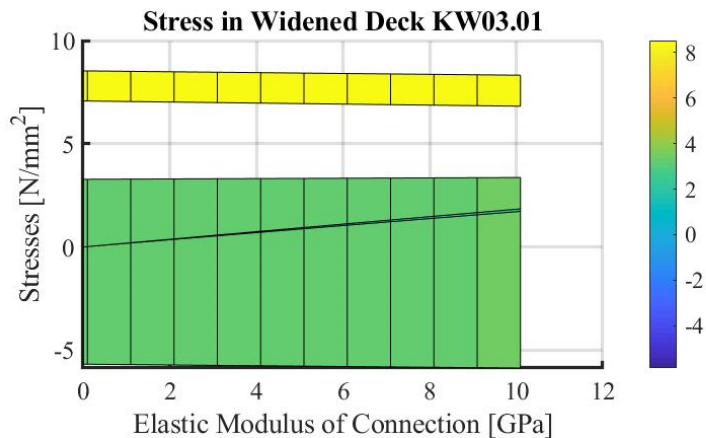


Figure 170: Front-view of Figure 167.

\*The colour in the image represents the mean stress resulting from the imposed deformation in applied to old deck, connection and old deck. This figure shows the impact of decreased elastic modulus on the stress calculated by Mechanics 1.

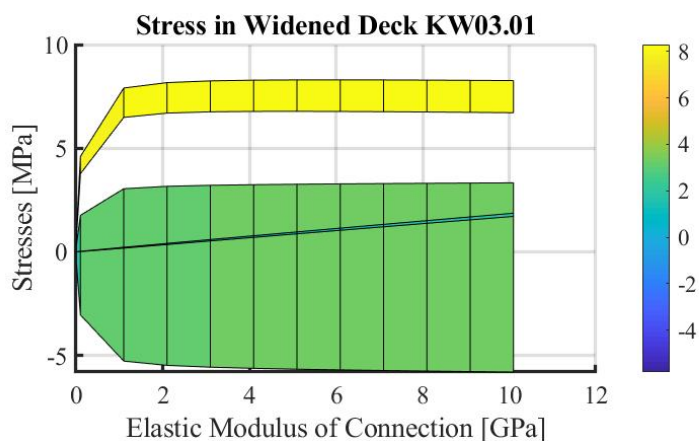


Figure 171: Front-View of Figure 169.

\*The colour in the image represents the mean stress resulting from the imposed deformation in applied to old deck, connection and old deck. This figure shows the impact of decreased elastic modulus on the stress calculated by Mechanics 2.

The calculation carried out above is only about in-plane situation. However, as shown in Appendix A15.3, suppose out-of-plane loads are also taken into account, as shown in Appendix A2.5, the maximum tensile stress resulting from out-of-plane loads in cross-section at mid-span varies from  $\sigma_d = 9.9$  MPa to  $\sigma_d = 15.6$  MPa, which is always larger than the maximum compressive stress resulting from in-plane loads. As a result, suppose the tensile strength of concrete is neglected, new decks are always cracked no matter when connections are made.

Out-of-plane loads result in out-of-plane cracking. According to Appendix A16, cracking decreases the stiffness of new deck. Same as the re-calculation in Appendix A19.2, the decreased stiffness is represented into a fictitious elastic modulus of concrete which is smaller than the original one. The original elastic modulus of concrete in new deck is  $E_{cm}(t) = 17.9$  GPa. So, during the additional calculation, the fictitious elastic modulus of concrete in connection varies from  $E_{cm}(t) = 1$  Pa to  $E_{cm}(t) = 17.9$  GPa, see Figure 172.

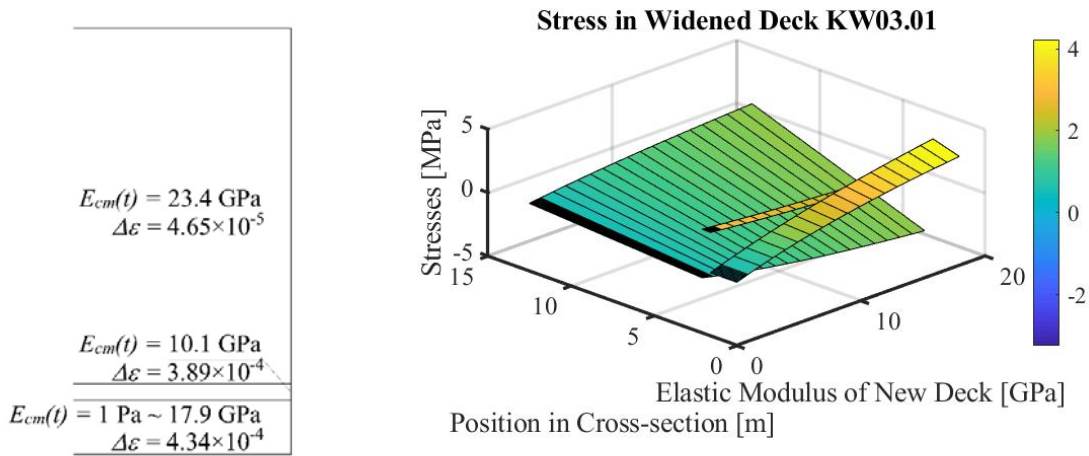


Figure 172: Material Properties and Imposed Deformation in the South Part ( $\Delta t_{I-III} = 28$  days). Figure 173: Stress Distribution in Example 3 Calculated by Mechanics 2 (M2) Corresponding to a Series of Elastic Modulus Applied to New Decks.

\*The colour in the image represents the mean stress resulting from the imposed deformation applied to old deck, connection and old deck. This three-dimensional image shows the impact of decreased elastic modulus on the stress calculated by Mechanics 2.

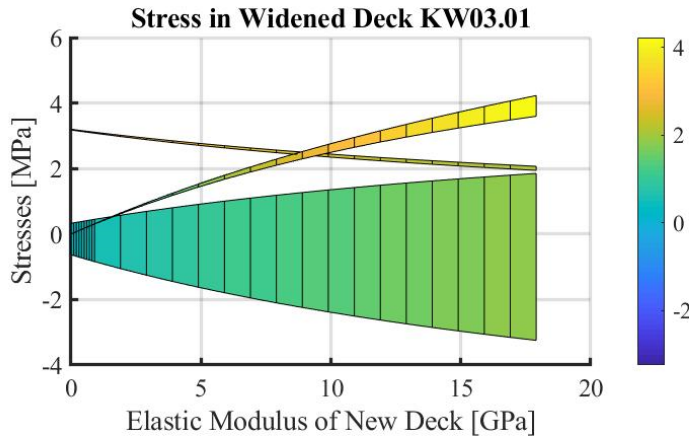


Figure 174: Front-view of Figure 173.

\*The colour in the image represents the mean stress resulting from the imposed deformation in applied to old deck, connection and old deck. This figure shows the impact of decreased elastic modulus on the stress calculated by Mechanics 2.

As shown in Appendix A2.5, tensile stress in concrete resulting from load case 6.10 a are  $\sigma_{d,6.10a} = 24.8$  MPa and  $\sigma_{d,6.10a} = 14.2$  MPa at 6X and 8X. For simplification, the maximum linear elastic deformation of concrete at Cross-section 6X and Cross-section 8X are calculated respectively as follow:

**maximum elastic deformation at Cross-section 6X**

$$\epsilon_{d,6.10a} = \frac{14.2 \text{ MPa}}{17.9 \text{ GPa}} = 7.93 \times 10^{-4}$$

**maximum elastic deformation at Cross-section 8X**

$$\epsilon_{d,6.10a} = \frac{24.8 \text{ MPa}}{17.9 \text{ GPa}} = 1.39 \times 10^{-3}$$

Substitute the maximum linear elastic deformation  $\varepsilon_{d,6.10a}$  as imposed deformation into the expressions shown in Appendix A16 to calculate the minimum elastic modulus of concrete at Cross-section 6X and Cross-section 8X. The results of calculation are as follow:

**minimum elastic modulus at Cross-section 6X**

$$E_{cm,6.10a}(t) = 1.7 \text{ GPa}$$

**minimum elastic modulus at Cross-section 8X**

$$E_{cm,d,6.10a}(t) = 2.9 \text{ GPa}$$

Suppose the compressive stress in cross-section has no impact on the magnitude of elastic modulus of concrete, the elastic modulus of concrete in the whole cross-section are as follow:

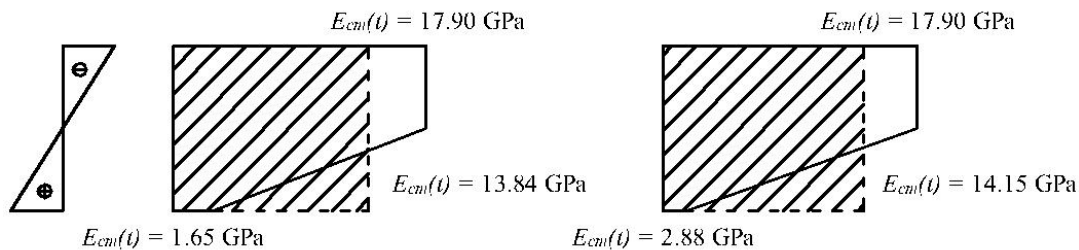


Figure 175: Mean Elastic Modulus of Concrete under Out-of-plane Loads.

**mean elastic modulus at Cross-section 6X**

$$E_{cm,d,6.10a}(t) = 13.8 \text{ GPa}$$

**mean elastic modulus at Cross-section 8X**

$$E_{cm,d,6.10a}(t) = 14.2 \text{ GPa}$$

According to Figure 174, due to the decrement of elastic modulus of concrete, stress resulting from imposed deformation would decrease to 84%, where the absolute stress decrement is 0.7 MPa. Although the out-of-plane loads may decrease the stress resulting from imposed deformation, the decrement cannot help avoid cracking.

## A19.4 Conclusion

In general, in terms of widened deck KW03.01, the impact of cracking and the advantage of Mechanics 2 is significant only when the elastic modulus of concrete in connections decrease to about 40% or less. However, the elastic modulus of concrete decreases to 96% and 99% in south and north respectively, which are much larger than 40%. Therefore, the impact of cracking on the stress resulting from imposed deformation and the prestress consumption in proportion is small.

In conclusion, both Mechanics 1 and Mechanics 2 without the impact of cracking is capable to calculate the stress resulting from imposed deformation in widened deck KW03.01. In terms of prestress consumption, the timing to make connection  $\Delta t_{II-III}$  is more critical than the impact of cracking.

Suppose out-of-plane loads are taken into account, it is expected that the stress resulting from imposed deformation would be decreased to 84%. However, such a decrement cannot help avoid cracking.

## A20 Impact of Reduced Prestressing Force on Prestress Consumption

### A20.1 General

As shown in Section 9.4, since the prestress loss in proportion is large due to imposed deformation and the prestressing itself is one of the sources of imposed deformation, an investigation is carried out to see whether it is possible to get similar remaining compressive stress in widened deck KW03.01 with reduced prestressing force.

### A20.2 Results

The investigation is carried out to the widened deck KW03.01. During the investigation, a series of prestress are applied to new deck. The magnitude of the prestress varies from 2000 kN/cable to 4000 kN/cable. For simplicity, hereby only summarized the final stress and prestress consumption in proportion, where the impact of cracking is taken into account, see Figure 176 to Figure 179.

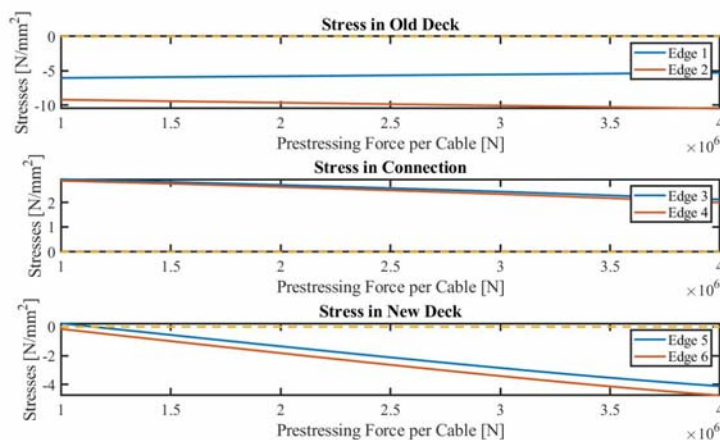


Figure 176: Final Resulting Stress in South Corresponding to Different Prestressing Forces per Cable.

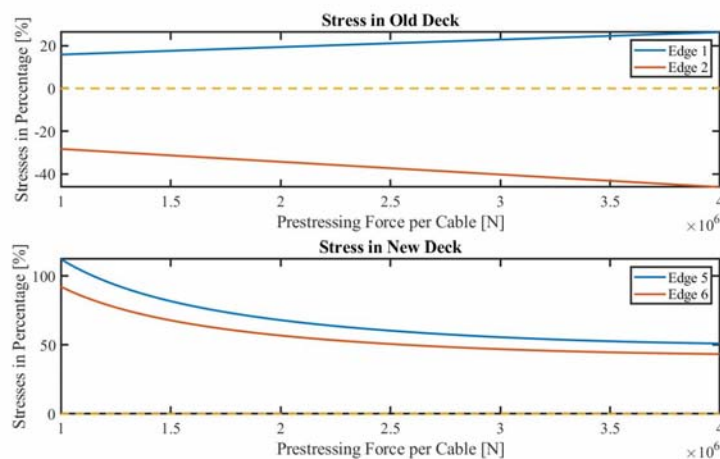


Figure 177: Prestress Consumption in South Corresponding to Different Prestressing Forces per Cable.

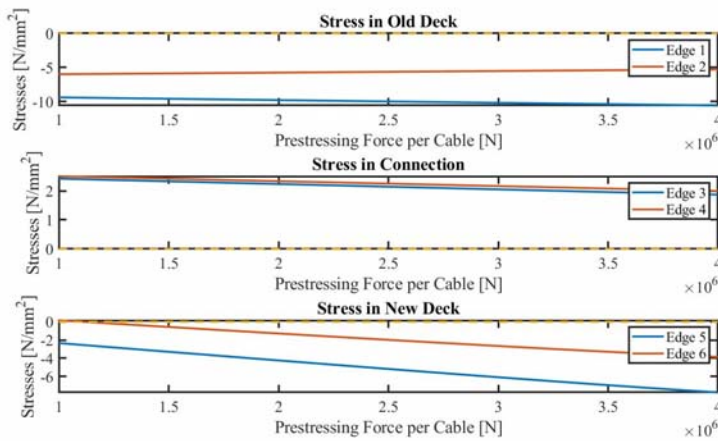


Figure 178: Final Resulting Stress in North Corresponding to Different Prestressing Forces per Cable.

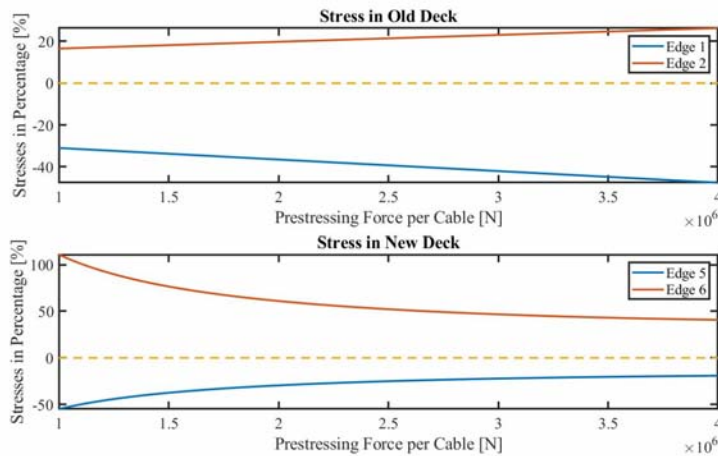


Figure 179: Prestress Consumption in North Corresponding to Different Prestressing Forces per Cable.

As shown in Figure 176 to Figure 179, the impact of reduced prestressing force on final resulting stress and prestress consumption is different in old deck, connection and new deck. Old decks are always in compression. The reduced prestressing force decreases the maximum prestress consumption in old decks. In contrast, connections are always in tension. The reduced prestressing force increases the tensile stress in connections. Due to the tensile stress, connections are cracked. One on hand, cracking decreases the stiffness of connections, which would decrease the stress resulting from imposed deformation. On the other hand, reduced prestressing forces increases the difference of imposed deformation in connections and new decks, which would increase the stress resulting from imposed deformation. According to Figure 176 to Figure 179, in terms of final resulting stress and prestress consumption, the difference of imposed deformation in connections and new decks is more critical to the resulting stress than the stiffness of connection.

The situation of new decks is more complex than those of old decks and connections. In most cases, when prestressing force is not extremely small, new decks are in compression. Otherwise, parts of new decks are in tension. As shown in Figure 176 to Figure 179, reduced prestressing force increases prestress consumption. Suppose the prestressing force per cable applied to new deck is extremely, the maximum prestress consumption would exceed 100%.

In addition, as shown in Figure 176 to Figure 179, if the prestressing force applied to new decks is 4000 kN/cable or more, the magnitude of prestressing force will have no impact on the maximum prestress consumption in new decks.

### A20.3 Conclusion

Reduced prestressing force increases the prestress consumption, or in other words decreases the remaining compressive stress in concrete. Suppose prestressing force applied to new decks is extremely small, prestress consumption would exceed 100%. As a result, to decrease prestress consumption, a larger prestress should be applied.

As shown in Appendix A20.2, if the prestressing force applied to new decks is 4000 kN/cable or more, the magnitude of prestressing force will have no impact on the maximum prestress consumption in new decks. As shown in Appendix A7.1, prestressing force applied to new decks is 3956 kN/cable. Therefore, neither increasing or decreasing the prestressing force in new decks would help reduce prestress consumption.

## A21 Expressions for Elastic Modulus of Concrete

### A21.1 General

According to Section 9.3.2, different expressions are used to evaluate the elastic modulus of concrete in the calculation carried out by SCIA and the simple approach. As for the calculation carried out by SCIA, Expression 124 is used, while, as for the simple approach, the expressions introduced in Appendix A16 are used.

According to Table 179, Expression 124 is mainly for the eccentrically reinforced rectangular section which is subjected to bending without normal force (Normalisatie, 1995). However, the stress in connection resulting from imposed deformation shows that the connections of widened deck KW03.01 are in tension, see Section 9.2. As a result, it is required to discuss whether it is proper to evaluate the elastic modulus of cracked concrete with Expression 124.

$$E_f = 3100 + 6700 \cdot 100 \cdot \rho \quad (124)$$

$E_f$ N/mm <sup>2</sup>			
$f'_{ck}$ N/mm <sup>2</sup>	buiging en normaalkracht symmetrisch gewapende rechthoekige doorsnede		buiging zonder normaalkracht; excentrisch gewapende rechthoekige doorsnede
	$\alpha_n \leq 0.5$	$0.5 < \alpha_n \leq 0.9$	
15	$1300 + 4100 \bar{\omega}_{ot} + (9000 - 1300 \bar{\omega}_{ot}) \alpha_n \leq 2900$	$(8700 + 5175 \bar{\omega}_{ot})(1 - 2/3 \alpha_n)$	$2200 + 4900 \bar{\omega}_o \leq 2900$
25	$1600 + 4200 \bar{\omega}_{ot} + (14000 - 1600 \bar{\omega}_{ot}) \alpha_n \leq 3600$	$(12900 + 5100 \bar{\omega}_{ot})(1 - 2/3 \alpha_n)$	$2500 + 5500 \bar{\omega}_o \leq 3600$
35	$1900 + 4300 \bar{\omega}_{ot} + (19000 - 1900 \bar{\omega}_{ot}) \alpha_n \leq 4300$	$(17100 + 5025 \bar{\omega}_{ot})(1 - 2/3 \alpha_n)$	$2800 + 6100 \bar{\omega}_o \leq 4300$
45	$2200 + 4400 \bar{\omega}_{ot} + (24000 - 2200 \bar{\omega}_{ot}) \alpha_n \leq 5000$	$(21300 + 4950 \bar{\omega}_{ot})(1 - 2/3 \alpha_n)$	$3100 + 6700 \bar{\omega}_o \leq 5000$
55	$2500 + 4500 \bar{\omega}_{ot} + (29000 - 2500 \bar{\omega}_{ot}) \alpha_n \leq 5700$	$(25500 + 4875 \bar{\omega}_{ot})(1 - 2/3 \alpha_n)$	$3400 + 7300 \bar{\omega}_o \leq 5700$
65	$2800 + 4600 \bar{\omega}_{ot} + (34000 - 2800 \bar{\omega}_{ot}) \alpha_n \leq 6400$	$(29700 + 4800 \bar{\omega}_{ot})(1 - 2/3 \alpha_n)$	$3700 + 7900 \bar{\omega}_o \leq 6400$
waarin:			waarin:
$\bar{\omega}_{ot} = \frac{A_s + A'_s}{A_b} 100$		$\alpha_n = \frac{N'_d}{A_b f'_c + (A_s + A'_s) f_s}$	$\bar{\omega}_o = \frac{A_s}{A_b} 100$

Table 179: Fictitious Elastic Modulus  $E_f$

### A21.2 Discussion

The expressions shown in Table 179 are derived from a  $M - \kappa$  relationship, see Figure 180, while the  $M - \kappa$  relationship is derived basing on a bi-linear concrete compressive stress – strain diagram was used. Therefore, as shown in Table 179, only two situations are taken into account. One is eccentrically reinforced rectangular section with bending and compressive normal force, while the other is eccentrically reinforced rectangular section with bending only.

Since connections are not prestressed, suppose there are out-of-plane loads only taken into account, cross-sections of connections are mainly subjected to bending. In this case, it is suggested to use Expression 124. However, when there is in-plane loads only taken into account, the connections of widened deck KW03.01 are in tension, see Section 9.2. As a result, neither the expressions with nor without normal force suit the in-plane situation.

As a result, the expressions introduced in Appendix A16 are recommended to evaluate the elastic modulus of cracked concrete when there is in-plane load only. Suppose there are out-of-plane loads taken into account, it is recommended to first calculate the possible linear elastic deformation in whole cross-section with out-of-plane loads. Then use the expressions introduced in Appendix A16 to calculate the elastic modulus of concrete in whole cross-section, and use the mean elastic modulus of concrete in whole cross-section to calculate the stress resulting from in-

plane loads. Appendix A19.3 shows an example of evaluating mean elastic modulus of concrete in whole cross-section.

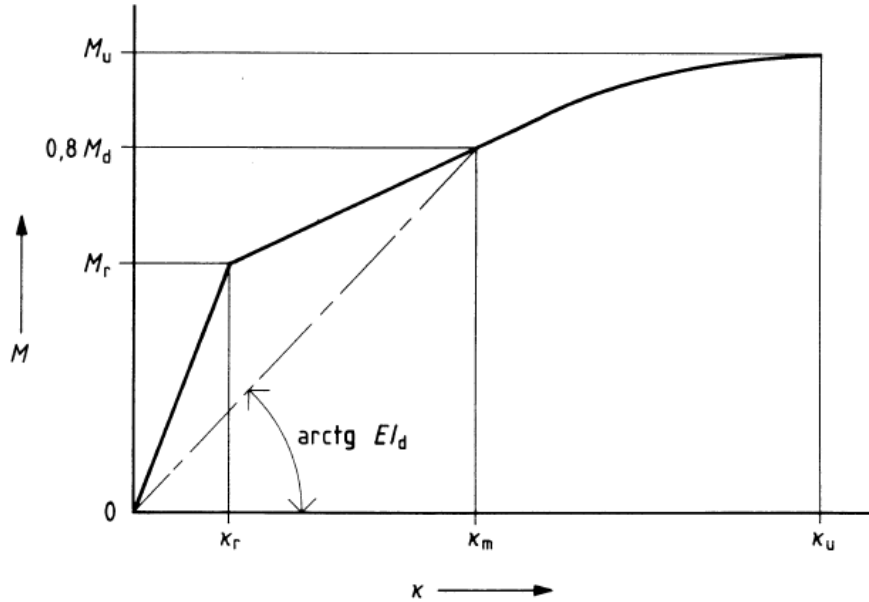


Figure 180: Determine of Bending Stiffness from  $M - \kappa$  Diagram

### A21.3 Conclusion

When in-plane loads are taken into account, instead of the expressions shown in Table 179, the expressions introduced in Appendix A16 are recommended to evaluate the elastic modulus of cracked concrete.